SUBSTITUTION CHEMISTRY OF THE COBALT COMPLEXES $[Co_2(CO)_6(PhC{\equiv}CR)$ (R = Ph, H) AND $PhCCo_3(CO)_9]$ WITH THE DIPHOSPHINE LIGANDS [BIS(DIPHENYLPHOSPHINO)MALEIC ANHYDRIDE (BMA) AND (Z)-$Ph_2PCH{=}CHPPh_2$]. REVERSIBLE CHELATE-TO-BRIDGE DIPHOSPHINE LIGAND EXCHANGE, PHOSPHORUS-CARBON BOND CLEAVAGE AND PHOSPHORUS-CARBON BOND FORMATION.

DISSERTATION

Presented to the Graduate Council of the
University of North Texas in Partial
Fulfillment of the Requirements

For the Degree of

DOCTOR OF PHILOSOPHY

By

Kaiyuan Yang, B.S., M.S.
Denton, Texas
December, 1994

SUBSTITUTION CHEMISTRY OF THE COBALT COMPLEXES $[Co_2(CO)_6(PhC{\equiv}CR)$ (R = Ph, H) AND $PhCCo_3(CO)_9]$ WITH THE DIPHOSPHINE LIGANDS [BIS(DIPHENYLPHOSPHINO)MALEIC ANHYDRIDE (BMA) AND (Z)-$Ph_2PCH{=}CHPPh_2$]. REVERSIBLE CHELATE-TO-BRIDGE DIPHOSPHINE LIGAND EXCHANGE, PHOSPHORUS-CARBON BOND CLEAVAGE AND PHOSPHORUS-CARBON BOND FORMATION.

DISSERTATION

Presented to the Graduate Council of the
University of North Texas in Partial
Fulfillment of the Requirements

For the Degree of

DOCTOR OF PHILOSOPHY

By

Kaiyuan Yang, B.S., M.S.
Denton, Texas
December, 1994

Yang, Kaiyuan, Substitution Chemistry of the Cobalt Complexes $[Co_2(CO)_6(\mu\text{-}PhC{\equiv}CR)$ (R = Ph, H) and $PhCCo_3(CO)_9]$ with the Diphosphine Ligands [Bis(diphenylphosphino)maleic Anhydride (BMA) and (Z)-$Ph_2PCH{=}CHPPh_2$]. Reversible Chelate-to-Bridge Diphosphine Ligand Exchange, Phosphorus-Carbon Bond Cleavage and Phosphorus-Carbon Bond Formation. Doctor of Philosophy (Chemistry), December, 1994, 192 pp., 26 tables, 21 figures, references list, 267 titles.

The tricobalt cluster $PhCCo_3(CO)_9$ (**1**) reacts with the bidentate phosphine ligand 2,3-bis(diphenylphosphino)maleic anhydride (bma) in the presence of added Me_3NO to give the diphosphine-substituted cluster $PhCCo_3(CO)_7$(bma) (**2**). Cluster **2** is unstable in solution, readily losing CO to afford $Co_3(CO)_6[\mu_2\text{-}\eta^2,\eta^1\text{-}C(Ph)\overline{C{=}C(PPh_2)C(O)OC(O)}](\mu_2\text{-}PPh_2)$ (**3**) as the sole observed product. VT-^{31}P NMR measurements on cluster **2** indicate that the bma ligand functions as both a chelating and a bridging ligand. At -97 °C, ^{31}P NMR analysis of **2** reveals a K_{eq} of 5.7 in favor of the bridging isomer. The bridged bma cluster **2** is the only observed species above -50°C. The solid-state structure of **2** does not correspond to the major bridging isomer observed in solution but rather the minor chelating isomer. The conversion of **2** to **3** followed first-order kinetics, with the reaction rates being independent of the nature of the reaction solvent and strongly suppressed by added CO, supporting a dissociative loss of CO as the rate-determining step. The activation parameters for CO loss were determined to be $\Delta H^{\neq} = 29.9 \pm 2.2$ kcal/mol and $\Delta S^{\neq} = 21.6 \pm 6$ eu.

Treatment of the cluster **3** with 1.0 equivalent PMe_3 at -78 °C gives

the cluster $Co_3(CO)_5(\mu\text{-}CO)(PMe_3)[\mu_2\text{-}\eta^2,\eta^1\text{-}C(Ph)\overline{C=C(PPh_2)C(O)OC(O)}](\mu_2\text{-}PPh_2)$ (**5**), via site-selective PMe_3 addition to the PPh_2(maleic anhydride)-substituted cobalt center. Cluster **5** readily loses CO at room temperature and transforms to the mono-substituted cluster $Co_3(CO)_5(PMe_3)[\mu_2\text{-}\eta^2,\eta^1\text{-}C(Ph)\overline{C=C(PPh_2)C(O)OC(O)}](\mu_2\text{-}PPh_2)$ (**6**). Cluster **6** reacts further with additional PMe_3 to afford the di-substituted cluster $Co_3(CO)_4(PMe_3)_2[\mu_2\text{-}\eta^2,\eta^1\text{-}C(Ph)\overline{C=C(PPh_2)C(O)OC(O)}](\mu_2\text{-}PPh_2)$ (**7**).

The reactions of the alkyne-bridged binuclear complexes $Co_2(CO)_6(\mu\text{-}PhC{\equiv}CR)$ (R = Ph, H) with the diphosphine ligand bma in the presence of Me_3NO give $Co_2(CO)_4(\mu\text{-}PhC{\equiv}CR)$(bma) (R = Ph, H) with chelating ligand (**8a**, **11a**). Chelate (**8a**, **11a**)-to-bridge (**8b**, **11b**) ligand equilibration is promoted by photolysis and thermolysis conditions. These transformations proceed by dissociative CO loss. The products (**9**, **12**) formed from $Co_2(CO)_6(\mu\text{-}PhC{\equiv}CR)$ (R = Ph, H) and (Z)-$Ph_2PCH{=}CHPPh_2$ exhibit a chelating diphosphine ligand, with no evidence for the analogous chelate-to-bridge exchange. Compound **8** undergoes P-C(maleic anhydride) bond cleavage coupled with alkyne-C(maleic anhydride) and alkyne-PPh_2 bond formation at 83 °C to give $Co_2(CO)_4[\eta^2,\eta^2,\eta^1,\eta^1\text{-}(Z)\text{-}Ph_2PC(Ph){=}(Ph)C\text{-}\overline{C=C(PPh)_2C(O)OC(O)}]$ (**10**) while the compound **11** affords the zwitterionic hydrocarbyl complex $Co_2(CO)_4[\eta^2,\eta^2,\eta^1,\eta^1\text{-}(Z)\text{-}Ph_2PC(Ph){=}(Ph)C\text{-}\overline{C=C(PPh)_2C(O)OC(O)}]$ (**13**) by a regioselective attack of one of the PPh_2 moieties on the terminal alkyne carbon.

The redox properties of **8**, **9**, and **10** have been examined by cyclic voltammetry. The nature of the HOMO and LUMO levels in **8** and **9** has been determined by extended Hückel MO calculations, the results of which are discussed with respect to the redox chemistry.

The reactivity of **13** with PMe_3 has been examined. The addition of

PMe_3 to **13** leads to CO insertion to afford the novel binuclear complex $Co_2(CO)_3(PMe_3)[\mu\text{-}\eta^2,\eta^2,\eta^1,\eta^1\text{-}Ph(CO)C{=}C(H)PPh_2\overline{C{=}C(PPh_2)C(O)OC(O)}]$ (**14**) in quantitative yield.

All new complexes have been fully characterized by IR and NMR spectroscopies. The solid-state structures of **2-11**, **13**, and **14** have been determined by single crystal X-ray diffraction analyses.

ACKNOWLEDGMENTS

The author wishes to express his sincere gratitude to Professor Michael G. Richmond for his kind guidance, never-ending encouragement, assistance in directing the described research, and serving as the chairman of my advisory committee. I am especially grateful to Dr. Richmond for his model role as a professor and researcher, his efforts in stressing new knowledge, and his insistence for academic excellence, all of which are benefits that will assist me in my future endeavors. Dr. Simon G. Bott is acknowledged for his assistance with all of the X-ray crystallographic structures. Drs. W. E. Acree, Jr, M. Schwartz, R. W. Bates, and D. A. Kunz are thanked for serving on my advisory committee. The help given to me by my colleagues, both graduate and undergraduate, has also been appreciated.

I am very grateful to my wife, Xiaohua, for her support and encouragement throughout the years.

Finally, I wish to thank the University of North Texas for support in the form of a teaching assistantship and the Robert A. Welch Foundation for financial support in the form of a research assistantship.

TABLE OF CONTENTS

LIST OF TABLES

LIST OF FIGURES

CHAPTER I

INTRODUCTION

The chemistry of transition-metal complexes and their phosphine-substituted derivatives has been extensively investigated. A diverse group of tertiary phosphines has been used widely in the field of organometallic chemistry to stabilize metal-hydrogen, metal-carbon, and metal-olefin bonds. Such phosphine ligands appear to be extremely versatile in their ability to stabilize a wide variety of metals in a wide variety of oxidation states. By changing the substituent groups, one can alter the tertiary phosphine's ability to influence the activity, selectivity, and stability of a catalytic system via electronic and/or steric considerations. Six areas of organometallic chemistry are presented in this dissertation. They encompass the areas of (1) P-C bond cleavage reactions involving the bma-substituted complexes $PhCCo_3(CO)_7(bma)$ and $Co_2(CO)_4(bma)(\mu\text{-}PhC{\equiv}CPh)$ [where bma = bis(di-phenylphosphino)maleic anhydride]; (2) the reversible chelate-to-bridge bma ligand exchange reactions in the tricobalt cluster $PhCCo_3(CO)_7(bma)$ and the dinuclear complexes $Co_2(CO)_4(bma)(\mu\text{-}PhC{\equiv}CR)$ (R = H, Ph); (3) phosphido ligand mediated polyhedral cluster expansion and ligand substitution reactivity in the trinuclear cobalt cluster $Co_3(CO)_6[\mu_2\text{-}\eta^2,\eta^1\text{-}C(Ph)C{=}C(PPh_2)C(O)OC(O)](\mu_2\text{-}PPh_2)$; (4) the formation of the zwitterionic hydrocarbyl complex by intramolecular phosphine attack on a coordinated alkyne ligand in the dinuclear complex $Co_2(CO)_4(bma)(\mu\text{-}PhC{\equiv}CH)$; (5) CO insertion reactivity in the dinuclear zwitterionic hydrocarbyl complex $Co_2(CO)_4[\mu\text{-}$

$\eta^2,\eta^2,\eta^1,\eta 1$–PhC=C(H)$PPh_2$C=C($PPh_2$)C(O)OC(O)]; and (6) the redox chemistry and the extended Hückel molecular orbital calculations in the dinuclear complexes $Co_2(CO)_4$(bma)(μ-PhC≡CPh) (chelating and bridging isomers) and $Co_2(CO)_4$(μ-PhC≡CPh)[(Z)-Ph_2PCH=CHPPh_2].

A. Tertiary Phosphines and Related Ligands

Tertiary phosphines are the most commonly encountered ancillary ligands associated with organotransition-metal compounds. Many investigations involving transition-metal carbonyl compounds have used phosphines (PR_3) as ligands, because they constitute one of the few series of ligands in which the electronic and steric properties can be altered in a systematic and predictable fashion over a wide range of R groups. Examples of monodentate, bidentate, tridentate, and higher chelating phosphines are well-documented in the literature. [1-3] A list of representive tertiary phosphines and related ligands is shown in Figure 1.1. These ligands exhibit a wide range of steric and electronic effects. For example, PH_3 is very small compared to PCy_3, whereas PF_3 and $(R_FO)_3P$ (R_F is any perfluoroalkyl group) are sufficiently electron withdrawing, which permits them to act as strong π-acids, rivalling the coordination properties of the CO ligand. Bidentate phosphines such as diphos are also commonly employed and they generally lead to the formation of chelated five membered-ring complexes in the case of mononuclear systems. Although most bidentate phosphines hold the phosphine groups in mutually cis positions, certain specially designed bidentate phosphines can keep the two phosphine donors in a trans orientation. Chiral phosphines are also known and they are very important as ligands in the asymmetric hydrogenation of prochiral olefins and other

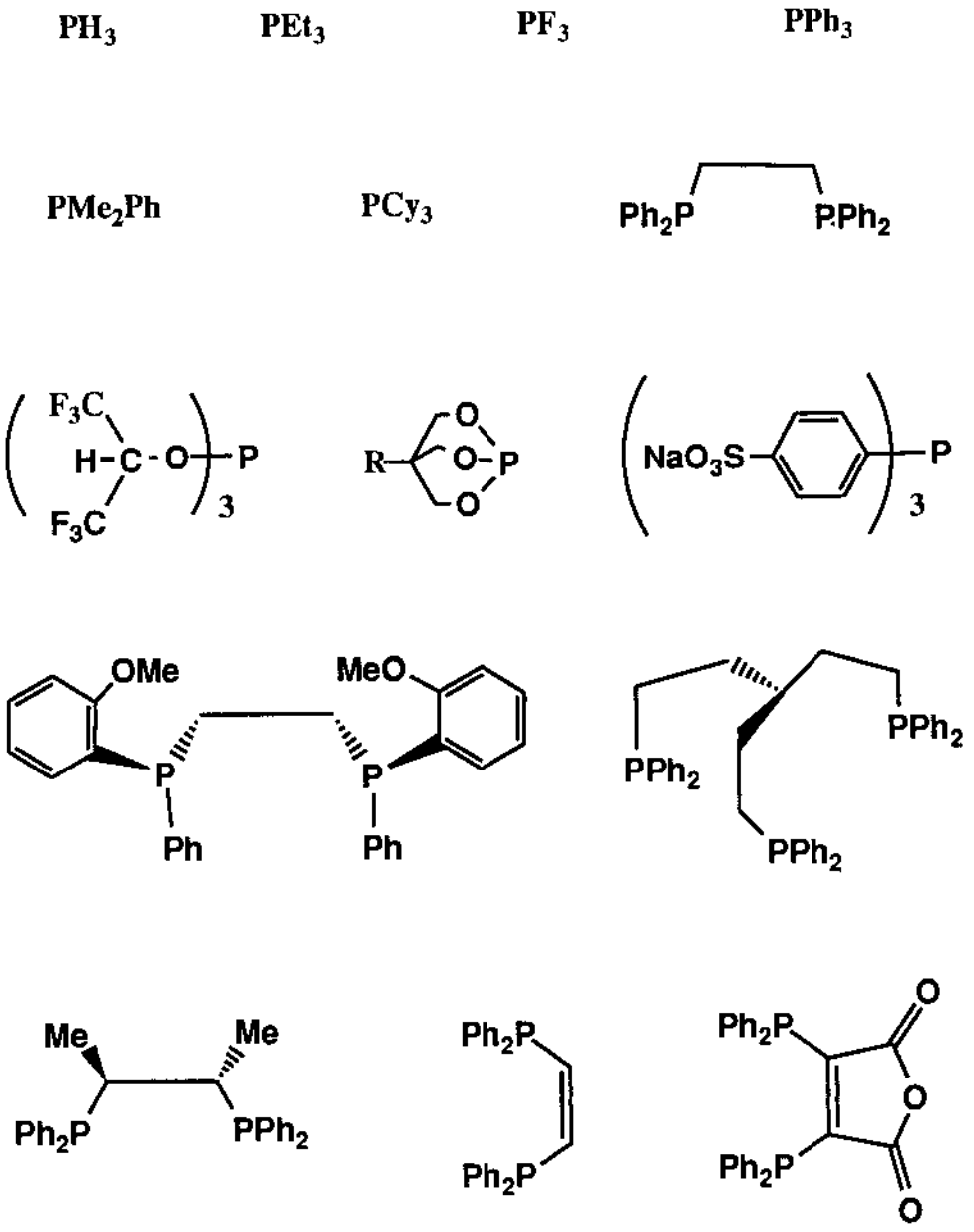

Figure 1.1 Tertiary Phosphines and Related Ligands

synthetic transformations involving asymmetric induction. Recently, water-soluble phosphines, such as sulfonated phosphines, have attracted a large amount of attention since water is a cheap and clean solvent. [4]

Phosphines have a lone-electron pair on the central atom that can be donated to metal. However, they are also π acceptors. In the case of the CO ligand, it has long been recognized that it is the π* orbitals that accept electron density from the metal. In the case of PR_3 ligands, it has been suggested that the σ* orbital of the P-R bonds plays the role of an acceptor orbital (Figure 1. 2). [5,6] Figure 1.2 reveals that as the P group becomes more electron rich, the orbital that the R fragment uses to bond to phosphorus becomes more stable. This implies that σ* orbital of the P-R bond also becomes more stable. At the same time, the phosphorus contribution to σ* increases, so does the size of σ* lobe that points toward the metal. Both of these factors make the σ* more accessible for back donation. The final order of increasing π-acceptor character is :

$$PMe_3 < PAr_3 < P(OMe)_3 < P(OAr)_3 < P(NR_2)_3 < PCl_3 < CO < PF_3$$

The dependence of the electronic effect of various PR_3 ligands on the nature of the R group has been quantified by Tolman, [7] who compared the ν (CO) frequencies of a series of complexes of the type $LNi(CO)_3$, containing different PR_3 ligands. The stronger donor phosphines increase the electron density on Ni, which passes some of this increased electrondensity along to the CO's by π backbonding, which in turn lowers ν (CO). Tolman has also quantified the steric effect of phosphines by using the concept of the cone angle. [7] This is obtained by taking a space-filling model of the $M(PR_3)$ group, folding back the R substituents away from the metal as far as they will go, and measuring the apex of the cone at the metal. Table 1.1 summarizes the cone

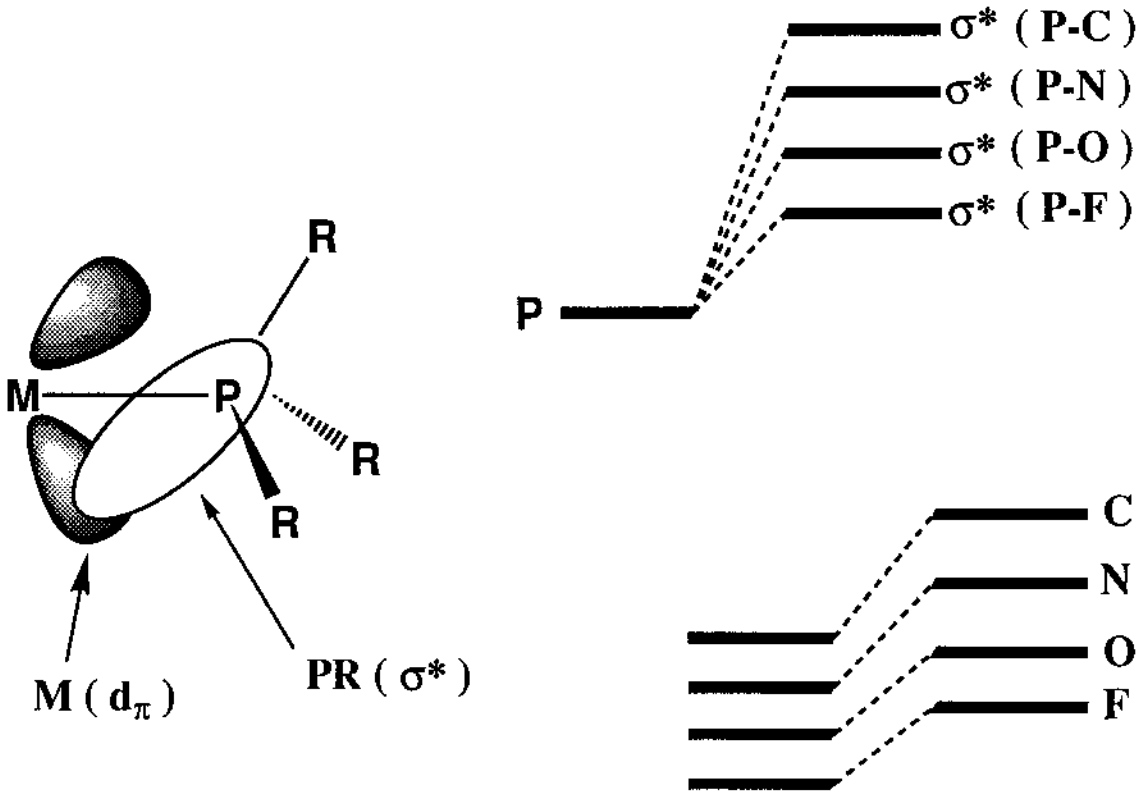

Figure 1.2 The σ* orbitals of the P-R bond play the acceptor role in metal complexes of phosphorus ligands. As the atom attached to phosphorus becomes more electronegative, the empty σ* orbitals of the P-X bond move to lower energy and become more accessible; the PX_3 molecule, therefore, becomes a better acceptor from the metal.

angles of phosphine ligands. [1-3]

The steric bulk of phosphine ligands is their most important structural property. Bulky tertiary phosphines such as triphenylphosphine distort the surrounding ligands and shield the metal, thus, markedly affecting the chemistry of phosphine-substituted metal complexes. Bulky phosphines also tend to bind trans to one another. [8] The presence of several bulky phosphine ligands in the same metal coordination sphere can cause deviations from an idealized coordination geometry, which facilitates ligand dissociation. [8] One must be cautious in the separation of steric and electronic effects since they are often interrelated in transition-metal phosphine complexes.

The use of ^{31}P NMR spectroscopy has proved to be the most important method for studying organometallic complexes, though the underlying theory for explaining chemical shift values associated phosphine complexes is poorly understood. [9,10] The ^{31}P nucleus has a spin of $I = 1/2$, is 100% abundant, and displays moderate NMR sensitivity. ^{31}P NMR data are quite useful for fingerprinting compounds and for distinguishing between related compounds. For example, the size of different phosphine chelate rings can be accessed, and unidentate and bidentate coordination of diphosphines can be easily determined. [9,10] Moreover, the stereochemistry of many metal-phosphine complexes can be deduced from the phosphorus-phosphorus coupling constants, because trans phosphines display a larger coupling constant than cis phosphines. The ^{31}P NMR information from both chemical shift and coupling constants is often used to determine the geometry of many complexes. [9,10]

Table 1.1 Cone Angles of Tertiary Phosphine Ligands

Ligands PR_3	Cone Angle Θ°
PH_3	87
$P(OCH_2)_3CR$	101
PH_2Ph	101
PF_3	104
$P(OMe)_3$	107
PMe_3	118
PMe_2Ph	122
$PPh_2CH_2CH_2PPh_2$	123
PEt_3	132
PPh_3	145
$PPh_2(t\text{-}Bu)$	157
PCy_3	170
$PPh(t\text{-}Bu)_2$	170
$P(t\text{-}Bu)_3$	182
$P(C_6F_5)_3$	184
P(mesityl)$_3$	212

B. Phosphorus Ligands Other than Phosphines

In addition to the well-known trivalent phosphines, other valences of phosphorus have been developed. [11] The chemistry of these other phosphorus ligands represents a rapidly growing research area which combines the chemistry of organotransition metals with that of the main-group elements. Figure 1.3 outlines a variety of phosphorus ligands that exhibit different valences. Most of these ligands are not stable unless they are bound to a metal atom. Sometimes these phosphorus ligands are amphoteric, and as such, can confer upon the metal a different formal oxidation state, coordination geometries, and coordination numbers.

Compared to simple tertiary phosphines, phosphorus ligands such as phosphides and phosphinidenes are much more reactive. Electrocyclic reactions and the addition of both electrophiles and nucleophiles have been observed when these ligands are coordinated to a metal. [11] The phosphido (or phosphenium) ligand has been increasingly explored as an ancillary ligand in organometallic compounds. This ligand can exist in either one of two discrete amphoteric states: (1) as a formally positive "phosphenium" ligand and (2) as a formally negative "phosphido" ligand. The former has a double bond between the metal and the phosphorus atoms, whereas the latter has a lone-electron pair on the phosphorus atom (Figure 1.4). Phosphenium complexes have a planar geometry about the P atom and a short M-P bond, indicating $d\pi$-$p\pi$ double-bond character. The phosphido complexes known exhibit a pyramidal geometry at the phosphorus atom and a long M-P bond (usually longer than that of a tertiary phosphine complex), which indicate the presence of a lone-electron pair on the phosphorus atom. The lone-electron pair on the phosphido ligand is stereo-chemically active,

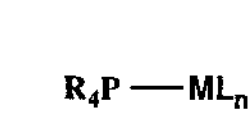

Metallated Phosphorane

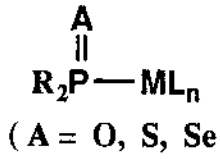

(A = O, S, Se)

Metallated P (V)

Phosphido or Phosphenium

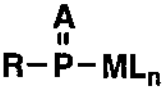

(A = O, NR, CR_2, PR)

Metallated P (III)

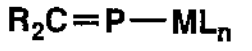

Metallated Phosphaalkene

Phosphinidene

Phosphide

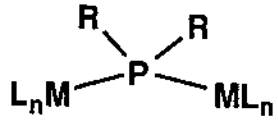

μ_2-Phosphido

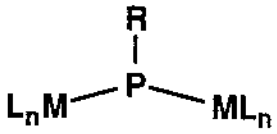

μ_2-Phosphinidene

(planar P)

μ_2-Phosphinidene

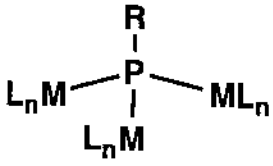

μ_3-Phosphinidene

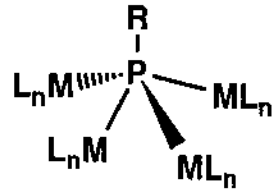

μ_4-Phosphinidene

Figure 1.3 Phosphorus Ligands Other Than Tertiary Phosphines

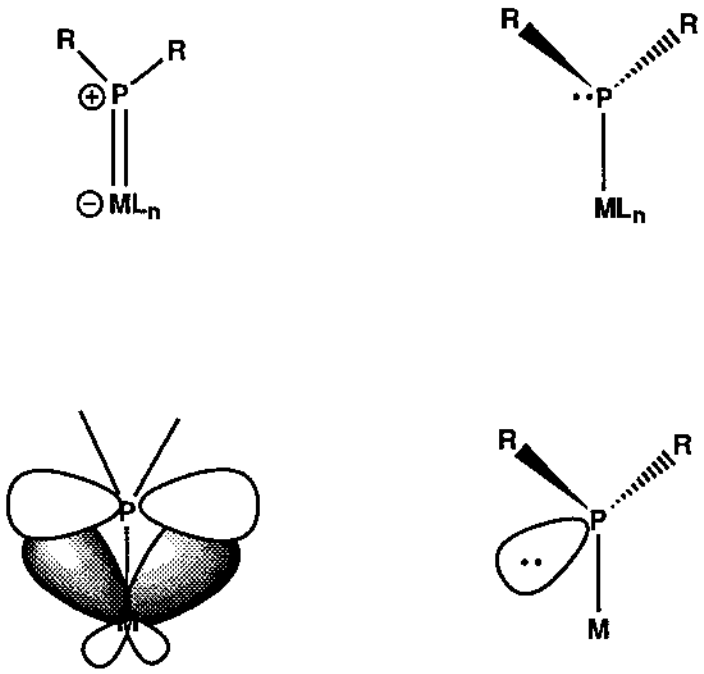

Figure 1.4 Phosphenium and Phosphido
(left) (right)

since it assumes a conformational position orthogonal to the metal HOMO.[12]

For the purpose of oxidation-state formalism, the phosphenium fragment bears a formal positive charge, whereas the phosphido fragment bears a formal negative charge. Both are formal two-electron donors. Conversion of the former to the latter results in a formal two-electron oxidation of the coordinated metal and should create a vacant coordination site. This situation is similar to that of the nitrosyl group, which is the classic case of an amphoteric or non-innocent ligand. [13] Terminal phosphido ligands are very reactive. In the pyramidal form the lone-electron pair on

the phosphorus can be alkylated, protonated, coordinated to another metal or combined with an oxidizing agent. [11]

C. Catalyst Deactivation by Transition-Metal-Mediated Cyclometallation and Phosphorus-Carbon Bond Cleavage

Tertiary phosphines and other phosphorus ligands have been widely used in organometallic chemistry, on the basis of the belief that tertiary phosphine ligands have good thermal stability and do not themselves undergo chemical reactions under common catalysis conditions. Related to this belief, special catalysis attention has been given to a variety of polydentate phosphines, arsines, and other similar ligands. Polydentate ligands have the ability to maintain the integrity of polymetallic cores and to ensure that possible metal-metal bond scission might be reversible in cluster-mediated catalysis. [11d,14-16]

It was recognized many years ago that a metal can react with an aryl or alkyl carbon-hydrogen bond of a phosphorus ligand to form a metal-carbon bond. Trofimenko [17] first introduced the term "cyclometallation" to describe reactions in which a ligand undergoes an intramolecular metallation with concomitant formation of a chelated ring containing a metal-carbon bond. For metallations of phenyl-substituted ligands the term "ortho metallation" has been used and through the years the terms have been used interchangeably (Equation 1.1). However, such cyclometallation reactions were considered to be trivial since they were found to be reversible and the catalytic activity was not destroyed in hydrogenation processes. [18]

It is now clear that many tertiary phosphine metal complexes are chemically reactive and liable with respect to carbon-phosphorus bond

scission, reactivity which is dependent upon the specific reaction conditions.[19] A striking example of a transition-metal-mediated P-C bond cleavage reaction is that between $Os_3(CO)_{12}$ and PPh_3 (1 : 2 ratio) in

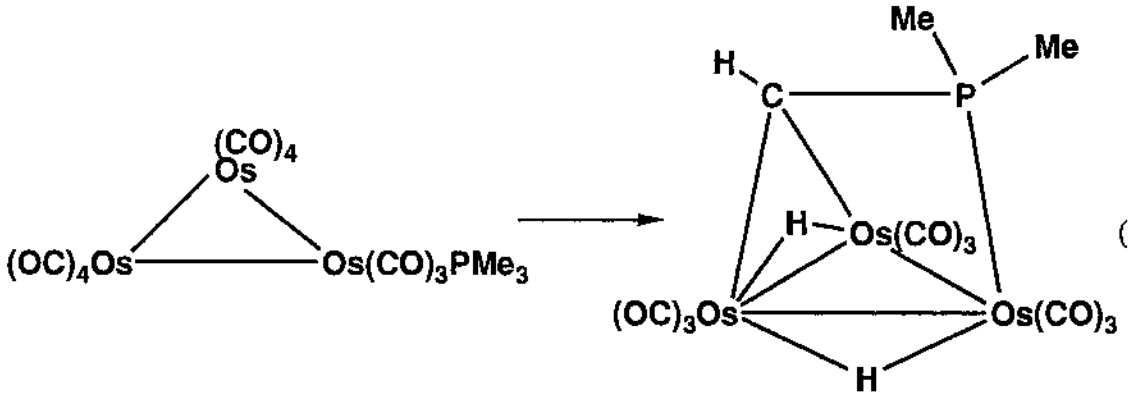

(1.1)

refluxing xylene. Nine different products derived from both cyclometallation and P-C bond cleavage pathways have been isolated and fully characterized by single-crystal X-ray diffraction analyses. [20] In the current literature, many P-C bond cleavage reactions were found by first synthesizing the desired phosphine complexes and then studying their thermolysis reactions in various solvents. Among the complexes which have been investigated, the Iron, [19-44] Cobalt, [19,45-55] and Nickel [19,56-58] subgroups have attracted the most attention.

The cleavage of the P-Ph bond in R'R''P-Ph is one of the commonly observed pathways in P-C bond scission reactions. [19,59] This usually leads to phosphido-bridged derivatives, in addition to benzene, [25,53] benzyne, [21,35] benzaldehyde, [53,60] or biphenyl. [51,53] The intermediates involved in these reactions have been claimed to be σ-phenyl-μ-dialkylposphido derivatives, but very few such complexes have been isolated and characterized. Cabeza and co-workers have recently prepared an η^1-aryl-bridged triruthenium

cluster complex by treating $[Ru_3(\mu\text{-}H)(\mu_3\text{-ampy})(PPh_3)_2(CO)_7]$ (ampy = 2-amino-6-methylpyridinate) with H_2 gas in toluene at 110 °C. They found that both triphenylphosphine ligands in $[Ru_3(\mu\text{-}H)(\mu_3\text{-ampy})(PPh_3)_2(CO)_6]$ underwent a P-C bond scission to give the η^1-phenyl-bridged derivative $[Ru_3(\mu\text{-}Ph)(\mu_3\text{-ampy})(PPh_2)_2(CO)_6]$. [44] The interaction of the η^1-bridging-phenyl group with the trimetallic fragment has been examined by using extended Hückel molecular orbital calculations. [44] Carty and co-workers have also carried out extensive investigations on the reactions of metal clusters with a series of phosphinoacetylene ($Ph_2PC{\equiv}CR$) ligands and demonstrated the ease by which the Ph_2P-C(alkyne) bond undergoes bond scission at a variety of metal centers. The observed C-P bond cleavage reactivity depends on the hybridization of carbon atom of the phosphine ligand, following the order P-C (sp) > P-C (sp^2) > P-C (sp^3). [22] The cleavage of the P-C (sp) bond of the phosphine-acetylene ligand is facile and in certain circumstances occurs under ambient conditions. Examples of P-C (sp^3) cleavage were rare until several cases were recently reported. [38,58] The data on the effect of substituents exhibit a trend for PR_3 (R = P-C_6H_4X) decomposition as a function of the X group: CF_3 > Cl > Me > OMe. [19,53] It is seen that the P-C bond cleavage is enhanced by the presence of electron-withdrawing substituents and inhibited by electron-donating substituents. The theoretical aspects for the shift of an alkyl or aryl group from a coordinated phosphine to a 16-electron d^8 metal center have been examined by Hoffmann and co-workers. They concluded that such migrations are symmetry allowed and thermodynamically accessible. [61] Little is known about the thermodynamic stability of the starting materials or reaction products of phosphorus-carbon activation processes. Estimation of the thermodynamic

stability of the P-C bond comes from the bond dissociation energy of triethylphosphine. Smith and Patrick [62] have conducted low-pressure pyrolysis studies on PEt_3 and derived a $\Delta H^{\neq}$ of 68 ± 2 kcal/mol. This can be compared to values of 104, 102, 88, and 84 kcal/mol for H-H, CH_3-H, CH_3-OH, and CH_3-CH_3 bonds, respectively. All evidence currently points to a P-C "oxidation addition" to the metal (Equation 1.2), which is considered to be the critical step for the P-C bond cleavage sequence. [19,45,55] Although some

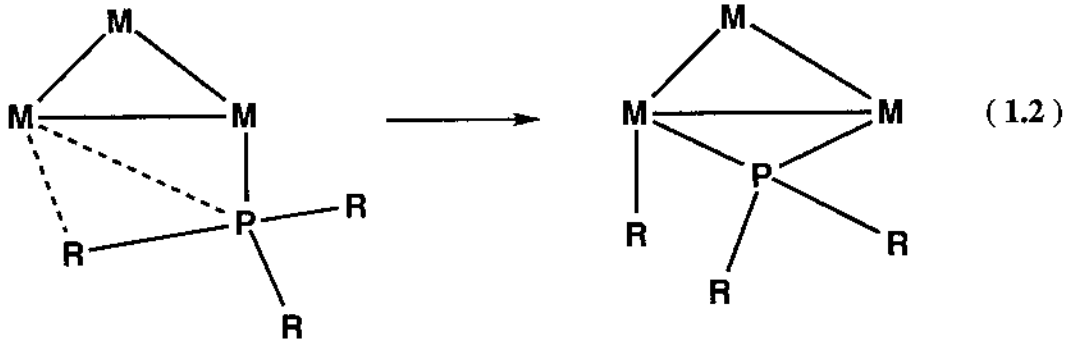

(1.2)

plausible mechanisms have been proposed for P-C cleavage in hydroformylation and hydrogenation, [19,53] only very limited data can be

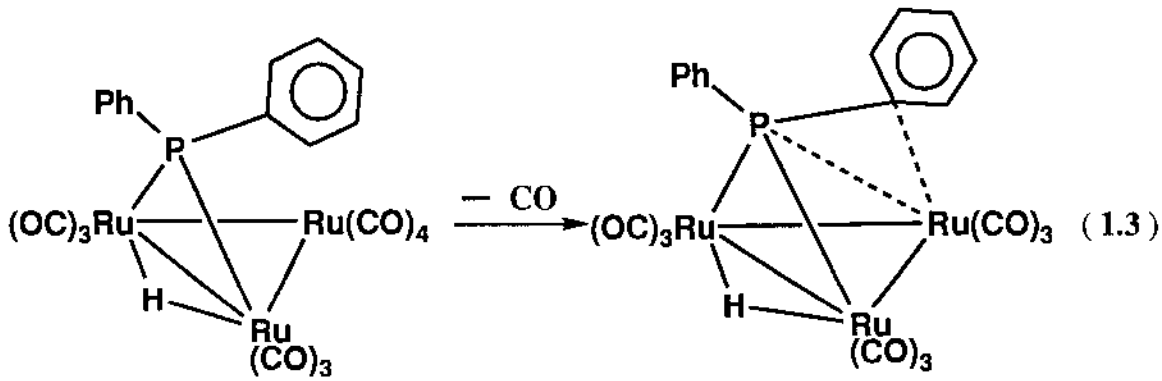

(1.3)

directly related to the key P-C bond oxidation step. Carty and co-workers [19,27] observed a facile reduction of the μ-PPh_2 group in $Ru_3(CO)_{10}(\mu_2\text{-}H)(\mu_2\text{-}PPh_2)$ via an intermediate electron-deficient hydride, which contains a weak P-Ph interaction with a Ru atom. This metal-ligand interaction provides a unique view of an intermediate stage in P-C bond activation and cleavage (Equation 1.3).

D. Phosphines as Nucleophiles and Formation of Zwitterionic Species

Tertiary phosphines can also serve as neutral nucleophiles. Tertiary phosphines can readily add to unsaturated hydrocarbon ligands in cationic complexes such as the cyclohexadienyl complex $[Fe(CO)_3(C_6H_7)][BF_4]$, [63] the alkene complex $[Fe(CO)_2(C_5H_5)(C_2H_4)][BF_4]$, [64] and the arene complex $[Fe(C_6H_6)_2][PF_6]_2$ [65] to give adducts in which the positive charge is localized at the phosphonium substituent on the hydrocarbon ligand. The electron-withdrawing properties of the metal atom in each cation render the carbon atom of the polyene electrophilic, reversing the normal reactivity of the free organic ligand.

It is now clear that tertiary phosphines can also attack neutral complexes to afford zwitterionic species. Carty [66-79], Deeming, [80-84] and others [85-87] have reported numerous mono-, di-, and trimetallic zwitterionic species by adding various nucleophiles, including phosphines, to correspondent neutral complexes. As a C_2 hydrocarbyl with the highest degree of unsaturation and unsurpassed versatility as a bridging ligand, acetylide ligands have received the most attention. The reactivity patterns for these multi-bound ligands have been established. The chemistry of μ_3-η^2-acetylides toward nucleophiles, which has been studied extensively by

Deeming and co-workers, [82] is dominated by attack at C_α, although reaction at C_β has been observed (Equation 1.4). Semiempirical CNDO calculations have indicated that the regiospecificity observed in these reactions is charge controlled. [88] Edge-bridging μ_2-η^2-acetylides also have a rich chemistry with nitrogen, phosphorus, and carbon nucleophiles. Seyferth's group [86] has

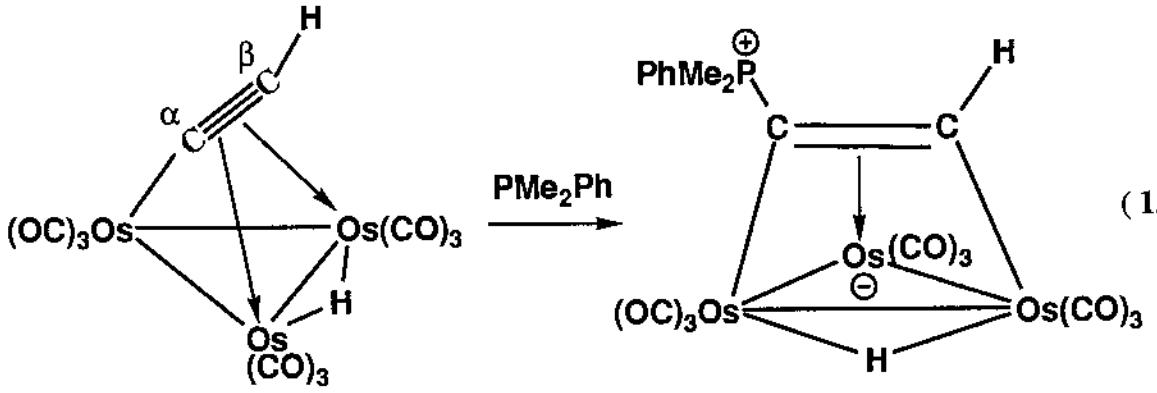

(1.4)

reported similar reactivity for the thiolate-bridged acetylides $Fe_2(CO)_6(\mu_3$-η^2-C≡CR′)(μ-SR). In these systems, nucleophiles can add at the β–carbon of the acetylide to form a one-carbon bridged product, or at the acetylide α–carbon atom to form a two carbon bridge (Equation 1.5). [69] The reactivity

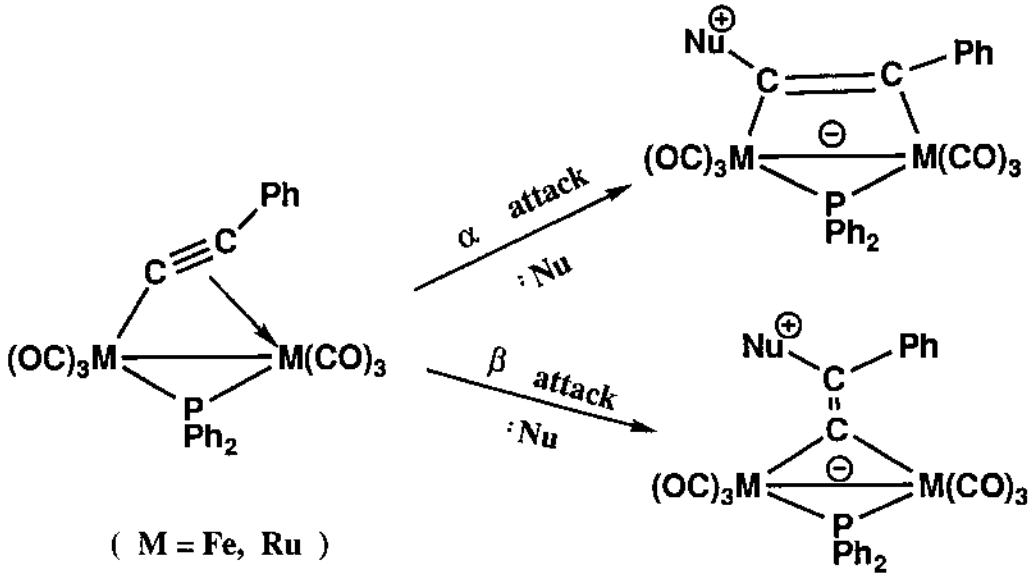

(M = Fe, Ru)

(1.5)

patterns for μ-η¹:η²-allenyl complexes have also been established. Reaction of the bimetallic allenyl complex $Ru_2(CO)_6$ (μ-η¹:η²-PhC=C=CH_2) with carbon, nitrogen, and phosphorus nucleophiles has led to the formation of dimetallacyclopentanes and dimetallacyclopentenes (Equation 1.6). [79] Carty has summarized the ^{13}C NMR chemical shift data for several classes of zwitterionic hydrocarbyl-bridged dimetallic compounds and used the data to

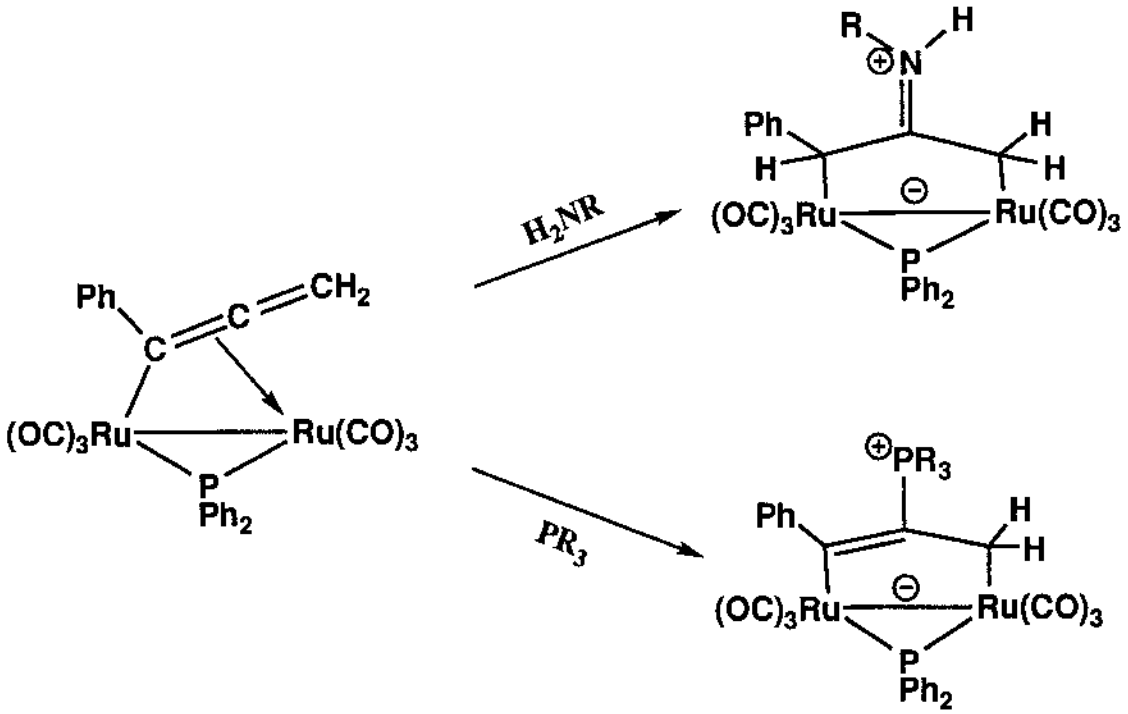

(1.6)

ascertain the amount of carbene character in various types of two-carbon bridges. [67]

In contrast to the coordinated acetylide chemistry, examples of PR_3 attack on a coordinated alkyne ligand to afford a zwitterionic complex that contains a μ-η²,η¹- hydrocarbyl moiety are rare. The only known complex involves the reaction between CpRh(CO)(PMe_3) and $Os(CO)_4$(η²-CH≡CH), which yields $CpRhOs(CO)_3$(μ-CO)[μ-η²,η¹-HCCH(PMe_3)], presumably as a result of an intermolecular PMe_3 attack on the acetylide ligand (Equation 1.7).

[90] Prior to 1994, there was no precedent in the literature for an intra-molecular phosphine attack on a coordinated alkyne ligand (vide infra).

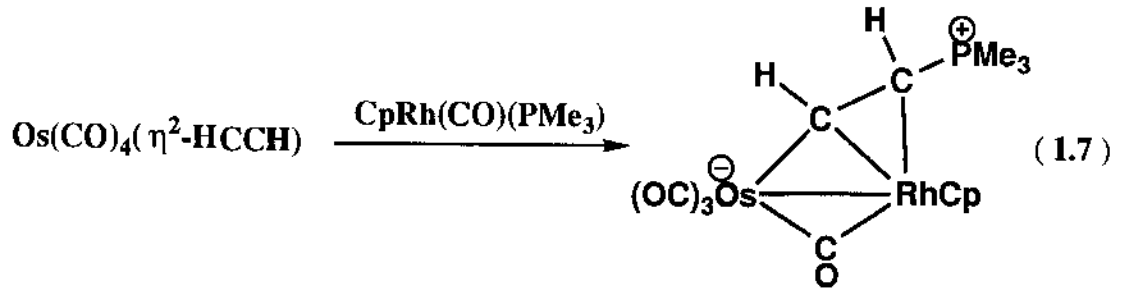

(1.7)

The formation of zwitterionic species by PR_3 attack on a coordinated alkyne is remarkably facile. In most cases, the zwitterions are air-stable and can be prepared in high yields. The fact that tertiary phosphines can undergo the P-C bond cleavage in certain circumstances, coupled with the formation of zwitterions by PR_3 nucleophilic attack on coordinated ligands, may limit the usefulness of phosphines in technological applications involving homogeneous and heterogeneous catalysts.

E. A Novel P-C Bond Cleavage Reaction Between $PhCCo_3(CO)_9$ and Bis(diphenylphosphino)maleic Anhydride (bma)

As one of my beginning practice projects, the reaction between $PhCCo_3(CO)_9$ and the bidentate phosphine ligand bis(diphenylphosphino) maleic anhydride (bma) was examined as part of my interest in the synthesis and reactivity of polynuclear clusters bearing redox-active phosphine ligands. The bma ligand is unique on the basis of the work of Fenske [91] and Tyler [92], who have demonstrated that this ligand assists in the stabilization of

mononuclear 19-electron complexes through electron delocalization with the low-lying π^* orbital of the phosphine ligand. Thus, the initial plan was to prepare the cluster $PhCCo_3(CO)_7(bma)$, which would allow for the examination of the redox chemistry and stability of the corresponding one-electron reduction product $[PhCCo_3(CO)_7(bma)]^{\bullet-}$. The effect of the bma ligand on the redox properties of the cluster can be easily assessed by a comparison with the extensive electrochemical data of the known phosphine-substituted $PhCCo_3(CO)_7P_2$ clusters.[93] However, when the reaction between $PhCCo_3(CO)_9$ and bma was initially examined in toluene solvent at 75 °C, the expected $PhCCo_3(CO)_7(bma)$ cluster was not observed, and it was subsequently shown that $Co_3(CO)_6[\mu_2\text{-}\eta^2,\eta^1\text{-}C(Ph)C{=}C(PPh_2)C(O)C(O)](\mu_2\text{-}PPh_2)$ was present (Equation 1.8).

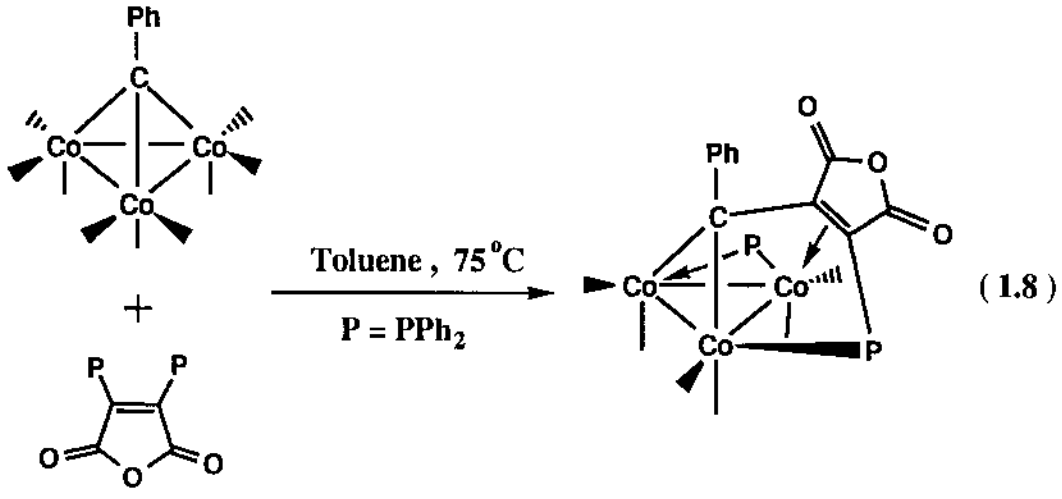

(1.8)

The novelty of this cluster resides in the facile P-C bond cleavage observed in the bma ligand and activation of the μ_3-benzylidyne capping ligand in $PhCCo_3(CO)_9$ and its conversion to a μ_2-benzylidene ligand. The

transformation of the μ_3-benzylidyne capping ligand to a μ_2-benzylidene ligand, coupled with P-C bond cleavage during the thermal substitution reaction condition, is unprecedented in this type of cluster. Thus, an effort was made to explore the full details of the above P-C cleavage reaction. The intermediate tricobalt cluster $PhCCo_3(CO)_7$(bma) involved in the formation of $Co_3(CO)_6[\mu_2\text{-}\eta^2,\eta^1\text{-}C(Ph)\overline{C=C(PPh_2)C(O)OC(O)}](\mu_2\text{-}PPh_2)$ has been successfully prepared from the reaction between $PhCCo_3(CO)_9$ and bma in either THF or CH_2Cl_2 by Me_3NO-promoted oxidative decarbonylation. A kinetic investigation for the transformation from $PhCCo_3(CO)_7$(bma) to $Co_3(CO)_6[\mu_2\text{-}\eta^2,\eta^1\text{-}C(Ph)\overline{C=C(PPh_2)C(O)OC(O)}](\mu_2\text{-}PPh_2)$ has been undertaken and the rate constants and activation parameters determined. This kinetic study represents the first kinetic investigation on a P-C bond scission process in an organometallic complex. The corresponding tricobalt cluster $PhCCo_3(CO)_7$[(Z)-$Ph_2PCH=CHPPh_2$], which is expected to be structurally similar yet electronically different compared to the cluster $PhCCo_3(CO)_7$(bma), has also been synthesized and studied under conditions analogous to $PhCCo_3(CO)_7$(bma) in order to highlight reactivity differences between them.

F. Phosphido-Ligand-Mediated Polyhedral Cluster Expansion and PMe_3 Ligand Substitution in the Tricobalt Cluster $Co_3(CO)_6[\mu_2\text{-}\eta^2,\eta^1\text{-}C(Ph)\overline{C=C(PPh_2)C(O)OC(O)}](\mu_2\text{-}PPh_2)$

The ligand substitution behavior of multinuclear metal carbonyl complexes with metal-metal bonds has been an important topic in transition-metal organometallic chemistry. Ligand substitution studies at multinuclear metal complexes are not only of academic interest but are of significance in providing a detailed analysis of homogeneous catalytic processes. The three

possible intimate mechanisms for ligand substitution processes in mononuclear metal complexes have been classified as (a) dissociative (D), (b) associative (A), and (c) interchange (I). [94] The interchange mechanism may be divided into I_a and I_b processes, depending on the binding strength of both the entering and leaving ligands to the metal in the transition state. In addition to these substitution pathways, Darensbourg has distinguished that polynuclear metal compounds can have other mechanisms which include metal-metal bond dissociation with and without cluster fragmentation. [95,96]

The dissociative mechanism is one of the most common pathways for ligand substitution reactions, with many examples having been reported in the current literature. For example, the ligand substitution reaction of $Os_3(CO)_{11}(NCMe)$ with phosphines has been shown to be quantitative, resulting in replacement of the CH_3CN ligand. [97] The rate constants were found to be independent of both the nature and concentration of the entering phosphine ligands. The trinuclear ruthenium hydride anion $HRu_3(CO)_{11}^-$ undergoes facile CO substitution with PPh_3 in THF. [98] At a given [PPh_3], k_{obsd} decreased with increasing [CO], suggesting a reaction pathway proceeding by CO dissociation.

While the associative mechanism is not common, it may hold for electron-poor metal clusters. For example, the triplatinum clusters $Pt_3(CO)_3L_3$ (L = phosphine) have been found to undergo a facile ligand substitution reaction with phosphines. [99] In these platinum clusters each metal center formally contains 16 electrons. The reaction rate was found to be dependent on both the nature and concentration of the incoming phosphine ligand. Basolo has stated the following rule : substitution reactions

involving 18-electron transition-metal organometallic compounds may proceed by an associative mechanism provided that the metal complex can delocalize a pair of electrons onto one of its ligands like NO, cyclopentadienyl, or arenes. [100]

The polyhedral expansion of certain clusters during ligand addition reactions has been documented. [11c,101,102] According to the current literature, the majority of cluster opening reactions involves ligand attack at a metal center and assistance from one or more of the ancillary CO groups. Here the formal transfer of the two electrons in the ruptured metal-metal bond is ultimately redistributed about the cluster polyhedron, giving rise to coordinatively saturated metal centers. CO loss and reformation of the metal-metal bond complete the overall sequence for the net substitution of CO by the incoming ligand in many transition-metal clusters. [102]

In this dissertation, data will be presented on the addition reaction of PMe_3 to the arachno cluster $Co_3(CO)_6[\mu_2\text{-}\eta^2,\eta^1\text{-}C(Ph)\overline{C=C(PPh_2)C(O)OC(O)}](\mu_2\text{-}PPh_2)$, which proceeds to give the hypho cluster $Co_3(CO)_5(\mu\text{-}CO)(PMe_3)[\mu_2\text{-}\eta^2,\eta^1\text{-}C(Ph)\overline{C=C(PPh_2)C(O)OC(O)}](\mu_2\text{-}PPh_2)$. The addition reaction is accompanied by cleavage of one of the Co-Co bonds in $Co_3(CO)_6[\mu_2\text{-}\eta^2,\eta^1\text{-}C(Ph)\overline{C=C(PPh_2)C(O)OC(O)}](\mu_2\text{-}PPh_2)$ and a formal change in how the μ_2-phosphido ligand distributes its three available bonding electrons to the ligated cobalt centers in $Co_3(CO)_5(\mu\text{-}CO)(PMe_3)[\mu_2\text{-}\eta^2,\eta^1\text{-}C(Ph)\overline{C=C(PPh_2)C(O)OC(O)}](\mu_2\text{-}PPh_2)$. This flexibility in the ligand donation properties of the μ_2-phosphido group is believed to be a key factor in promoting the observed polyhedral cluster expansion. There is no precedent in the literature for the phosphido ligand assisted redistribution of electron density in a ligand substitution reaction involving a tricobalt cluster. The interception and

characterization of $Co_3(CO)_5(\mu\text{-}CO)(PMe_3)[\mu_2\text{-}\eta^2,\eta^1\text{-}C(Ph)\overbrace{C=C(PPh_2)C(O)OC}(O)](\mu_2\text{-}PPh_2)$ as a kinetic product en route to the mono-substituted cluster $Co_3(CO)_5(PMe_3)[\mu_2\text{-}\eta^2,\eta^1\text{-}C(Ph)\overbrace{C=C(PPh_2)C(O)OC}(O)](\mu_2\text{-}PPh_2)$ represent another rare example of metal-metal bond reactivity in a substitution reaction involving a polynuclear system.

G. Reversible Chelate-to-Bridge Ligand Exchange in $Co_2(CO)_4(\mu\text{-}PhC{\equiv}CPh)$(bma) and Alkyne-Diphosphine Ligand Coupling

The reactivity of transition-metal complexes possessing an ancillary alkyne ligand continues to be investigated by a diverse group of researchers. [103] While many metal-alkyne complexes are known, probably the most thoroughly studied class of alkyne complexes is that derived from dicobalt hexacarbonyl, i.e., $Co_2(CO)_6(\mu\text{-alkyne})$. [104] Such complexes have found wide use in various organic transformations. For example, it has been demonstrated that cobalt-complexed propargyl cations function as propargyl cation synthons in carbon-carbon bond formation reactions, [105,106] while the protection of alkynes and the marking of acetylide steroids by the $Co_2(CO)_6$ moiety are routinely employed in organic syntheses [107] and biochemical receptor recognition studies, [108] respectively. Another well-known use of cobalt-alkyne compounds involves the cobalt-mediated ene-yne reaction, otherwise known as the Pauson-Khand reaction. Here complex carbocyclic ring systems are prepared regio- and stereoselectively under relatively mild conditions. [109]

Phosphine ligand substitution in $Co_2(CO)_6(\mu\text{-alkyne})$ has also been extensively studied from both mechanistic and theoretical aspects. [110] In the case of bidentate phosphine ligands both bridged and chelated products of the

form $Co_2(CO)_{6-2n}(\mu\text{-alkyne})(L\text{-}L)_n$ (where n = 1, 2) are observed, with the exact product being dependent on the nature of the phosphine and the mode of dinuclear complex activation. [111] Thermal ligand substitution with the common phosphines dppm and dppe yields the phosphine-bridged alkyne dinuclear compounds, whereas electron transfer catalysis has been successfully utilized to give chelated or bridged dimers with impressive stereochemical control. [112] By comparison, ligand substitution studies with unsaturated diphosphine ligands have received less attention. [113]

The reaction between $PhCCo_3(CO)_9$ and the bidentate phosphine ligand bis(diphenylphosphino)maleic anhydride (bma) initially afforded the expected cluster $PhCCo_3(CO)_7$ (bma). Thermolysis or photolysis of this cluster led to the new cluster $Co_3(CO)_6[\mu_2\text{-}\eta^2,\eta^1\text{-}C(Ph)\overline{C=C(PPh_2)C(O)OC(O)}](\mu_2\text{-}PPh_2)$ as a result of P-C(maleic anhydride) bond cleavage coupled with C(μ-benzylidyne)-C(maleic anhydride) bond reductive elimination. [45,46] On the basis of the isolobal relationship between $PhCCo_3(CO)_9$ and $Co_2(CO)_6(\mu\text{-}PhC{\equiv}CPh)$ [114] and my desire to explore the generality of the bma P-C bond cleavage in different cluster systems, the reaction between $Co_2(CO)_6(\mu\text{-}PhC{\equiv}CPh)$ and bma was also studied. The synthesis and characterization of both the chelating and bridging isomers of $Co_2(CO)_4(\mu\text{-}PhC{\equiv}CPh)$(bma) and the transformation to the P-C bond cleavage product $Co_2(CO)_4[\eta^2,\eta^1,\eta^1,\eta^1\text{-}(Z)\text{-}Ph_2PC(Ph){=}(Ph)C\text{-}\overline{C=C(PPh_2)C(O)OC(O)}]$ have been summarized in this dissertation. The corresponding dinuclear complex $Co_2(CO)_4(\mu\text{-}PhC{\equiv}CPh)$ [(Z)-$Ph_2PCH{=}CHPPh_2$] has also been synthesized and studied under conditions analogous to $Co_2(CO)_4(\mu\text{-}PhC{\equiv}CPh)$(bma) in order to highlight reactivity differences between the two diphosphine-substituted complexes.

H. Intramolecular Phosphine Attack on a Coordinated Alkyne Ligand in $Co_2(CO)_4(\mu\text{-PhC}{\equiv}CH)(bma)$

The thermolysis reaction of $Co_2(CO)_4(\mu\text{-PhC}{\equiv}CPh)(bma)$ in 1,2-dichloroethane results in an initial isomerization to give the corresponding bma-bridged complex; this latter isomer then undergoes an alkyne-diphosphine ligand coupling and formation of $Co_2(CO)_4[\eta^2,\eta^1,\eta^1,\eta^1\text{-(Z)-}Ph_2PC(Ph)=(Ph)C\text{-}\overline{C=C(PPh_2)C(O)OC(O)}]$. [55] However, while examing the reactivity of the corresponding phenylacetylene complex $Co_2(CO)_4(\mu\text{-PhC}{\equiv}CH)(bma)$, a different course of reactivity was observed upon thermolysis. Refluxing a 1,2-dichloroethane solution of $Co_2(CO)_4(\mu\text{-PhC}{\equiv}CH)(bma)$ leads to the formation of the zwitterionic hydrocarbyl complex $Co_2(CO)_4[\mu\text{-}\eta^2,\eta^2,\eta^1,\eta 1\text{–PhC=C(H)PPh}_2\overline{C=C(PPh_2)C(O)OC(O)}]$, in an isolated yield of 70%. The migration of one of the phosphine moieties associated with the bma ligand to the terminal alkyne carbon of the coordinated phenylacetylene ligand has been established by X-ray diffraction analysis. This regioselective transformation gives rise to the first $\mu_2\text{-}\eta^2,\eta^1$–hydrocarbyl ligand complex formed from an intramolecular P-ligand attack on a coordinated alkyne moiety. [115] The full details of the this novel reaction are summarized in this dissertation.

The corresponding dinuclear complex $Co_2(CO)_4(\mu\text{-PhC}{\equiv}CH)[(Z)\text{-}Ph_2PCH=CHPPh_2]$ has also been synthesized and studied under conditions analogous to $Co_2(CO)_4(\mu\text{-PhC}{\equiv}CH)(bma)$ in order to highlight reactivity differences between the two diphosphine-substituted complexes.

The reaction of the zwitterionic hydrocarbyl complex $Co_2(CO)_4[\mu\text{-}\eta^2,\eta^2,\eta^1,\eta^1\text{–PhC=C(H)PPh}_2\overline{C=C(PPh_2)C(O)OC(O)}]$ with PMe_3 has also been investigated. The novel CO insertion product $Co_2(CO)_3(PMe_3)[\mu\text{-}\eta^2,\eta^2,\eta^1,\eta 1\text{–}$

$Ph(CO)C{=}C(H)PPh_2\overline{C{=}C(PPh_2)C(O)OC(O)}$] has been isolated and characterized by spectroscopic methods and X-ray diffraction analysis.

CHAPTER REFERENCES

1. Collman, J. P.; Hegedus, L. S.; Norton, J. R.; Finke, R. G. "Principles and Applications of Organotransition Metal Chemistry," University Science Books, Mill Valley, CA, **1987**, Chapter 2.

2. Clark, H. C. Israel J. Chem. **1976/77**, 15, 210.

3. (a) Levason, W.; McAuliffe, C. A. Acc. Chem. Res. **1978**, 11, 363. (b) Levason, W.; McAuliffe, C. A. Adv. Inorg. Chem. Radiochem. **1972**, 14, 173. (c) McAuliffe, C. A. Ed.; "Transition-Metal Complexes of Phosphorus, Arsenic, and Antimony Ligands," Wiley: New York, **1973**.

4. Darensbourg, D.; Bischoff, C. J. Inorg. Chem. **1993**, 32, 47.

5. Orpen, A. G. J. Chem. Soc., Chem. Commun. **1985**, 1310.

6. (a) Xiao, S.-X.; Trogler, W. C.; Ellis, D. E.; Berkovitch-Yellin, Z. J. Am. Chem. Soc. **1983**, 105, 7033. (b) Morris, R. J.; Girolami, G. S. Inorg. Chem. **1990**, 29, 4167.

7. Tolman, C. A. Chem. Rev. **1977**, 77, 313.

8. (a) Hitchcock, P. B.; McPartlin, M.; Mason, R. Chem. Commun. **1969**, 1367. (b) Bennett, M. J.; Donaldson, P. B.; Inorg. Chem. **1977**, 16, 655.

9. Davies, J. A.; In "The Chemistry of the Metal-Carbon Bond," Hartley, F. R., Ed.; Wiley-Interscience: New York, **1982**, Chapter 21, p880.

10. Pregosin, P. S.; Kunz, R. W. In "NMR Basic Principles and Progress," Springer-Verlag: Heidelberg, **1979**, Vol. 16, p55.

11. (a) Richmond, M. G.; Kochi, J. K. Inorg. Chem. **1986**, 25, 656. (b) Richmond, M. G.; Kochi, J. K. Inorg. Chem. **1986**, 25, 1334. (c) Richmond, M. G.; Kochi, J. K. Inorg. Chem. **1987**, 26, 541. (d) Richmond, M. G.; Kochi, J. K. Organometallics **1987**, 6, 254. (e) Richmond, M. G.; Kochi, J. K. Organometallics **1987**, 6, 777. (f) Edsworth, E. A. V.; Holloway, J. H.; Pilkington, N. J.; Rankin, D. W. H. Angew. Chem., Int. Ed. Engl. **1984**, 23, 630. (g) Baker, R. T.; Krusic, P. J.; Tulip, T. H.; Calabrese, J. C.; Wreford, S. S. J. Am. Chem. Soc. **1985**, 107, 3346. (h) Cowley, A. H.; Norman, N. C. Quashie, S. J. Am. Chem. Soc. **1984**, 106, 5007. (i) Marinetti, A.; Mathey, F. J. Am. Chem. Soc. **1982**, 104, 4484.

(j) Huttner, G.; Muller, H. P.; Frank, A.; Lorenz, H. Angew. Chem., Int. Ed. Engl. **1977**, 16, 482. (k) Burt, J. C.; Schmid, G. J. Chem. Soc., Dalton Trans. **1978**, 1385. (l) Richter, F.; Beurich, H.; Vahrenkamp, H. J. Organomet. Chem. **1979**, 204, C10. (m) Natarajan, K.; Zsolnai, L.; Huttner, G. J. Organomet. Chem. **1981**, 209, 85.

12. Buhro, W. E.; Georgiou, S.; Hutchinson, J. P.; Gladysz, J. A. J. Am. Chem. Soc. **1985**, 107, 3346.

13. (a) McCleverty, J. Chem. Rev. **1979**, 79, 53. (b) Feltham, R. D.; Enemark, J. H. In "Topics in Inorganic and Organometallic Stereochemistry", Wiley: New York, **1981**, 12, 155. (c) Caulton, K. G. Coord. Chem. Rev. **1975**, 14, 317. (d) Enermark, J. H.; Feltham, R. D. Coord. Chem. Rev. **1974**, 13, 339

14. (a) de Boer, J. J.; van Doorn, J. A.; Osborn, J. A.; Masters, C. J. Chem. Soc., Chem. Commun. **1978**, 1005. (b) Masters, C. Adv. Organomet. Chem. **1979**, 17, 61.

15. (a) Arduini, A. A.; Bahsoun, A. A.; Osborn, J. A.; Voelker, C. Angew. Chem., Int. Ed. Engl. **1980**, 19, 1024. (b) Bahsoun, A. A.; Osborn, J. A.; Voelker, C.; Bonnet, J. J.; Lavingne, G. Organometallics **1982**, 1, 1114.

16. (a) Chini, P.; Heaton, B. Top. Curr. Chem. **1977**, 71, 53. (b) Dombek, B. D. J. Am. Chem. Soc. **1980**, 102, 6855. (c) Bor, G.; Dietler, U. K.; Pino, P.; Poe, A. J. Organomet. Chem. **1978**, 154, 301. (d) Vidal, J. L.; Walker, W. E. Inorg. Chem. **1981**, 20, 249. (e) Whyman, R. J. Chem. Soc., Dalton Trans. **1972**, 2294.

17. Trofimenko, S. Inorg. Chem. **1973**, 12, 1215.

18. Parshall, G. W. Acc. Chem. Res. **1970**, 3, 139.

19. Garrou, P. E. Chem. Rev. **1985**, 171 and references therein.

20. (a) Bradford, C. W.; Nyholm, R. S. J. Chem. Soc., Chem. Commun. **1972**, 87. (b) Bradford, C. W.; Nyholm, R. S. J. Chem. Soc., Dalton Trans. **1973**, 529. (c) Deeming, A. J.; Kimber, R. E.; Underhill, M. J. Chem. Soc., Dalton Trans. **1973**, 2589. (d) Deeming, A. J.; Underhill, M. J. Chem. Soc., Dalton Trans. **1973**, 2727.

21. Bruce, M. I.; Shaw, G.; Stone, F. G. A. J. Chem. Soc., Dalton Trans. **1972**, 2094.

22. Carty, A. J. Pure Appl. Chem. **1982**, 54, 113 and references therein. (b) Carty, A. J.; Tayler, N. J.; Smith, W. F. J. Chem. Soc., Chem. Commun. **1979**, 750.

23. Reed, J.; Schultz, A. J.; Pierpoint, C. G.; Eisenberg, R. Inorg. Chem. **1973**, 12, 2949.

24. Foley, H. C.; Finch, W. C.; Pierpoint, C. G.; Geoffroy, G. L. Organometallics **1982**, 1, 1379.

25. Sabo, S.; Chaudret, B.; Gervais, D. J. Organomet. Chem. **1983**, 258, C19.

26. Chaudiet, B. N.; Cole-Hamilton, D. J.; Nohr, R. S.; Wilkinson, G. J. Chem. Soc., Dalton Trans. **1977**, 1546.

27. MacLaughlin, S. A.; Carty, A. J.; Taylor, N. J. Can. J. Chem. **1982**, 60, 88.

28. Patel, V. D.; Taylor, N. J.; Carty, A. J. J. Chem. Soc., Chem. Commun. **1984**, 99.

29. Bergounhou, C.; Bonnet, J.-J.; Fompeyrine, P.; Lavingne, G.; Lugan, N.; Mansilla, F. Organometallics **1986**, 5, 60 and references therein.

30. Gastel, F. V.; MacLaughlin, S. A.; Lynch, M.; Carty, A. J.; Sappa, E. J. Organomet. Chem. **1987**, 326, C65.

31. Doherty, N. M.; Hogarth, G.; Knox, S. A. R.; Macpherson, K. A.; Melchior, F.; Orpen, A. G. J. Chem. Soc., Chem. Commun. **1986**, 540.

32. Bruce, M. I. J. Organomet. Chem. **1990**, 394, 365.

33. Bruce, M. I.; Humphrey, P. A.; Skelton, B. W.; White, A. H.; Williams, M. L. J. Organomet. Chem. **1985**, 394, 365.

34. Bitterer, F.; Brauer, D. J.; Dörrenbach, F.; Stelzar, O. J. Organomet. Chem. **1990**, 399, C4.

35. Knox, S. A. R.; Lloyd, B. R.; Morton, D. A. V.; Nicholls, S. M.; Orpen, G.; Viñas, J. M.; Weber, M.; Williams, G. K. J. Organomet. Chem. **1990**, 394, 385 and references therein.

36. Hogarth, G. J. Organomet. Chem. **1991**, 407, 91.

37. Elliot, D. J.; Holah, D. J.; Hughes, A. N.; Mirza, H. A.; Zawada, E. J. Chem. Soc., Chem. Commun. **1990**, 32.

38. Hogarth, G.; Knox, S. A. R.; Turner, M. L. J. Chem. Soc., Chem. Commun. **1990**, 145 and references therein.

39. Manojlovic-Muir, L.; Brandes, D. A.; Puddephatt, R. J. Organomet. Chem. **1987**, 332, 201.

40. Bruce, M. I.; Horn, Ernst; Shawkataly, O. B.; Snow, M. R.; Tiekink, E. R. T.; Williams, M. L. J. Organomet. Chem. **1986**, 316, 187.

41. Benlaarab, H.; Chaudret, B.; Dahan, F.; Poilblanc, R. J. Organomet. Chem. **1987**, 320, C51.

42. Lugan, N.; Lavingne, G.; Bonnet, J.-J. Inorg. Chem. **1987**, 26, 585.

43. Lu, K. L.; Chen, H. J.; Lu, P. Y.; Li, S. Y.; Hong, F. E.; Peng, S. M.; Lee, G. H. Organometallics **1994**, 13, 585.

44. Cabeza, J. A.; Franco, R. J.; Llamazares, A.; Riera, V.; Pérez-Carreño, E.; Van der Maelen, J. F. Organometallics **1994**, 13, 55 and references therein.

45. Yang, K.; Smith, J. M.; Bott, S. G.; Richmond, M. G. Inorg. Chim. Acta. **1993**, 212, 1.

46. Yang, K.; Smith, J. M.; Bott, S. G.; Richmond, M. G. Organometallics **1993**, 12, 4779 and references therein.

47. Mason, R.; Sotofte, I.; Robinson, S. D.; Uttley, M. F. J. Organomet. Chem. **1972**, 46, C61.

48. Bellon, P. L.; Benedicenti, C.; Caglio, G.; Manassero, M. J. Chem. Soc., Chem. Commun. **1973**, 946.

49. Blickensderfer, J. R.; Knobler, C. B.; Kasez, H. D. J. Am. Chem. Soc. **1975**, 97, 2686.

50. Blickensderfer, J. R.; Kasez, H. D. J. Am. Chem. Soc. **1975**, 97, 2681.

51. Lewin, M.; Aizenshtat, Z.; Blum, J. J. Organomet. Chem. **1980**, 184, 255.

52. Blum, O.; Frolow, F.; Milstein, D. J. Chem. Soc., Chem. Commun. **1991**, 258.

53. Dubois, R. A.; Garrou, P. E.; Lavin, K. D.; Allock, H. R. Organometallics **1986**, 5, 460 and references therein.

54. Benvenutti, M. H. A.; Vargas, D.; Braga, D.; Grepioni, F.; Parisini, E.; Mann, B. E. Organometallics **1993**, 12, 2955.

55. Yang, K.; Bott, S. G.; Richmond, M. G. Organometallics **1994**, 13, in press.

56. Bergamini, P.; Sostero, S.; Traverso, O.; Kemp, T. J. J. Chem. Soc., Dalton Trans. **1989**, 2017.

57. Sommovigo, M.; Pasquali, M.; Leoni, P.; Braga, D.; Sabatino, P. Chem. Ber. **1991**, 124, 97 and references therein.

58. Alcock, N. W.; Bergamini, P.; Kemp, T. J.; Pringle, P. G. J. Chem. Soc., Chem. Commun. **1987**, 235.

59. Shriver, D. F.; Adams, R. D.; Kasez, H. D. "The Chemistry of Metal Cluster Complexes," VCH Publishers: New York, **1990**.

60. (a) Lugan, N.; Lavingne, G.; Bonnet, J.-J.; Réau, R.; Neibecker, D.; Tkatchenko, I. J. Am. Chem. Soc. **1988**, 110, 5369. (b) Abatjoglou, A. G.; Billig, E.; Bryant, D. R. Organometallics **1984**, 3, 923.

61. Ortiz, J. V.; Havias, Z.; Hoffmann, R. Helv. Chim. Acta. **1984**, 67, 1.

62. Smith, G. P.; Patrick, R. Int. J. Chem. Kinet. **1983**, 15, 167.

63. John, G. R.; Kane-Maguire, L. A. P. J. Chem. Soc., Dalton Trans. **1979**, 873.

64. (a) Lennon, P.; Madhavarao, M.; Rosan, A.; Rosenblum, M. J. Organomet. Chem. **1976**, 108, 93. (b) Noth, W. H. Inorg. Chem. **1975**, 14, 1566. (c) Cosslett, L.; Kane-Maguire, L. A. P. J. Organomet. Chem. **1979**, 178, C17.

65. Davis, S. G.; Gelfaud, L. G.; Sweigart, D. A. J. Chem. Soc., Chem. Commun. **1979**, 762. (b) Domaille, D. J.; Ittel, S. D.; Jesson, J. P.; Sweigart, D. A. J. Organomet. Chem. **1980**, 202, 191.

66. Cherkas, A. A.; Hagheri, N.; Carty, A. J.; Sappa, E.; Pellinghelli, M. A.; Tiripicchio, A. Organometallics **1990**, 9, 1887.

67. Cherkas, A. A.; Randall, L. H.; Taylor, N. J.; Mott, G. N.; Yule, J. E.; Guinamart, J. L.; Carty, A. J. Organometallics **1990**, 9, 1677.

68. Wong, Y. S.; Paik, H. N.; Chieh, P. C.; Carty, A. J. J. Chem. Soc., Chem. Commun. **1975**, 309.

69. Carty, A. J.; Mott, G. N.; Taylor, N. J.; Yule, J. E.; J. Am. Chem. Soc. **1978**, 100, 3051.

70. Carty, A. J.; Mott, G. N.; Taylor, N. J.; Ferguson, G.; Khan, M. A.; Roberts, P. J. J. Organomet. Chem. **1978**, 149, 345.

71. Cherkas, A. A.; Carty, A. J.; Sappa, E.; Pellinghelli, M. A.; Tiripicchio, A. Inorg. Chem. **1987**, 26, 3201.

72. MacLaughlin, S. A.; Johnson, J. P.; Taylor, N. J.; Carty, A. J.;

Sappa, E. Organometallics **1983**, 2, 352.

73. Carty, A. J.; Taylor, N. J.; Smith, W. F.; Lappert, M. F.; Pye, P. L. J. Chem. Soc., Chem. Commun. **1978**, 1017.

74. Carty, A. J.; Mott, G. N.; Taylor, N. J.; Paik, H. N.; Smith, W.; Yule, J. G. J. Chem. Soc., Chem. Commun. **1976**, 41.

75. Carty, A. J.; Mott, G. N.; Taylor, N. J. J. Organomet. Chem. **1981**, 212, C54.

76. Carty, A. J.; Mott, G. N.; Taylor, N. J. J. Organomet. Chem. **1979**, 182, C69.

77. Cherkas, A. A.; Mott, G. N.; Granby, R.; MacLaughlin, S. A.; Yule, J. E.; Taylor, N. J.; Carty, A. J. Organometallics **1988**, 7, 1115.

78. Cherkas, A. A.; Doherty, S.; Cleroux, M.; Hogarth, G.; Randall, L. H.; Breckenridge, S. M.; Taylor, N. J.; Carty, A. J. Organometallics **1992**, 11, 1701.

79. Breckenridge, S. M.; Taylor, N. J.; Carty, A. J. Organometallics **1991**, 10, 837.

80. Henrick, K.; McPartlin, M.; Deeming, A. J.; Hasso, S.; Manning, P. J. Chem. Soc., Dalton Trans. **1982**, 899.

81. Boyar, E. R.; Deeming, A. J.; Kabir, S. E. J. Chem. Soc., Chem. Commun. **1986**, 577.

82. Deeming, A. J.; Kabir, S. S.; Nuel, D.; Powell, N. I. Organometallics **1989**, 8, 717.

83. Deeming, A. J.; Hasso, S. J. Organomet. Chem. **1976**, 112, C39.

84. Deeming, A. J. Adv. Organomet. Chem. **1986**, 26, 1.

85. Churchill, M. R.; DeBoer, B. G.; Shapley, J. R.; Keister, J. B. J. Am. Chem. Soc. **1976**, 98, 2357.

86. Seyferth, D.; Hoke, J. B.; Wheeler, D. R. J. Organomet. Chem. **1988**, 341, 421.

87. Hoffman, D. M.; Huffman, J. C.; Lappas, D.; Wierda, D. A. Organometallics **1993**, 12, 4312 and references therein.

88. Granozzi, G.; Tondello, E.; Bertoncello, R.; Aime, S.; Osella, D. Inorg. Chem. **1983**, 22, 744.

90. Takats, J.; Washington, J.; Santarsiero, B. D. Organometallics **1994**, 13, 1078 and references therein.

91. (a) Fenske, D.; Becher, H. J. Chem. Ber. **1974**, 107, 117. (b) Fenske, D.; Becher, H. J. Chem. Ber. **1975**, 108, 2115. (c) Fenske, D. Chem. Ber. **1979**, 112, 363.

92. (a) Mao, F.; Tyler, D. R.; Keszler, J. J. Am. Chem. Soc. **1989**, 111, 130. (b) Mao, F.; Philbin, C. E.; Weakley, T. J. R.; Tyler, D. R. Organometallics **1990**, 9, 1510. (c) Mao, F.; Tyler, D. R.; Rieger, A. L.; Rieger, P. H. J. Chem. Soc., Faraday Trans. **1991**, 87, 3113. (d) Mao, F.; Sur, S. K.; Tyler, D. R. Organometallics **1991**, 10, 419. (e) Tyler, D. R. Acc. Chem. Res. **1991**, 24, 325. (f) Avey, A.; Schut, D. M.; Weakley, T. J. R. Inorg. Chem. **1993**, 32, 233.

93. (a) Downard, A. J.; Robinson, B. H.; Simpson, J. Organometallics **1986**, 5, 1132, 1140. (b) Hinkelmann, K.; Keinze, J.; Schacht, H.-T.; Field, J. S.; Vahrenkamp, H. J. Am. Chem. Soc. **1989**, 111, 5078.

94. Langford, C. H.; Gray, H. B. In "Ligand Substitution Processes," New York: Benjamin, **1965**.

95. Knoll, K.; Huttner, G.; Zsolnai, L.; Jibril, I.; Wasincionek, M. J. Organomet. Chem. **1985**, 294, 91.

96. (a) Brodie, N.; Poë, A. J.; Sekhar, V. C. J. Chem. Soc., Chem. Commun. **1985**, 1090. (b) Poë, A. J.; Sekhar, V. C. Inorg. Chem. **1985**, 24, 4376.

97. Dahlinger, K.; Poë, A. J.; Sayal, P. K.; Sekhar, V. C. J. Chem. Soc., Dalton Trans. **1986**, 2145.

98. Taube, D. J.; Ford, P. C. Organometallics **1986**, 5, 99.

99. Browning, C. S.; Farrar, D. H.; Gukathasan, R. R.; Morris, S. A. Organometallics **1985**, 4, 1750.

100. Basolo, F. Inorg. Chim. Acta. **1981**, 50, 65.

101. (a) Bogan, L. E.; Lesch, D. A.; Rauchfuss, T. B. J. Organomet. Chem. **1983**, 250, 429. (b) Adams, R. D.; Yang, L. W. J. Am. Chem. Soc. **1983**, 105, 1983. (c) Martin, L. R.; Einstein, F. W. B.; Pomeroy, R. K. Organometallics **1988**, 7, 294. (d) Tulyathan, B.; Geiger, W. E. J. Am. Chem. Soc. **1985**, 107, 5960. (e) Vahrenkamp, H. Adv. Organomet. Chem. **1983**, 22, 169 and references therein.

102. Planalp, R. P.; Vahrenkamp, H. Organometallics **1987**, 6, 492. (b) Schneider, J.; Minelli, M.; Huttner, G. J. Organomet. Chem. **1985**, 294, 75. (c) Darensbourg, D. J. in "The Chemistry of Metal Cluster Complexes," Shriver, D. F.; Kasez, H. D.; Adams, R. D. Eds.; VCH Publishers, Inc.: New York, **1990**, Chapter 4.

103. (a) Nuel, D.; Dahan, F.; Mathieu, R. J. Am. Chem. Soc. **1985**, 107, 1658. (b) Wang, J.; Sabat, M.; Lyons, L. J.; Shriver, D. F. Inorg. Chem. **1991**, 30, 382. (c) Adams, R. D.; Babin, J. E.; Tasi, M.; Wolfe, T. A. Organometallics **1987**, 6, 2228. (d) Adams, R. D.; Horváth, I. T. Prog. Inorg. Chem. **1985**, 32, 127. (e) Templeton, J. L. Adv. Organomet. Chem. **1989**, 29, 1. (f) Adams, R. D.; Chen, G.; Chen, L.; Wu, W.; Yin, J. Organometallics **1993**, 12, 3431. (g) Bantel, H.; Powell, A. K.; Vahrenkamp, H. Chem. Ber. **1990**, 123, 1607.

104. Dickson, R. S.; Fraser, P. J. Adv. Organomet. Chem. **1974**, 12, 323 and references therein.

105. (a) Nicholas, K. M.; Acc. Chem. Res. **1987**, 20, 207. (b) Tester, R.; Varghese, V.; Montana, A. M.; Khan, M.; Nicholas, K. M. J. Org. Chem. **1990**, 55, 186.

106. Schreiber, S. L.; Klimas, M. T.; Sammakia, T. J. Am. Chem. Soc. **1987**, 109, 5749.

107. Rubin, Y.; Knobler, C. B.; Diederich, F. J. Am. Chem. Soc. **1990**, 112, 4966. (b) Melikyan, G. G.; Mineif, A.; Vostrowsky, O.; Bestmann, H. J. Synthesis **1991**, 633. (c) Osella, D.; Stein, E.; Jaouen, G.; Zanello, P. J. Organomet. Chem. **1991**, 401, 37. (d) Osella, D.; Fiedler, J. Organometallics **1992**, 11, 3875.

108. Osella, D.; Dutto, G.; Jaouen, G.; Vessiéres, A.; Raithby, P. R.; De Benedetto, L.; McGlinchey, M. J. Organometallics **1993**, 12, 4545.

109. (a) Harrington, P. J.; "Transition Metals in Total Synthesis," John Wiley & Sons: New York, **1990**, Chapter 9. (b) Kraft, M. E.; Juliano, C. A.; Scott, I. L.; Wright, C.; McEachin, M. D. J. Am. Chem. Soc. **1991**, 113, 1693. (c) Krafft, M. E.; Scott, I. L.; Romero, R. H.; Feibelmann, S.; Van Pelt, C. E. J. Am. Chem. Soc. **1993**, 115, 7199.

110. (a) Heck, R. F. J. Am. Chem. Soc. **1963**, 85, 657. (b) Aggarwal, R. P.; Connelly, N. G.; Crespo, M. C.; Dunne, B. J.; Hopkins, P. M.; Orpen, A. G. J. Chem. Soc., Chem. Commun. **1989**, 33. (c) Aggarwal, R. P.; Connelly, N. G.; Crespo, M. C.; Dinne, B. J.; Hopkins, P. M.; Orpen, A. G. J. Chem. Soc., Dalton Trans. **1992**, 655. (d) Arewgoda, C. M.; Robinson, B. H.; Simpson, J. J. Chem. Soc., Chem. Commun. **1982**, 284. (e) Arewgoda, C. M.; Robinson, B. H.; Simpson, J. J. Am. Chem. Soc. **1983**, 105, 1893. (f) Casagrande, L. V.; Chen, T.; Reiger, P. H.; Robinson, B. H.; Simpson, J.; Visco, S. J. Inorg. Chem. **1984**, 23, 2019.

111. (a) Chia, L. S.; Cullen, W. R.; Franklin, M.; Manning, A. R. Inorg. Chem. **1975**, 14, 2521. (b) Bird, P. H.; Fraser, A. R.; Hall, D. N. Inorg. Chem. **1977**, 16, 1923. (c) Bianchini, C.; Dapporto, P.;

Meli, A. J. Organomet. Chem. **1979**, 174, 205.

112. (a) Cunnighame, R. G.; Hanton, L. R.; Jenson, S. D.; Robinson, B. H.; Simpson, J. Organometallics **1987**, 1470. (b) Jenson, S. D.; Robinson, B. H.; Simpson, J. Organometallics **1987**, 12, 1479.

113. Crow, J. P.; Cullen, W. R. Inorg. Chem. **1971**, 10, 2165.

114. (a) Hoffmann, R. Angew. Chem., Int. Ed. Engl. **1982**, 21, 711. (b) Albright, T. A.; Burdett, J. K.; Whangbo, M. H. "Orbital Interactions in Chemistry," Wiley: New York, **1985**.

115. Yang, K.; Bott, S. G.; Richmond, M. G. Organometallics , **1994**, 13, in press.

CHAPTER II

EXPERIMENTAL

A. Materials

1. Solvents

CH_2Cl_2, $ClCH_2CH_2Cl$, and MeCN were distilled from CaH_2. THF, Bu_2O, Et_2O, toluene, and 2,5-Me_2THF were distilled from sodium/benzophenone ketyl. The deuterated solvents benzene-d^6 and THF-d^8 were vacuum distilled from CaH_2, while CD_2Cl_2 and $CDCl_3$ were distilled from P_2O_5. All distilled solvents were stored under argon in Schlenk vessels equipped with Teflon stopcocks.

2. Reagents

$Co_2(CO)_8$ and (Z)-$Ph_2PCH{=}CHPPh_2$ were purchased from Pressure Chemical Co. and used as received. The ^{13}C-enriched carbon monoxide (99 % ^{13}C) was obtained from Isotec, Inc. The Ph_2PTMS used in the synthesis of bma was prepared according to the published procedure. [1] $PhCCo_3(CO)_9$ was prepared by the procedure reported by Seyferth, [2] and the bma ligand was synthesized by using the method of Tyler. [3] $Co_2(CO)_6(\mu\text{-}PhC{\equiv}CR)$ (R = H, Ph) were prepared according to the published procedure. [4] Trimethylphosphine, [5] cobaltocene, [6] and $[Cp_2Fe][BF_4]$ [7] were prepared from known literature procedures.

MeLi (1.0 M in Et_2O), n-BuLi (2.5 M in hexane), PhMgBr (1.0 M in

Et_2O), and Me_3NO were all purchased from Aldrich and used as received. MeLi and BuLi were titrated against diphenylacetic acid prior to use. [8] The tetra-n-butylammonium perchlorate (TBAP) used in the electrochemical studies was purchased from Johnson Matthey Electronics and recrystallized from ethyl acetate/petroleum ether and dried in vacuo for 2 days.

B. Instrumentation

All reactions were conducted under argon using Schlenk techniques or in a nitrogen-filled Vacuum Atmosphere DXL series inert-atmosphere Dri-Box. [9] Routine infrared spectra were recorded on a Nicolet 20SXB FT-IR spectrometer in 0.1 mm NaCl cells. Low-temperature IR spectra were recorded on the same spectrometer with a Specac Model P/N 21.000 variable-temperature cell equipped with inner and outer CaF_2 windows. Dry ice/acetone was used as coolant, and the reported cell temperature, taken to be accurate to ±1 °C, was determined with a copper-constantan thermocouple. ^1H, ^{13}C, ^{31}P NMR spectra were recorded at 300, 75, and 121 MHz, respectively, on a Varian 300-VXR spectrometer. The reported ^{31}P chemical shifts are referenced to external H_3PO_4 (85 %), taken to have $\delta = 0$. Positive chemical shifts are to low field of the external standard. C and H analyses were performed by Atlantic Microlab, Atlanta, GA.

Cyclic voltammetric measurements were conducted with a PAR Model 273 potentiostat/galvanostat, equipped with positive feedback circuitry to compensate for IR drop. The CV cell used was of airtight design and based on a three-electrode configuration, which enabled all cyclic voltammograms to be obtained free from oxygen and water. The CV experiments employed a platinum disk (area = 0.0079 cm^2) as the working electrode and a coiled

platinum wire as the auxiliary electrode. All voltammograms utilized a silver wire quasi-reference electrode and all potential data are referenced relative to the formal potential of the Cp_2Fe/Cp_2Fe^+ redox couple run under identical conditions, taken to have an $E_{1/2}$ = 0.306 V. [10]

The bulk electrolysis experiments were carried out in the constant-potential mode at desired potentials in an airtight bulk-electrolysis cell at the desired temperature in CH_2Cl_2 solvent containing 0.1 M TBAP. After the electrolysis was completed, the solution was examined by IR spectroscopy, using a low-temperature IR cell.

C. Extended Hückel Molecular Orbital Calculations.

All calculations were carried out by using the original program developed by Hoffmann, [11] as modified by Mealli and Proserpio. [12] The HOMO and LUMO orbitals shown in the dissertation were done with CACAO drawing program of Mealli and Proserpio.

D. Preparation of Compounds

1. $PhCCo_3(CO)_7$(bma)

To a mixture of 0.2 g (0.39 mmol) of $PhCCo_3(CO)_9$ and 0.2 g (0.42 mmol) of bma in 20 ml of THF was added 0.06 g (0.80 mmol) of Me_3NO. The color of the solution changed from brown to green-black immediately. The reaction, which was monitored by IR, was complete after 0.5 hr. The reaction solution was removed in vacuo at 0 °C, and $PhCCo_3(CO)_7$(bma) was isolated by column chromatography at -78 °C using CH_2Cl_2/petroleum ether (1 : 1). Yield: 0.25 g (70 %). IR (CH_2Cl_2) : ν (CO) 2065 (s), 2015 (s), 1986 (s), 1824 (w,

asymmetric bma C=O), 1772 (m, symmetric bma C=O) cm^{-1}. $^{31}P\{^1H\}$ NMR (THF, -97 °C) : δ 62 (chelate), 54 (chelate), 37 (bridge). $^{13}C\{^1H\}$ NMR (THF, -97 °C) : δ 209 (2C, bridge), 207 (chelate), 204 (2C, bridge), 202 (3C, bridge). The $PhCCo_3(CO)_7$(bma) was not submitted for combustion analysis because of its thermal instability.

2. $Co_3(CO)_6[\mu_2\text{-}\eta^2, \eta^1\text{-}C(Ph)\overbrace{C=C(PPh_2)C(O)OC}(O)](\mu_2\text{-}PPh_2)$

To 0.5 g (0.96 mmol) of $PhCCo_3(CO)_9$ and 0.47 g (1.0 mmol) of bma was added 50 ml of toluene, after which the solution was heated at 75 °C overnight. Upon cooling, TLC analysis revealed the presence of the desired product along with a trace of the parent cluster. Purification was achieved by column chromatography on silica gel using CH_2Cl_2 as the eluant. The analytically pure sample was obtained by recrystallization from benzene/isooctane (1 : 1). Yield: 0.5 g (58 %). IR (CH_2Cl_2) : ν (CO) 2062 (m), 2042 (vs), 2025 (vs), 2010 (sh), 1939 (b, m), 1811 (m, asymmetric bma C=O), 1748 (m, symmetric bma C=O) cm^{-1}. $^{31}P\{^1H\}$ NMR (THF, -97 °C) : δ 201.0 (μ_2-phosphido), 12.0 (phosphine). $^{13}C\{^1H\}$ NMR (THF, -97 °C) : δ 210.5 (1C, $J_{P\text{-}C}$ = 12.3 Hz), 202.9 (1C, $J_{P\text{-}C}$ = 7.9 Hz), 202.5 (1C), 201.9 (1C), 197.0 (1C), 192.8 (1C). Anal. Calcd for $C_{41}H_{25}Co_3O_9P_2$: C, 54.69 (54.55); H, 2.80 (2.88).

3. $PhCCo_3(CO)_7$[(Z)-$Ph_2PCH{=}CHPPh_2$]

To a Schlenk tube containing 0.2 g (0.39 mmol) of $PhCCo_3(CO)_9$ and 0.17 g (0.43 mmol) of (Z)-$Ph_2PCH{=}CHPPh_2$ was added 20 ml of toluene via syringe. The reaction was heated at 75 °C overnight and then allowed to cool to room temperature. TLC examination showed the presence of a single product. Purification was achieved by using silica gel chromatography with

petroleum ether/CH_2Cl_2 as the eluant. An analytically pure sample was obtained from a CH_2Cl_2 solution containing $PhCCo_3(CO)_7$[(Z)-Ph_2PCH=CH PPh_2] that had been layered with heptane. Yield : 0.26 g (78 %). IR (CH_2Cl_2) : ν (CO) 2057 (s), 2006 (vs), 1831 (w, b) cm^{-1}. $^{31}P\{^1H\}$ NMR ($CDCl_3$, -65 °C) : δ 36.2. $^{13}C\{^1H\}$ NMR ($CDCl_3$, -65 °C): δ 211 (2C), 204 (2C), 203 (3C). Anal. Calcd for $C_{40}H_{27}Co_3O_7P_2 \cdot 1/3\ CH_2Cl_2$: C, 54.61 (54.63); H, 3.20 (3.15).

4. $Co_3(CO)_5(\mu\text{-}CO)(PMe_3)[\mu_2\text{-}\eta^2,\eta^1\text{-}C(Ph)\overline{C=C(PPh_2)C(O)OC(O)}](\mu_2\text{-}PPh_2)$

To the 0.2 g (0.20 mmol) $Co_3(CO)_6[\mu_2\text{-}\eta^2, \eta^1\text{-}C(Ph)\overline{C=C(PPh_2)C(O)OC(O)}](\mu_2\text{-}PPh_2)$ in 20 ml CH_2Cl_2 at -78°C was added 1.1 equiv. of PMe_3 (0.47 ml of a 0.48 M solution of PMe_3 in THF) by syringe. The reaction was instantaneous as judged by the color change from brown to red brown and IR spectroscopy. The reaction solution was treated with 50 ml of cold petroleum ether and then maintained at -78 °C for 1 hr. The solvent was decanted, and the resulting solid was washed twice with cold petroleum ether. Crystals suitable for X-ray diffraction and combustion analyses were grown at -20 °C from a toluene/heptane solution (1 : 1) containing $Co_3(CO)_5(\mu\text{-}CO)(PMe_3)[\mu_2\text{-}\eta^2,\eta^1\text{-}C(Ph)\overline{C=C(PPh_2)C(O)OC(O)}](\mu_2\text{-}PPh_2)$ that had been layered with a small amount of diethyl ether. Yield: 0.18 g (ca. 90%). IR (CH_2Cl_2) : ν (CO) 2035 (s), 2010 (vs), 1999 (vs), 1900 (w), 1795 (m, asymmetric bma C=O), 1736 (s, symmetric bma C=O). $^{31}P\{^1H\}$ NMR (THF, -95 °C) : δ 184.3 (1P), 55.4 (1P, $J_{P\text{-}P}$ = 51 Hz), 0.3 (1P, $J_{P\text{-}P}$ = 51 Hz). $^{13}C\{^1H\}$ NMR (THF, -95 °C) : δ 212.5 (1C, dd, $J_{P\text{-}C}$ = 67 Hz, $J_{P\text{-}C}$ = 29 Hz), 208.3 (2C), 205.0 (1C), 202.1 (1C), 201.4 (1C). Anal. Calcd for $C_{44}H_{34}Co_3O_9P_3 \cdot 1/4$ heptane : C, 54.86 (54.65); H, 3.82 (4.09).

5. $Co_3(CO)_5(PMe_3)[\mu_2\text{-}\eta^2,\eta^1\text{-}C(Ph)C{=}C(PPh_2)C(O)OC(O)](\mu_2\text{-}PPh_2)$

To 0.2 g (0.2 mmol) of $Co_3(CO)_6[\mu_2\text{-}\eta^2,\eta^1\text{-}C(Ph)C{=}C(PPh_2)C(O)OC(O)](\mu_2\text{-}PPh_2)$ in 20 ml of CH_2Cl_2 at 0 °C was added 1.1 equiv of PMe_3 (0.47 ml of a 0.48 M solution of PMe_3 in THF) by syringe. The initially formed product $Co_3(CO)_5(\mu\text{-}CO)(PMe_3)[\mu_2\text{-}\eta^2,\eta^1\text{-}C(Ph)C{=}C(PPh_2)C(O)OC(O)](\mu_2\text{-}PPh_2)$, transformed into the mono-substituted cluster $Co_3(CO)_5(PMe_3)[\mu_2\text{-}\eta^2,\eta^1\text{-}C(Ph)C{=}C(PPh_2)C(O)OC(O)](\mu_2\text{-}PPh_2)$ after stirring at room temperature for 3 hrs. The reaction solution was removed in vacuo and product was isolated by column chromatography using CH_2Cl_2 as the eluant. Yield : 0.15 g (ca. 70%). IR (CH_2Cl_2) : ν (CO) 2040 (s), 2006 (vs), 1984 (s), 1801 (m, asymmetric bma C=O), 1741 (s, symmetric bma C=O). $^{31}P\{^1H\}$ NMR (THF, -95 °C) : δ 190.5 (1P, phosphido), 14.3 and 7.8 [Ph_2P(maleic anhydride) and PMe_3 groups]. $^{13}C\{^1H\}$ NMR (THF, -95 °C) : δ 216.1 (1C, d, $J_{P\text{-}C}$ = 23.1 Hz), 206.4 (1C), 204.6 (1C), 200.5 (1C), 191.9 (1C, $J_{P\text{-}C}$ = 29 Hz). Anal. Calcd for $C_{43}H_{34}Co_3O_8P_3{\cdot}CH_2Cl_2$: C, 51.19 (51.34); H, 3.51 (3.55).

6. $Co_3(CO)_4(PMe_3)_2[\mu_2\text{-}\eta^2,\eta^1\text{-}C(Ph)C{=}C(PPh_2)C(O)OC(O)](\mu_2\text{-}PPh_2)$

To the 0.2 g (0.2 mmol) of $Co_3(CO)_6(\mu_2\text{-}\eta^2,\eta^1\text{-}C(Ph)C{=}C(PPh_2)C(O)OC(O)](\mu_2\text{-}PPh_2)$ in 20 ml CH_2Cl_2 at room temperature was added 2.1 equiv of PMe_3 (0.94 ml of a 0.48 M solution of PMe_3 in THF) by syringe. The color of the solution changed from brown to brown-green. The reaction, which was monitored by IR, was complete after 3 hrs. The reaction solution was then removed in vacuo and $Co_3(CO)_4(PMe_3)_2[\mu_2\text{-}\eta^2,\eta^1\text{-}C(Ph)C{=}C(PPh_2)C(O)OC(O)](\mu_2\text{-}PPh_2)$ was isolated by column chromatography using CH_2Cl_2/acetone (95 : 5). The analytical sample was obtained by recrystallization from benzene/heptane (1 : 1). Yield : 0.15 g (ca. 70 %). IR (CH_2Cl_2) : ν (CO) 1993 (sh),

1976 (vs), 1864 (w, broad), 1993 (sh), 1976 (vs), 1864 (w, broad), 1791 (m, asymmetric bma C=O), 1728 (m, symmetric bma C=O). $^{31}P\{^1H\}$ NMR (THF, -95 °C) : δ 172.9 (1P, phosphido), 7.0, 0.8 and -10.0 [Ph_2P (maleic anhydride) and two PMe_3 groups]. $^{13}C\{^1H\}$ NMR (THF, -95 °C) : δ 224.0 (1C, d, J_{P-C} = 25.5 Hz), 207.4 (1C), 206.7 (2C). Anal. Calcd for $C_{45}H_{43}Co_3O_7P_4 \cdot 1/2\ C_6H_6$: C, 55.67 (55.29); H, 4.48 (4.77).

7. $Co_2(CO)_4(\mu\text{-PhC}{\equiv}\text{CPh})$(bma) (chelating isomer)

To a mixture of 0.5 g $Co_2(CO)_6(\mu\text{-PhC}{\equiv}\text{CPh})$ (1.08 mmol) and 0.5 g of bma (1.07 mmol) in 50 ml of THF was added 0.16 g of Me_3NO (2.13 mmol). The color of the solution gradually changed from brown to black-green. The reaction, which was monitored by IR, was complete after 1 hr. The reaction solution was removed in vacuo and $Co_2(CO)_4(\mu\text{-PhC}{\equiv}\text{CPh})$(bma) (chelating) was isolated by column chromatography at -78°C using CH_2Cl_2/petroleum ether (3 : 1). Yield : 0.65 g (69 %). IR (CH_2Cl_2) : ν (CO) 2047 (vs), 1993(vs), 1952 (sh), 1842 (w, asymmetric bma C=O), 1775 (m, symmetric bma C=O) cm^{-1}. $^{31}P\{^1H\}$ NMR ($CDCl_3$, -56 °C) : δ 60.3. $^{13}C\{^1H\}$ NMR (THF , - 91 °C) : δ 207.5 (1C, bma-substituted cobalt), 201.1 (3C, $Co(CO)_3$). Anal. Calcd for $C_{46}H_{30}Co_2O_7P_2 \cdot 1/2\ CH_2Cl_2$: C, 60.84 (60.73); H, 3.49 (3.40).

8. $Co_2(CO)_4(\mu\text{-PhC}{\equiv}\text{CPh})$(bma) (bridging isomer)

To a Schlenk tube containing 0.2 g of the chelating isomer of $Co_2(CO)_4(\mu\text{-PhC}{\equiv}\text{CPh})$(bma) (0.23 mmol) was added 40 ml of 1,2-dichloroethane, after which the solution was heated at 45 °C overnight. IR analysis at this point revealed the presence of a mixture of the desired bridging isomer and chelating isomer in a 1 : 1 ratio. Longer reaction times

did not change the ratio of the chelating and bridging isomers. Due to inefficient compound separation on silica gel, column chromatography could not be employed in the purification of this isomeric mixture. The solvent was instead removed by vacuum, followed by repeated crystallizations using CH_2Cl_2/petroleum ether. By this method, a pure sample of the bridging isomer was ultimately isolated from the mother liquor. The analytical sample was recrystallized from CH_2Cl_2/pentane (1 : 1). Yield : 0.02g (10 %). IR (CH_2Cl_2) : ν (CO) 2032 (s), 2009 (vs), 1982 (s), 1818 (w, asymmetric bma C=O), 1765(m, symmetric bma C=O) cm^{-1}. $^{31}P\{^1H\}$ NMR (THF, -95 °C) : δ 30.5. $^{13}C\{^1H\}$ NMR (THF, -95°C) : δ 203.2 (4C). Anal. Calcd for $C_{46}H_{30}Co_2O_7P_2 \bullet CH_2Cl_2$: C, 58.48 (58.83); H, 3.49 (3.36).

9. $Co_2(CO)_4(\mu\text{-PhC}{\equiv}\text{CPh})[(Z)\text{-}Ph_2PCH{=}CHPPh_2]$

To a Schlenk tube containing 0.2 g of the $Co_2(CO)_6(\mu\text{-PhC}{\equiv}\text{CPh})$ (0.43 mmol) and 0.17 g $(Z)\text{-}Ph_2PCH{=}CHPPh_2$ (0.43 mmol) was added 50 ml of CH_2Cl_2, after which the solution was treated with 64.5 mg of Me_3NO (0.86 mmol). Stirring was continued for 3 hr, after which time IR analysis indicated the presence of the desired product (>90%). Product purification was achieved by chromatography over silica gel using CH_2Cl_2/petroleum ether (1 : 1). Yield : 0.25g (73 %). IR (CH_2Cl_2) : ν (CO) 2039 (vs), 1983 (vs). $^{31}P\{^1H\}$ NMR (THF, -95 °C) : δ 71.8. $^{13}C\{^1H\}$ NMR (THF , - 95 °C) : δ 208.8 (1C, P_2-substituted cobalt), 202.8 (3C, $Co(CO)_3$). Anal. Calcd for $C_{44}H_{32}Co_2O_4P_2$: C, 65.68 (65.77); H, 4.01 (4.01).

10. $Co_2(CO)_4[\eta^2,\eta^2,\eta^1,\eta^1\text{–}(Z)\text{–}Ph_2P\text{-}C(Ph){=}(Ph)C\text{-}\overline{C{=}C(PPh_2)C(O)\overline{OC(O)}}]$

To 0.25 g of $Co_2(CO)_6(\mu\text{-PhC}\equiv\text{CPh})$ (0.54 mmol) and 0.25 g of bma (0.54 mmol) was added 30 ml of 1,2-dichloroethane solvent by syringe, after which the solution was heated to reflux for 5 hr and then allowed to cool to room temperature. TLC examination showed the presence of only one slow moving spot. Purification was achieved by using silica gel chromatography with CH_2Cl_2 as the eluant. Yield : 0.05 g (10%). IR (CH_2Cl_2) : ν (CO) 2049 (s), 2025 (vs), 2008 (s), 1981 (m), 1808 (w, asymmetric bma C=O), 1745 (m, symmetric bma C=O) cm^{-1}. $^{31}P\{^1H\}$ NMR (THF, -90 °C) : δ 46.7 (1P, $J_{P\text{-}P}$ = 17.0 Hz), 27.8 (1P, broad). $^{13}C\{^1H\}$ NMR (THF, – 90 °C): δ 193.7 (1C), 196.9 (1C), 201.1 (1C, $J_{P\text{-}C}$ = 19.6 Hz), 202.1 (1C). Anal. Calcd for $C_{46}H_{30}Co_2O_7P_2$: C, 62.82 (63.18); H, 3.94 (3.46).

11. $Co_2(CO)_4(\mu\text{-PhC}\equiv\text{CH})$(bma) (chelating)

To a mixture of 0.1 g (0.26 mmol) $Co_2(CO)_6(\mu\text{-PhC}\equiv\text{CH})$ and 0.13 g of bma (0.27 mmol) in 20 ml of THF was added 0.039 g of Me_3NO (0.53 mmol). The color of the solution immediately changed from brown to black-green. The reaction, which was monitored by IR, was complete after 0.5 hr. The reaction solution was removed in vacuo and $Co_2(CO)_4(\mu\text{-PhC}\equiv\text{CH})$(bma) (chelating) was isolated by column chromatography at -78°C using CH_2Cl_2/ petroleum ether (3 : 1). Yield : 0.13 g. IR (CH_2Cl_2) : ν (CO) 2046 (s), 1985 (vs), 1841 (w asymmetric bma C=O), 1775 (m, symmetric bma C=O) cm^{-1}. $^{31}P\{^1H\}$ NMR (CH_2Cl_2) : δ 54.3, 64.6 (1P each for pseudo-axial and pseudo-equatorial bma PPh_2 groups). $^{13}C\{^1H\}$ NMR (CH_2Cl_2 , - 60 °C) : δ 201.8 (3C), 206.9 (1C), Anal. Calcd for $C_{40}H_{26}Co_2O_7P_2 \bullet 1/3\ CH_2Cl_2$: C, 58.52 (58.59); H, 3.42 (3.25).

12. $Co_2(CO)_4(\mu\text{-}PhC{\equiv}CH)[(Z)\text{-}Ph_2PCH{=}CHPPh_2]$

To a Schlenk tube containing 0.2 g of the $Co_2(CO)_6(\mu\text{-}PhC{\equiv}CH)$ (0.43 mmol) and 0.17 g $(Z)\text{-}Ph_2PCH{=}CHPPh_2$ (0.43 mmol) was added 50 ml of CH_2Cl_2, after which the solution was treated with 64.5 mg of Me_3NO (0.86 mmol). Stirring was continued for 3 hr, after which time IR analysis indicated the presence of the product (>90%). The purification was achieved by chromatography over silica gel using CH_2Cl_2/petroleum ether (1 : 1). Yield : 0.25g (73 %) IR (CH_2Cl_2) : ν (CO) 2041 (vs), 1984 (vs). $^{31}P\{^1H\}$ NMR (THF, -95 °C) : δ 85.5, 76.0 (1P each for pseudo-axial and pseudo-equatorial (Z)-$Ph_2PCH{=}CHPPh_2$ PPh_2 groups). Anal. Calcd for $C_{38}H_{28}Co_2O_4P_2$: C, 62.65 (62.72); H, 3.87 (3.93).

13. $Co_2(CO)_4[\mu\text{-}\eta^2,\eta^2,\eta^1,\eta^1\text{–}PhC{=}C(H)PPh_2\overline{C{=}C(PPh_2)C(O)OC(O)}]$

To 0.20 g (0.25 mmol) of $Co_2(CO)_6(\mu\text{-}PhC{\equiv}CH)$ and 0.25 g (0.25 mmol) of bma was added 20 ml of 1,2-dichloroethane solvent by syringe, after which the solution was heated to reflux for 1 hr and then allowed to cool to room temperature. TLC examination showed the presence of a single product. Purification was achieved by using silica gel chromatography with CH_2Cl_2 as the eluant. Yield : 0.3 g (70 %). IR (CH_2Cl_2) : ν (CO) 2035 (s), 2006 (vs), 1984 (m), 1969 (m), 1795 (w, asymmetric bma C=O), 1742 (m, symmetric bma C=O) cm^{-1}. $^{31}P\{^1H\}$ NMR (CH_2Cl_2, -90 °C) : δ 10.6 (1P, $J_{P\text{-}P}$ = 48.6 Hz), 38.3 (1P, $J_{P\text{-}P}$ = 48.4 Hz). $^{13}C\{^1H\}$ NMR (CH_2Cl_2 , - 90 °C) : δ 201.1 (1C, $J_{P\text{-}C}$ = 19.6 Hz), 203.2 (1C), 203.0 (1C), 208.1 (1C). Anal. Calcd for $C_{40}H_{26}Co_2O_7P_2 \bullet 1/2CH_2Cl_2$: C, 57.84 (57.87); H, 3.24 (3.26).

14. $Co_2(CO)_3(PMe_3)[\mu\text{-}\eta^2,\eta^2,\eta^1,\eta^1\text{–}PhC(CO)=C(H)PPh_2C=C(PPh_2)C(O)OC(O)]$

To the 0.2 g (0.2 mmol) of $Co_2(CO)_4[\mu\text{-}\eta^2,\eta^2,\eta^1,\eta^1\text{–}PhC=C(H)PPh_2C=C(PPh_2)C(O)OC(O)]$ in 15 ml of CH_2Cl_2 was added 0.4 ml of 0.5 M PMe_3 (0.2 mmol) in THF by syringe. The color of the solution immediately changed from brown to black-green. The reaction, which was monitored by IR, was complete after 5 minutes. The reaction solution was removed in vacuo and product was isolated by column chromatography using CH_2Cl_2/acetone (95 : 5). Yield : 0.18 g. IR (CH_2Cl_2) : ν (CO) 2022 (vs), 1985 (vs), 1777 (w, asymmetric bma C=O), 1719 (m, symmetric bma C=O), 1555 (broad, acyl) cm-1. $^{31}P\{^1H\}$ NMR (THF, -90 °C) : δ 31.2 (1P, $J_{P\text{-}P}$ = 69.1Hz), 7.4 (1P, $J_{P\text{-}P}$ = 69.1 Hz), 4.6 (1P). $^{13}C\{^1H\}$ NMR (THF , - 90 °C) : δ 234.5 (1C, $J_{P\text{-}C}$ = 15.0 Hz), 206.6 (2C), 197.8 (1C, $J_{P\text{-}C}$ = 11.4 Hz). Anal. Calcd for $C_{43}H_{35}Co_2O_7P_3$: C, 59.06 (58.36); H, 4.03 (4.38).

15. Preparation of Sealed NMR Tube Reactions

Starting material and solvent (0.8 ml for a 5 mm NMR tube) were transferred into a NMR tube under argon. After the tube was shaken well, the NMR tube and its contents were cooled to -78 °C and desired reagent was added. The tube was then evacuated to ca. 10^{-4} mm Hg prior to flame sealing.

E. Kinetic Study on the Conversion of $PhCCo_3(CO)_7$(bma) to $Co_3(CO)_6[\mu_2\text{-}\eta^2, \eta^1\text{-}C(Ph)C=C(PPh_2)C(O)OC(O)](\mu_2\text{-}PPh_2)$

All kinetic reactions involving the conversion of $PhCCo_3(CO)_7$(bma) to $Co_3(CO)_6[\mu_2\text{-}\eta^2,\eta^1\text{-}C(Ph)C=C(PPh_2)C(O)OC(O)](\mu_2\text{-}PPh_2)$ were carried out in Schlenk tubes under argon and monitored for a minimum of 2-3 half-lives by

following the IR absorbance of the 1772 cm^{-1} band. Plots of ln A_t vs. time gave the first-order rate constants, k_{obsd}. The activation parameters ($\Delta H^{\neq}$ and $\Delta S^{\neq}$) were determined by using the Eyring equation, and error limits were calculated by using the available least-squares regression program. [13]

F. X-Ray Crystallography

1. $PhCCo_3(CO)_7(bma)$

A dark green-black crystal, which was grown from a CH_2Cl_2 solution of $PhCCo_3(CO)_7(bma)$ that had been layered with heptane, of dimensions 0.04 x 0.42 x 0.10 mm^3 was sealed inside a Lindemann capillary and mounted on the goniometer of an Enraf-Nonius CAD-4 diffractometer. The radiation used was Mo Kα monochromatized by a crystal of graphite. Cell constants were obtained from a least-squares refinement of 25 reflections with $2\theta > 28°$. Intensity data in the range $2.0 \leq 2\theta \leq 40.0°$ were collected at 298 K using the ω–scan technique in the variable-scan speed mode. Three reflections (800, 080, 00-6) were measured after every 3600 seconds of exposure time in order to monitor crystal decay (< 2 %). The structure was solved by SHELX-86, which revealed the positions of the Co and P atoms. All remaining non-hydrogen atoms were located with difference Fourier maps and blocked-matrix least-squares refinement. With the exception of the phenyl and CO carbons, all non-hydrogen atoms were refined anisotropically. Refinement converged at $R = 0.0367$ and $R_w = 0.0391$ for 1344 unique reflections with $I > 3\sigma(I)$.

2. $Co_3(CO)_6[\mu_2\text{-}\eta^2, \eta^1\text{-}C(Ph)C{=}C(PPh_2)C(O)OC(O)](\mu_2\text{-}PPh_2)$

A black crystal, which was grown from a CH_2Cl_2 solution of

$Co_3(CO)_6[\mu_2\text{-}\eta^2,\eta^1\text{-}C(Ph)\overline{C=C(PPh_2)C(O)OC(O)}](\mu_2\text{-}PPh_2)$ that had been layered with heptane, of dimensions 0.04 x 0.42 x 0.10 mm^3 was sealed inside a Lindemann capillary and mounted on the goniometer of an Enraf-Nonius CAD-4 diffractometer. The radiation used was Mo Kα monochromatized by a crystal of graphite. Cell constants were obtained from a least-squares refinement of 25 reflections with $2\theta > 25°$. Intensity data in the range $2.0 \leq 2\theta \leq 44.0°$ were collected at 298 K using the ω–scan technique in the variable-scan speed mode. Three reflections (600, 080, 0012) were measured after every 3600 seconds of exposure time in order to monitor crystal decay (< 1 %). The structure was solved by MULTAN, which revealed the positions of the Co and P atoms. All remaining non-hydrogen atoms were located with difference Fourier maps and blocked-matrix least-squares refinement. With the exception of the phenyl and CO carbons, all non-hydrogen atoms were refined anisotropically. Refinement converged at R = 0.0392 and R_w = 0.0432 for 2012 unique reflections with $I > 3\sigma(I)$.

3. $PhCCo_3(CO)_7[(Z)\text{-}Ph_2PCH{=}CHPPh_2]$

A black crystal, which was grown from a CH_2Cl_2 solution of $PhCCo_3(CO)_7[(Z)\text{-}Ph_2PCH{=}CHPPh_2]$ that had been layered with heptane, of dimensions 0.08 x 0.22 x 0.43 mm^3 was sealed inside a Lindemann capillary and mounted on the goniometer of an Enraf-Nonius CAD-4 diffractometer. The radiation used was Mo Kα monochromatized by a crystal of graphite. Cell constants were obtained from a least-squares refinement of 25 reflections with $2\theta > 25°$. Intensity data in the range $2.0 \leq 2\theta \leq 44.0°$ were collected at 298 K using the $\theta/2\theta$-scan technique in the variable-scan speed mode. Three reflections (600, 180, 008) were measured after every 3600 seconds of exposure

time in order to monitor crystal decay (< 1 %). The structure was solved by MULTAN, which revealed the positions of the Co and P atoms. All remaining non-hydrogen atoms were located with difference Fourier maps and blocked-matrix least-squares refinement. With the exception of the phosphorus phenyl carbons, all non-hydrogen atoms were refined anisotropically. Refinement converged at R = 0.0445 and R_w = 0.0488 for 4559 unique reflections with $I > 3\sigma(I)$.

4. $Co_3(CO)_5(\mu\text{-}CO)(PMe_3)[\mu_2\text{-}\eta^2,\eta^1\text{-}C(Ph)\overline{C=C(PPh_2)C(O)OC}(O)](\mu_2\text{-}PPh_2)$

A black crystal, which was grown from a toluene/heptane solution (1 : 1) of $Co_3(CO)_5(\mu\text{-}CO)(PMe_3)[\mu_2\text{-}\eta^2,\eta^1\text{-}C(Ph)\overline{C=C(PPh_2)C(O)OC}(O)](\mu_2\text{-}PPh_2)$ that had been layered with a small amount of diethyl ether, of dimensions 0.08 x 0.22 x 0.48 mm^3 was sealed inside a Lindemann capillary and mounted on the goniometer of an Enraf-Nonius CAD-4 diffractometer. The radiation used was Mo Kα monochromatized by a crystal of graphite. Cell constants were obtained from a least-squares refinement of 25 reflections with $2\theta > 25°$. Intensity data in the range $2.0 \leq 2\theta \leq 40°$ were collected at 298 K using the $\theta/2\theta$ scan technique in the variable-scan speed mode. Three reflections (500, 050, 007) were measured after every 3600 seconds of exposure time in order to monitor crystal decay (< 8 %). The structure was solved by SIR, which revealed the positions of the Co and P atoms. All remaining non-hydrogen atoms were located with difference Fourier maps and blocked-matrix least-squares refinement. With the exception of the cobalt and phosphorus atoms, all other atoms were refined isotropically. Refinement converged at R = 0.0667 and R_w = 0.0816 for 1768 unique reflections with $I > 3\sigma(I)$.

5. $Co_3(CO)_5(PMe_3)[\mu_2\text{-}\eta^2,\eta^1\text{-}C(Ph)\overline{C=C(PPh_2)C(O)OC(O)}](\mu_2\text{-}PPh_2)$

A black crystal, which was grown from a CH_2Cl_2 solution of $Co_3(CO)_5(PMe_3)[\mu_2\text{-}\eta^2,\eta^1\text{-}C(Ph)\overline{C=C(PPh_2)C(O)OC(O)}](\mu_2\text{-}PPh_2)$ that had been layered with heptane, of dimensions 0.08 x 0.28 x 0.48 mm^3 was sealed inside a Lindemann capillary and mounted on the goniometer of an Enraf-Nonius CAD-4 diffractometer. The radiation used was Mo Kα monochromatized by a crystal of graphite. Cell constants were obtained from a least-squares refinement of 25 reflections with $2\theta > 25°$. Intensity data in the range $2.0 \leq 2\theta \leq 44.0°$ were collected at 298 K using the ω-scan technique in the variable-scan speed mode. Three reflections (600, 0120, 006) were measured after every 3600 seconds of exposure time in order to monitor crystal decay (< 1 %). The structure was solved by SIR, which revealed the positions of the Co and P atoms. All remaining non-hydrogen atoms were located with difference Fourier maps and blocked-matrix least-squares refinement. With the exception of the phenyl carbons, all non-hydrogen atoms were refined anisotropically. Refinement converged at R = 0.0469 and R_w = 0.0577 for 2623 unique reflections with $I > 3\sigma(I)$.

6. $Co_3(CO)_4(PMe_3)_2[\mu_2\text{-}\eta^2,\eta^1\text{-}C(Ph)\overline{C=C(PPh_2)C(O)OC(O)}](\mu_2\text{-}PPh_2)$

A black crystal, which was grown from a CH_2Cl_2 solution of $Co_3(CO)_4(PMe_3)_2[\mu_2\text{-}\eta^2,\eta^1\text{-}C(Ph)\overline{C=C(PPh_2)C(O)OC(O)}](\mu_2\text{-}PPh_2)$ that had been layered with heptane, of dimensions 0.25 x 0.27 x 0.30 mm^3 was sealed inside a Lindemann capillary and mounted on the goniometer of an Enraf-Nonius CAD-4 diffractometer. The radiation used was Mo Kα monochromatized by a crystal of graphite. Cell constants were obtained from a least-squares refinement of 25 reflections with $2\theta > 30°$. Intensity data in the range $2.0 \leq 2\theta$

$\leq 44.0°$ were collected at 298 K using the ω-scan technique in the variable-scan speed mode. Three reflections (600, 0110, 0010) were measured after every 3600 seconds of exposure time in order to monitor crystal decay (< 1 %). The structure was solved by SHELX-86, which revealed the positions of the Co and P atoms. All remaining non-hydrogen atoms were located with difference Fourier maps and blocked-matrix least-squares refinement. With the exception of the phosphorus phenyl carbons, all non-hydrogen atoms were refined anisotropically. Refinement converged at R = 0.0453 and R_w = 0.0489 for 3795 unique reflections with $I > 3\sigma(I)$.

7. $Co_2(CO)_4(\mu\text{-PhC}{\equiv}\text{CPh})(bma)$ (bridging isomer)

A dark green-black crystal, which was grown from a CH_2Cl_2 solution of $Co_2(CO)_4(\mu\text{-PhC}{\equiv}\text{CPh})(bma)$ (bridging) that had been layered with heptane, of dimensions 0.08 x 0.08 x 0.42 mm was sealed inside a Lindemann capillary and mounted on the goniometer of an Enraf-Nonius CAD-4 diffractometer. The radiation used was Mo Kα monochromatized by a crystal of graphite. Cell constants were obtained from a least-squares refinement of 25 reflections with $2\theta > 24°$. Intensity data in the range $2.0 \leq 2\theta \leq 44°$ were collected at 298 K using the ω-scan technique in the variable-scan speed mode and were corrected for Lorentz, polarization, and absorption (DIFABS). Three reflections (400, 060, 004) were measured after every 3600 seconds of exposure time in order to monitor crystal decay (< 2 %). The structure was solved by SIR, which revealed the positions of the Co and P atoms. All remaining non-hydrogen atoms were located with difference Fourier maps and blocked-matrix least-squares refinement. All non-hydrogen atoms were refined anisotropically. Refinement converged at R = 0.0697 and R_w = 0.0850 for 1711 unique

reflections with $I > 3\sigma(I)$.

8. $Co_2(CO)_4(\mu\text{-}PhC{\equiv}CPh)[(Z)\text{-}Ph_2PCH{=}CHPPh_2]$

A black crystal, which was grown from a CH_2Cl_2 solution of $Co_2(CO)_4(\mu\text{-}PhC{\equiv}CPh)[(Z)\text{-}Ph_2PCH{=}CHPPh_2]$ that had been layered with heptane, of dimensions 0.08 x 0.11 x 0.22 mm^3 was sealed inside a Lindemann capillary and mounted on the goniometer of an Enraf-Nonius CAD-4 diffractometer. The radiation used was Mo Kα monochromatized by a crystal of graphite. Cell constants were obtained from a least-squares refinement of 25 reflections with $2\theta > 25°$. Intensity data in the range $2.0 \leq 2\theta \leq 44°$ were collected at 298 K using the $\theta/2\theta$–scan technique in the variable-scan speed mode and were corrected for Lorentz, polarization, and absorption (DIFABS). Three reflections (500, 060, 006) were measured after every 3600 seconds of exposure time in order to monitor crystal decay (< 2 %). The structure was solved by SIR, which revealed the positions of the Co and P atoms. All remaining non-hydrogen atoms were located with difference Fourier maps and blocked-matrix least-squares refinement. With the exception of the phenyl carbons, all non-hydrogen atoms were refined anisotropically. Refinement converged at R = 0.0587 and R_w = 0.0650 for 2425 unique reflections with $I > 3\sigma(I)$.

9. $Co_2(CO)_4[\eta^2,\eta^2,\eta^1,\eta^1\text{–}(Z)\text{–}Ph_2P\text{-}C(Ph){=}(Ph)C\text{-}\overline{C{=}C(PPh_2)C(O)OC(O)}]$

A black crystal, which was grown from a CH_2Cl_2 solution of $Co_2(CO)_4[\eta^2,\eta^2,\eta^1,\eta^1\text{–}(Z)\text{–}Ph_2P\text{-}C(Ph){=}(Ph)C\text{-}\overline{C{=}C(PPh_2)C(O)OC(O)}]$ that had been layered with heptane, of dimensions 0.04 x 0.22 x 0.31mm^3 was sealed

inside a Lindemann capillary and mounted on the goniometer of an Enraf-Nonius CAD-4 diffractometer. The radiation used was Mo Kα monochromatized by a crystal of graphite. Cell constants were obtained from a least-squares refinement of 25 reflections with $2\theta > 25°$. Intensity data in the range $2.0 \leq 2\theta \leq 44°$ were collected at 298 K using the ω–scan technique in the variable-scan speed mode and were corrected for Lorentz, polarization, and absorption (DIFABS). Three reflections (600, 060, 0012) were measured after every 3600 seconds of exposure time in order to monitor crystal decay (< 2 %). The structure was solved by SIR, which revealed the positions of the Co and P atoms. All remaining non-hydrogen atoms were located with different Fourier maps and blocked-matrix least-squares refinement and refined anisotropically. Refinement converged at R = 0.0529 and R_w = 0.0608 for 1141 unique reflections with $I > 3\sigma(I)$.

10. $Co_2(CO)_4[\mu\text{-}\eta^2,\eta^2,\eta^1,\eta^1\text{–}PhC{=}C(H)PPh_2\overline{C{=}C(PPh_2)C(O)OC(O)}]$

A black crystal, which was grown from a CH_2Cl_2 solution of $Co_2(CO)_4[\mu\text{-}\eta^2,\eta^2,\eta^1,\eta^1\text{–}PhC{=}C(H)PPh_2\overline{C{=}C(PPh_2)C(O)OC(O)}]$ that had been layered with heptane, of dimensions 0.11 x 0.22 x 0.45 mm^3 was sealed inside a Lindemann capillary and mounted on the goniometer of an Enraf-Nonius CAD-4 diffractometer. The radiation used was Mo Kα monochromatized by a crystal of graphite. Cell constants were obtained from a least-squares refinement of 25 reflections with $2\theta > 30°$. Intensity data in the range $2.0 \leq 2\theta \leq 44°$ were collected at 298 K using the $\theta/2\theta$–scan technique in the variable-scan speed mode and were corrected for Lorentz, polarization, and absorption (DIFABS). Three reflections (500, 080, 008) were measured after every 3600 seconds of exposure time in order to monitor crystal decay (< 4 %).

The structure was solved by SIR, which revealed the positions of the Co and P atoms. All remaining non-hydrogen atoms were located with different Fourier maps and blocked-matrix least-squares refinement. With the exception of the phenyl carbons and hydrogens, all atoms were refined anisotropically. Refinement converged at R = 0.0365 and R_w = 0.0469 for 2749 unique reflections with $I > 3\sigma(I)$.

11. $Co_2(CO)_3(PMe_3)[\mu\text{-}\eta^2,\eta^2,\eta^1,\eta^1\text{–}PhC(CO)=C(H)PPh_2C=C(PPh_2)C(O)OC(O)]$

A black crystal, which was grown from a CH_2Cl_2 solution of $Co_2(CO)_3(PMe_3)[\mu\text{-}\eta^2,\eta^2,\eta^1,\eta^1\text{–}PhC(CO)=C(H)PPh_2C=C(PPh_2)C(O)OC(O)]$ that had been layered with heptane, of dimensions 0.08 x 0.11 x 0.24 mm^3 was sealed inside a Lindemann capillary and mounted on the goniometer of an Enraf-Nonius CAD-4 diffractometer. The radiation used was Mo Kα monochromatized by a crystal of graphite. Cell constants were obtained from a least-squares refinement of 25 reflections with $2\theta > 30°$. Intensity data in the range $2.0 \leq 2\theta \leq 44°$ were collected at 298 K using the ω–scan technique in the variable-scan speed mode and were corrected for Lorentz, polarization, and absorption (DIFABS). Three reflections (800, 0100, 0012) were measured after every 3600 seconds of exposure time in order to monitor crystal decay (< 1 %). The structure was solved by SHELX-86, which revealed the positions of the Co and P atoms. All remaining non-hydrogen atoms were located with different Fourier maps and blocked-matrix least-squares refinement. With the exception of phenyl carbons, all atoms were refined anisotropically. Refinement converged at R = 0.0427 and R_w = 0.0460 for 2127 unique reflections with $I > 3\sigma(I)$.

CHAPTER REFERENCES

1. Kuchen, W.; Buchward, H. Chem. Ber. **1959**, 92, 227.

2. Nestle, M. O.; Hallgren, J. E.; Seyferth, D. Inorg. Synth. **1980**, 20, 226.

3. Mao, F.; Philbin, C. E.; Weakly, T. J. R.; Tyler, D. R. Organometallics **1990**, 9, 1510.

4. Bor, G.; Kettle, S. F. A.; Stanghellini, P. L. Inorg. Chim. Acta **1976**, 18, L18.

5. Luetkens, M. L, Jr.; Sattelberger, A. P.; Murray, H. H.; Basil, J. D.; Fackler, Jr. Inorg. Synth. **1990**, 28, 305.

6. Eisch, J. J.; King, R. B.; "Organometallic Syntheses," Academic Press: New York, **1965**, pp. 70-71.

7. Hendrickson, D. N.; Sohn, Y. S.; Gray, H. B. Inorg. Chem. **1971**, 10, 1559.

8. Kofen, W. G.; Backlawski, L. M. J. Org. Chem. **1976**, 41, 1879.

9. Shriver, D. F.; "The Manipulation of Air-Sensitive Compounds," McGraw-Hill: New York, **1969**.

10. Bard, A. J.; Faulkner, L. R. "Electrochemical Methods," Wiley: New York, **1980**.

11. (a) Hoffmann, R. J. Chem. Phys. **1963**, 39, 1397. (b) Hoffmann, R.; Libscomb, W. N. J. Chem. Phys. **1962**, 36, 3179.

12. Mealli, C.; Proserpio, D. M. J. Chem. Ed. **1990**, 67, 399.

13. Gordon, A. J.; Ford, R. A. "The Chemist's Companion," Wiley-Interscience: New York, **1972**.

CHAPTER III

RESULTS

A. Synthesis and Spectroscopic Properties of $PhCCo_3(CO)_7(bma)$

The reaction between $PhCCo_3(CO)_9$ and bma was initially examined in toluene solvent at 75 °C in an effort to prepare the diphosphine-substituted cluster $PhCCo_3(CO)_7(bma)$ (**2**). While the conditions chosen were identical to those employed in the synthesis of $PhCCo_3(CO)_7[(Z)\text{-}Ph_2PCH{=}CHPPh_2]$ (**4**) [1] (vide infra), the spectral properties (IR and NMR) of the isolated product did not match that of the expected cluster **2**. It was subsequently shown that the isolated product from the thermolysis reaction was the tricobalt cluster $Co_3(CO)_6[\mu_2\text{-}\eta^2,\eta^1\text{-}C(Ph)\overline{C{=}C(PPh_2)C(O)OC(O)}](\mu_2\text{-}PPh_2)$ (**3**) (vide infra). When the same reaction was carried out at 50 °C with monitoring by IR spectroscopy, no intermediates were observed and cluster **3** was again the only observed product. On the basis of the many examples of diphosphine-substituted $PhCCo_3(CO)_7P_2$ clusters that have been prepared and characterized, cluster **2** was considered to be a logical precursor to cluster **3**.[2-5] Therefore, efforts were made to synthesize the cluster **2** by alternative routes since this would allow for the exploration of the mechanism leading to the cluster **3**.

Treatment of an equimolar mixture of $PhCCo_3(CO)_9$ and bma with 2 equivalents of the oxidative-decarbonylation reagent Me_3NO [6] in either CH_2Cl_2 or THF at room temperature led to an immediate reaction, as judged by the immediate color change of the reaction solution from red-brown to green. IR and TLC analyses also supported this premise. Cluster **2** was

isolated in 70-80% yield after passage across a short silica gel column. Maximum yields of **2** were obtained by flash-column chromatography at -78 °C using CH_2Cl_2/petroleum ether (2 : 1) as the eluting solvent. **2** is very soluble in polar solvents, yielding green color solutions. **2** does not appear to be overly air-sentive in solution; however, it is extremely temperature sensitive.

The IR spectrum of **2** exhibits two ν (CO) bands at 2065 and 2015 cm^{-1} along with a weak ν (CO) band at 1986 cm^{-1}, which are assignable to terminal cobalt-carbonyl groups. The coordinated bma ligand displays two ν (CO) bands at 1824 (w) and 1772 (m) cm^{-1}, representing the vibrationally coupled asymmetric and symmetric carbonyl stretches, respectively. [7] The possibility that these last two assignments may represent μ_2-bridging carbonyl groups was ruled out by the preparation of cluster **2** that was isotopically enriched with ^{13}CO gas. Only the frequencies of the latter two carbonyl bands were unaffected, consistent with their anhydride nature.

A single, broad resonance at δ 37 in the $^{31}P\{^1H\}$ NMR spectrum was observed for cluster **2** in THF at room temperature. The presence of only one ^{31}P resonance along with its high-field location suggests that the ancillary bma ligand bridges adjacent cobalt centers. The same sample was next examined at -97 °C in order to reduce the scalar coupling between the ^{31}P and ^{59}Co nuclei. Reduced temperatures effectively serve to shorten the molecular correlation time (τ_c) and have been shown to afford sharper ^{31}P resonances in other phosphine-substituted cobalt clusters. [8] The low-temperature $^{31}P\{^1H\}$ NMR spectrum of **2** revealed the same bridging ^{31}P resonance that was observed at room temperature and the presence of two additional ^{31}P resonances at δ 54 and 62. These latter two resonances are deshielded relative

to the bridging bma resonance, making them readily assignable to a chelating bma ligand. [9] The fact that two new inequivalent ^{31}P resonances were observed at low temperatures indicates that both PPh_2 groups cannot reside in the equatorial plane defined by the cobalt atoms. This is, however,

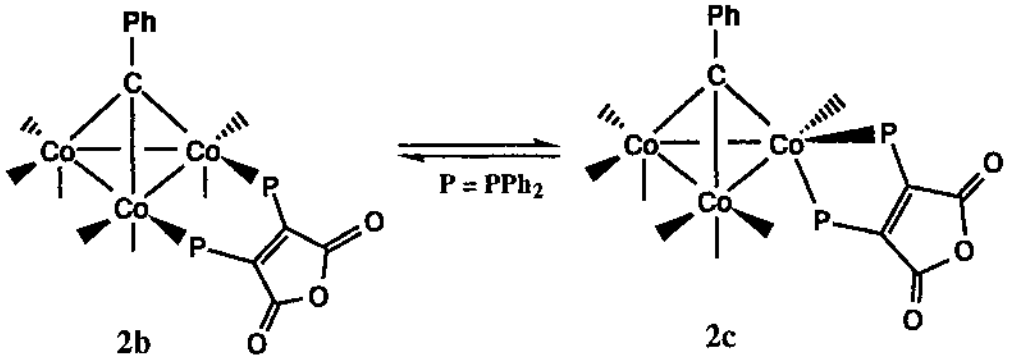

(3.1)

consistent with the presence of a chelating isomer with equatorial and axial PPh_2 groups. Warming this sample to -50°C led to the disappearance of the chelating ^{31}P resonances and was accompanied by the expected increase in the resonance at δ 37. Cooling the sample back down to -97 °C afforded the original spectrum and demonstrated the reversible nature of the interconversion between the bridging and chelating isomers of cluster **2**. This equilibration process is depicted in Equation 3.1, and a representative $^{31}P\{^1H\}$ NMR spectrum of **2** exhibiting both the bridging and chelating ^{31}P resonances is seen in Figure 3.1. Concern over the possibility that the chelating isomer may only reflect the existence of a separate and discrete impurity was eliminated by the invariant bridge/chelate ratio measured for different samples of **2**. $^{31}P\{^1H\}$ NMR measurements of **2** consistently gave a Keq = 5.7 in favor of the bridging isomer at -97 °C. Reactivity studies

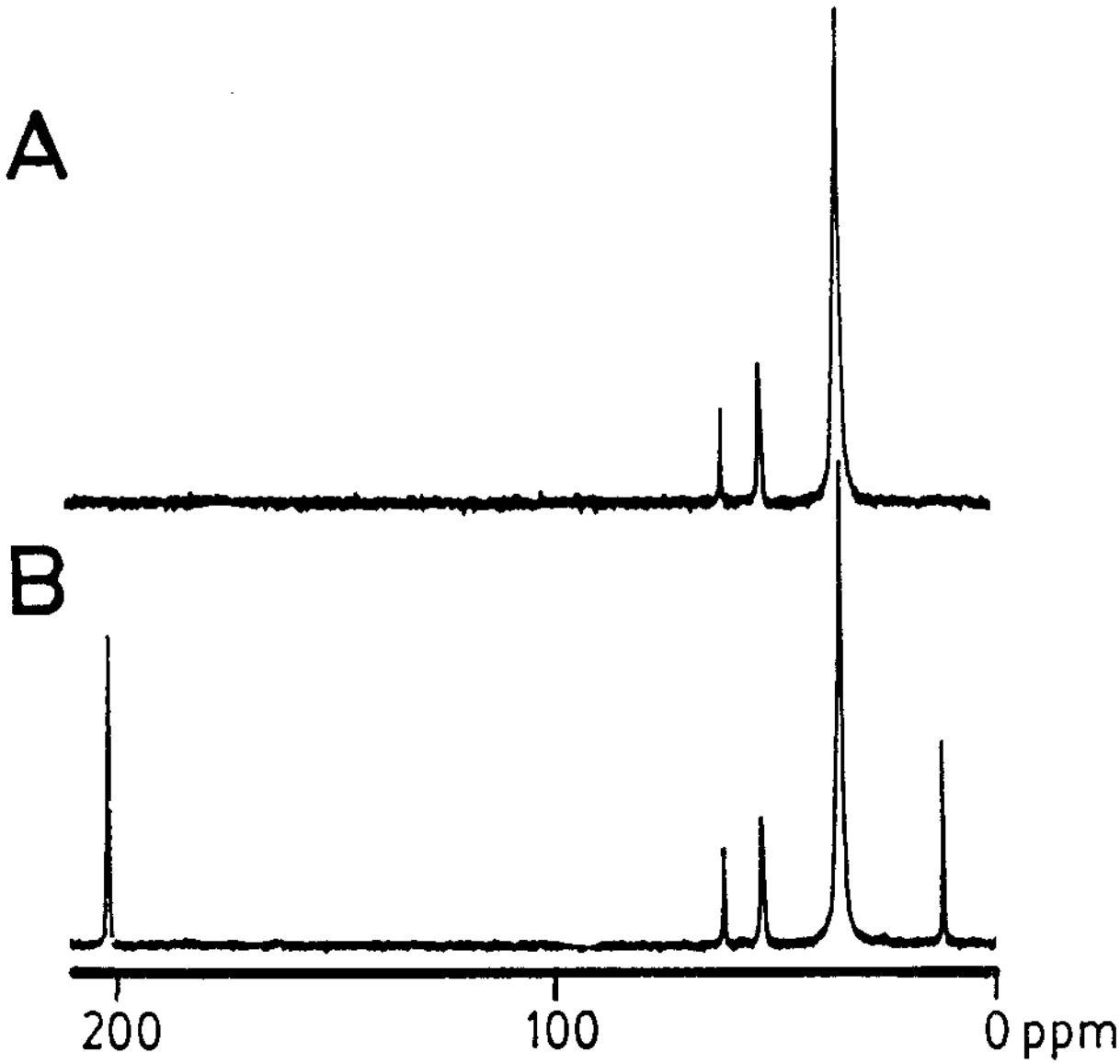

Figure 3.1 $^{31}P\{^{1}H\}$ NMR spectra of (A) $PhCCo_3(CO)_7(bma)$ before the thermolysis at 45 °C and (B) $PhCCo_3(CO)_7(bma)$ and $Co_3(CO)_6[\mu_2\text{-}\eta^2,\eta^1\text{-}C(Ph)\overline{C=C(PPh_2)C(O)OC(O)}](\mu_2\text{-}PPh_2)$ after the thermolysis at 45 °C. All $^{31}P\{^{1}H\}$ NMR spectra were recorded at -97 °C in THF.

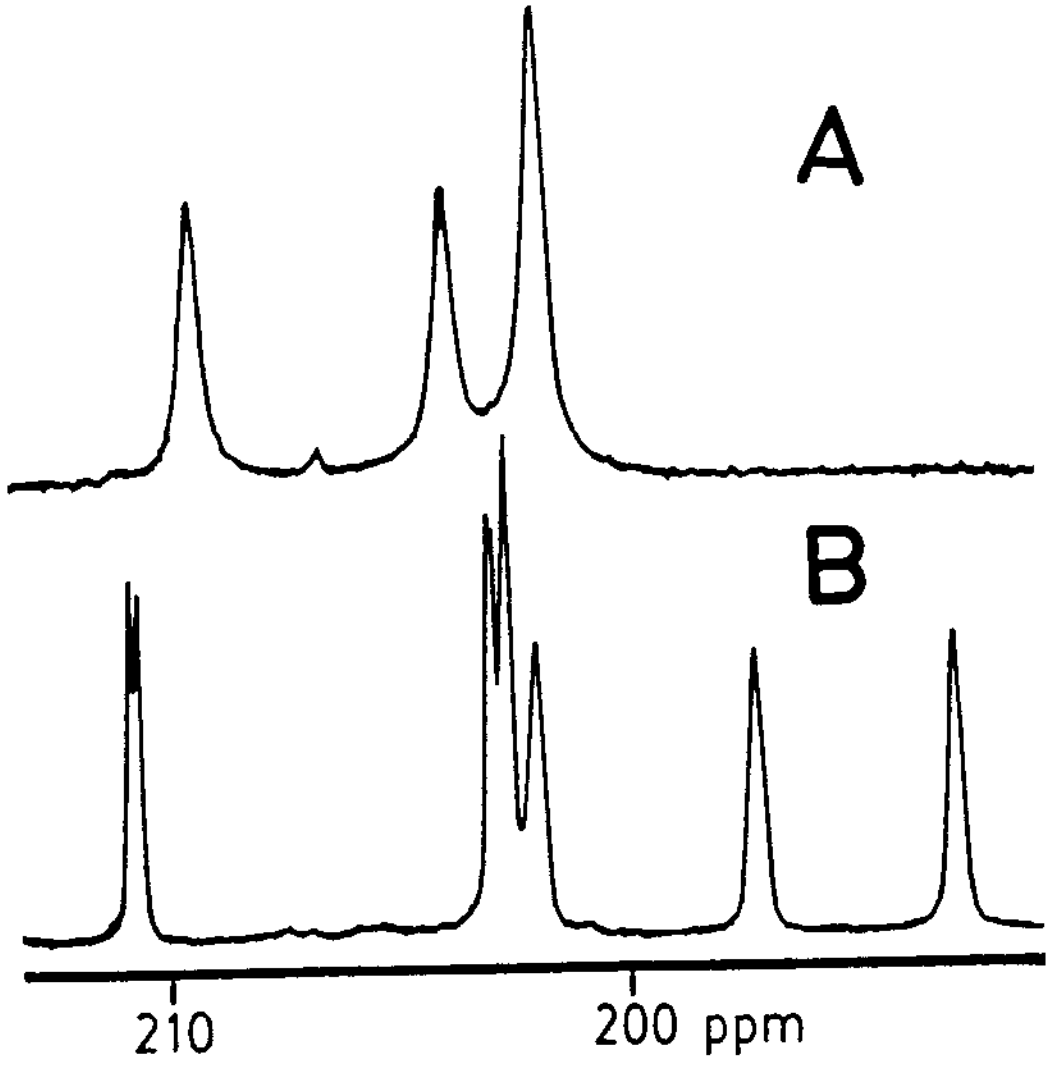

Figure 3.2. $^{13}C\{^1H\}$ NMR of (A) $PhCCo_3(CO)_7(bma)$ and (B) $Co_3(CO)_6[\mu_2\text{-}\eta^2,\eta^1\text{-}C(Ph)\overline{C=C(PPh_2)C(O)OC(O)}](\mu_2\text{-}PPh_2)$ recorded at -97 °C in THF.

involving the conversion of **2** to **3** also support the proposed temperature-dependent bma ligand equilibration process in **2** (vide infra).

It is believed that this bridge/chelate bma ligand equilibration is the first of its kind, and the olefinic bond of the bma ligand is believed to play a role in the equilibration process based on the absence of similar ^{31}P NMR behavior in the cluster $PhCCo_3(CO)_7(dppe)$, which contains a saturated diphosphine ligand. Here the bridging ^{31}P resonance is the only observed resonance over all temperatures measured. [10]

The solution structure of **2** was also investigated by variable-temperature $^{13}C\{^1H\}$ NMR spectroscopy. At -97 °C, three terminal carbonyl resonances at δ 209 (2C), 204 (2C), 202 (3C) with an integral ratio of 2 : 2 : 3, respectively, are observed. The above spectrum is identical to the published $^{13}C\{^1H\}$ NMR spectra for the diphosphine-bridged clusters $PhCCo_3(CO)_7(dppe)$ and $PhCCo_3(CO)_7[(Z)\text{-}Ph_2PCH{=}CHPPh_2]$ (vida infra), whose chemical shift assignments and CO exchange pathways have been thoroughly discussed. [1] The major isomer of **2** in solution by both ^{31}P and ^{13}C NMR spectroscopy clearly possesses an equatorially disposed bridging bma ligand. Besides these three major carbonyl resonances, a small resonance at ~δ 207 is seen and assigned to the minor chelating bma isomer of **2**. The presence of only one carbonyl resonance for this isomer indicates that intramolecular CO exchange is still rapid at -97 °C, conditions which would give rise to the single observed resonance. Alternatively, the other carbonyl groups of **2** (chelating) may be obscured by the CO groups associated with the bridged isomer of **2**. The former explanation is favored at this point since it is known that CO scrambling is, as a rule of thumb, generally faster than that of the phosphine-ligand scrambling. [5,8b] The low-temperature ^{13}C NMR spectrum

of **2** is shown in Figure 3.2.

As the temperature is raised to -50 °C, the carbonyl resonances broaden, more or less at the same rate, and merge to give a single, broad resonance at δ 205, which is in agreement with the weighted-average chemical shift for the bridging isomer of **2**. Further warming to room temperature leads to a slight sharpening of the resonance at δ 205. This ^{13}C NMR behavior is fully reversible as evidenced by repeated cooling and warming cycles. The ^{13}C NMR data of **2** agree well with the reported $^{31}P\{^1H\}$ NMR data, where the bridging isomer is the major isomer in solution at ambient temperature. The dynamic NMR behavior underscores the extreme ease by which the ancillary bma and CO groups interconvert in solution.

B. Synthesis and Spectroscopic Properties of $Co_3(CO)_6[\mu_2\text{-}\eta^2, \eta^1\text{-}C(Ph)C{=}C(PPh_2)C(O)OC(O)](\mu_2\text{-}PPh_2)$

Cluster **2** readily loses CO and transforms to cluster **3** upon gentle heating in a variety of solvents. These thermolysis reactions unequivocally establish the intermediacy of the diphosphine cluster **2** in the formation of **3** and allow the overall reaction to be delineated as illustrated in Equation 3.2. The inability to observe cluster **2** in the thermolysis reactions involving $PhCCo_3(CO)_9$ and bma provides an important view on the relative rates of formation for clusters **2** and **3**. Starting from cluster $PhCCo_3(CO)_9$, the observation of cluster **2** is not expected if the subsequent reactions leading to **3** all occur at faster rates. Independent kinetic measurements that confirm this scenario are discussed in the next section.

Cluster **3** was isolated by chromatography over silica gel using CH_2Cl_2

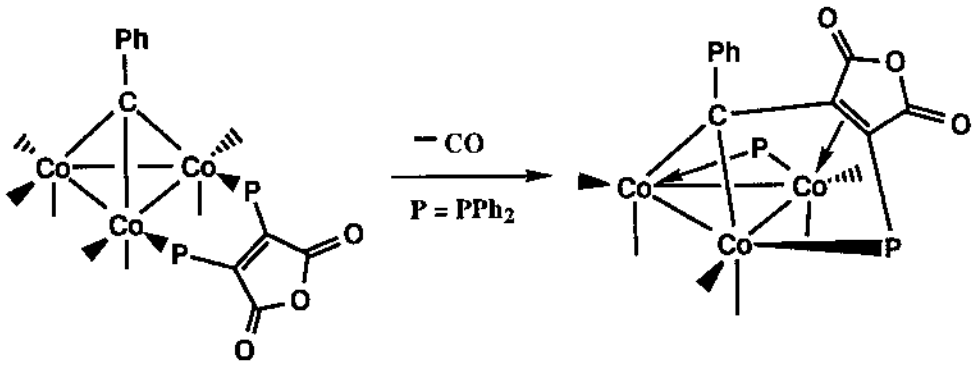

(3.2)

solvent and characterized spectroscopically in solution. The IR spectrum of **3** displays terminal carbonyl stretching bands at 2062 (m), 2042 (vs), 2025 (vs), 2010 (s), and 1939 (m) cm^{-1} along with the characteristic bma carbonyl bands at 1811 and 1749 cm^{-1}. As with the precursor cluster **2**, these latter two bands are assigned to the asymmetric and symmetric ν (C=O) modes of the anhydride moiety. [7] The $^{31}P\{^1H\}$ NMR spectrum of **3** showed a pair of equal intensity resonances at δ 201.0 and 12.0, which are attributed to a μ_2-phosphido and a coordinated Co-PR_3 group, respectively. A ^{13}C-enriched sample of **3** was prepared and the $^{13}C\{^1H\}$ NMR spectrum was recorded at -97 °C to reduce the undesired quadrupolar broadening between the Co-CO nuclei. The resulting spectrum exhibited six, equal-intensity resonances as shown in Figure 3.2b. Of these resonances, the two downfield resonances centered at δ 210.5 and 202.9 reveal phosphorus coupling with $J_{P\text{-}C}$ values of 12.3 and 7.9 Hz, respectively. No further effort has been made to assign these resonances to a specific CO group. The observation of six CO groups supports the static structure of **3** shown in Equation 3.2. In comparison to the dynamic ligand behavior observed in **2**, **3** maintains a static structure over the temperature range of -97 °C to room temperature.

A study of the conversion of **2** to **3** was carried out by $^{31}P\{^1H\}$ NMR spectroscopy, which strongly supports the equilibrium between the chelating

and bridging isomers of **2**. The -97 °C $^{31}P\{^1H\}$ NMR spectrum of a 0.034 M THF solution of **2** was initially examined before the thermolysis reaction. The spectrum is shown in Figure 3.1a, and as discussed, a Keq value of about 5.7 in favor of the bridged-bma isomer was obtained. The same sample was next removed from the spectrometer probe and placed in a temperature-controlled bath at 45 °C for a period of time sufficient to effect partial conversion to cluster **3**. After quenching the sample in a dry ice/acetone bath, the $^{31}P\{^1H\}$ NMR spectrum was recorded again at -97 °C. The resulting spectrum, which is shown in Figure 3.1b, reveals the presence of cluster **3**, on the basis of the resonances at δ 201.0 and 12.0, and cluster **2**. More importantly, the ratio of the bridging and chelating isomers of **2** remained unchanged relative to the initial spectrum, evidence which supports a facile equilibrium between these two isomers.

C. Synthesis and Spectroscopic Properties of $PhCCo_3(CO)_7[(Z)\text{-}Ph_2PCH=CHPPh_2]$

A clean reaction between $PhCCo_3(CO)_9$ and $(Z)\text{-}Ph_2PCH=CHPPh_2$ was observed when equimolar amounts of reactants were heated overnight at 75 °C. TLC analysis revealed the presence of a slower moving material that is readily assigned to the product cluster, $PhCCo_3(CO)_7[(Z)\text{-}Ph_2PCH=CHPPh_2]$ (**4**). Cluster **4** was isolated in 75% yield by chromatography using silica gel

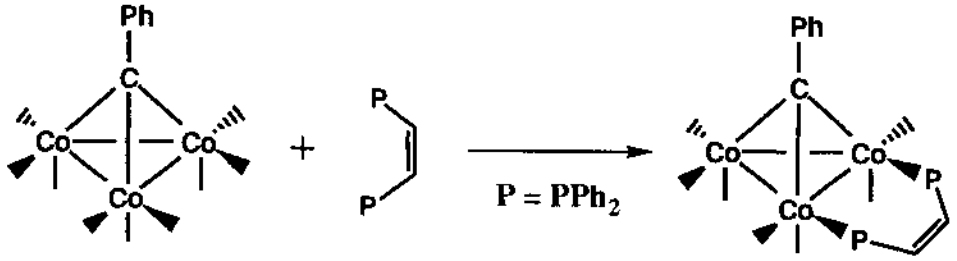

(3.3)

and CH_2Cl_2/petroleum ether mixture solvent. Alternative synthetic methods were also examined as a route to cluster **4**. Me_3NO-promoted oxidative decarbonylation [6] and sodiobenzophenone ketyl-initiated electron-transfer chain (ETC) [11] reactions also gave cluster **4** in isolated yields that ranged from 50 to 70% (Equation 3.3).

The IR spectrum of **4** in CH_2Cl_2 revealed two prominent ν (CO) bands at 2057 (s) and 2006 (vs) cm^{-1}, which are assigned to terminal carbonyl groups, along with a very weak ν (CO) band at 1831 cm^{-1}. The intensity pattern and frequency of these terminal carbonyl bands are in agreement with the IR data reported for the diphosphine-bridged cluster $PhCCo_3(CO)_7(dppe)$.[4] The $^{31}P\{^1H\}$ NMR spectrum of a sample of **4**, recorded at -57 °C, exhibited a major (> 95%) ^{31}P resonance at δ 36.2 along with a pair of equal intensity resonances at δ 77.7 and 103.6. The major resonance is assigned to cluster **4** with a bridging diphosphine ligand, while the minor species is ascribed to the isomeric cluster possessing a chelating diphosphine ligand. A chelating diphosphine ligand may be rationalized due to the existence of two highly deshieled, inequivalent ^{31}P resonances. [2b,9] The possibility of a chelate-to-bridge equilibration reaction involving $PhCCo_3(CO)_7[(Z)\text{-}Ph_2PCH{=}CHPPh_2]$ has been ruled out since the amount of the chelating isomer remained unchanged relative to the bridging isomer in a variety of solvents and different temperatures.

The variable-temperature $^{13}C\{^1H\}$ NMR behavior of **4** was examined next by using a sample of **4** that was ~ 20-30% enriched in ^{13}CO. The limiting spectrum of **4** at -97 °C reveals the presence of three terminal carbonyl resonances at δ 211, 204, and 203 with a relative integral ratio of 2 : 2 : 3, respectively. The two resonances at δ 211, 204 are assigned to the pairwise

equivalent axial and equatorial carbonyl groups at the phosphine-substituted cobalt centers. [5,12] The remaining high-field resonance at δ 203 represents the carbonyls associated with the cobalt tricarbonyl group, which are rendered magnetically equivalent as a result of rapid, intramolecular 3-fold carbonyl scrambling. [13] As the temperature is raised to -57 °C, the carbonyl resonances broaden, more or less at the same rate, and merge to give a single, broad resonance at δ 206, which is in agreement with the weighted-average chemical shift. Further warming to room temperature promotes rapid, intramolecular carbonyl scrambling about the cluster polyhedron; this gives rise to a ^{13}C NMR spectrum possessing a single sharp resonance at δ 206. Using the CO exchange pathways proposed by McGlinchey [5] for related tetrahedron clusters along with the knowledge of the limiting ^{13}C chemical shifts and the coalescence temperature, τ_c, an activation energy of ~ 9.6 kcal/mol for the complete carbonyl scrambling in **4** is calculated. [14] This value is in excellent agreement with the data reported by McGlinchey. [5]

D. Kinetic Study on the Transformation of 2 to 3.

The kinetics for the reaction of **2** to **3** were investigated by IR spectroscopy in THF solution over the temperature range of 27-57 °C. The reaction followed first-order kinetics over a period of 2-3 half-lives, and the reported first-order rate constants, which are quoted in Table 3.1, were calculated by monitoring the absorbance decrease in the bma band at 1772 cm^{-1} of **2**. Changing the solvent from THF to either CH_2Cl_2 or 2,5-dimethyl-THF (entries 3 and 6) did not affect the rate of the reaction, but the introduction of CO (1 atm) resulted in a sharp retardation in the rate. Entries 2 and 4 allow for a direct comparison of the effect of the CO on this reaction.

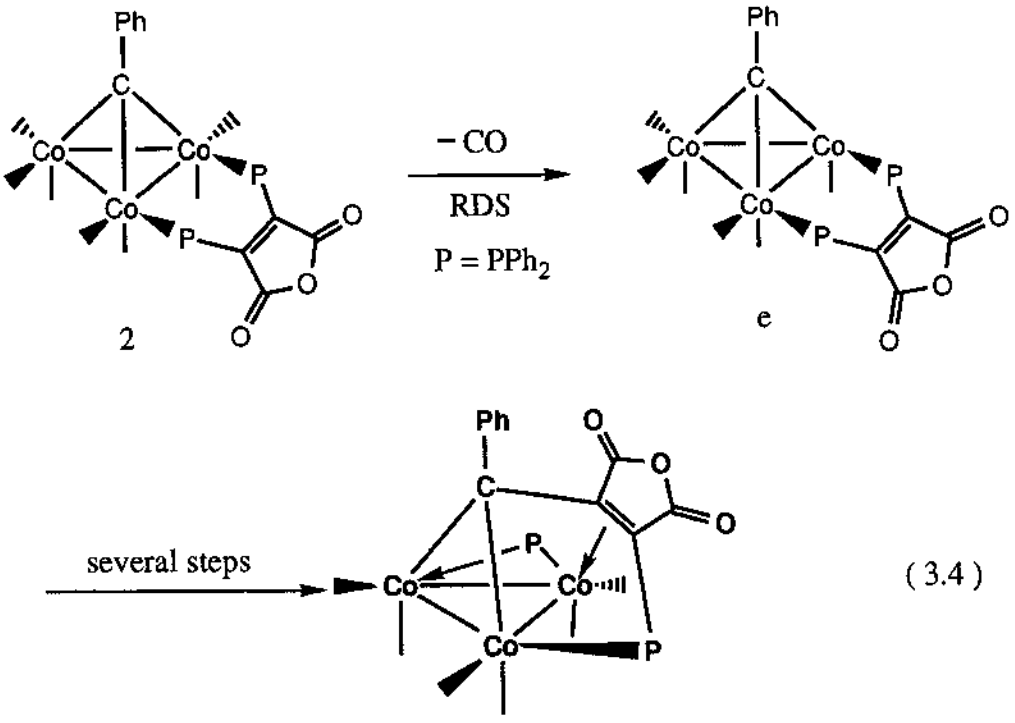

(3.4)

The presence of CO slows the formation of cluster **3** down by a factor of almost 36. These data suggest that the rate-determing step is best described by an unimolecular mechanism involving dissociative CO loss, as outlined in Equation 3.4. Treating the unsaturated intermediate $PhCCo_3(CO)_6(bma)$ (**e**) within the steady-state approximation affords the rate law:

$$\text{rate} = \frac{k_1 k_2[PhCCo_3(CO)_7(bma)]}{k_{-1}[CO] + k_2}$$

which, in the absence of added CO ($k_2 > k_{-1}[CO]$), reduces to rate = $k_1[PhCCo_3(CO)_7(bma)]$, as expected for a dissociative mechanism. The observed CO inhibition and the enthalpy of activation ($\Delta H^{\neq} = 29.9 \pm 2.2$

Table 3.1 Experimental Rate Constants for the Reaction of $PhCCo_3(CO)_7(bma)$ (**2**) to $Co_3(CO)_6[\mu_2\text{-}\eta^2,\eta^1\text{-}C(Ph)\overline{C=C(PPh_2)C(O)C(O)}](\mu_2\text{-}PPh_2)$ (**3**) [a]

Entry no.	Temperature (°C)	$10^5 k_{obsd}$,[b] s^{-1}
1	27.0	3.7 ± 0.8
2	34.2	18.10 ± 0.02
3[c]	34.2	20 ± 1
4[d]	34.2	0.51 ± 0.06
5	43.6	63 ± 6
6[e]	43.6	63 ± 9
7	50.2	185 ± 24
8	57.0	368 ± 18

[a]From ~ 8.2×10^{-3} M $PhCCo_3(CO)_7(bma)$ in THF by following the disappearance of the 1772 cm^{-1} IR band. All THF kinetic data quoted represent the average of two measurements. [b]Error limits at 95% confidence level. [c]CH_2Cl_2 used as solvent. [d]In the presence of 1 atm of CO. [e]2,5-Me_2THF used as solvent.

kcal/mol) and the entropy of activation ($\Delta S^{\neq} = 21 \pm 6$ eu) are fully consistent with the proposed mechanism. It is noteworthy to mention here that this mechanism does not give any information concerning the timing of the P-C bond cleavage of the bma ligand and formation of the μ_2-η^2,η^1-benzylidene(diphenylphosphino)-maleic anhydride ligand because these steps occur after the rate-determing step. However, the lower limit for the rates of these steps cannot be less than the reported rates in Table 3.1.

E. X-Ray Diffraction Structure of $PhCCo_3(CO)_7$(bma)

Single crystals of **2** were grown from CH_2Cl_2 solution containing **2** that had been layered with heptane. Compound **2** exists as discrete molecules in the unit cell with no unusually short inter- or intramolecular contacts. The X-ray data collection and processing parameters for **2** are given in Table 3.2, with the selected bond distances and angles given in Table 3.3. The ORTEP diagram is shown in Figure 3.3.

F. X-Ray Diffraction Structure of $Co_3(CO)_6[\mu_2$-η^2,η^1-$C(Ph)\overline{C=C(PPh_2)C(O)C(O)}](\mu_2$-$PPh_2)$

Single crystals of **3** were grown from CH_2Cl_2 solution containing **3** that had been layered with heptane. Compound **3** exists as discrete molecules in the unit cell with no unusually short inter- or intramolecular contacts. The X-ray data collection and processing parameters for **3** are given in Table 3.4, with the selected bond distances and angles given in Table 3.5. The ORTEP diagram is shown in Figure 3.4.

Table 3.2. X-Ray Crystallographic Collection and Processing Data for $PhCCo_3(CO)_7(bma)$ (**2**)

Space group	$Pna2_1$, orthorhombic
Cell Constants	
a, Å	20.488 (2)
b, Å	10.620 (1)
c, Å	17.665 (1)
V, Å^3	3843.8 (9)
mol formula	$C_{42}H_{25}Co_3O_{10}P_2$
fw	928.41
formula units per cell (Z)	4
p, g • cm^{-3}	1.604
abs coeff (μ), cm^{-1}	14.17
radiation Mo Kα (λ), Å	0.71073
collection range, deg	$2.0 \leq 2\theta \leq 40.0$
scan speed range, deg•min^{-1}	0.67-8.0
total data collected	2080
independent data	2080
independent data, $I > 3\sigma(I)$	1344
R	0.0367
R_w	0.0391
weights	$[0.04F^2 + (\sigma F)^2]^{-1}$

Table 3.3. Selected Bond Distances (Å) and Angles (deg) for $PhCCo_3(CO)_7(bma)$ (**2**)[a]

		bond distances	
Co(1)-Co(2)	2.504(3)	Co(1)-Co(3)	2.505(2)
Co(2)-Co(3)	2.411(3)	Co(1)-P(1)	2.247(4)
Co(1)-P(2)	2.198(4)	Co(1)-C(1)	1.80(1)
Co(1)-C(7)	1.89(1)	Co(1)-C(16)	1.91(1)
Co(2)-C(1)	2.24(1)	Co(2)-C(2)	1.79(2)
Co(2)-C(3)	1.74(2)	Co(2)-C(4)	1.88(2)
Co(2)-C(16)	1.94(1)	Co(3)-C(4)	2.02(2)
Co(3)-C(5)	1.77(1)	Co(3)-C(6)	1.74(2)
Co(3)-C(7)	1.91(1)	Co(3)-C(16)	1.96(1)
O(1)-C(1)	1.16(2)	O(2)-C(2)	1.13(2)
O(3)-C(3)	1.15(2)	O(4)-C(4)	1.15(2)
O(5)-C(5)	1.16(2)	O(6)-C(6)	1.16(2)
O(7)-C(7)	1.21(2)	O(12)-C(12)	1.14(2)
O(13)-C(12)	1.40(2)	O(13)-C(14)	1.39(2)
O(14)-C(14)	1.19(2)	C(11)-C(12)	1.53(2)
C(11)-C(15)	1.33(2)	C(14)-C(15)	1.47(2)
C(16)-C(17)	1.39(2)		
		bond angles	
Co(2)-Co(1)-Co(3)	57.53(8)	Co(1)-Co(2)-Co(3)	61.25(7)
Co(1)-Co(3)-Co(2)	61.21(7)	Co(2)-Co(1)-P(1)	123.1(1)
Co(2)-Co(1)-P(2)	144.4(1)	Co(2)-Co(1)-C(1)	60.2(4)
Co(3)-Co(1)-C(7)	48.9(4)	P(1)-Co(1)-P(2)	90.5(1)

Table 3.3. continued

P(1)-Co(1)-C(16)	172.0(4)	P(2)-Co(1)-C(16)	97.3(4)
Co(3)-Co(2)-C(4)	54.4(5)	C(2)-Co(2)-C(3)	102.8(7)
C(2)-Co(2)-C(16)	158.4(6)	C(3)-Co(2)-C(16)	96.7(7)
C(5)-Co(3)-C(6)	102.3(7)	C(5)-Co(3)-C(16)	160.2(6)
C(6)-Co(3)-C(16)	97.3(7)	Co(1)-C(1)-O(1)	160.(1)
Co(2)-C(1)-O(3)	124.(1)	Co(2)-C(2)-O(2)	175.(1)
Co(2)-C(3)-O(3)	176.(2)	Co(2)-C(4)-Co(3)	76.5(5)
Co(2)-C(4)-O(4)	148.(2)	Co(3)-C(4)-O(6)	177.(2)
Co(1)-C(7)-Co(3)	82.5(5)	Co(1)-C(7)-O(7)	143.(1)
Co(3)-C(7)-O(7)	135.(1)		

[a]Numbers in parentheses are estimated standard deviations in the least significant digits.

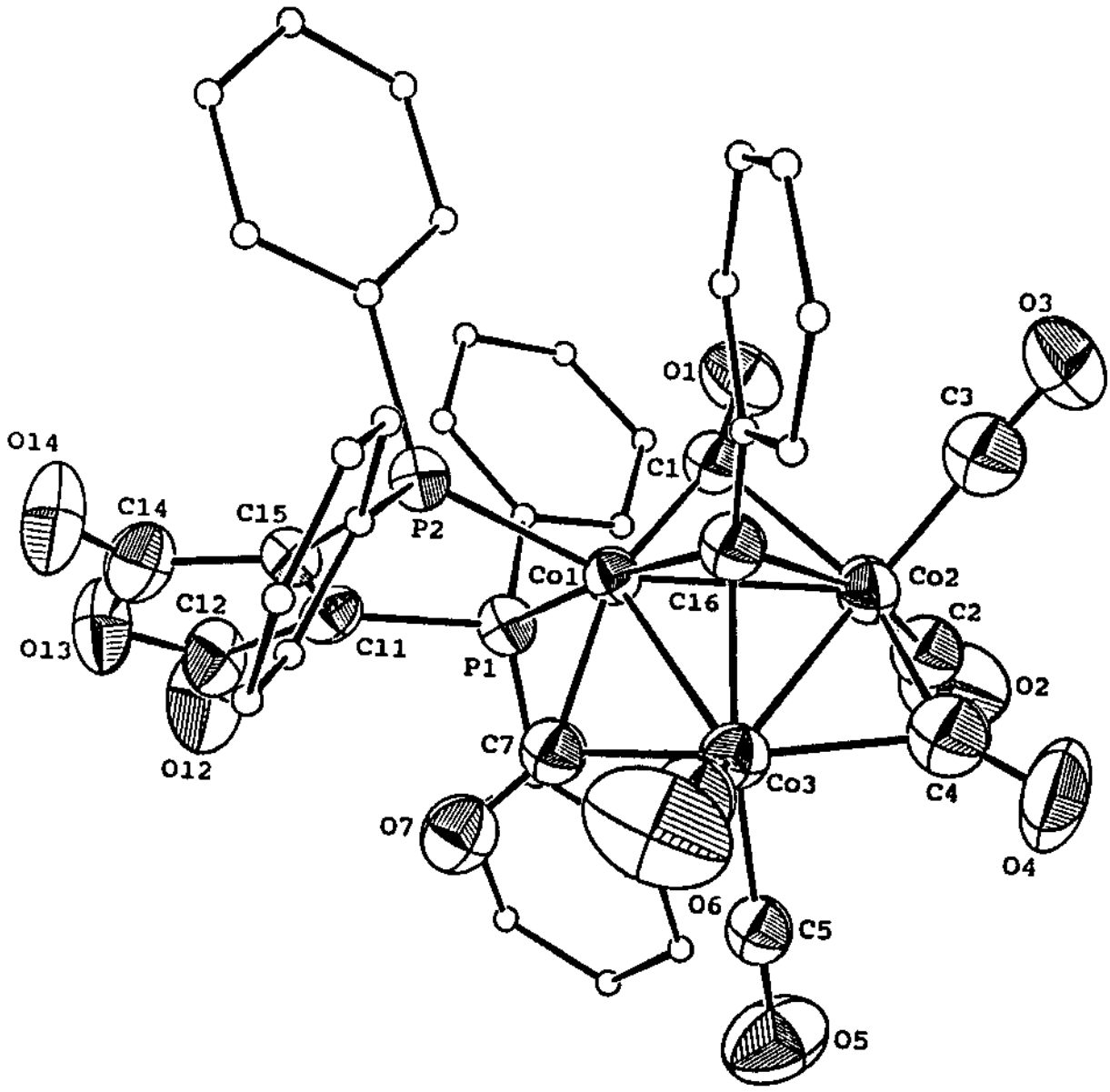

Figure 3.3. ORTEP diagram of the tricobalt cluster $PhCCo_3(CO)_7(bma)$ with the thermal ellipsoids drawn at the 50% probability level. H atoms are omitted for clarity.

Table 3.4. X-Ray Crystallographic Collection and Processing Data for $Co_3(CO)_6[\mu_2\text{-}\eta^2,\eta^1\text{-}C(Ph)\overline{C=C(PPh_2)C(O)OC(O)}](\mu_2\text{-}PPh_2)$ (3)

Space group	P 2_1/n, monoclinic (#14)
Cell Constants	
a, Å	11.538 (1)
b, Å	17.0754 (8)
c, Å	19.506 (1)
β, deg	92.108 (7)
V, Å^3	3840.4 (7)
mol formula	$C_{41}H_{25}Co_3O_9P_2$
fw	900.40
formula units per cell (Z)	4
p, g • cm^{-3}	1.557
abs coeff (μ), cm^{-1}	14.14
radiation Mo Kα (λ), Å	0.71073
collection range, deg	$2.0 \leq 2\theta \leq 44.0$
scan speed range, deg•min^{-1}	0.67-8.0
total data collected	5169
independent data	4898
independent data, $I > 3\sigma(I)$	2012
R	0.0392
R_w	0.0432
weights	$[\,0.04F^2 + (\sigma F)^2\,]^{-1}$

Table 3.5. Selected Bond Distances (Å) and Angles (deg) for $Co_3(CO)_6[\mu_2\text{-}\eta^2,\eta^1\text{-}C(Ph)C{=}C(PPh_2)C(O)C(O)](\mu_2\text{-}PPh_2)$ (3)[a]

bond distances			
Co(1)-Co(2)	2.576(2)	Co(1)-Co(3)	2.412(2)
Co(2)-Co(3)	2.696(2)	Co(1)-C(1)	1.72(1)
Co(1)-C(2)	1.75(1)	Co(1)-C(16)	1.92(1)
Co(2)-P(1)	2.264(3)	Co(2)-C(3)	1.79(1)
Co(2)-C(4)	1.78(1)	Co(2)-C(11)	2.06(1)
Co(2)-C(15)	2.12(1)	Co(3)-P(2)	2.234(3)
Co(3)-C(5)	1.81(1)	Co(3)-C(6)	1.79(1)
Co(3)-C(16)	2.023(9)	C(1)-O(1)	1.17(1)
C(2)-O(2)	1.15(1)	C(3)-O(3)	1.14(1)
C(4)-O(4)	1.15(1)	Co(1)-P(1)	2.129(3)
C(5)-O(5)	1.13(1)	C(6)-O(6)	1.13(1)
C(12)-O(12)	1.20(1)	C(12)-O(13)	1.40(1)
O(13)-C(14)	1.39(1)	C(14)-O(14)	1.18(1)
C(16)-C(15)	1.47(1)	C(11)-C(15)	1.45(1)
bond angles			
Co(2)-Co(1)-Co(3)	65.34(6)	Co(1)-Co(2)-Co(3)	54.40(5)
Co(1)-Co(3)-Co(2)	60.26(5)	Co(3)-Co(1)-C(16)	54.2(3)
P(1)-Co(1)-C(1)	101.0(4)	P(1)-Co(1)-C(2)	108.6(4)
C(1)-Co(1)-C(2)	106.1(5)	C(1)-Co(1)-C(16)	106.3(5)
C(2)-Co(1)-C(16)	98.0(5)	P(1)-Co(2)-C(11)	150.9(3)
P(1)-Co(2)-C(15)	110.9(3)	C(3)-Co(2)-C(4)	97.4(5)
C(3)-Co(2)-C(11)	100.3(4)	C(3)-Co(2)-C(15)	101.9(4)

Table 3.5. continued

C(4)-Co(2)-C(11)	104.8(4)	C(4)-Co(2)-C(15)	142.7(4)
C(11)-Co(2)-C(15)	40.6(4)	Co(1)-Co(3)-C(16)	50.4(3)
Co(2)-Co(3)-C(16)	73.5(3)	P(2)-Co(3)-C(5)	108.0(3)
P(2)-Co(3)-C(6)	103.7.(4)	P(2)-Co(3)-Co(16)	85.8(3)
C(5)-Co(3)-C(6)	96.3(5)	C(5)-Co(3)-C(16)	158.8(4)
C(6)-Co(3)-C(16)	95.8(4)	Co(1)-P(1)-Co(2)	71.7(1)
Co(1)-C(1)-O(1)	169(1)	Co(1)-C(2)-O(2)	174.(1)
P(2)-Co(3)-C(6)	103.7.(4)	P(2)-Co(3)-Co(16)	85.8(3)
Co(2)-C(3)-O(3)	179(1)	Co(2)-C(4)-O(4)	176(1)
Co(3)-C(5)-O(5)	177(1)	Co(3)-C(6)-O(6)	176(1)

[a]Numbers in parentheses are estimated standard deviations in the least significant digits.

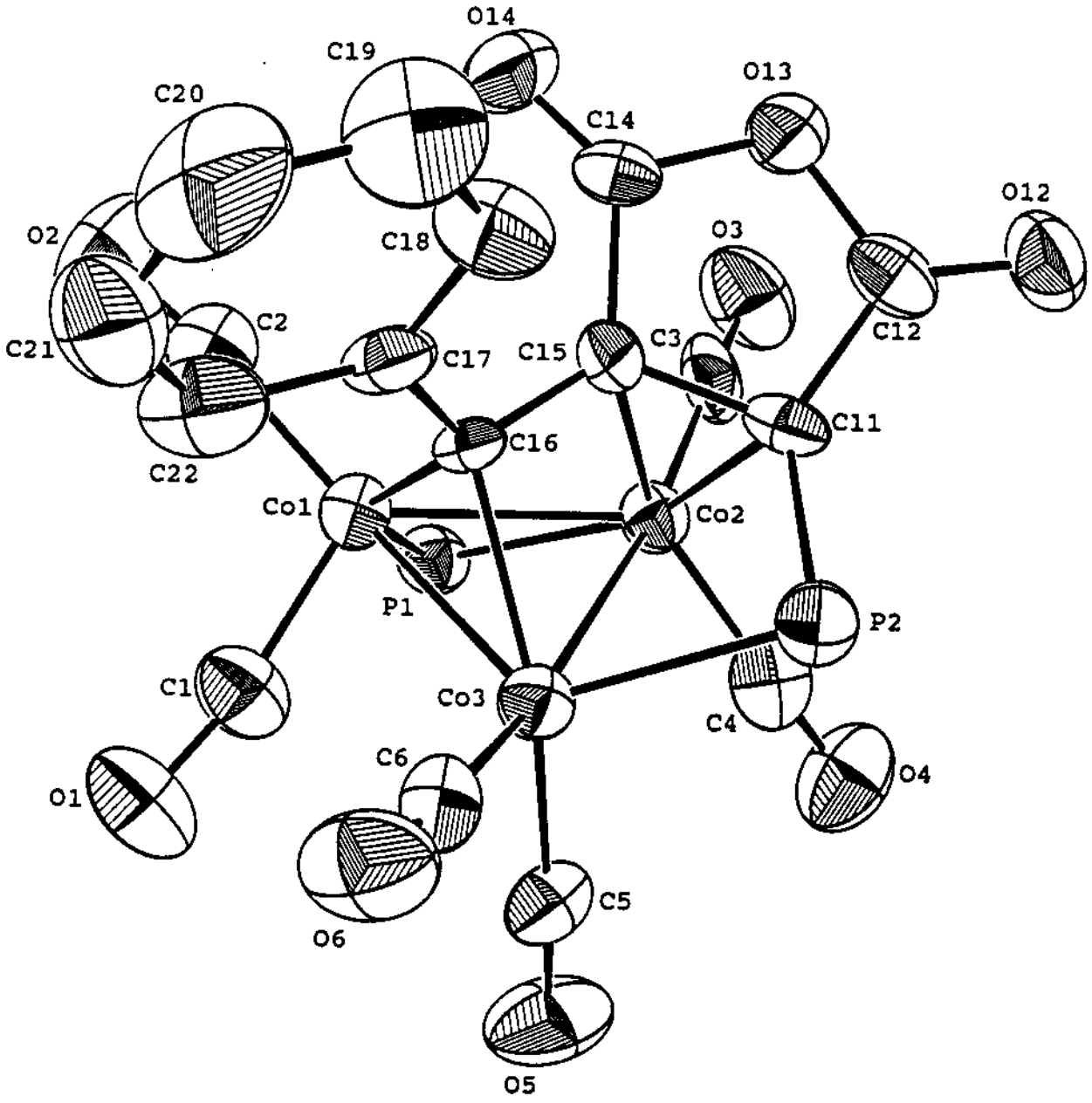

Figure 3.4. ORTEP diagram of $Co_3(CO)_6[\mu_2\text{-}\eta^2,\eta^1\text{-}C(Ph)\overline{C=C(PPh_2)C(O)OC(O)}](\mu_2\text{-}PPh_2)$ with the thermal ellipsoids drawn at the 50% probability level. H atoms are omitted for clarity.

Table 3.6. X-Ray Crystallographic Collection and Processing Data for $PhCCo_3(CO)_7[(Z)\text{-}Ph_2PCH{=}CHPPh_2]$ (4)

Space group	P $2_1/n$, monoclinic
Cell Constants	
a, Å	12.7065 (9)
b, Å	18.385 (2)
c, Å	15.943 (1)
β, deg	98.025 (6)
V, Å^3	3688.0 (5)
mol formula	$C_{40}H_{27}Co_3O_7P_2$
fw	858.40
formula units per cell (Z)	4
ρ, g • cm^{-3}	1.546
abs coeff (μ), cm^{-1}	14.65
radiation Mo Kα (λ), Å	0.71073
collection range, deg	$2.0 \leq 2\theta \leq 44.0$
scan speed range, deg•min^{-1}	0.67-8.0
total data collected	5169
independent data	4786
independent data, $I > 3\sigma(I)$	2021
R	0.0445
R_w	0.0488
weights	$[(\sigma F_o)^2]^{-1}$

Table 3.7. Selected Bond Distances (Å) and Angles (deg) for $PhCCo_3(CO)_7[(Z)\text{-}Ph_2PCH{=}CHPPh_2]$ (**4**)[a]

		bond distances	
Co(1)-Co(2)	2.473(2)	Co(1)-Co(3)	2.483(2)
Co(1)-P(1)	2.206(3)	Co(1)-C(1)	1.75(1)
Co(1)-C(2)	1.79(1)	Co(1)-C(10)	1.88(1)
Co(2)-Co(3)	2.486(2)	Co(1)-C(1)	1.75(1)
Co(1)-P(2)	2.206(3)	Co(2)-C(4)	1.75(1)
Co(3)-C(5)	1.75(1)	Co(3)-C(7)	1.74(1)
C(1)-O(1)	1.16(1)	P(2)-C(9)	1.81(1)
C(2)-O(2)	1.14(1)	C(3)-O(3)	1.14(1)
Co(2)-C(3)	1.79(1)	C(4)-O(4)	1.16(1)
C(6)-O(6)	1.15(2)	C(7)-O(7)	1.17(2)
C(8)-C(9)	1.31(1)	Co(2)-C(3)	1.79(1)
Co(2)-C(10)	1.90(1)	Co(3)-C(6)	1.80(1)
Co(3)-C(10)	1.94(1)	P(1)-C(8)	1.816(9)
		bond angles	
Co(2)-Co(1)-Co(3)	60.22(6)	C(3)-Co(2)-C(4)	98.9(6)
C(3)-Co(2)-C(10)	143.0(4)	C(4)-Co(2)-C(10)	106.7(5)
C(1)-Co(1)-C(2)	99.8(5)	C(1)-Co(1)-C(10)	107.0(5)
C(2)-Co(1)-C(10)	140.2(5)	C(5)-Co(3)-C(6)	101.9(6)
C(5)-Co(3)-C(7)	94.0(6)	C(6)-Co(3)-C(7)	107.2(6)
C(6)-Co(3)-C(10)	141.9(5)	C(7)-Co(3)-C(10)	96.5(5)
Co(1)-P(1)-C(8)	117.8(4)	Co(2)--P(2)-C(9)	118.1(3)
Co(2)-C(3)-O(3)	177.(1)	Co(2)-C(4)-O(4)	178.(1)

Table 3.7. continued

Co(3)-C(5)-O(5)	178.(1)	Co(3)-C(6)-O(6)	178.(1)
Co(3)-C(7)-O(7)	176.(1)	P(1)-C(8)-C(9)	126.0(8)
P(2)-C(9)-C(8)	128.0(7)	C(10)-C(11)-C(12)	123.(1)
C(10)-C(11)-C(16)	120(1)	C(12)-C(11)-C(16)	117(1)
C(11)-C(12)-C(13)	121.(1)	C(12)-C(13)-C(14)	120.(1)
C(13)-C(14)-C(15)	120.(1)	C(14)-C(15)-C(16)	120.(1)
C(11)-C(16)-C(15)	122.(1)	P(1)-Co(1)-C(1)	94.2(4)
P(1)-Co(1)-C(10)	101.3(3)	P(2)-Co(2)-C(3)	103.6(4)
P(2)-Co(2)-C(10)	101.1(3)	P(2)-Co(2)-C(4)	93.5(4)
P(1)-C(9)-C(8)	128.0(7)	Co(1)-Co(3)-Co(2)	59.69(6)
Co(1)-Co(3)-Co(5)	151.9(4)	Co(1)-Co(3)-Co(6)	97.7(5)
Co(1)-Co(3)-C(7)	99.1(5)	Co(1)-Co(3)-C(10)	48.3(3)
Co(2)-Co(3)-C(5)	96.2(4)	Co(2)-Co(3)-C(6)	102.8(5)
Co(2)-Co(3)-C(7)	145.5(4)	Co(2)-Co(3)-C(10)	49.0(3)
Co(1)-C(10)-Co(2)	81.8(4)	Co(1)-C(10)-C(11)	136.5(8)
Co(2)-C(10)-Co(3)	80.7(4)	Co(2)-C(10)-C(11)	131.8(7)
Co(3)-C(10)-C(11)	124.9(7)		

[a]Numbers in parentheses are estimated standard deviations in the least significant digits.

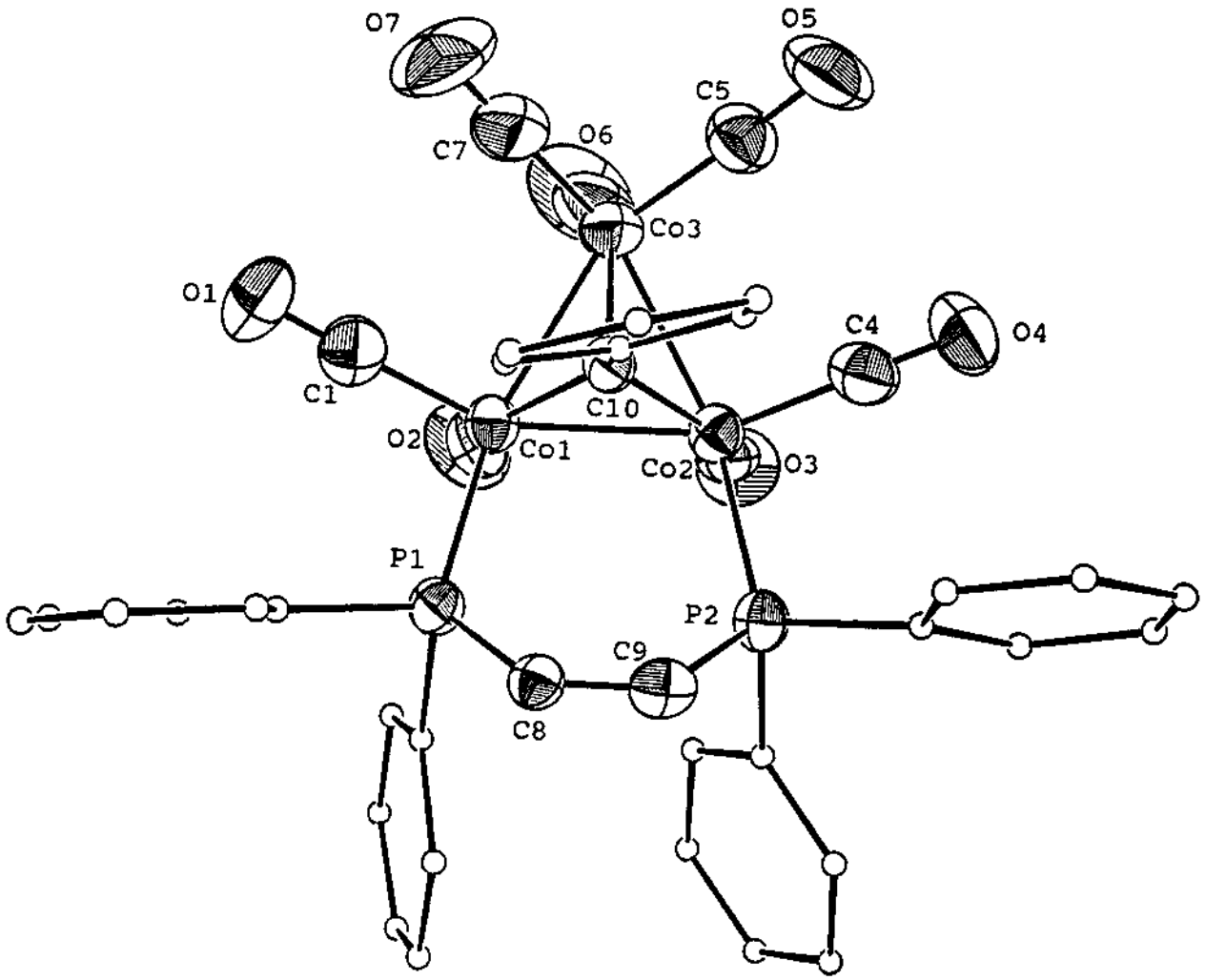

Figure 3.5. ORTEP diagram of $PhCCo_3(CO)_7[(Z)\text{-}Ph_2PCH{=}CHPPh_2]$ with the thermal ellipsoids drawn at the 50% probability level. H atoms are omitted for clarity.

G. X-Ray Diffraction Structure of $PhCCo_3(CO)_7[(Z)\text{-}Ph_2PCH{=}CHPPh_2]$

Single crystals of **4** were grown from a CH_2Cl_2 solution containing **4** that had been layered with heptane and the molecular structure was determined. Cluster **4** exists as discrete molecules in the unit cell with no unusually inter- or intramolecular contacts. The X-ray data collection and processing parameters for **4** are given in Table 3.6, with the selected bond distances and angles given in Table 3.7. The ORTEP diagram is shown in Figure 3.5.

H. Synthesis and Spectroscopic Properties of $Co_3(CO)_5(\mu\text{-}CO)(PMe_3)[\mu_2\text{-}\eta^2,\eta^1\text{-}C(Ph)C{=}C(PPh_2)C(O)OC(O)](\mu_2\text{-}PPh_2)$

The reaction between the cluster $Co_3(CO)_6[\mu_2\text{-}\eta^2,\eta^1\text{-}C(Ph)C{=}C(PPh_2)C(O)OC(O)](\mu_2\text{-}PPh_2)$ (**3**) and PMe_3 was initially examined at room temperature in CH_2Cl_2 solvent in an attempt to explore the substitution chemistry associated with **3**. When a CH_2Cl_2 solution of **3** was treated

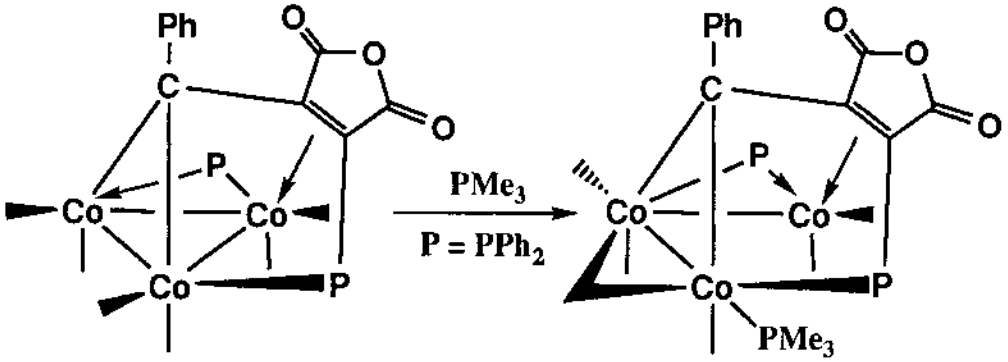

3 **5** (3.5)

with 1.1 equivalent of PMe_3, an instantaneous reaction took place and the reaction solution acquired a red-brown color (Equation 3.5). The new cluster **5** was found to be unstable at room temperature, transforming into a new

species, **6**, during a period of 3 h in CH_2Cl_2. It was subsequently shown that cluster **6** is the mono-substituted cluster $Co_3(CO)_5(PMe_3)[\mu_2\text{-}\eta^2,\eta^1\text{-}C(Ph)C{=}C(PPh_2)C(O)C(O)](\mu_2\text{-}PPh_2)$, where the PMe_3 group coordinates to the cobalt center that is not bridged by the ancillary phosphido group (vide infra). The intermediacy of **5** as a precursor to **6** is of interest with respect to metal cluster reactivity and crucial for understanding of the formation of **6**.

The stability of cluster **5** in solution was greatly improved when the reaction was conducted at -78 °C. Pure **5** was isolated in >90% yield by treating the reaction solution with excess petroleum ether at -78°C. **5** does not appear to be overly air sensitive in solution, but it is extremely temperature sensitive.

The IR spectrum of **5** exhibits terminal carbonyl stretching bands at 2034 (m), 2009 (vs), 2000 (vs), 1996 (vs), 1960 (sh) cm^{-1} along with the characteristic bma carbonyl bands at 1795 (m) and 1736 (m) cm^{-1}.[7] Compared to the starting cluster **3**, the carbonyl bands are shifted to lower frequencies, consistent with the stronger electron donating ability of the PMe_3 ligand. The possibility that the 1795 (m) and 1736 (m) cm^{-1} carbonyl bands may represent bridging carbonyl groups was ruled out by the preparation of cluster **5** that was isotopically enriched with ^{13}CO gas. Only the frequencies of these two bands were not affected, consistent with their anhydride nature. The ^{31}P NMR spectrum of **5** in THF at -95 °C displayed three equal-intensity resonances at δ 184.3, 55.4 ($J_{p\text{-}p}$ = 51 Hz), and 0.6 ($J_{p\text{-}p}$ = 51 Hz). The most downfield resonance is easily assigned to the μ_2-phosphido ligand, while the resonances at δ 55.4 and 0.6 are attributed to coordinated Co-PR_3 groups (bma phosphine and PMe_3 groups). The solution structure was also probed by ^{13}C NMR spectroscopy. Over temperature range of -97 °C to 0 °C in THF, **5**

displayed five carbonyl resonances at δ 212.3, 208.3, 205.0, 202.1, and 201.4 with an integral ratio of 1 : 2 : 1 : 1 : 1. No attempt has been made to assign these resonances to specific carbonyl groups. The observation of six CO groups from the ^{13}C NMR data and three phosphorous resonances from the ^{31}P NMR data in **5** suggests that the reaction between cluster **3** and PMe_3 involves no CO loss and that **5** is an adduct of cluster **3** and PMe_3.

I. X-Ray Diffraction Structure of $Co_3(CO)_5(\mu\text{-}CO)(PMe_3)[\mu_2\text{-}\eta^2,\eta^1\text{-}C(Ph)\overline{C=C(PPh_2)C(O)C(O)}](\mu_2\text{-}PPh_2)$

Single crystals of **5** were grown and the molecular structure was determined. **5** exists as discrete molecules in the unit cell with no unusual short inter- and intramolecular contacts. Table 3.8 lists the X-ray data collection and processing parameters, while Table 3.9 gives the selected bond distances and angles. The ORTEP diagram is shown in Figure 3.6.

J. Synthesis and Spectroscopic Properties of $Co_3(CO)_5(PMe_3)[\mu_2\text{-}\eta^2,\eta^1\text{-}C(Ph)\overline{C=C(PPh_2)C(O)C(O)}](\mu_2\text{-}PPh_2)$ (6)

Cluster **5** readily loses CO and transforms to cluster **6** upon stirring in a variety of solvents at room temperature. The overall reaction between cluster **3** and 1.1 equivalent of PMe_3 can now be delineated as that illustrated in Equation 3.6.

Cluster **6** was isolated by chromatography over silica gel using CH_2Cl_2 solvent and characterized spectroscopically in solution. The IR spectrum displays terminal carbonyl stretching bands at 2040 (m), 2006 (vs), 1980 (sh), 1884 (w) cm^{-1}, along with the characteristic bma carbonyl bands at 1801 (w) and 1741 (s) cm^{-1}. The $^{31}P\{^1H\}$ NMR spectrum of **6** exhibits three, equal-

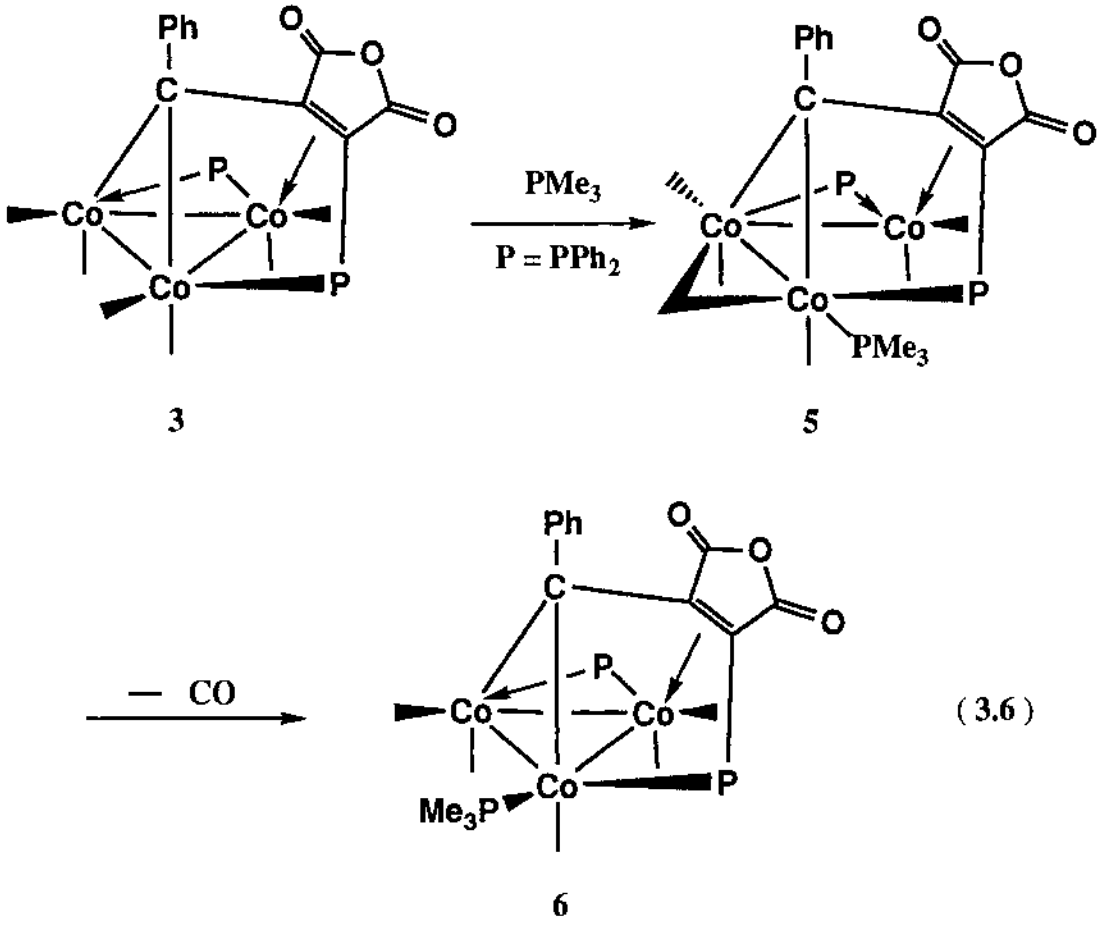

(3.6)

intensity resonances at δ 190.5, 14.3, and 7.8, which are attributed to a μ_2-phosphido and coordinated Co-PR_3 groups (bma Ph_2P and PMe_3 groups), respectively. A sample of **6** enriched with ^{13}CO was prepared and the $^{13}C\{^1H\}$ NMR spectrum was recorded at -97 °C to reduce the undesired quadrupolar broadening between the Co-CO nuclei. The resulting spectrum exhibited five, equal-intensity resonances at δ 216.1, 206.4, 204.6, 200.5 and 191.9. Of these resonances, the most downfield resonance centered at δ 216.1 and the highest field resonance centered at 191.9 reveal phosphorus coupling with $J_{P\text{-}C}$ values of 23.1 and 7.9 Hz, respectively. No further effort has been made to assign these resonances to specific CO groups. The observation of five CO

Table 3.8. X-Ray Crystallographic Collection and Processing Data for $Co_3(CO)_5(\mu\text{-}CO)(PMe_3)[\mu_2\text{-}\eta^2,\eta^1\text{-}C(Ph)\overline{C=C(PPh_2)C(O)OC(O)}](\mu_2\text{-}PPh_2)$

Space group	P1/triclinic
Cell Constants	
a, Å	11.236 (2)
b, Å	12.802 (4)
c, Å	17.886 (1)
α, deg	86.41 (2)
β, deg	73.26 (2)
γ, deg	83.79 (2)
V, $Å^3$	2448 (1)
mol formula	$C_{51}H_{50}Co_3O_9P_3$
fw	1076.68
p, g • cm^{-3}	1.461
abs coeff (μ), cm^{-1}	11.53
radiation Mo Kα (λ), Å	0.71073
collection range, deg	$2.0 \leq 2\theta \leq 40.0$
total data collected	4544
independent data, $I > 3\sigma(I)$	4544
R	0.0667
R_w	0.0816
weights	$[0.04F^2 + (\sigma F)^2]^{-1}$

Table 3.9. Selected Bond Distances (Å) and Angles (deg) for $Co_3(CO)_5(\mu\text{-}CO)(PMe_3)[\mu_2\text{-}\eta^2,\eta^1\text{-}C(Ph)\overbrace{C=C(PPh_2)C(O)OC(O)}]$ $(\mu_2\text{-}PPh_2)$ (**5**)[a]

		bond distances	
Co(1)-Co(2)	2.663(4)	Co(2)-Co(3)	2.523(4)
Co(1)-P(2)	2.129(7)	Co(1)-C(1)	1.73(3)
Co(1)-C(2)	1.68(3)	Co(1)-C(11)	2.02(2)
Co(1)-C(15)	2.07(2)	Co(2)-P(2)	2.188(6)
Co(2)-C(3)	1.71(2)	Co(2)-C(4)	1.75(3)
Co(6)-C(6)	2.28(2)	Co(2)-C(16)	2.02(2)
Co(3)-P(3)	2.278(8)	Co(3)-C(5)	1.72(2)
Co(3)-C(6)	1.69(2)	Co(3)-C(16)	2.04(2)
P(1)-C(11)	1.83(2)	O(1)-C(1)	1.18(3)
O(2)-C(2)	1.20(3)	O(3)-C(3)	1.18(3)
O(4)-C(4)	1.17(4)	O(5)-C(5)	1.16(3)
O(6)-C(6)	1.21(3)	O(12)-C(12)	1.22(3)
O(13)-C(12)	1.22(3)	O(13)-C(14)	1.38(2)
O(14)-C(14)	1.23(3)	C(11)-C(12)	1.46(3)
C(11)-C(15)	1.43(3)	C(14)-C(15)	1.43(3)
C(15)-C(16)	1.48(3)	C(16)-C(17)	1.49(3)
		bond angles	
Co(2)-Co(1)-P(2)	52.9(2)	Co(2)-Co(2)-Co(3)	97.5(1)
Co(1)-Co(2)-P(2)	50.9(2)	Co(1)-Co(2)-C(16)	76.2(5)
Co(3)-Co(2)-P(2)	147.3(2)	Co(3)-Co(2)-C(16)	52.1(6)
P(2)-Co(2)-C(16)	105.0(6)	Co(2)-Co(3)-P(1)	97.8(2)

Table 3.9. continued

Co(2)-Co(3)-P(3)	124.7(2)	Co(2)-Co(3)-C(16)	51.1(6)
P(1)-Co(3)-C(16)	86.9(6)	P(3)-Co(3)-C(16)	174.2(6)
Co(3)-P(1)-C(11)	101.0(7)	Co(1)-P(2)-Co(2)	76.2(2)
C(12)-O(13)-C(14)	110(2)	Co(1)-C(11)-P(1)	115(1)
Co(1)-C(11)-C(12)	109(1)	Co(1)-C(11)-C(12)	127(2)
P(1)-C(11)-C(15)	113(1)	C(12)-C(11)-C(15)	109(2)
O(12)-C(12)-O(13)	125(2)	O(12)-C(12)-C(11)	129(2)
O(13)-C(12)-C(11)	106(2)	O(13)-C(14)-O(14)	116(2)
O(13)-C(14)-C(15)	111(2)	O(14)-C(14)-C(15)	133(2)
Co(1)-C(15)-C(11)	68(1)	Co(1)-C(15)-C(14)	105(1)
Co(1)-C(15)-C(16)	110(1)	C(11)-C(15)-C(14)	104(2)
C(11)-C(15)-C(16)	123.(2)	C(14)-C(15)-C(16)	129(2)
Co(2)-C(16)-Co(3)	76.8(9)	Co(2)-C(16)-C(15)	103(1)
Co(2)-C(16)-C(17)	128(1)	Co(3)-C(16)-C(15)	114(1)

[a]Numbers in parentheses are estimated standard deviations in the least significant digits.

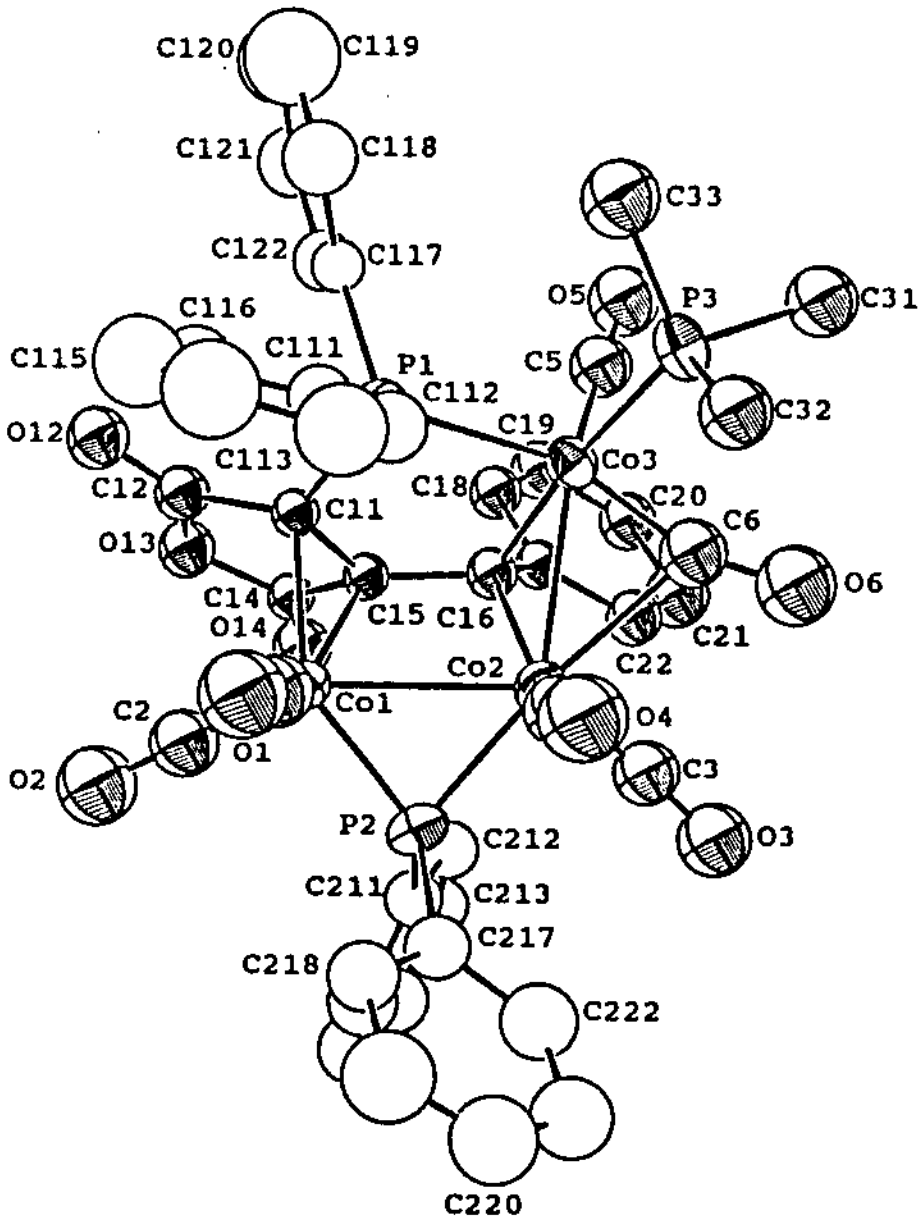

Figure 3.6. ORTEP diagram of $Co_3(CO)_5(\mu\text{-}CO)(PMe_3)[\mu_2\text{-}\eta^2,\eta^1\text{-}C(Ph)\overline{C=C(PPh_2)C(O)OC(O)}](\mu_2\text{-}PPh_2)$ (**5**) with the thermal ellipsoids drawn at the 50% probability level. H atoms are omitted for clarity.

groups supports the proposed structure of **6** and reveals that the ancillary CO groups do not participate in any intramolecular scrambling about the cluster core.

K. X-Ray Diffraction Structure of $Co_3(CO)_5(PMe_3)[\mu_2\text{-}\eta^2,\eta^1\text{-}C(Ph)C{=}C(PPh_2)C(O)OC(O)](\mu_2\text{-}PPh_2)$ (6)

Single crystals of **6** were grown and the molecular structure was determined. **6** exists as discrete molecules in the unit cell with no unusual short inter- and intramolecular contacts. Table 3.10 lists the X-ray data collection and processing parameters, while Table 3.11 gives the selected bond distances and angles. The ORTEP diagram is shown in Figure 3.7.

L. Synthesis and Spectroscopic Properties of $Co_3(CO)_4(PMe_3)_2[\mu_2\text{-}\eta^2,\eta^1\text{-}C(Ph)C{=}C(PPh_2)C(O)OC(O)](\mu_2\text{-}PPh_2)$

Cluster **6** reacts with additional PMe_3 to afford the disubstituted cluster **7** (Equation 3.7). The same result can be obtained by treating a

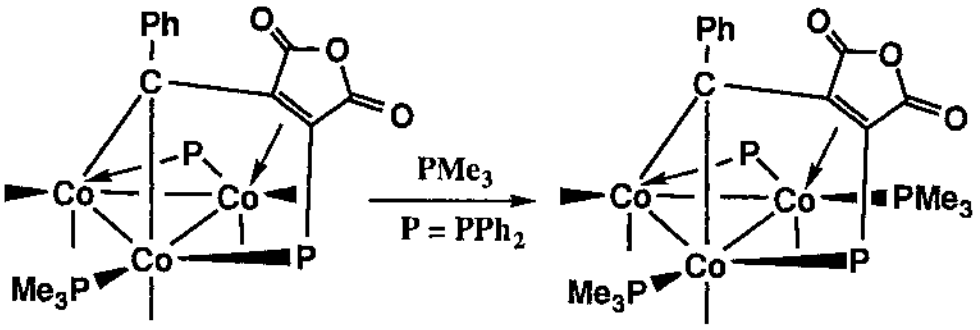

(3.7)

6 **7**

CH_2Cl_2 solution of **3** at room temperature with excess PMe_3. Unlike the reaction between **3** and PMe_3, which gave cluster **5** as an intermediate, no

Table 3.10. X-Ray Crystallographic Collection and Processing Data for $Co_3(CO)_5(PMe_3)[\mu_2\text{-}\eta^2,\eta^1\text{-}C(Ph)\overline{C=C(PPh_2)C(O)OC(O)}](\mu_2\text{-}PPh_2)\bullet CH_2Cl_2$ (6)[a]

Space group	$P2_1ln$/monoclinic
Cell Constants	
a, Å	10.256 (2)
b, Å	28.398 (2)
c, Å	15.405 (1)
β, deg	73.26 (2)
V, Å^3	4405.5 (9)
mol formula	$C_{44}H_{36}Cl_2Co_3O_8P_3$
fw	1033.40
formula units per cell (Z)	4
p, g • cm^{-3}	1.558
abs coeff (μ), cm^{-1}	13.95
collection range, deg	$2.0 \leq 2\theta \leq 44$
total data collected	5876
independent data, $I > 3\sigma(I)$	5527
R	0.0469
R_w	0.0577
weights	$[0.04F^2 + (\sigma F)^2]^{-1}$

Table 3.11. Selected Bond Distances (Å) and Angles (deg) for $Co_3(CO)_5(PMe_3)[\mu_2\text{-}\eta^2,\eta^1\text{-}C(Ph)\overbrace{C=C(PPh_2)C(O)OC(O)}](\mu_2\text{-}PPh_2)$ (**6**)[a]

		bond distances	
Co(1)-Co(2)	2.571(2)	Co(1)-Co(3)	2.779(2)
Co(1)-P(2)	2.253(3)	Co(1)-C(1)	1.79(1)
Co(1)-C(2)	1.79(1)	Co(1)-C(15)	2.14(1)
Co(1)-Co(11)	2.035(9)	Co(2)Co(3)	2.437(2)
Co(2)-C(3)	1.77(1)	Co(2)-C(4)	1.73(1)
Co(2)-C(16)	1.90(1)	Co(2)-P(2)	2.135(3)
Co(3)-P(1)	2.240(3)	Co(3)-P(3)	2.256(3)
Co(3)-C(5)	1.79(1)	Co(3)-C(16)	2.01(1)
P(1)-C(111)	1.82(1)	P(1)-C(117)	1.82(1)
P(2)-C(11)	1.776(9)	P(2)-C(211)	1.82(1)
P(2)-C(217)	1.80(1)	P(3)-C(31)	1.79(1)
P(3)-C(32)	1.82(1)	P(3)-C(33)	1.82(1)
O(1)-C(1)	1.14(1)	O(2)-C(2)	1.13(1)
O(3)-C(3)	1.15(1)	O(4)-C(4)	1.16(1)
O(5)-C(5)	1.12(1)	O(12)-C(12)	1.18(1)
O(13)-C(12)	1.41(1)	O(13)-C(14)	1.39(1)
O(14)-C(14)	1.17(1)	C(11)-C(12)	1.48(2)
C(11)-C(15)	1.43(1)	C(14)-C(15)	1.43(1)
C(15)-C(16)	1.46(1)	C(16)-C(17)	1.47(1)
C(17)-C(18)	1.39(1)	C(17)-C(22)	1.39(2)
C(18)-C(19)	1.38(2)	C(19)-C(20)	1.35(2)

Table 3.11. continued

C(20)-C(21)	1.34(2)	C(21)-C(22)	1.43(2)
	bond angles		
Co(2)-Co(1)-Co(3)	54.02(5)	Co(2)-Co(1)-P(2)	52.01(8)
Co(2)-Co(1)-C(11)	98.4(3)	Co(3)-Co(1)-P(2)	93.17(9)
Co(3)-Co(1)-C(15)	65.4(3)	P(2)-Co(2)-C(16)	135.7(3)
Co(2)-Co(1)-Co(3)	54.02(5)	Co(2)-Co(1)-P(2)	52.01(8)
Co(2)-Co(1)-C(11)	98.4(3)	Co(2)-Co(1)-C(15)	62.4(3)
Co(3)-Co(2)-P(1)	93.17(9)	Co(3)-Co(2)-C(11)	71.9(3)
Co(3)-Co(1)-C(15)	65.4(3)	P(2)-Co(1)-C(11)	148.7(3)
P(2)-Co(1)-C(15)	109.0(3)	C(11)-Co(1)-C(15)	39.9(4)
Co(2)-Co(3)-Co(1)	58.64(5)	Co(2)-Co(3)-P(3)	126.6(1)
Co(2)-Co(3)-P(1)	119.7(1)	Co(2)-Co(3)-C(16)	49.4(3)
Co(1)-Co(3)-P(1)	70.93(8)	Co(1)-Co(3)-P(3)	170.0(1)
Co(1)-Co(3)-C(16)	72.9(3)	P(1)-Co(3)-P(3)	99.7(1)
P(1)-Co(3)-C(16)	87.2(3)	P(3)-Co(3)-C(16)	103.7(3)
Co(2)-P(2)-Co(1)	71.7(1)	Co(3)-P(1)-C(11)	91.3(3)
C(12)-O(13)-C(14)	111.6(8)	Co(1)-C(11)-P(1)	101.0(5)
Co(1)-C(11)-C(15)	74.0(5)	P(1)-C(11)-C(12)	132.0(7)
C(12)-C(11)-C(15)	107.0(8)	O(12)-C(12)-O(13)	119.(1)
O(12)-C(12)-C(11)	134(1)	O(13)-C(14)-O(14)	122.(1)
O(13)-C(14)-C(15)	106.1(8)	O(14)-C(14)-C(15)	132(1)

[a]Numbers in parentheses are estimated standard deviations in the least significant digits.

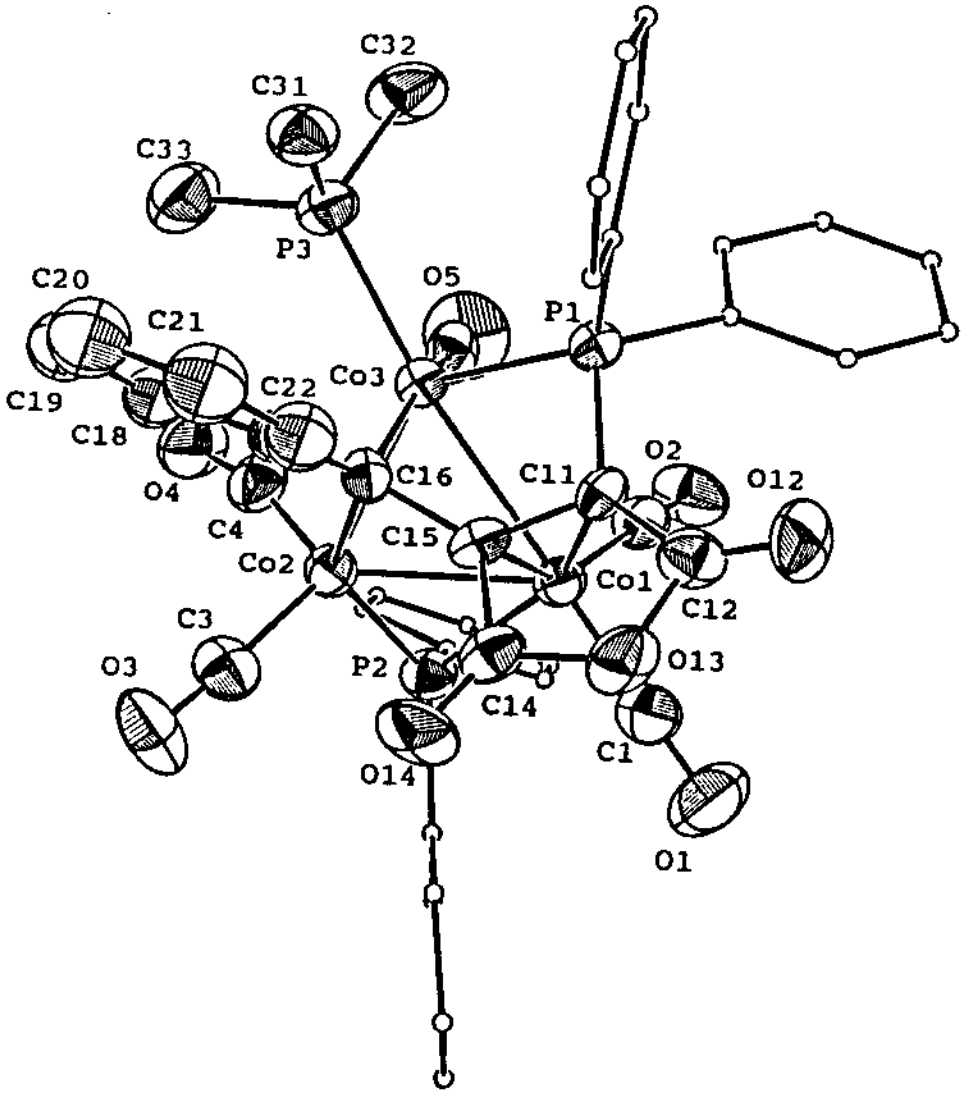

Figure 3.7. ORTEP diagram of $Co_3(CO)_5(PMe_3)[\mu_2\text{-}\eta^2,\eta^1\text{-}C(Ph)\overline{C=C(PPh_2)C(O)OC(O)}](\mu_2\text{-}PPh_2)$ with the thermal ellipsoids drawn at the 50% probability level. H atoms are omitted for clarity.

intermediates were observed when the reaction between **6** and PMe_3 was monitored by IR spectroscopy. Cluster **7** was isolated by chromatography over silica gel using a mixture solvent of CH_2Cl_2/acetone (95 : 5) and characterized spectroscopically in solution. The IR spectrum of **7** displays terminal carbonyl stretching bands at 1993 (sh), 1976 (vs), 1864 (w, broad) cm^{-1}, along with the characteristic bma carbonyl bands at 1791 and 1728 cm^{-1}. The $^{31}P\{^1H\}$ NMR spectrum of **7** exhibits four equal-intensity resonances at δ 172.9, 7.2, 0.8, and -10.0, which are attributed to a μ_2-phosphido and coordinated Co-PR_3 groups (bma Ph_2P and two PMe_3 groups), respectively. A ^{13}CO-enriched sample of **7** was prepared and the $^{13}C\{^1H\}$ NMR spectrum recorded at -97 °C. The resulting spectrum exhibited three resonances at δ 224.0, 207.4, and 206.7 with an integral ratio of 1 : 1 : 2. Of these resonances, the most downfield resonance at δ 224.0 reveals phosphorus coupling with a $J_{P\text{-}C}$ value of 25.5 Hz. No further effort has been made to assign these resonances to specific CO groups. The observation of four CO groups supports a static structure of **7**, which is maintained over the temperature range of -97 °C to room temperature.

M. X-Ray Diffraction Structure of $Co_3(CO)_4(PMe_3)_2[\mu_2\text{-}\eta^2,\eta^1\text{-}C(Ph)\overline{C=C(PPh_2)C(O)OC(O)}](\mu_2\text{-}PPh_2)$

Single crystals of **7** were grown and the molecular structure was determined. **7** exists as discrete molecules in the unit cell with no unusual short inter- and intramolecular contacts. Table 3.12 lists the X-ray data collection and processing parameters, while Table 3.13 gives the selected distances and angles. The ORTEP diagram is shown in Figure 3.8.

Table 3.12. X-Ray Crystallographic Collection and Processing Data for $Co_3(CO)_4(PMe_3)_2[\mu_2\text{-}\eta^2,\eta^1\text{-}C(Ph)\overline{C=C(PPh_2)C(O)OC(O)}](\mu_2\text{-}PPh_2)$ (7)

Space group	$P2_1/n$/monoclinic
Cell Constants	
a, Å	11.0047(8)
b, Å	19.558(2)
c, Å	17.683(1)
β, deg	94.947(6)
V, Å^3	4664.4(6)
mol formula	$C_{45}H_{43}Co_3O_7P_4$
fw	996.54
formula units per cell (Z)	4
ρ, g • cm^{-3}	1.419
abs coeff (μ), cm^{-1}	12.33
radiation Mo Kα (λ), Å	0.71073
total data collected	6253
independent data, $I > 3\sigma(I)$	5906
R	0.0453
R_w	0.0489
weights	$[\ 0.04F^2 + (\sigma F)^2\ ]^{-1}$

Table 3.13. Selected Bond Distances (Å) and Angles (deg) for $Co_3(CO)_4(PMe_3)_2[\mu_2\text{-}\eta^2,\eta^1\text{-}C(Ph)\overline{C=C(PPh_2)C(O)C}(O)](\mu_2\text{-}PPh_2)$ (7)[a]

		bond distances	
Co(1)-Co(2)	2.422(1)	Co(1)-Co(3)	2.832(1)
Co(1)-P(1)	2.235(2)	Co(1)-P(3)	2.242(2)
Co(1)-C(16)	2.035(7)	Co(2)-Co(3)	2.592(1)
Co(2)-P(2)	2.139(2)	Co(2)-C(15)	2.377(7)
Co(2)-C(16)	1.900(7)	Co(3)-P(2)	2.241(2)
Co(3)-P(4)	2.265(2)	Co(3)-C(11)	2.068(7)
Co(3)-C(15)	2.198(7)	P(1)-C(11)	1.788(7)
O(12)-C(12)	1.201(9)	O(13)-C(12)	1.405(9)
O(13)-C(14)	1.402(9)	O(14)-C(14)	1.180(9)
C(11)-C(12)	1.45(1)	C(11)-C(15)	1.47(1)
C(14)-C(15)	1.48(1)	C(15)-C(16)	1.44(1)
		bond angles	
Co(2)-Co(1)-Co(3)	58.51(4)	Co(2)-Co(1)-P(1)	118.14(7)
Co(2)-Co(1)-P(3)	127.28(7)	Co(2)-Co(1)-C(16)	49.5(2)
Co(3)-Co(1)-P(1)	70.15(6)	Co(3)-Co(1)-P(3)	170.33(8)
Co(3)-Co(1)-C(16)	74.3(2)	P(1)-Co(1)-P(3)	100.48(8)
P(1)-Co(1)-C(16)	86.8(2)	P(3)-Co(1)-C(16)	103.4(2)
Co(1)-Co(2)-Co(3)	68.68(4)	Co(1)-Co(2)-P(2)	106.31(7)
Co(1)-Co(2)-C(15)	68.7(2)	Co(1)-Co(2)-C(16)	82.5(2)
P(2)-Co(2)-C(16)	137.9(2)	C(15)-Co(2)-C(16)	37.4(3)
Co(1)-Co(3)-Co(2)	52.81(3)	Co(1)-Co(3)-P(2)	91.38(6)

Table 3.13. continued

Co(1)-Co(3)-P(4)	170.82(7)	Co(1)-Co(3)-C(11)	71.1(2)
Co(1)-Co(3)-C(15)	63.7(2)	Co(2)-Co(3)-P(2)	51.91(6)
Co(2)-Co(3)-P(4)	133.15(7)	Co(2)-Co(3)-C(11)	95.3(2)
Co(2)-Co(3)-C(15)	58.8(2)	P(2)-Co(3)-C(11)	145.8(2)
P(2)-Co(3)-C(15)	105.9(2)	P(4)-Co(3)-C(11)	100.3(2)
P(4)-Co(3)-C(15)	112.0(2)	C(11)-Co(3)-C(15)	144.2(3)
Co(1)-P(1)-C(11)	92.2(2)	C(12)-O(13)-C(14)	110.5(5)
Co(3)-C(11)-P(1)	99.7(3)	Co(3)-C(11)-C(15)	74.6(4)
Co(3)-C(11)-C(12)	130.2(5)	P(1)-C(11)-C(12)	120.9(5)
P(1)-C(11)-C(15)	111.6(5)	C(12)-C(11)-C(15)	106.4(6)
O(12)-C(12)-O(13)	119.1(7)	O(12)-C(12)-C(11)	132.3(7)
O(13)-C(12)-C(11)	108.5(6)	O(13)-C(14)-O(14)	120.8(7)
O(13)-C(14)-C(15)	107.3(6)	O(14)-C(14)-C(15)	131.8(7)
Co(2)-C(15)-Co(3)	68.9(2)	Co(2)-C(15)-C(11)	126.6(5)
Co(2)-C(15)-C(14)	115.7(4)	Co(2)-C(15)-C(16)	53.1(3)
Co(3)-C(15)-C(11)	65.1(4)	Co(3)-C(15)-C(14)	112.7(5)
Co(3)-C(15)-C(16)	109.7(5)	C(11)-C(15)-C(16)	106.1(6)

[a]Numbers in parentheses are estimated standard deviations in the least significant digits.

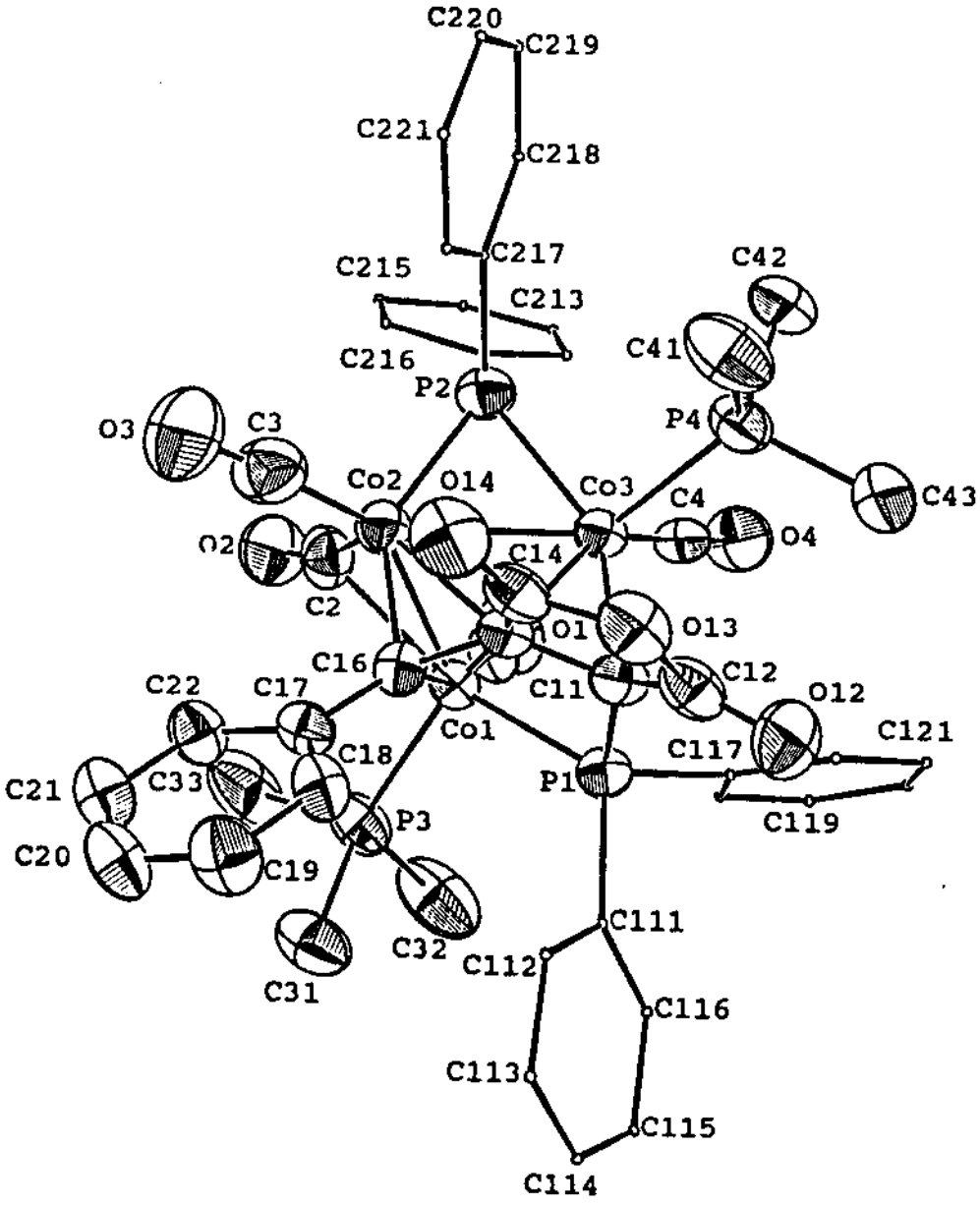

Figure 3.8. ORTEP diagram of $Co_3(CO)_4(PMe_3)_2[\mu_2\text{-}\eta^2,\eta^1\text{-}C(Ph)\overline{C=C(PPh_2)\,C(O)C(O)}](\mu_2\text{-}PPh_2)$ with the thermal ellipsoids drawn at the 50% probability level. H atoms are omitted for clarity.

N. Synthesis and Spectroscopic Properties of $Co_2(CO)_4(\mu\text{-}PhC{\equiv}CPh)(bma)$ and $Co_2(CO)_4(\mu\text{-}PhC{\equiv}CPh)[(Z)\text{-}Ph_2PCH{=}CHPPh_2]$

The reaction between the dinuclear complex $Co_2(CO)_4(\mu\text{-}PhC{\equiv}CPh)$ and bma was initially examined in CH_2Cl_2 at room temperature using the oxidative-decarbonylation reagent Me_3NO, as a route to $Co_2(CO)_4(\mu\text{-}PhC{\equiv}CPh)(bma)$ (Equation 3.8). A clean and immediate reaction was

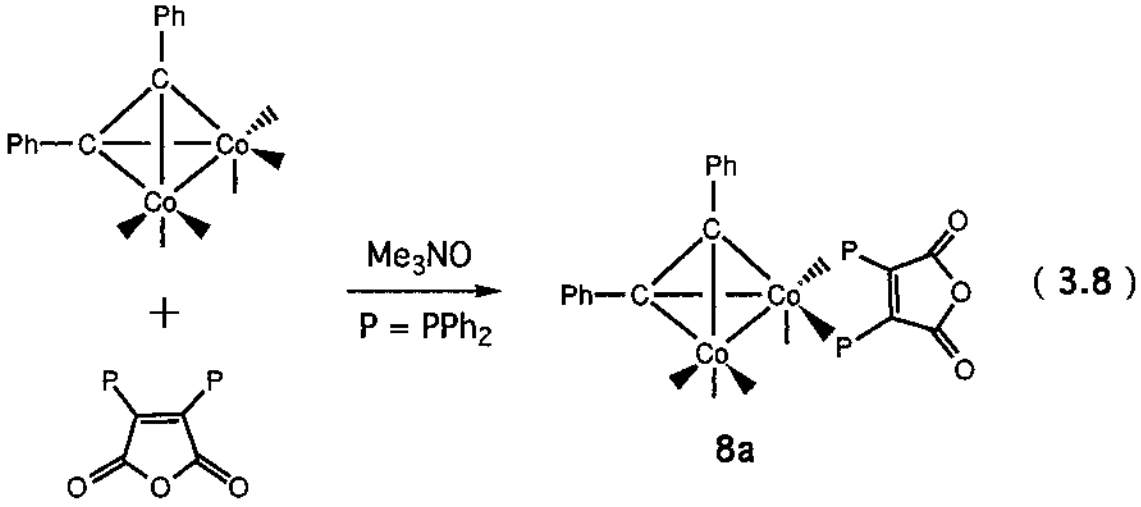

(3.8)

observed when the reaction was monitored by IR spectroscopy. TLC analysis revealed the presence of small amount of starting material and product (>90%). The resulting green solution was purified by chromatography over a short silica gel column at -78 °C to give $Co_2(CO)_4(\mu\text{-}PhC{\equiv}CPh)(bma)$ as an air-sensitive solid in routinely isolated yields of 50-60%. The lowered yield of isolated product compared to the reaction solution stems from the partial decomposition of $Co_2(CO)_4(\mu\text{-}PhC{\equiv}CPh)(bma)$ on the silica gel, presumably the result of anhydride ring hydrolysis.

Two prominent terminal ν (CO) bands at 2047 (vs) and 1993 (vs) cm^{-1} were observed for $Co_2(CO)_4(\mu\text{-}PhC{\equiv}CPh)(bma)$ in CH_2Cl_2 solution, in addition to a weak shoulder at 1952 cm^{-1}. The symmetry of this IR spectrum

is inconsistent with the IR data reported for other diphosphine-bridged $Co_2(CO)_4(\mu\text{-alkyne})P_2$ complexes. Accordingly, the bma ligand was assigned to a chelating role in the chromatographed material. The expected ν (CO) bands associated with the bma ligand were observed at 1842 (w) and 1775 (s) cm^{-1} and ascribed to the vibrationally coupled asymmetric and symmetric bma carbonyl stretches, [7] respectively. These latter two IR assignments were unequivocally established by an isotope study. Repeating the experiment depicted in Eq. 3.8 with a sample of $Co_2(CO)_6(\mu\text{-PhC}\equiv\text{CPh})$ that was 20-30% enriched in ^{13}CO afforded the dinuclear complex $Co_2(CO)_4(\mu\text{-PhC}\equiv\text{CPh})$(bma) with unchanged bma carbonyl bands.

The $^{31}P\{^1H\}$ spectrum of $Co_2(CO)_4(\mu\text{-PhC}\equiv\text{CPh})$(bma) in $CDCl_3$ solution displayed a single resonance at ~δ 60 over the temperature range -56°C to room temperature. The low-field location of the ^{31}P resonance supports the chelating nature of the bma ligand in $Co_2(CO)_4(\mu\text{-PhC}\equiv\text{CPh})$ (bma) , as it is known that five-membered diphosphine-metal chelate rings experience a large nuclear deshielding of the ^{31}P centers, causing a lower-field resonance relative to the alternative six-membered ring isomer (vide infra). [9] The $^{13}C\{^1H\}$ NMR spectrum of $Co_2(CO)_4(\mu\text{-PhC}\equiv\text{CPh})$(bma), prepared from ^{13}CO enriched $Co_2(CO)_6(\mu\text{-PhC}\equiv\text{CPh})$, bma, and Me_3NO, was recorded as a function of temperature in THF solution. At room temperature two, broad resonances at δ 207.5 and 201.1 were observed in an integral ratio 1 : 3, for the lone CO group at the bma-chelated cobalt center and the unsubstituted $Co(CO)_3$ center, respectively. Reducing the temperature to -91 °C led only to the sharpening of these resonances, as a result of the diminution of the dinuclear complex's molecular correlation time (τ_c), which is expected to afforded sharper ^{13}C resonances. [2a,15] The variable-temperature NMR data

indicate that intramolecular carbonyl scrambling between the two cobalt centers is not important in $Co_2(CO)_4(\mu\text{-PhC}{\equiv}\text{CPh})$(bma).

While the ^{31}P and ^{13}C NMR data clearly show that the sole product from the reaction between $Co_2(CO)_6(\mu\text{-PhC}{\equiv}\text{CPh})$ and bma under Me_3NO-induced carbonyl activation is the chelating isomer of $Co_2(CO)_4(\mu\text{-PhC}{\equiv}\text{CPh})$(bma), the thermolysis reaction between $Co_2(CO)_6(\mu\text{-PhC}{\equiv}\text{CPh})$ and bma yields a mixture of chelating and bridging isomers of $Co_2(CO)_4(\mu\text{-PhC}{\equiv}\text{CPh})$(bma). Refluxing an equimolar mixture of the dinuclear complex $Co_2(CO)_6(\mu\text{-PhC}{\equiv}\text{CPh})$ and bma in CH_2Cl_2 overnight led to a more complicated IR spectrum than previously recorded, and this suggested the existence of an isomeric mixture of bridging and chelating $Co_2(CO)_4(\mu\text{-PhC}{\equiv}\text{CPh})$(bma). Examination of the $^{31}P\{^1H\}$ spectrum of the crude thermolysis product revealed the presence of two ^{31}P resonances at δ 60.6 and 30.3, assignable to the chelating and bridging isomers of $Co_2(CO)_4(\mu\text{-PhC}{\equiv}\text{CPh})$(bma), respectively. The solubility of the bridging isomer of $Co_2(CO)_4(\mu\text{-PhC}{\equiv}\text{CPh})$(bma) in common solvents is slightly higher than that of the chelating isomer and this allowed, after repeated recrystallizations, the isolation of small quantities of pure bridging isomer from the mother liquor. Three terminal ν (CO) bands at 2031 (s), 2009 (vs), and 1982 (sh) cm^{-1} are observed in the IR spectrum of this isomer, which are identical to the IR data reported the analogous dppm- and dppe-substituted complexes.[16,17] The ν (CO) bands at 1818 (w) and 1765 (s) cm^{-1} belong to the bridging bma ligand. It is interesting to note that these latter two stretches are ~24 and 10 cm^{-1} lower than the corresponding bma stretches in the chelating isomer. The bridged isomer exhibits a $^{13}C\{^1H\}$ NMR spectrum with a broad carbonyl resonance at δ 203 at room temperature, which upon cooling to -91 °C sharpens only

slightly. Two separate carbonyl resonances were expected at low temperature given the NMR studies on related dppm-bridged cobalt-alkyne complexes published by Hansen. [18] In that report, dynamic ^{13}C NMR behavior is derived from a rocking motion of the coordinated acetylene ligand within the nido polyhedronal core of the cobalt dinuclear complex. Two possible explanations for the low-temperature ^{13}C NMR behavior in bridged isomer are resonable, namely (1) a small chemical shift difference exists between the unique carbonyl groups, or (2) the diphenylacetylene ligand is still rocking rapidly within the nido polyhedral core .

Since it was not immediately clear whether the formation of both of the isomers of $Co_2(CO)_4(\mu\text{-PhC}\equiv\text{CPh})$(bma) proceeded by separate pathways or if a chelate-to-bridge isomerization sequence was operative, the thermolysis reactivity of the pure chelating isomer of $Co_2(CO)_4(\mu\text{-PhC}\equiv\text{CPh})$(bma) was next examined. Refluxing the chelating isomer in CH_2Cl_2 slowly afforded $Co_2(CO)_4(\mu\text{-PhC}\equiv\text{CPh})$(bma) as an isomeric mixture. The resulting IR and ^{31}P NMR spectra were identical to those obtained from the thermolysis reaction between $Co_2(CO)_6(\mu\text{-PhC}\equiv\text{CPh})$ and bma (vide supra). The equilibrium nature of this reaction was also demonstrated by exploring the ratio of the bridging-to-chelating isomers of $Co_2(CO)_4(\mu\text{-PhC}\equiv\text{CPh})$(bma) by ^{31}P NMR spectroscopy. Heating a 0.03 M sample of $Co_2(CO)_4(\mu\text{-PhC}\equiv\text{CPh})$(bma) (chelating) in $CDCl_3$ in a sealed NMR tube at 45 °C for 48 hrs gave a Keq (bridge/chelate) of ~1. No other phosphorus-containing products were observed in this reaction. The same results were also obtained when the equilibration was approached by heating a 0.01 M sample of $Co_2(CO)_4(\mu\text{-PhC}\equiv\text{CPh})$(bma) (bridging) in dichloroethane overnight at 45 °C. Moreover, added CO strongly suppresses isomer equilibration. No isomerization was

observed after 2 days at 45 °C when $Co_2(CO)_4(\mu\text{-PhC}\equiv\text{CPh})$(bma) (chelating) was stirred under 100 psi of CO. Consistent with the isomerization inhibition by CO is the fact that near-UV photolysis of $Co_2(CO)_4(\mu\text{-PhC}\equiv\text{CPh})$(bma) (chelating) also gives an isomeric mixture of $Co_2(CO)_4(\mu\text{-PhC}\equiv\text{CPh})$(bma). Here optical excitation is expected to promote CO dissociation and, thus, initiates the isomerization sequences. Taken collectively, the ligand substitution data strongly support consecutive reaction pathways, where the initially formed chelating isomer gives rise to the corresponding bridging isomer as outlined in Equation 3.9.

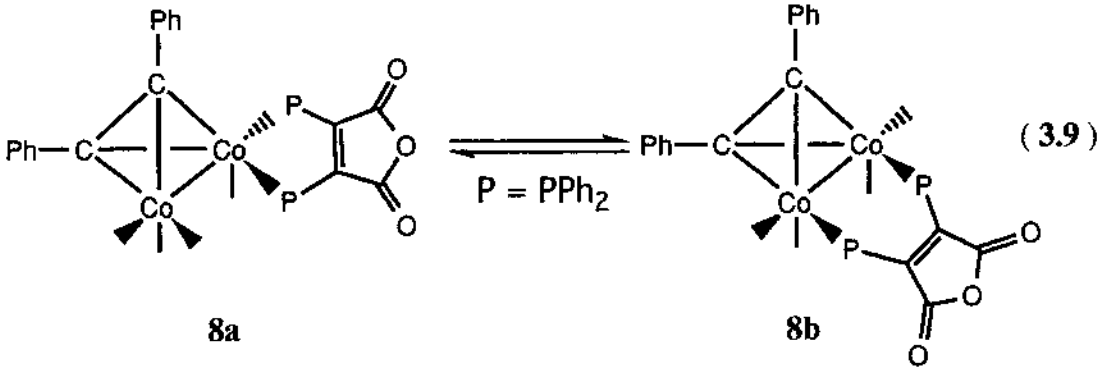

8a **8b** **(3.9)**

The reaction between $Co_2(CO)_6(\mu\text{-PhC}\equiv\text{CPh})$ and (Z)-$Ph_2PCH{=}CHPPh_2$ was studied next because the anticipated product $Co_2(CO)_4(\mu\text{-PhC}\equiv\text{CPh})$[(Z)-$Ph_2PCH{=}CHPPh_2$] would allow for disparate reactivity between $Co_2(CO)_4(\mu\text{-PhC}\equiv\text{CPh})$(bma) and $Co_2(CO)_4(\mu\text{-PhC}\equiv\text{CPh})$[(Z)-$Ph_2PCH{=}CHPPh_2$] to be probed. Since the two compounds are expected to be structurally similar, it could be argued that any observed reactivity differences would have their origin in the electronic properties inherent to each ancillary diphosphine ligand. The dinuclear compound $Co_2(CO)_4(\mu\text{-PhC}\equiv\text{CPh})$[(Z)-$Ph_2PCH{=}CH$ PPh_2] was obtained exclusively as the chelating isomer when $Co_2(CO)_6(\mu$-

PhC≡CPh) was allowed to react with (Z)-$Ph_2PCH=CHPPh_2$ in either dichloromethane at 50 °C or with Me_3NO in CH_2Cl_2 at room temperature (Equation 3.10). The IR spectrum of $Co_2(CO)_4$(μ-PhC≡CPh)[(Z)-$Ph_2PCH=CHPPh_2$] exhibits two terminal ν (CO) bands at 2039 (vs) and 1983 (vs) cm^{-1}. These ν (CO) bands are ~10 cm^{-1} lower in energy than the analogous carbonyl bands in $Co_2(CO)_4$(μ-PhC≡CPh)(bma) (chelating), which reflects the better donor properties of the (Z)-$Ph_2PCH=CHPPh_2$ ligand relative to the bma ligand, with its electron-withdrawing anhydride ring. The chelating nature

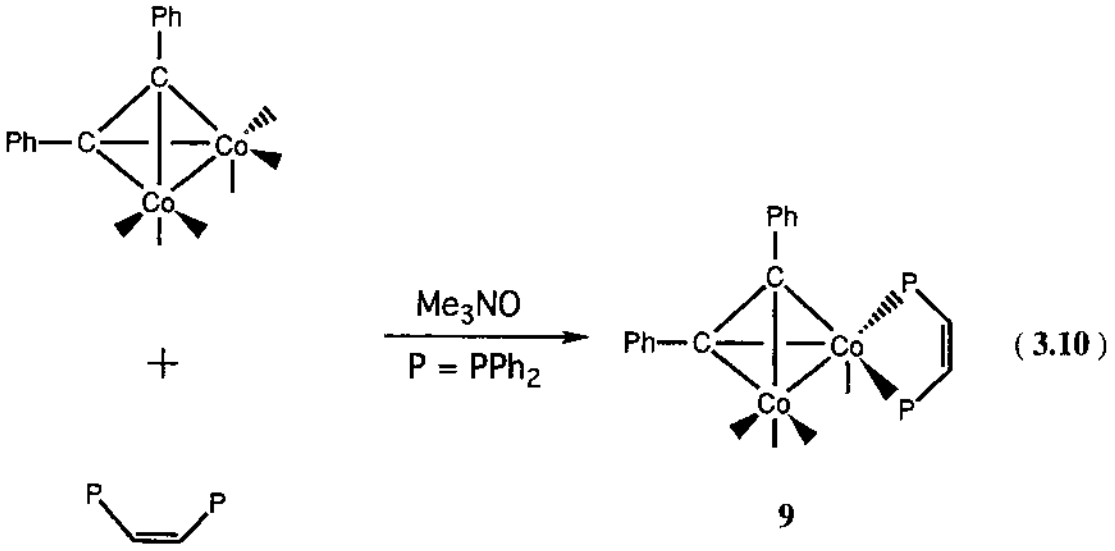

(**3.10**)

9

of the ancillary diphosphine was ascertained by ^{31}P and ^{13}C NMR spectroscopies, where a single resonance at δ 71.8 and two resonances at δ 208.8 (1C) and 202.8 (3C), respectively, have been recorded at -91 °C in THF solution.

The thermolysis and photolysis reactivity of $Co_2(CO)_4$(μ-PhC≡CPh)[(Z)-$Ph_2PCH=CHPPh_2$] under conditions comparable to those employed in the isomerization of $Co_2(CO)_4$(μ-PhC≡CPh)(bma) did not afford any of the bridging isomer. In both cases, the only observed reaction was the

decomposition of $Co_2(CO)_4(\mu\text{-}PhC{\equiv}CPh)[(Z)\text{-}Ph_2PCH{=}CHPPh_2]$, with decomposition from the thermolysis reaction being more extensive than that from the photolysis reaction. The absence of isomerization in $Co_2(CO)_4(\mu\text{-}PhC{\equiv}CPh)[(Z)\text{-}Ph_2PCH{=}CHPPh_2]$ suggests that the diphosphine remains associated with the cobalt center and does not become free, a condition that would be required for isomerization.

O. Synthesis and Spectroscopic Properties of $Co_2(CO)_4[\eta^2,\eta^2,\eta^1,\eta^1\text{-}(Z)\text{-}Ph_2PC(Ph){=}(Ph)C\text{-}C{=}C(PPh_2)C(O)OC(O)]$

During the course of the investigation on the isomerization of $Co_2(CO)_4(\mu\text{-}PhC{\equiv}CPh)$(bma) in refluxing dichloroethane or toluene solutions, the appearance of a new product was found by IR and TLC analyses. It was subsequently shown that at temperatures higher than 75 °C the compound $Co_2(CO)_4(\mu\text{-}PhC{\equiv}CPh)$(bma) was unstable, giving as the only isolable product the new complex $Co_2(CO)_4[\eta^2,\eta^2,\eta^1,\eta^1\text{-}(Z)\text{-}Ph_2PC(Ph){=}(Ph)C\text{-}C{=}C(PPh_2)C(O)OC(O)]$ (**10**) as shown in Eq. 3.11 . This same product is obtained from the reaction between $Co_2(CO)_6(\mu\text{-}PhC{\equiv}CPh)$ and bma in refluxing dichloroethane,

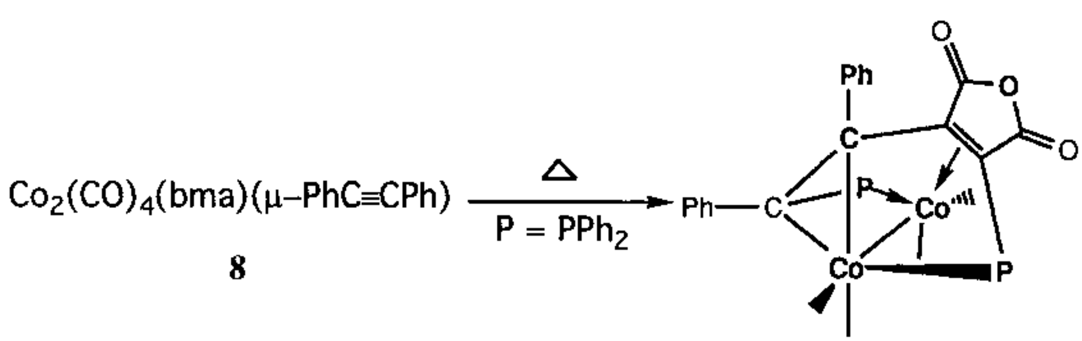

8 **10** (3.11)

by way of $Co_2(CO)_4(\mu\text{-}PhC{\equiv}CPh)$(bma). The dinuclear complex **10**, which

results from the formal coupling of the diphenylacetylene and bma ligands, was isolated in 10% yield by column chromatography and characterized in solution by IR and NMR spectroscopies. When the thermolysis reaction was repeated under CO (100 psi) using either isomer of $Co_2(CO)_4(\mu\text{-PhC}\equiv\text{CPh})$ (bma), no reaction was observed. Only unreacted starting material was isolated at the end of these reactions.

The IR spectrum of **10** in CH_2Cl_2 shows four terminal ν (CO) bands at 2050 (s), 2025 (vs), 2008 (s), and 1981 (m) cm^{-1}, in agreement with the highly asymmetric structure of the dinuclear complex which should yield a greater number of carbonyl stretching bands relative to the starting bma-substituted compound. The ν (CO) bands derived from bma ligand are observed at 1809 (w) and 1745 (m) cm^{-1}. At -91 °C four, equal-intensity carbonyl resonances were observed at δ 202.1, 201.1 (d, $J_{C\text{-}P}$ = 15.3 Hz), 196.9, and 193.7 in the $^{13}C\{^1H\}$ NMR spectrum of **10**. The doublet resonance at δ 201.1 is presumed to result from coupling with one of the phosphine atoms in **10**. The ^{31}P NMR spectrum of **10** recorded under comparable conditions shows the presence of two inequivalent phosphine ligands at δ 46.7 (broad) and 27.8 (d, $J_{P\text{-}P}$ = 17.0 Hz). While no attempt has been made to assign the ^{13}C and ^{31}P resonances to specific groups, we note that the NMR data are consistent with the structure of **10**. Warming these samples to room temperature led only to the broadening of these resonances as ^{59}Co quadrupolar-induced line broadening becomes more pronounced.

P. X-Ray Diffraction Structure of $Co_2(CO)_4(\mu\text{-PhC}\equiv\text{CPh})$(bma) (bridging)

Single crystals of **8b** were grown and the molecular structure was determined. **8b** exists as discrete molecules in the unit cell with no unusual

Table 3.14. X-Ray Crystallographic Collection and Processing Data for $Co_2(CO)_4(\mu$-PhC≡CPh)(bma) (bridging isomer) (8a)

Space group	P1/triclinic
Cell Constants	
a, Å	10.712 (1)
b, Å	11.1467 (4)
c, Å	19.944 (1)
α, deg	78.311 (6)
β, deg	89.029 (7)
γ, deg	68.169 (7)
V, Å^3	2160.4 (3)
mol formula	$C_{47}H_{32}Cl_2Co_3O_7P_2$
fw	959.49
formula units per cell (Z)	2
ρ, g • cm^{-3}	1.475
abs coeff (μ), cm^{-1}	10.13
radiation Mo Kα (λ), Å	0.71073
collection range, deg	$2.0 \leq 2\theta \leq 44.0$
total data collected	5230
independent data, $I > 3\sigma(I)$	1711
R	0.0697
R_w	0.085
weights	$[0.04F^2 + (\sigma F)^2]^{-1}$

Table 3.15. Selected Bond Distances (Å) and Angles (deg) for $Co_2(CO)_4(\mu\text{-PhC}{\equiv}\text{CPh})(bma)$ (bridging isomer **8a**)[a]

		bond distances	
Co(1)-Co(2)	2.469(4)	Co(1)-C(1)	1.77(3)
Co(1)-P(1)	2.223(6)	Co(1)-C(2)	1.71(2)
Co(1)-C(5)	1.91(2)	Co(1)-C(6)	2.01(2)
Co(2)-P(2)	2.214(5)	Co(2)-C(3)	1.75(3)
Co(2)-C(4)	1.65(2)	Co(2)-C(5)	1.91(2)
Co(2)-C(6)	1.93(2)	P(1)-C(11)	1.81(2)
P(2)-C(16)	1.78(2)	O(1)-C(1)	1.15(3)
O(2)-C(2)	1.18(3)	O(3)-C(3)	1.15(3)
O(4)-C(4)	1.21(3)	O(12)-C(12)	1.19(3)
O(13)-C(12)	1.38(3)	O(13)-C(14)	1.32(3)
O(14)-C(14)	1.21(3)	C(5)-C(6)	1.29(3)
C(11)-C(12)	1.48(3)	C(11)-C(15)	1.42(3)
C(14)-C(15)	1.48(3)		
		bond angles	
Co(2)-Co(1)-P(1)	108.3(2)	P(1)-Co(1)-C(1)	109.4(6)
P(1)-Co(1)-C(2)	97.0(8)	P(1)-Co(1)-C(5)	138.2(7)
P(1)-Co(1)-C(6)	100.0(6)	C(1)-Co(1)-C(2)	97(1)
Co(1)-Co(2)-P(2)	96.8(2)	P(2)-Co(2)-C(3)	106.6(6)
P(2)-Co(2)-C(4)	103.4(8)	P(2)-Co(2)-C(5)	142.9(5)
P(2)-Co(2)-C(6)	110.8(5)	C(3)-Co(2)-C(4)	99(1)
Co(1)-P(1)-C(11)	115.6(6)	Co(2)-P(2)-C(15)	113.3(6)
Co(1)-C(1)-O(1)	177(2)	Co(1)-C(2)-O(2)	179(3)

Table 3.15. continued

Co(2)-C(3)-O(3)	169.(2)	Co(2)-C(4)-O(4)	175.(2)
Co(1)-P(1)-C(111)	108.1(6)	Co(1)-P(1)-C(117)	122.9(8)
C(1)-Co(1)-C(2)	97.(1)	C(1)-Co(1)-C(5)	107.5(9)
C(1)-Co(1)-C(6)	140.1(9)	C(2)-Co(1)-C(5)	96.9(9)
C(2)-Co(1)-C(6)	105.(1)	C(5)-Co(1)-C(6)	38.2(9)
C(3)-Co(2)-C(4)	99.(1)	C(3)-Co(2)-C(5)	96.8(9)
C(3)-Co(2)-C(6)	135.8(9)	C(4)-Co(2)-C(5)	100.9(9)
C(4)-Co(2)-C(6)	95.(1)	C(5)-Co(2)-C(6)	39.1(9)
C(11)-P(1)-C(111)	105.(1)	C(11)-P(1)-C(117)	101.6(9)
C(111)-P(1)-C(117)	101.3(9)	Co(1)-C(5)-Co(2)	80.4(6)
Co(1)-C(5)-C(51)	139.(2)	Co(2)-C(5)-C(6)	71.(1)
Co(2)-C(5)-C(51)	129.(1)	Co(1)-C(6)-C(5)	67.(1)
Co(2)-C(6)-C(5)	69.(1)	P(1)-C(11)-C(12)	127.(1)
P(1)-C(11)-C(15)	127.(2)	C(12)-C(11)-C(15)	106.(2)
O(12)-C(12)-O(13)	119.(2)	O(12)-C(12)-C(11)	132.(2)
O(13)-C(12)-C(11)	110.(2)	O(13)-C(12)-C(11)	110.(2)
O(13)-C(14)-O(14)	122.(2)	O(13)-C(14)-C(15)	113.(2)
O(14)-C(14)-C(15)	125.(2)	P(2)-C(15)-C(11)	125.(2)
P(2)-C(15)-C(14)	131.(2)	C(11)-C(15)-C(14)	104.(2)

[a]Numbers in parentheses are estimated standard deviations in the least significant digits.

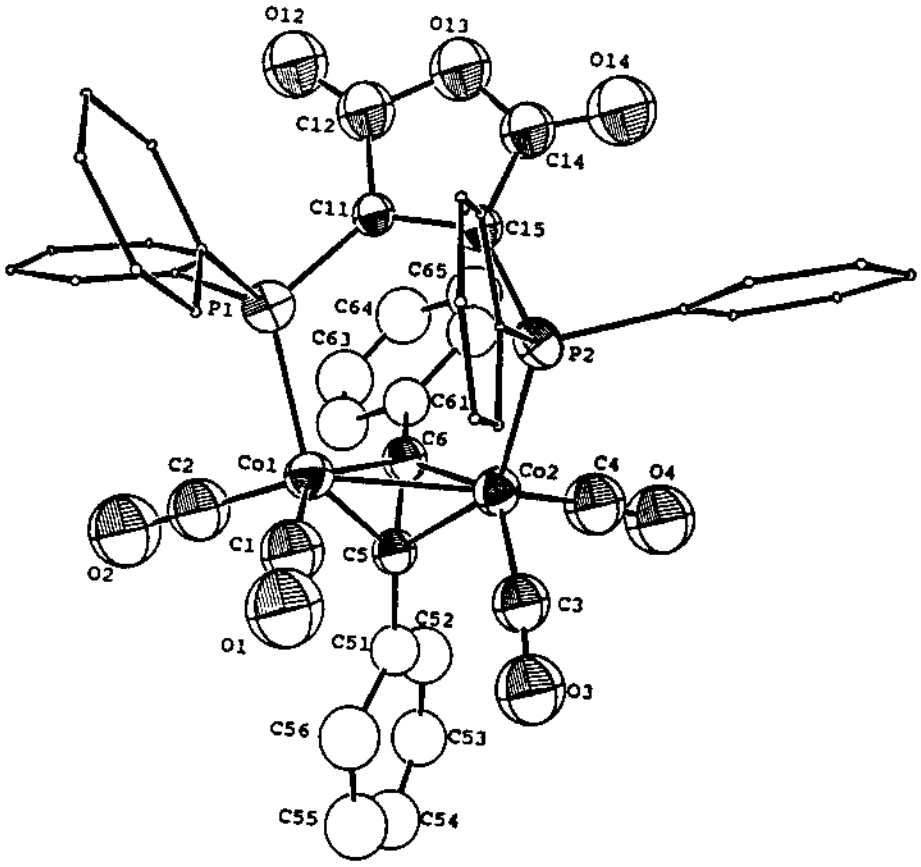

Figure 3.9. ORTEP diagram of $Co_2(CO)_4(\mu\text{-PhC}{\equiv}\text{CPh})$(bma) (bridging isomer **8a**) with the thermal ellipsoids drawn at the 50% probability level. H atoms are omitted for clarity.

Table 3.16. X-Ray Crystallographic Collection and Processing Data for the Dinuclear Complex $PhCCPhCo_2(CO)_4$ [(Z)-$Ph_2PCH=CHPPh_2$] (9)

Space group	P1/triclinic
Cell Constants	
a, Å	9.993 (2)
b, Å	12.047 (2)
c, Å	16.657 (2)
α, deg	74.67 (1)
β, deg	77.99 (1)
γ, deg	84.52 (1)
V, $Å^3$	1889.2 (6)
mol formula	$C_{44}H_{32}Co_2O_4P_2$
fw	804.56
formula units per cell (Z)	2
ρ, g • cm^{-3}	1.414
abs coeff (μ), cm^{-1}	10.00
collection range, deg	$2.0 \leq 2\theta \leq 44.0$
total data collected	4836
independent data, $I > 3\sigma(I)$	2425
R	0.0587
R_w	0.0658
weights	$[\,0.04F^2 + (\sigma F)^2\,]^{-1}$

3.17. Selected Bond Distances (Å) and Angles (deg) for $Co_2(CO)_4(\mu$-PhC≡CPh)[(Z)-Ph_2PCH=$CHPPh_2$] (**9**)[a]

		bond distances	
Co(1)-Co(2)	2.485(2)	Co(1)-C(1)	1.78(1)
Co(1)-P(1)	2.237(3)	Co(1)-P(2)	2.188(3)
Co(1)-C(21)	1.930(9)	Co(1)-C(22)	1.92(1)
Co(2)-C(2)	1.77(1)	Co(2)-C(3)	1.79(1)
Co(2)-C(4)	1.71(1)	Co(2)-C(21)	1.99(1)
Co(2)-C(22)	1.98(1)	O(1)-C(1)	1.15(2)
O(2)-C(2)	1.16(2)	O(3)-C(3)	1.13(2)
O(4)-C(4)	1.17(1)	C(11)-C(12)	1.31(2)
		bond angles	
P(1)-Co(1)-P(2)	87.7(1)	P(1)-Co(1)-C(1)	106.6(4)
P(2)-Co(1)-C(1)	96.8(4)	C(2)-Co(2)-C(3)	104.2(6)
C(2)-Co(2)-C(4)	103.8(7)	C(3)-Co(2)-C(4)	98.5(7)
Co(1)-C(1)-O(1)	171.8(9)	Co(2)-C(2)-O(2)	179(1)
Co(2)-C(3)-O(3)	175(1)	Co(2)-C(4)-O(4)	176(1)

[a]Numbers in parentheses are estimated standard deviations in the least significant digits.

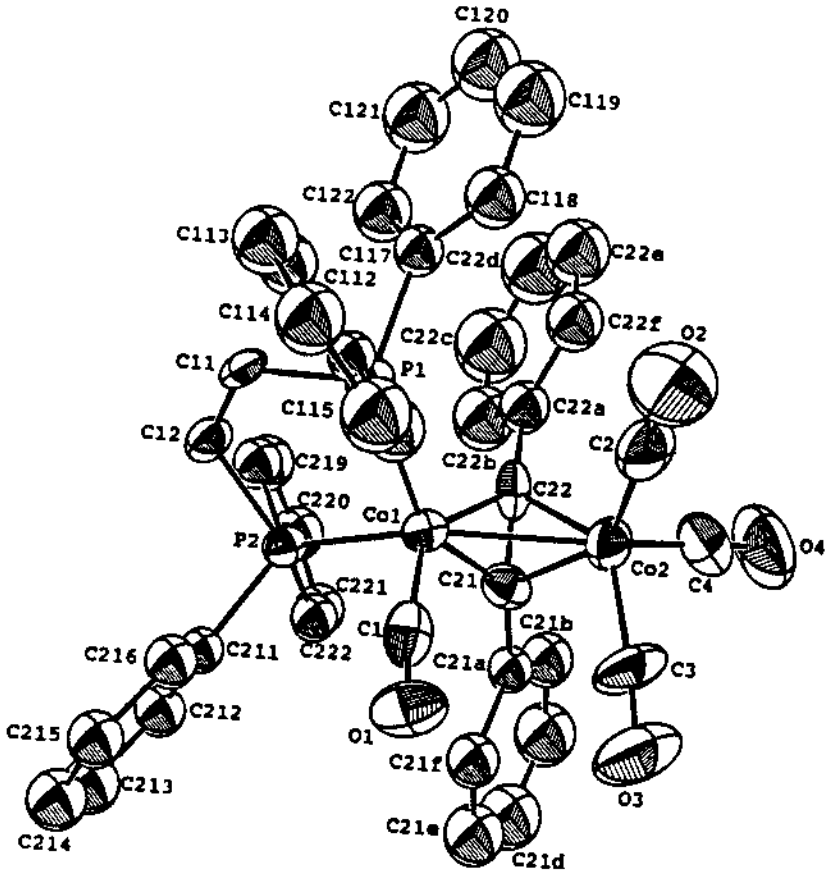

Figure 3.10. ORTEP diagram of $Co_2(CO)_4(\mu\text{-PhC}{\equiv}\text{CPh})[(Z)\text{-}Ph_2PCH{=}CHPPh_2]$ with the thermal ellipsoids drawn at the 50% probability level. H atoms are omitted for clarity.

short inter- and intramolecular contacts. Table 3.14 lists the X-ray data collection and processing parameters, while Table 3.15 gives the selected distances and angles. The ORTEP diagram is shown in Figure 3.9.

Q. X-Ray Diffraction Structure of $Co_2(CO)_4(\mu\text{-}PhC{\equiv}CPh)[(Z)Ph_2PCH{=}CHPPh_2]$

Single crystals of **9** were grown and the molecular structure was determined. **9** exists as discrete molecules in the unit cell with no unusual short inter- and intramolecular contacts. Table 3.16 lists the X-ray data collection and processing parameters, while Table 3.17 gives the selected distances and angles. The ORTEP diagram is shown in Figure 3.10.

R. X-Ray Diffraction Structure of $Co_2(CO)_4[\eta^2,\eta^2,\eta^1,\eta^1\text{-}(Z)\text{-}Ph_2PC(Ph)=(Ph)C\text{-}\overline{C=C(PPh_2)C(O)OC(O)}]$

Single crystals of **10** were grown and the molecular structure was determined. **10** exists as discrete molecules in the unit cell with no unusual short inter- and intramolecular contacts. Table 3.18 lists the X-ray data collection and processing parameters, while Table 3.19 gives the selected distances and angles. The ORTEP diagram is shown in Figure 11.

S. Cyclic Voltammetric Investigation of $Co_2(CO)_4(\mu\text{-}PhC{\equiv}CPh)(bma)$, $Co_2(CO)_4(\mu\text{-}PhC{\equiv}CPh)[(Z)\text{-}Ph_2PCH{=}CHPPh_2]$ and $Co_2(CO)_4[\eta^2,\eta^2,\eta^1,\eta^1\text{-}(Z)\text{-}Ph_2PC(Ph)=(Ph)C\text{-}\overline{C=C(PPh_2)C(O)OC(O)}]$.

The electrochemical behavior of the dinuclear complexes $Co_2(CO)_4(\mu\text{-}PhC{\equiv}CPh)(bma)$, $Co_2(CO)_4(\mu\text{-}PhC{\equiv}CPh)[(Z)\text{-}Ph_2PCH{=}CHPPh_2]$ and $Co_2(CO)_4[\eta^2,\eta^2,\eta^1,\eta^1\text{-}(Z)\text{-}Ph_2PC(Ph)=(Ph)C\text{-}\overline{C=C(PPh_2)C(O)OC(O)}]$ was next examined

Table 3.18. X-Ray Crystallographic Collection and Processing Data for $Co_2(CO)_4[\eta^2,\eta^2,\eta^1,\eta^1$–(Z)-$Ph_2PC(Ph)=(Ph)CC(=C(PPh_2)C(O)OC(O)]$ (10)

Space group	$P2_12_12_1$/orthorhombic
Cell Constants	
a, Å	10.352 (1)
b, Å	15.883 (1)
c, Å	23.437 (2)
V, Å^3	3853.5 (6)
mol formula	$C_{46}H_{30}Co_2O_7P_2$
fw	874.56
formula units per cell (Z)	4
ρ, g • cm^{-3}	1.507
abs coeff (μ), cm^{-1}	9.92
radiation Mo Kα (λ), Å	0.71073
collection range, deg	$2.0 \leq 2\theta \leq 44.0$
scan speed range, deg•min^{-1}	0.67-8.0
max scan time, (s)	120
total data collected	2694
independent data, $I > 3\sigma(I)$	1141
R	0.0529
R_w	0.0608
weights	$[0.04F^2 + (\sigma F)^2]^{-1}$

Table 3.19. Selected Bond Distances (Å) and Angles (deg) for $Co_2(CO)_4[\eta^2,\eta^2,\eta^1,\eta^1$-(Z)-$Ph_2PC(Ph)=(Ph)C$-$\overline{C(O)OC(O)}$-$\overline{C=C(PPh_2)}$] (**10**)[a]

		bond distances	
Co(1)-Co(2)	2.594(4)	Co(1)-P(1)	2.244(6)
Co(1)-C(1)	1.77(2)	Co(1)-C(2)	1.73(2)
Co(1)-C(16)	2.09(2)	Co(1)-C(17)	2.11(2)
Co(2)-P(2)	2.179(6)	Co(2)-C(3)	1.76(2)
Co(2)-C(4)	1.81(2)	Co(2)-C(11)	2.11(2)
Co(2)-C(15)	2.00(2)	P(1)-C(11)	1.76(2)
P(2)-C(17)	1.81(2)	O(1)-C(1)	1.16(2)
O(2)-C(2)	1.17(3)	O(3)-C(3)	1.19(3)
O(4)-C(4)	1.12(3)	O(12)-C(12)	1.22(3)
O(13)-C(12)	1.42(3)	O(13)-C(14)	1.39(2)
O(14)-C(14)	1.19(3)	C(14)-C(15)	1.53(3)
C(15)-C(16)	1.45(3)	C(16)-C(17)	1.51(3)
		bond angles	
Co(2)-Co(1)-P(1)	71.8(2)	Co(2)-Co(1)-C(1)	174.3(7)
Co(2)-Co(1)-C(2)	94.3(7)	C(1)-Co(1)-C(2)	90(1)
C(1)-Co(1)-C(16)	100.5(9)	C(1)-Co(1)-C(17)	96.5(9)
C(2)-Co(1)-C(16)	161.5(9)	C(2)-Co(1)-C(17)	122.2(9)
P(2)-Co(2)-C(15)	84.5(7)	C(3)-Co(2)-C(4)	94(1)
C(4)-Co(2)-C(11)	115.5(9)	C(4)-Co(2)-C(15)	155(1)
Co(1)-P(1)-C(11)	92.7(7)	Co(1)-C(1)-O(1)	175(2)
Co(1)-C(2)-O(2)	170(2)	Co(2)-C(16)-C(17)	115(2)

Table 3.19 continued

Co(2)-C(4)-O(4)	178(2)	C(15)-C(16)-C(17)	115.(2)
P(1)-Co(1)-C(1)	110.4(6)	P(1)-Co(1)-C(1)	110.4(6)
P(1)-Co(1)-C(2)	102.0(7)	P(1)-Co(1)-C(16)	88.2(6)
P(1)-Co(1)-C(17)	127.9(6)	P(2)-Co(2)-C(3)	101.8(7)
P(2)-Co(2)-C(4)	110.4(8)	P(2)-Co(2)-C(15)	84.5(7)
Co(1)-P(1)-C(111)	119.4(8)	Co(1)-P(1)-C(117)	122.2(7)
C(11)-P(1)-C(111)	109.(1)	C(11)-P(1)-C(117)	112.(1)
C(111)-P(1)-C(117)	101.(1)	P(1)-C(11)-C(12)	141.(2)
P(1)-C(11)-C(15)	111.(2)	C(12)-C(11)-C(15)	106.(2)
O(12)-C(12)-O(13)	115.(2)	O(12)-C(12)-C(11)	132.(2)
O(13)-C(12)-C(11)	113.(2)	O(13)-C(14)-O(14)	121.(2)
O(13)-C(14)-C(15)	109.(2)	O(14)-C(14)-C(15)	130.(2)
C(14)-C(15)-C(16)	122.(2)	C(11)-C(15)-C(14)	103.(2)
C(11)-C(15)-C(16)	124.(2)	P(2)-C(17)-C(16)	112.(1)
Co(1)-C(17)-P(2)	91.6(9)	Co(1)-C(17)-C(16)	68.(1)
Co(1)-C(17)-C(171)	126.(1)	C(16)-C(17)-C(171)	124.(2)
Co(1)-C(16)-C(161)	119.(1)		

[a]Numbers in parentheses are estimated standard deviations in the least significant digits.

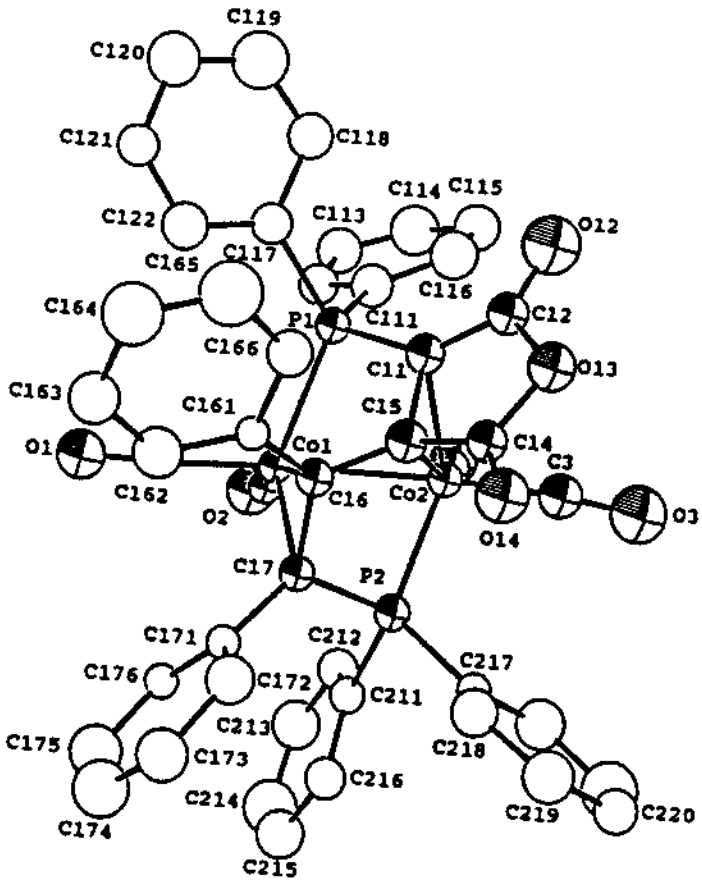

Figure 3.11. ORTEP diagram of $Co_2(CO)_4[\eta^2,\eta^2,\eta^1,\eta^1$–(Z)-$Ph_2PC(Ph)=(Ph)C\text{-}\overline{C=(PPh_2)C(O)OC(O)}]$ with the thermal ellipsoids drawn at the 50% probability level. H atoms are omitted for clarity.

as part of my interest in redox-active polynuclear systems that bear a pendant redox-active ligand. [2a] Here the dinuclear complexes with the bma ligand would be expected to display redox properties different from the analogous phosphine-substituted $Co_2(CO)_{6-n}(\mu\text{-alkyne})P_n$ (where n = 1, 2). [17,19,20]

The cyclic voltammetry studies were conducted in CH_2Cl_2 containing 0.1 M tetra-n-butylammonium perchlorate (TBAP) as the supporting electrolyte at a platinum electrode. The two isomers of $Co_2(CO)_4(\mu\text{-PhC}\equiv\text{CPh})$(bma) allow a direct comparison regarding the redox properties as function of the coordination mode adopted by the bma ligand. Both of these isomers display three well-defined redox responses as shown by the cyclic voltammograms (CV) in Figure 3.12, while Table 3.20 gives the pertinent potential data for all of the compounds studied. The 0/-1 redox couple of both isomers of $Co_2(CO)_4(\mu\text{-PhC}\equiv\text{CPh})$(bma) is reversible, on the basis of peak current (Ip^a/Ip^c) ratios of unity and plots of the current function (Ip) vs. the square root of the scan rate ($v^{1/2}$), [21] which were linear over the scan rates examined. Calibration of the peak currents against ferrocene also supports the one-electron nature of this couple. The second reduction step is less reversible as judged by the diminished current ratios of 0.58 and 0.88 for the chelating and bridging isomers, respectively. The reduction waves of both isomers exhibit only slight potential differences and no significance is attached to these potentials as a function of the coordination mode of the bma ligand. How the bma ligand coordinates to the Co-Co core does, however, affect the potential of the 0/+1 redox couple. It can be seen that $Co_2(CO)_4(\mu\text{-PhC}\equiv\text{CPh})$(bma) (chelating) is oxidized at 0.13 V more positive than $Co_2(CO)_4(\mu\text{-PhC}\equiv\text{CPh})$(bma) (bridging). This is of interest because such an effect has not been previously reported for a dinuclear complex. [22] The 0/+1

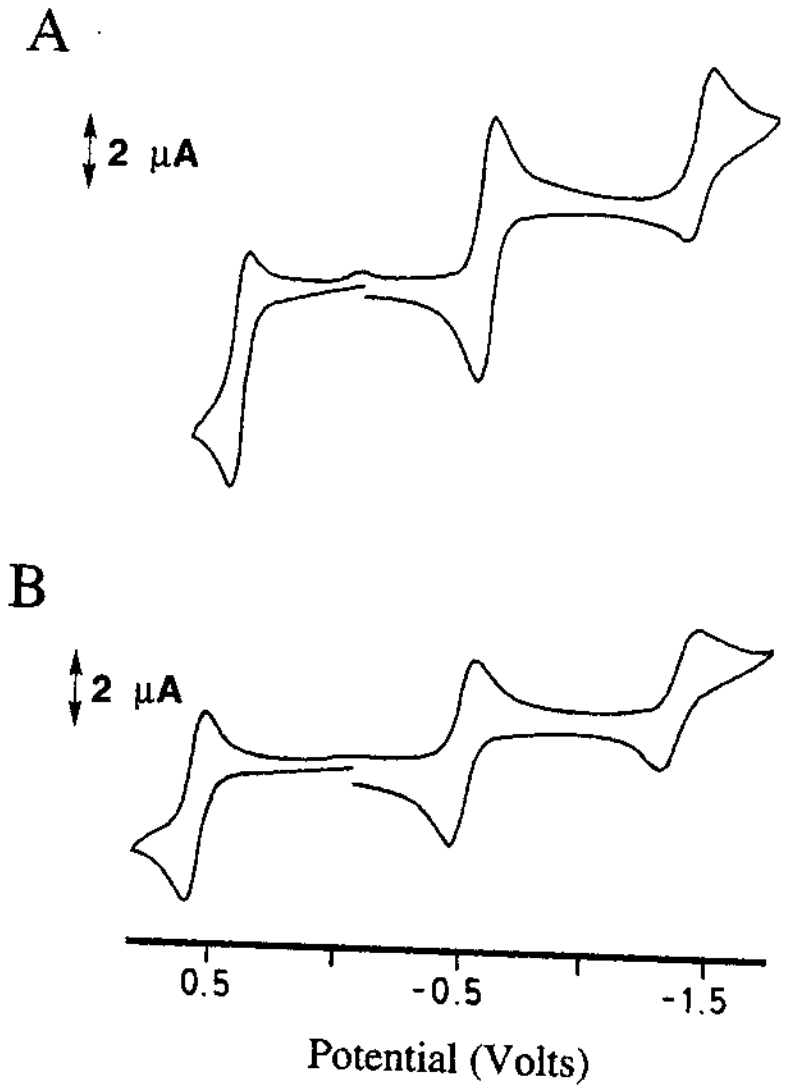

Figure 3.12. Anodic Scan Cyclic Voltammogram of (A) **8a** (chelating) (ca. 3.2 x 10^{-3} M) and (B) **8b** (bridging) (ca. 1.9 x 10^{-3} M) in CH_2Cl_2 containing 0.1 M TBAP at 100 mv/s.

Table 3.20. Cyclic Voltammetry Data[a] for the Dinuclear Complexes **8a**, **9**, **10**, $Co_2(CO)_6(\mu\text{-PhC}{\equiv}\text{CPh})$, and bma.

Redox Couple : [b]	0/+1			0/-1			-1/-2		
Compound	$E_p{}^a$	$E_p{}^c$	$E_{1/2}$	$E_p{}^a$	$E_p{}^c$	$E_{1/2}$	$E_p{}^a$	$E_p{}^c$	$E_{1/2}$
8a (bridging)	0.48	0.39	0.44	-0.61	-0.53	-0.57	-1.50	-1.39	-1.45
8b (chelating)	0.61	0.53	0.57	-0.56	-0.47	-0.52	-1.47	-1.33	-1.40
9	0.26	0.18	0.22	-	-	-	-	-	-
10	1.06	-	-	-0.87	-0.77	-0.82	-1.62	-1.44	-1.53
$Co_2(CO)_6(\mu\text{-PhC}{\equiv}\text{CPh})$ [c]	0.98	-	-	-1.35	-	-	-	-	-
bma (free ligand) [d]	-	-	-	-0.67	-0.58	-0.63	-1.44	-1.32	-1.38

[a] In ~ 10^{-3} M CH_2Cl_2 solution containg 0.1 M TBAP at room temperature and a scan rate of 0.1 V s^{-1}. Potentials are in Volts relative to a silver wire quasi-reference electrode, calibrated against ferrocene. [b] $E_p{}^a$ and $E_p{}^c$ refer to the anodic and cathodic peak potentials of the CV waves. The half-wave potential $E_{1/2}$, which represents the chemically reversible redox couple, is defined as $(E_p{}^a + E_p{}^c)/2$. [c] See ref. 23(a). [d] See ref. 20.

redox couple in both isomers is only partially reversible, as then current ratio for both isomers is ~ 0.8 at room temperature. Moreover, the small amount of unknown material in the CV at -0.05 V (Fig. 3.12a) and 0.01 V (Fig. 3.12b) arises from the radical cation of each isomer. Lowering the temperature to 0°C renders the oxidation wave fully reversible.

The CV of $Co_2(CO)_4(\mu\text{-PhC}{\equiv}\text{CPh})[(Z)\text{-}Ph_2PCH{=}CHPPh_2]$ reveals the presence of a quasi-reversible oxidation (Ip^c/Ip^a ~ 0.50) at $E_{1/2}$ = 0.22 V. No reduction wave was observed when the CV was scanned out to the - 2 V. The lack of a reduction wave(s) in $Co_2(CO)_4(\mu\text{-PhC}{\equiv}\text{CPh})[(Z)\text{-}Ph_2PCH{=}CHPPh_2]$ is consistent with the data reported for other diphosphine-substituted dinuclear complexes of this type, [18] as the LUMO is predicted to be an antibonding Co-Co orbital. [23,24] Since the $Co_2(CO)_4(\mu\text{-PhC}{\equiv}\text{CPh})$(bma) isomers display low-energy reduction waves, this suggest that the bma ligand is the site of electron accession, a fact supported by the work of Fenske and Tyler in addition to the MO calculations reported here (vide infra). [20,25,26]

The dinuclear complex $Co_2(CO)_4[\eta^2,\eta^2,\eta^1,\eta^1\text{–}(Z)\text{-}Ph_2PC(Ph){=}(Ph)C\overline{C{=}C(PPh_2)C(O)O\overline{C(O)}}]$ exhibits similar reductive CV behavior with respect to the isomers of $Co_2(CO)_4(\mu\text{-PhC}{\equiv}\text{CPh})$(bma), showing two redox waves at $E_{1/2}$ = -0.82 and -1.53 V. The assignments for these waves are the same as those for $Co_2(CO)_4(\mu\text{-PhC}{\equiv}\text{CPh})$(bma) (i.e., bma-based reductions). Unlike the quasi-reversible 0/+1 wave found in each isomer of $Co_2(CO)_4(\mu\text{-PhC}{\equiv}\text{CPh})$(bma) and $Co_2(CO)_4(\mu\text{-PhC}{\equiv}\text{CPh})[(Z)\text{-}Ph_2PCH{=}CHPPh_2]$, an irreversible oxidation (Ip^a = 1.06 V) is recorded for $Co_2(CO)_4[\eta^2,\eta^2,\eta^1,\eta^1\text{–}(Z)\text{-}Ph_2PC(Ph){=}(Ph)C\text{-}\overline{C{=}C(PPh_2)C(O)O\overline{C(O)}}]$.

The CV of the parent complex $Co_2(CO)_6(\mu\text{-PhC}{\equiv}\text{CPh})$ has been recorded under conditions identical to those used for $Co_2(CO)_4(\mu\text{-PhC}{\equiv}\text{CPh})$(bma) ,

$Co_2(CO)_4(\mu\text{-}PhC{\equiv}CPh)[(Z)\text{-}Ph_2PCH{=}CHPPh_2]$, and $Co_2(CO)_4[\eta^2,\eta^2,\eta^1,\eta^1\text{–}(Z)\text{-}Ph_2PC(Ph){=}(Ph)C\text{-}\overline{C{=}C(PPh_2)C(O)OC(O)}]$ and is included for comparative purposes only, as the electrochemical behavior of this compound has been fully explored. [23a] In CH_2Cl_2 solvent, both the oxidation and reduction waves are irreversible at a scan rate of 0.1 V s^{-1}. Since the substitution of two CO ligands in $Co_2(CO)_6(\mu\text{-}PhC{\equiv}CPh)$ by P-ligands is anticipated to decrease the reduction potential of $Co_2(CO)_6(\mu\text{-}PhC{\equiv}CPh)$ by ~ 0.2 V per P-ligand, [27] the absence of a reduction wave for $Co_2(CO)_4(\mu\text{-}PhC{\equiv}CPh)[(Z)\text{-}Ph_2PCH{=}CHPPh_2]$ is not surprising. However, the observation of multiple reduction waves for both isomers of $Co_2(CO)_4(\mu\text{-}PhC{\equiv}CPh)$(bma) and $Co_2(CO)_4[\eta^2,\eta^2,\eta^1,\eta^1\text{–}(Z)\text{-}Ph_2PC(Ph){=}(Ph)C\text{-}\overline{C{=}C(PPh_2)C(O)OC(O)}]$ surely attests to the ability of the bma ligand to control the electron transfer process by stabilizing the added electron in a low-energy π^* orbital associated with the anhydride ring. The CV responses of the bma ligand have been included in Table 3.20, and the presence of two reduction waves at potentials close to those reported for the dinuclear complexes $Co_2(CO)_4(\mu\text{-}PhC{\equiv}CPh)$(bma) and $Co_2(CO)_4[\eta^2,\eta^2,\eta^1,\eta^1\text{–}(Z)\text{-}Ph_2PC(Ph){=}(Ph)C\text{-}\overline{C{=}C(PPh_2)C(O)OC(O)}]$ supports the LUMO as being a primarily bma-based orbital.

$Co_2(CO)_4(\mu\text{-}PhC{\equiv}CPh)$(bma) (chelating) was also examined by constant-potential coulometry in order to verify the electron stoichiometry associated with the 0/-1 redox couple and to explore the effect of electron accession on the IR stretching bands of the CO and bma ligands. The compound was reduced electrochemically at -0.60 V in CH_2Cl_2 solvent containing 0.1 M TBAP at -20 °C. The total charge passed upon completion of the reduction was Q = 0.97 coulombs per mole of $Co_2(CO)_4(\mu\text{-}PhC{\equiv}CPh)$(bma) in agreement with the one-electron nature of this redox couple. IR analysis of the catholyte at -20 °C

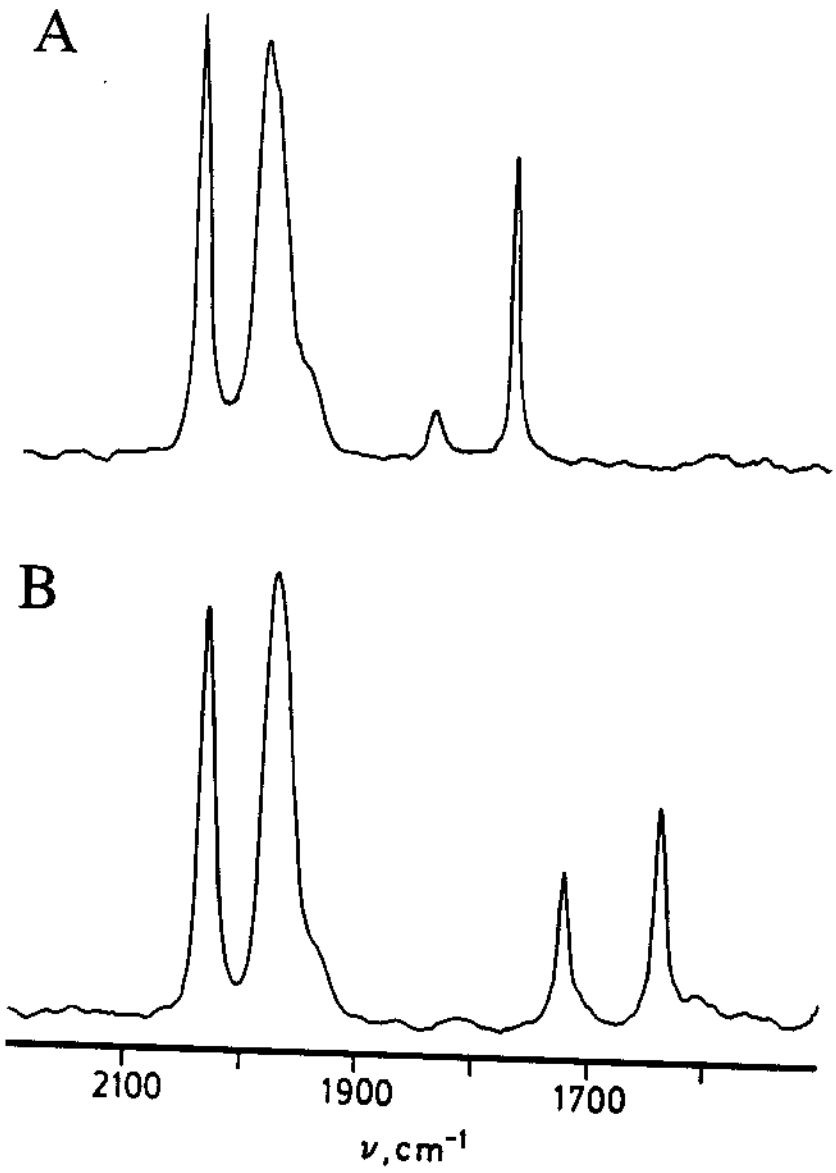

Figure 3.13. Infrared Spectra of the Carbonyl Region for (A) **8a** (chelating), and (B) **8a**$^{-\bullet}$ (chelating) in CH_2Cl_2 containing 0.1 M TBAP at -20°C.

shows the presence of four new ν (CO) bands at 2031 (vs), 1972 (vs), 1772 (s), and 1638 (s) cm^{-1}. The former two bands belong the same terminal carbonyl groups already described for the neutral chelating isomer $Co_2(CO)_4$(μ-PhC≡CPh)(bma) but shifted by 16 and 21 cm^{-1} to lower frequency. This slight shift observed in the terminal CO bands indicates that only a small amount of the added electron density is associated with these CO groups. [28] A much larger shift is found in the latter two bma ν (CO) bands, which reveals that extensive odd-electron density is localized in the anhydride ring of the bma ligand. [18,25,26] Figure 3.13 shows the IR data of $Co_2(CO)_4$(μ-PhC≡CPh)(bma) (chelating) and $Co_2(CO)_4$(μ-PhC≡CPh)(bma) (chelating)$^{\bullet-}$. In view of the current thinking on 18+δ complexes put forth by Brown and Tyler, [18,26,29], the radical anion derived from each isomer of $Co_2(CO)_4$(μ-PhC≡CPh)(bma) can be considered as a 36+δ complex, as opposed to formal 37-electron complex.

T. Extended Hückel Calculations.

The nature of the HOMO and LUMO in both isomers of $Co_2(CO)_4$(μ-PhC≡CPh)(bma) and $Co_2(CO)_4$(μ-PhC≡CPh)[(Z)-Ph_2PCH=CHPPh_2] was determined by carrying out extended Hückel molecular orbital calculations. For simplicity, the phenyl groups associated with the acetylene and diphosphine ligands were replaced by hydrogen groups. Figure 3.14 shows the three-dimensional CACAO drawings of these molecular orbitals along with their respective energies.

In each dinuclear complex examined, the HOMO, which is found at ~ -11.9 eV, can best be described as a metal-based orbital that is composed of an in-phase overlap of hybridized dyz orbitals. The nature of this hybridization has been fully analyzed by Hoffmann and co-workers in an earlier paper on

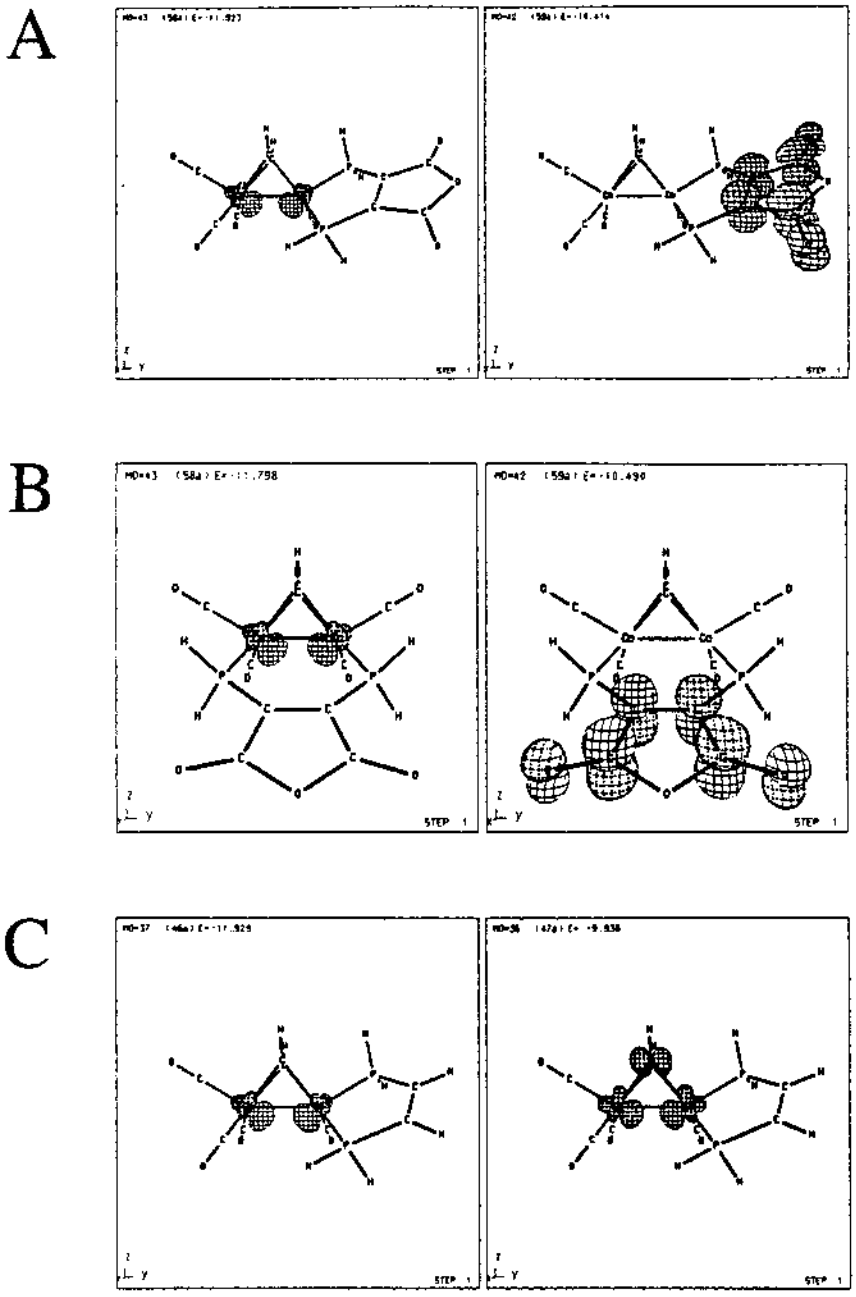

Figure 3.14. CACAO Drawings of the HOMO (left) and the LUMO (right) for (A) $Co_2(CO)_4(\mu\text{-}HC{\equiv}CH)(H_4\text{-bma})$ (chelating), and (B) $Co_2(CO)_4(\mu\text{-}HC{\equiv}CH)(H_4\text{-bma})$ (bridging), and (C) $Co_2(CO)_4(\mu\text{-}HC{\equiv}CH)[(Z)\text{-}H_2PCH{=}CHPH_2]$ (chelating).

the parent compound $Co_2(CO)_6(CH{\equiv}CH)$. [24,30-32] More importantly, the calculations clearly reveal that the LUMO in both isomers of the dinuclear complex $Co_2(CO)_4(\mu\text{-}PhC{\equiv}CPh)$(bma) resides primarily on the bma ligand, in full agreement with the electrochemical data and the 36+δ formalism ascribed to the one-electron reduction product derived from $Co_2(CO)_4(\mu\text{-}PhC{\equiv}CPh)$ (bma). The nodal pattern of the bma ligand in each LUMO of $Co_2(CO)_4(\mu\text{-}PhC{\equiv}CPh)$(bma) can be envisioned as arising from ψ_4 of an isolated six π-electron system (e.g., maleic anhydride or hexatriene). [33] The LUMO energy for each of these compounds is calculated at ~ -10.4 eV, and is substantially below the LUMO found for complex $Co_2(CO)_4(\mu\text{-}PhC{\equiv}CPh)[(Z)\text{-}Ph_2PCH{=}CHPPh_2]$, which does not possess a redox-active diphosphine ligand.

The LUMO in $Co_2(CO)_4(\mu\text{-}PhC{\equiv}CPh)[(Z)\text{-}Ph_2PCH{=}CHPPh_2]$ is represented by an out-of phase overlap of hybridized dyz orbitals, with a contribution from the acetylene π bond. This LUMO is the same as calculated by Hoffmann and co-workers for $Co_2(CO)_6(CH{\equiv}CH)$, [24] and is best described as an antibonding Co-Co orbital, whose energy is ~ -9.9 eV. The effect of the unsaturated ethano bridge on the HOMO and LUMO in $Co_2(CO)_4(\mu\text{-}PhC{\equiv}CPh)[(Z)\text{-}Ph_2PCH{=}CHPPh_2]$ was also probed by conducting calculations on the model compound $Co_2(CO)_4(PH_3)_2(\mu\text{-}CH{\equiv}CH)$ (1,1-substitution). The calculated HOMO and LUMO energy levels and the orbital compositions exhibited no major perturbations from those data obtained from the dinuclear complex $Co_2(CO)_4(\mu\text{-}PhC{\equiv}CPh)[(Z)\text{-}Ph_2PCH{=}CHPPh_2]$.

U. Synthesis and Spectroscopic Properties of $Co_2(CO)_4(\mu\text{-}PhC{\equiv}CH)$(bma) and $Co_2(CO)_4(\mu\text{-}PhC{\equiv}CH)[(Z)\text{-}Ph_2PCH{=}CHPPh_2]$

A clean and immediate reaction was observed when an equimolar

mixture of $Co_2(CO)_6(\mu\text{-PhC}\equiv\text{CH})$ and bma in THF was treated with 2.0 equivalents of the oxidative-decarbonylation reagent Me_3NO at room temperature (Equation 3.12). [6] TLC and IR analyses revealed the presence of small amount of starting material and product (>90%). The resulting green solution was purified by chromatography over a short silica gel column at -78 °C to give $Co_2(CO)_4(\mu\text{-PhC}\equiv\text{CH})$(bma) (**11a**) as an air-sensitive solid, that was

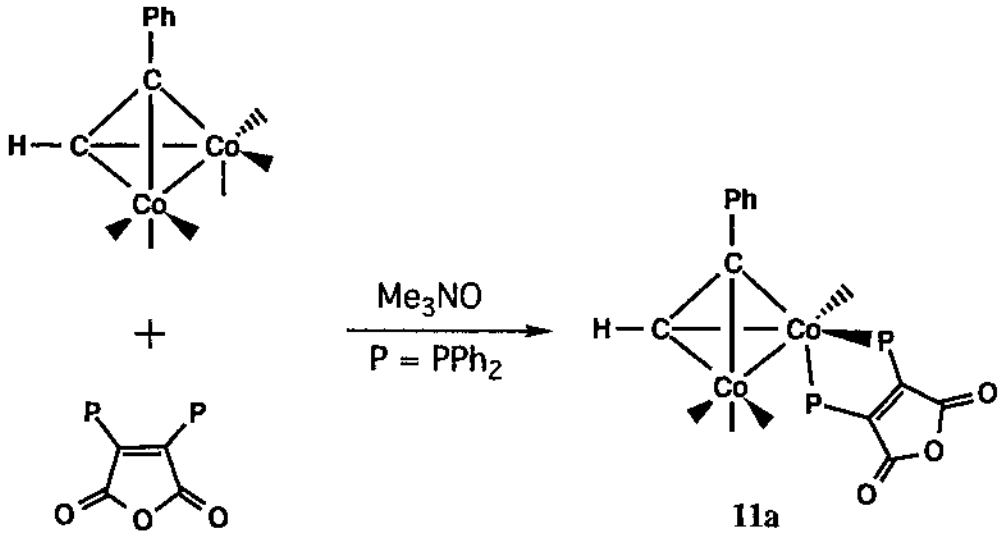

11a (3.12)

routinely isolated yields of 50-65%. The lowered yields of isolated product compared to the solution reactions stem from the partial decomposition of $Co_2(CO)_4(\mu\text{-PhC}\equiv\text{CH})$(bma) on the silica gel, presumably the result of anhydride ring hydrolysis.

The CH_2Cl_2 solution IR spectrum of $Co_2(CO)_4(\mu\text{-PhC}\equiv\text{CH})$(bma) reveals two prominent terminal ν (CO) bands at 2048 (vs), 1989 (vs) cm^{-1}. The symmetry of this IR spectrum is consistent with the IR data for the chelating isomer of $Co_2(CO)_4(\mu\text{-PhC}\equiv\text{CPh})$(bma). The expected ν(CO) bands of the coordinated bma ligand were observed at 1841 (m) and 1775 (s) and attributed

to the vibrationally coupled asymmetric and symmetric bma carbonyl stretches, respectively. [7] These latter two IR assignments were unequivocally established by an isotope study. Repeating the substitution reaction depicted in equation 3.12 with a sample of $Co_2(CO)_6(\mu\text{-}PhC{\equiv}CH)$ that was 20-30% enriched in ^{13}CO afforded the ^{13}CO-enriched compound $Co_2(CO)_4(\mu\text{-}PhC{\equiv}CH)(bma)$ with unchanged bma carbonyl bands.

The ^{31}P NMR spectrum of $Co_2(CO)_4(\mu\text{-}PhC{\equiv}CH)(bma)$ in CH_2Cl_2 solution displayed a pair of equal-intensity resonances located δ 64.6 and 54.4. The low-field location of the ^{31}P resonances supports the presence of a chelating bma ligand with pseudo-axial and pseudo-equatorial bma PPh_2 groups. [9] Furthermore, the ^{13}C NMR spectrum of $Co_2(CO)_4(\mu\text{-}PhC{\equiv}CH)$ (bma) in THF reveals the two terminal carbonyl resonances at δ 207.5 and 201.1 in an integral ratio of 1 : 3, for the lone CO group at the bma-chelated cobalt and the unsubstituted $Co(CO)_3$ centers, respectively. Raising the temperature from -95 °C to 25 °C did not lead to any major changes in the ^{13}C NMR spectrum.

The reaction between $Co_2(CO)_6(\mu\text{-}PhC{\equiv}CH)$ and (Z)-$Ph_2PCH{=}CHPPh_2$ was studied next because the anticipated product $Co_2(CO)_4(\mu\text{-}PhC{\equiv}CH)[(Z)\text{-}Ph_2PCH{=}CHPPh_2]$ would allow for an examination of disparate reactivity between $Co_2(CO)_4(\mu\text{-}PhC{\equiv}CH)(bma)$ and $Co_2(CO)_4(\mu\text{-}PhC{\equiv}CH)[(Z)\text{-}Ph_2PCH{=}CHPPh_2]$. Since the two compounds are expected to be structurally similar, it could be reasonably argued that any observed reactivity differences would have their origin in the electronic properties inherent to each ancillary diphosphine ligand. The complex $Co_2(CO)_4(\mu\text{-}PhC{\equiv}CH)[(Z)\text{-}Ph_2PCH{=}CHPPh_2]$ (**12**) was obtained exclusively as the chelating isomer when $Co_2(CO)_6(\mu\text{-}PhC{\equiv}CH)$ was allowed to react with (Z)-$Ph_2PCH{=}CHPPh_2$ in either 1,2-

dichloroethane at 50 °C or with Me_3NO [6] in THF at room temperature (Equation 3.13). The IR spectrum of $Co_2(CO)_4(\mu\text{-PhC}\equiv\text{CH})[(Z)\text{-}Ph_2PCH{=}CHPPh_2]$ exhibits two terminal ν (CO) bands at 2041 (vs) and 1982 (vs) cm^{-1}. These ν (CO) bands are ~10 cm^{-1} lower in energy than the analogous carbonyl bands in $Co_2(CO)_4(\mu\text{-PhC}\equiv\text{CH})$(bma) (chelating), which reflects the better donor properties of the $(Z)\text{-}Ph_2PCH{=}CHPPh_2$ ligand relative to the bma ligand, with its electron-withdrawing anhydride ring. The chelating

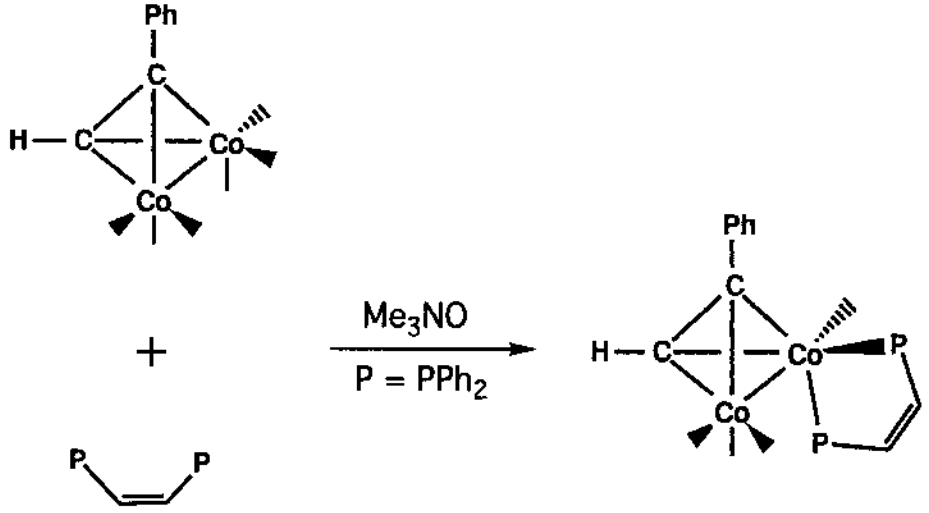

(3.13)

12

nature of the ancillary diphosphine was ascertained by ^{31}P and ^{13}C NMR spectroscopies. The ^{31}P NMR spectrum of $Co_2(CO)_4(\mu\text{-PhC}\equiv\text{CH})[(Z)\text{-}Ph_2PCH{=}CHPPh_2]$ in CH_2Cl_2 solution displayed a pair of equal-intensity resonances located at δ 85.5 and 76.0 with $J_{P\text{-}P}$ values of 19.4 Hz. The low-field location of the ^{31}P resonances supports the presence of a chelating bma ligand, which possesses pseudo-axial and pseudo-equatorial phosphine groups. [9]

The thermolysis and photolysis reactivity of $Co_2(CO)_4(\mu\text{-PhC}\equiv\text{CH})[(Z)\text{-}Ph_2PCH{=}CHPPh_2]$ under conditions comparable to those employed in the reactivity study of $Co_2(CO)_4(\mu\text{-PhC}\equiv\text{CH})$(bma) did not afford any of the

bridging isomer. In both cases the only observed reaction was the decomposition of the diphosphine-bridged cobalt complex, with decomposition from the thermolysis reaction being more extensive than that from the photolysis reaction. The absence of isomerization in $Co_2(CO)_4$(μ-PhC≡CPh)[(Z)-Ph_2PCH=$CHPPh_2$] suggests that the diphosphine remains associated with the cobalt center and does not become free, a condition that would be required for isomerization.

V. Synthesis and Spectroscopic Properties of the Zwitterionic Hydrocarbyl Complex $Co_2(CO)_4$[μ-$\eta^2,\eta^2,\eta^1,\eta^1$–PhC=C(H)$PPh_2$C=C($PPh_2$)C(O)OC(O)]

The thermolysis of $Co_2(CO)_4$(μ-PhC≡CH)(bma) in 1,2-dichloroethane was next investigated under the same conditions as employed in thermolysis of $Co_2(CO)_4$(μ-PhC≡CPh)(bma). The goal of this work was to explore the generality of the P-C bond cleavage exhibited by the coordinated bma ligand in different alkyne-substituted dinuclear cobalt complexes. However, refluxing a 1,2-dichloroethane solution of the chelating isomer of $Co_2(CO)_4$(μ-PhC≡CH)(bma) results in the attack of a PPh_2 moiety on the terminal alkyne carbon to give the zwitterionic hydrocarbyl complex $Co_2(CO)_4$[μ-$\eta^2,\eta^2,\eta^1,\eta^1$–PhC=C(H)$PPh_2$C=C($PPh_2$)C(O)OC(O)], rather than the P-C bond cleavage which was observed in $Co_2(CO)_4$(μ-PhC≡CPh)(bma) (Equation 3.14). The zwitterionic hydrocarbyl complex $Co_2(CO)_4$[μ-$\eta^2,\eta^2,\eta^1,\eta^1$–PhC=C(H)$PPh_2$C=C($PPh_2$)C(O)OC(O)] (**13**) was isolated in 70% yield after passage over a silica gel column using CH_2Cl_2 solvent. This new compound was characterized in solution by IR and NMR spectroscopies. The IR spectrum of **13** displays terminal carbonyl stretching bands at 2035 (s), 2005 (vs), 1983 (m), and 1966 (m) cm^{-1}, in agreement with the highly asymmetric structure

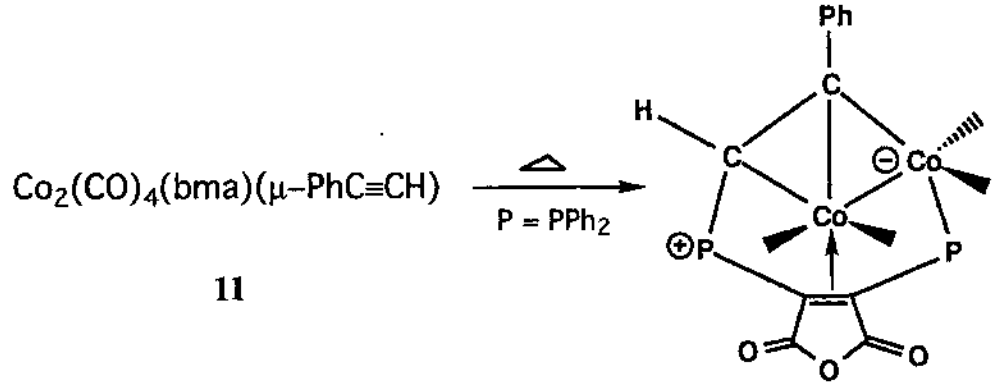

(3.14)

associated with this complex. The ν (CO) bands derived from the bma ligand are observed at 1796 (m) and 1741 (m) cm^{-1}, and are attributed to the vibrationally coupled asymmetric and symmetric bma carbonyl stretches, respectively. [7] The ^{31}P NMR spectrum of **13** reveals a pair of equal-intensity resonances at δ 31.3 and 4.7 ppm with a J_{P-P} value of 77.0 Hz. The higher field resonance has been assigned to the PPh_2 group attached to the cobalt center, while the lower field resonance has been assigned to the PPh_2 group attached to the terminal alkyne carbon. A ^{13}CO-enriched sample of $Co_2(CO)_4[\mu$-$\eta^2,\eta^2,\eta^1,\eta^1$–PhC=C(H)$PPh_2$C=C($PPh_2$)C(O)OC(O)] was prepared and the ^{13}C NMR spectrum recorded in CH_2Cl_2 solvent. At -95 °C, four, equal-intensity resonances were observed at δ 201.1 (J_{P-C} = 19.6 Hz), 203.2, 203.0, and 108.1 with an integral ratio of 1 : 1 : 1 : 1. The ^{13}C NMR spectrum did not change appreciably as the temperature was raised to room temperature. No attempt has been made to assign these resonances to specific CO groups. It is interesting to note that the IR and NMR (^{13}C and ^{31}P) spectra of **13** are very similar as those of the $Co_2(CO)_4[\eta^2,\eta^2,\eta^1,\eta^1$–(Z)-$Ph_2$PC(Ph)=(Ph)C-C=($PPh_2$)C(O)OC(O)], which suggest that **13** might be structurally similar to $Co_2(CO)_4$ [$\eta^2,\eta^2,\eta^1,\eta^1$–(Z)-$Ph_2$PC(Ph)=(Ph)C-C=($PPh_2$)C(O)OC(O)]. However, an X-ray

diffraction study of **13** revealed that this was not the case (vide infra).

The thermal reaction between $Co_2(CO)_6(\mu\text{-PhC}{\equiv}\text{CH})$ and bma was next examined in refluxing CH_2Cl_2 solvent. As discussed, the reaction between $Co_2(CO)_6(\mu\text{-PhC}{\equiv}\text{CPh})$ and bma in refluxing CH_2Cl_2 solvent resulted an equimolar mixture of bridging and chelating isomers of $Co_2(CO)_4(\mu\text{-PhC}{\equiv}\text{CPh})$(bma). [34] However, only the chelating isomer of $Co_2(CO)_4(\mu\text{-PhC}{\equiv}\text{CH})$(bma) was observed after refluxing an equimolar mixture of

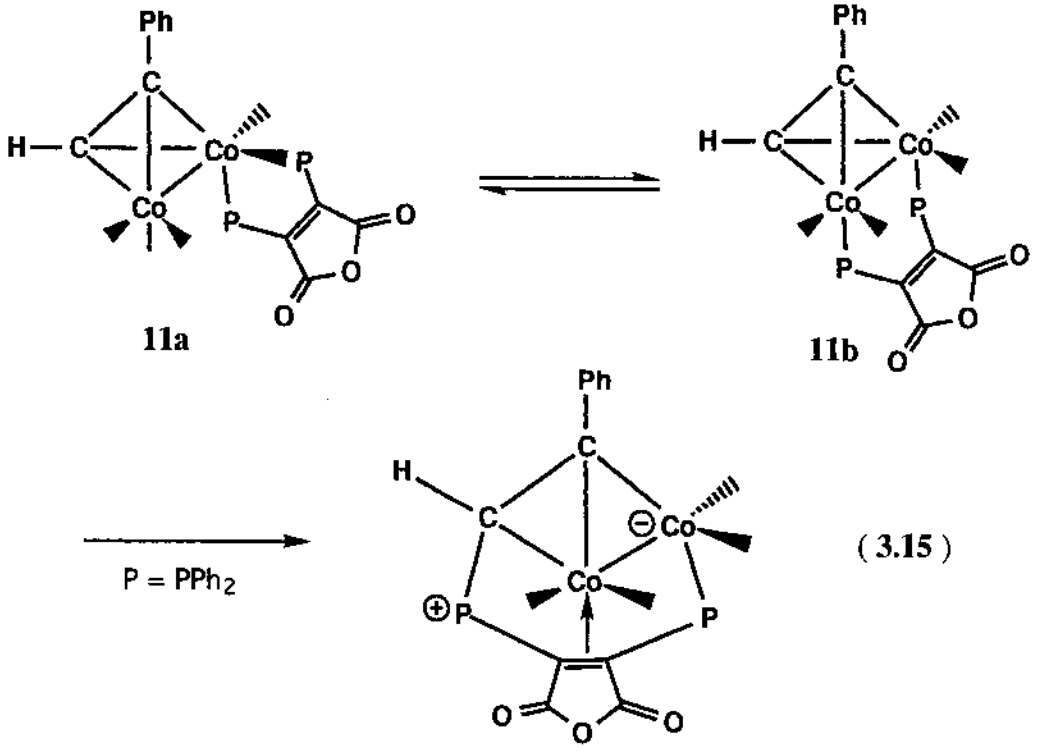

(3.15)

$Co_2(CO)_6(\mu\text{-PhC}{\equiv}\text{CH})$ and bma in CH_2Cl_2 overnight. Monitoring this reaction by IR spectroscopy did not reveal the presence of the bridging isomer. When the reaction was performed in a sealed NMR tube in 1,2-dichloroethane as solvent, a small amount of the bridging isomer of $Co_2(CO)_4(\mu\text{-PhC}{\equiv}\text{CH})$(bma)

was observed by ^{31}P NMR spectroscopy. Heating a sealed NMR tube containing the chelating isomer of $Co_2(CO)_4(\mu\text{-PhC}\equiv\text{CH})$(bma) in 1,2-dichloroethane at 83 °C, followed by quenching and ^{31}P NMR analysis at room temperature, revealed a new ^{31}P chemical shift at δ 25.9. The observed high-field shift of this new resonance is assigned to a bridging bma ligand in $Co_2(CO)_4(\mu\text{-PhC}\equiv\text{CH})$(bma) (**11b**), consistent with the ^{31}P chemical shift of the known bridging isomer of $Co_2(CO)_4(\mu\text{-PhC}\equiv\text{CPh})$(bma). [34] On the basis of the chemistry observed with the related complexes $PhCCo_3(CO)_7$(bma) and $Co_2(CO)_4(\mu\text{-PhC}\equiv\text{CPh})$(bma), the bridged isomer of $Co_2(CO)_4(\mu\text{-PhC}\equiv\text{CH})$(bma) is believed to serve as an intermediate en route to the zwitterionic hydrocarbyl complex **13** (Equation 3.15).

W. X-Ray Diffraction Structure of $Co_2(CO)_4[\mu\text{-}\eta^2,\eta^2,\eta^1,\eta^1\text{–PhC=C(H)PPh}_2\overline{\text{C=C(PPh}_2\text{)C(O)OC(O)}}]$

Single crystals of **13** were grown and the molecular structure was determined. **13** exists as discrete molecules in the unit cell with no unusual short inter- or intramolecular contacts. Table 3.21 lists the X-ray data collection and processing parameters, while Table 3.22 gives the selected bond distances and angles. The ORTEP diagram is shown in Figure 3.15.

X. Synthesis and Spectroscopic Properties of the $Co_2(CO)_3(PMe_3)[\mu\text{-}\eta^2,\eta^2,\eta^1,\eta^1\text{–PhC(CO)=C(H)PPh}_2\overline{\text{C=C(PPh}_2\text{)C(O)OC(O)}}]$

The reaction between cluster **13** with PMe_3 was next examined at room temperature in CH_2Cl_2 solvent in an attempt to explore the substitution chemistry associated with **13**. When a CH_2Cl_2 solution of **13** was treated with

Table 3.21. X-Ray Crystallographic Collection and Processing Data for $Co_2(CO)_4[\mu\text{-}PhC{=}C(H)PPh_2\overline{C{=}C(PPh_2)C(O)OC(O)}]$ (**13**)

Space group	P 1/triclinic
Cell Constants	
a, Å	9.8093 (7)
b, Å	12.215 (1)
c, Å	15.744 (2)
V, Å^3	1859.1 (3)
mol formula	$C_{40}H_{26}Co_2O_7P_2$
fw	798.46
formula units per cell (Z)	2
ρ, g • cm^{-3}	1.426
abs coeff (μ), cm^{-1}	10.21
radiation Mo Kα (λ), Å	0.71073
collection range, deg	$2.0 \leq 2\theta \leq 44.0$
scan speed range, deg•min^{-1}	0.67-8.0
max scan time, (s)	120
total data collected	4603
independent data, $I > 3\sigma(I)$	2749
R	0.0365
R_w	0.0469
weights	$[\,0.04F^2 + (\sigma F)^2\,]^{-1}$

Table 3.22. Selected Bond Distances (Å) and Angles (deg) for $Co_2(CO)_4[\mu\text{-}\eta^2,\eta^2,\eta^1,\eta^1\text{-}PhC{=}C(H)C{=}C(PPh_2)C(O)OC(O)]$ (13)[a]

		bond distances	
Co(1)-Co(2)	2.549(1)	Co(1)-P(1)	2.204(2)
Co(1)-C(1)	1.777(9)	Co(1)-C(2)	1.766(8)
Co(1)-C(21)	2.105(8)	Co(1)-C(22)	1.899(7)
Co(2)-C(3)	1.803(9)	Co(2)-C(4)	1.763(8)
Co(2)-C(11)	2.056(7)	Co(2)-C(15)	2.016(7)
Co(2)-C(22)	2.005(7)	P(1)-C(11)	1.811(7)
P(2)-C(15)	1.797(8)	P(2)-C(21)	1.758(7)
O(1)-C(1)	1.14(1)	O(2)-C(2)	1.14(1)
O(3)-C(3)	1.13(1)	O(4)-C(4)	1.13(1)
O(12)-C(12)	1.18(1)	O(13)-C(12)	1.38(1)
O(13)-C(14)	1.40(1)	O(14)-C(14)	1.20(1)
C(11)-C(12)	1.46(1)	C(11)-C(15)	1.43(1)
C(14)-C(15)	1.46(1)	C(21)-C(22)	1.43(1)
		bond angles	
Co(2)-Co(1)-P(1)	72.87(6)	Co(2)-Co(1)-C(1)	96.4(3)
Co(2)-Co(1)-C(2)	167.6(3)	Co(2)-Co(1)-C(21)	75.7(2)
Co(2)-Co(1)-C(22)	51.5(2)	P(1)-Co(1)-C(1)	106.5(3)
P(1)-Co(1)-C(2)	106.3(3)	P(1)-Co(1)-C(21)	112.1(2)
P(1)-Co(1)-C(22)	120.5(2)	C(21)-Co(1)-C(22)	124.0(4)
Co(1)-Co(2)-C(11)	83.5(2)	Co(1)-Co(2)-C(15)	90.2(2)
Co(1)-Co(2)-C(22)	47.4(2)	C(11)-Co(2)-C(15)	41.1(3)
C(11)-Co(2)-C(22)	118.4(3)	C(15)-Co(2)-C(22)	96.4(3)

Table 3.22 continued

Co(1)-P(1)-C(11)	100.1(2)	C(15)-P(2)-C(21)	105.9(4)
C(12)-O(13)-C(14)	109.7(6)	Co(2)-C(11)-C(12)	119.0(5)
Co(2)-C(11)-C(15)	68.0(4)	P(1)-C(11)-C(12)	129.9(6)
P(1)-C(11)-C(15)	120.2(5)	C(12)-C(11)-C(15)	107.3(6)
O(12)-C(12)-C(11)	133.3(8)	O(13)-C(12)-C(11)	108.2(7)
O(13)-C(14)-O(14)	118.7(7)	O(13)-C(14)-C(15)	108.2(6)
O(14)-C(14)-C(15)	108.2(6)	O(14)-C(14)-C(15)	133.0(8)
Co(2)-C(15)-P(2)	104.6(3)	Co(2)-C(15)-P(2)	104.6(3)
Co(2)-C(15)-C(11)	71.0(4)	Co(2)-C(15)-C(14)	114.1(5)
P(2)-C(15)-C(14)	119.5(6)	C(11)-C(15)-C(14)	106.3(6)
Co(1)-C(21)-P(2)	111.4(4)	Co(1)-C(21)-C(22)	64.3(4)
P(2)-C(21)-C(22)	115.8(5)	Co(1)-C(22)-Co(2)	81.5(3)
Co(1)-C(22)-C(21)	73.1(4)	C(1)-Co(1)-C(2)	95.7(4)
C(1)-Co(1)-C(21)	135.7(3)	C(1)-Co(1)-C(22)	98.6(3)
C(2)-Co(1)-C(21)	93.6(4)	C(2)-Co(1)-C(22)	124.0(4)
C(3)-Co(2)-C(4)	94.6(4)	C(3)-Co(2)-C(11)	109.8(3)
C(3)-Co(2)-C(15)	149.1(3)	C(3)-Co(2)-C(22)	110.6(3)
C(4)-Co(2)-C(11)	124.7(3)	C(4)-Co(2)-C(15)	97.5(3)
C(4)-Co(2)-C(22)	95.8(4)		

[a]Numbers in parentheses are estimated standard deviations in the least significant digits.

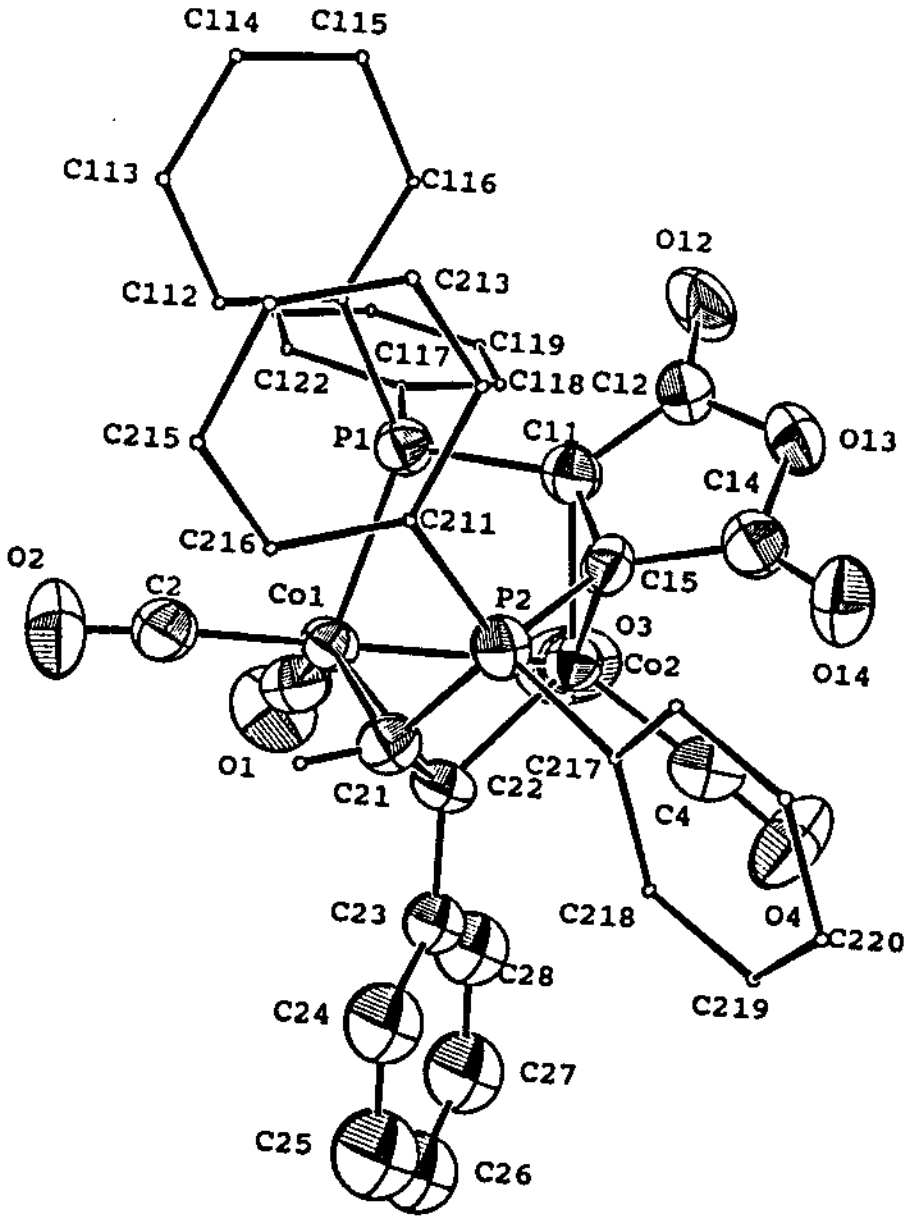

Figure 3.15. ORTEP diagram of $Co_2(CO)_4[\mu\text{-}\eta^2,\eta^2,\eta^1,\eta^1\text{-}PhC{=}C(H)C{=}C(PPh_2)C(O)OC(O)]$ with the thermal ellipsoids drawn at the 50% probability level. H atoms are omitted for clarity

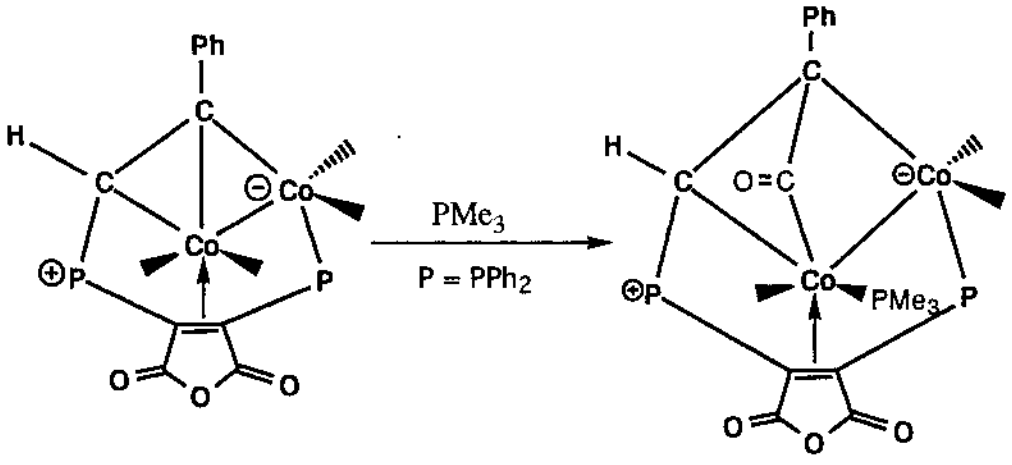

13 14 (3.16)

1.0 equivalent of PMe_3, an instantaneous reaction was observed and the reaction solution acquired a green color (Equation 3. 16). TLC analysis revealed that **14** was the only product. Compound **14** was purified by chromatography over silica gel column using CH_2Cl_2/acetone (95 : 5), giving **14** as an air-stable solid in routinely isolated yields of >80%.

The IR spectrum of **14** in CH_2Cl_2 solution reveals two prominent terminal carbonyl ν (CO) bands at 2022 (vs), 1985 (vs) cm^{-1}. The ν (CO) bands derived from the bma ligand are observed at 1777 (m) and 1719 (s) cm^{-1}, which are attributed to the vibrationally coupled asymmetric and symmetric bma carbonyl stretches, respectively. [7] Besides the terminal ν (CO) bands and the ν (CO) bands of the coordinated bma ligand, an additional weak, broad ν (CO) band was observed at 1555 cm^{-1}, which is assigned to the acyl moiety. [35] A ^{13}CO-enriched sample of **14** was prepared, and the ^{13}C NMR spectrum was recorded in THF solvent at -95 °C. The resulting spectrum exhibited three resonances observed at δ 234.5, 206.6, and 197.8, with an integral ratio of 1 : 2 : 1, respectively. Of these resonances, the downfield

resonance at δ 234.5 and high-field resonance at δ 197.8 reveal phosphorus coupling and $J_{P\text{-}C}$ values of 15.0 and 11.4 Hz, respectively. The downfield resonance at δ 234.5 is easily attributed to the acyl carbon, on the basis of the well-documented CO insertion chemistry [35] in other transition-metal complexes, while the other two resonances at δ 206.6, and 197.8 are assigned to the terminal CO groups. Changing the temperature from -95 °C to room temperature did not perturb the ^{13}C NMR spectrum of **14**.

The ^{31}P NMR spectrum of **14** in THF solution displayed three, equal-intensity resonances located at δ 31.2, 7.4, and 4.6, respectively. Of these resonances, the two downfield resonances centered at δ 31.2 and 7.4 reveal phosphorus-phosphorus coupling with $J_{P\text{-}P}$ values of 69.1 Hz. Compared to the starting complex **13** , the low-field resonance at δ 31.2 is assigned to the PPh_2 group attached to alkyne carbon while the resonances at 7.4, and 4.6 are assigned to the Co-PR_3 groups (maleic anhydride PPh_2 and PMe_3 groups). Other than some minor temperature-dependent chemical shift changes, the ^{31}P NMR spectrum of **14** remained unaltered over the temperature range of - 95 °C to room temperature.

Y. X-Ray Diffraction Analysis of $Co_2(CO)_3(PMe_3)[\mu\text{-}\eta^2,\eta^2,\eta^1,\eta^1\text{–}PhC(CO)=C(H)PPh_2C=C(PPh_2)C(O)OC(O)]$

Single crystals of **14** were grown and the molecular structure was determined. **14** exists as discrete molecules in the unit cell with no unusual short inter- or intramolecular contacts. Table 3.23 lists the X-ray data collection and processing parameters, while Table 3.24 gives the selected bond distances and angles. The ORTEP diagram is shown in Figure 3.16.

Table 3.23. X-Ray Crystallographic Collection and Processing Data for $Co_2(CO)_3(PMe_3)[\mu\text{-}\eta^2,\eta^2,\eta^1,\eta^1\text{–}PhC(CO)=C(H)PPh_2C=C(PPh_2)C(O)OC(O)]$ (**14**)

Space group	$P2_12_12_1$/orthorhomic
Cell Constants	
a, Å	10.2936 (7)
b, Å	17.471 (1)
c, Å	22.294 (2)
V, Å^3	4009.3 (5)
mol formula	$C_{43}H_{35}Co_2O_7P_3$
fw	874.54
formula units per cell (Z)	4
ρ, g • cm^{-3}	1.449
abs coeff (μ), cm^{-1}	9.91
radiation Mo Kα (λ), Å	0.71073
collection range, deg	$2.0 \leq 2\theta \leq 44.0$
scan speed range, deg•min^{-1}	0.67-8.0
total data collected	2811
independent data, $I > 3\sigma(I)$	2127
R	0.0427
R_w	0.0460
weights	$[\ 0.04F^2 + (\sigma F)^2\ ]^{-1}$

Table 3.24. Selected Bond Distances (Å) and Angles (deg) for $Co_2(CO)_3(PMe_3)[\mu\text{-}\eta^2,\eta^2,\eta^1,\eta^1\text{-}PhC(CO)=C(H)C=C(PPh_2)C(O)OC(O)]$ (**14**)[a]

		bond distances	
Co(1)-Co(2)	2.650(2)	Co(1)-P(1)	2.187(3)
Co(1)-C(1)	1.77(1)	Co(1)-C(2)	1.79(1)
Co(1)-C(16)	2.030(9)	Co(1)-C(17)	2.022(9)
Co(2)-P(3)	2.239(3)	Co(2)-C(4)	1.944(9)
Co(2)-C(11)	2.095(9)	Co(2)-C(15)	2.006(9)
P(1)-C(11)	1.7787(9)	P(1)-C(111)	1.81(1)
P(1)-C(117)	1.83(1)	P(2)-C(15)	1.776(9)
P(2)-C(16)	1.758(9)	P(2)-C(211)	1.800(9)
P(2)-C(217)	1.798(9)	P(3)-C(31)	1.81(1)
P(3)-C(32)	1.81(1)	P(3)-C(33)	1.80(1)
O(1)-C(1)	1.15(1)	O(2)-C(2)	1.14(1)
O(3)-C(3)	1.16(1)	O(4)-C(4)	1.23(1)
O(12)-C(12)	1.20(1)	O(13)-C(12)	1.42(1)
O(13)-C(14)	1.39(1)	O(14)-C(14)	1.19(1)
C(4)-C(17)	1.48(1)	C(11)-C(12)	1.44(1)
C(11)-C(15)	1.47(1)	C(14)-C(15)	1.47(1)
C(16)-C(17)	1.43(1)		
		bond angles	
Co(2)-Co(1)-P(1)	71.08(8)	Co(2)-Co(1)-C(1)	91.8(3)
Co(2)-Co(1)-C(2)	173.1(3)	Co(2)-Co(1)-C(16)	83.7(3)
Co(2)-Co(1)-C(17)	75.2(3)	P(1)-Co(1)-C(1)	104.2(3)

Table 3.24 continued

P(1)-Co(1)-C(2)	104.8(4)	P(1)-Co(1)-C(16)	106.3(3)
P(1)-Co(1)-C(17)	135.3(3)	Co(1)-Co(2)-P(3)	159.7(1)
Co(1)-Co(2)-C(11)	81.8(3)	Co(1)-Co(2)-C(15)	89.5(3)
Co(1)-P(1)-C(16)	109.6(4)	Co(1)-P(1)-C(11)	103.7(3)
P(3)-Co(2)-C(11)	116.3(3)	P(3)-Co(2)-C(15)	98.4(3)
C(11)-Co(2)-C(15)	41.9(4)	C(2)-C(15)-P(2)	110.8(5)
O(14)-C(14)-C(15)	132.5(9)	C(12)-C(11)-C(15)	106.5(8)
P(1)-C(11)-C(12)	123.4(7)	Co(2)-C(11)-P(1)	92.1(4)
Co(2)-C(4)-C(17)	114.7(6)	O(4)-C(4)-C(17)	121.2(8)
Co(2)-C(11)-C(12)	123.4(7)	Co(2)-C(11)-C(15)	65.8(5)
C(1)-Co(1)-C(2)	90.(1)	O(12)-C(12)-O(13)	118.2(9)
O(12)-C(12)-C(11)	133.(1)	C(1)-Co(1)-C(16)	145.4(4)
C(1)-Co(1)-C(17)	1043.(4)	C(2)-Co(1)-C(16)	93.6(4)
C(2)-Co(1)-C(17)	106.9(4)	C(3)-Co(2)-C(4)	98.0(5)
C(3)-Co(2)-C(11)	114.4(4)	C(3)-Co(2)-C(15)	155.5(4)
C(4)-Co(2)-C(11)	135.2(4)	C(4)-Co(2)-C(15)	105.3(4)
C(11)-P(1)-C(111)	109.1(4)	C(11)-P(1)-C(117)	107.0(4)
C(15)-P(2)-C(16)	109.6(4)		

[a]Numbers in parentheses are estimated standard deviations in the least significant digits.

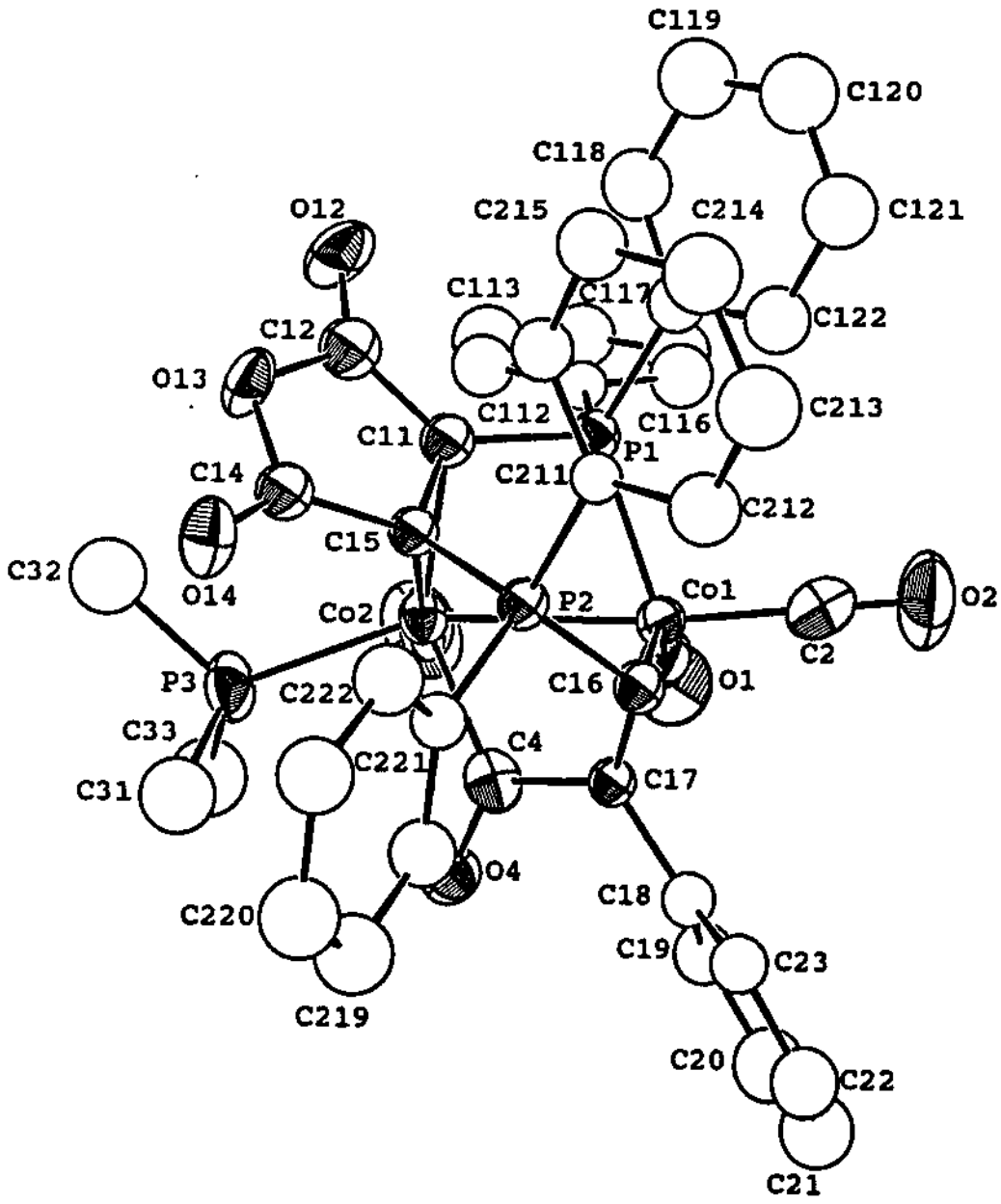

Figure 3.16. ORTEP diagram of the $Co_2(CO)_3(PMe_3)[\mu\text{-}\eta^2,\eta^2,\eta^1,\eta^1\text{-}PhC(CO)=C(H)\overline{C=C(PPh_2)C(O)OC(O)}]$ (**14**) with the thermal ellipsoids drawn at the 50% probability level. H atoms are omitted for clarity.

CHAPTER REFERENCES

1. Yang, K.; Bott, S. G.; Richmond, M. G. J. Organomet. Chem. **1993**, 454, 273.

2. (a) Watson, W. H.; Nagl, A.; Hwang, S.; Richmond, M. G. J. Organomet. Chem. **1993**, 445, 163. (b) Don, M.-J.; Richmond, M. G.; Watson, W. H.; Krawiec, M.; Kashyap, R. P. J. Organomet. Chem. **1991**, 418, 231.

3. (a) Balavoine, G.; Collin, J.; Bonnet, J. J.; Lavingne, G. J. Organomet. Chem. **1985**, 280, 429. (b) Aime, S.; Botta, M.; Gobetto, R.; Osella, D. J. Organomet. Chem. **1987**, 320, 229.

4. Downard, A. J.; Robinson, B. H.; Simpson, J. Organometallics **1986**, 5, 1122.

5. See also: Sutin, K. A.; Kolis, J. W.; Miekuz, M.; Bougeard, P.; Sayer, B. G.; Quilliam, M. A.; Faggiani, R.; Lock, C. J. L.; McGlinchey, M. J.; Jaouen, G. Organometallics **1987**, 6, 439.

6. (a) Koelle, U. J. Organomet. Chem. **1977**, 133, 53. (b) Albers, M. O.; Coville, N. J. Coord. Chem. Rev. **1984**, 53, 227.

7. Dolphin, D.; Wick, A. "Tabulation of Infrared Spectral Data," Wiley-Interscience: New York, **1977**.

8. (a) Schulman, C. L.; Richmond, M. G.; Watson, W. H.; Nagl, A. J. Organomet. Chem. **1989**, 368, 367. (b) Richmond, M. G.; Kochi, J. K. Organometallics **1987**, 6, 254.

9. Garrou, P. E. Chem. Rev. **1981**, 81, 229 and references therein.

10. Unpublished variable-temperature ^{31}P NMR results. See ref. 4 for the room-temperature ^{31}P chemical shift of $PhCCo_3(CO)_7(dppe)$.

11. (a) Bruce, M. I. Coord. Chem. Rev. **1987**, 76, 1. (b) Richmond, M. G.; Kochi, J. K. Organometallics **1987**, 6, 254.

12. Aime, S.; Milone, L.; Rosssetti, R.; Stanghellini, P. L. Inorg. Chim. Acta. **1977**, 25, 103.

13. (a) Don, M.-J.; Richmond, M. G.; Inorg. Chem. **1991**, 30, 1703. (b) Yuan, P.; Richmond, M. G.; Schwartz, M. Inorg. Chem. **1991**, 30, 679. (c) Yuan, P.; Don, M. -J.; Richmond, M. G.; Schwartz, M. Inorg. Chem. **1991**. 30, 3704. (d) Gates, R. A.;

D'Agostino, K. A.; Sutin, K. A.; McGlinchey, M. J.; Janik, T. S.; Churchill, M. R. Organometallics **1990**, 9, 20.

14. (a) Shanan-Atidi, H.; Bar-Eli, K. H. J. Phys. Chem. **1970**, 74, 961. (b) Sandström, J. "Dynamic NMR Spectroscopy," Academic Press, New York, **1992**.

15. (a) Mann, B. E.; Taylor, B. F. "^{13}C NMR Data for Organometallic Compounds," Academic Press: New York, **1981**. (b) Gragg, B. R.; Layton, W. J.; Niedenzu, K. J. Organomet. Chem. **1977**, 132, 29.

16. (a) Chia, L. S.; Cullen, W. R.; Franklin, M.; Manning, A. R. Inorg. Chem. **1975**, 14, 2521. (b) Bird, P. H.; Fraser, A. R.; Hall, D. N. Inorg. Chem. **1977**, 16, 1923. (c) BIanchini, C.; Dapporto, P.; Meli, A. J. Organomet. Chem. **1979**, 174, 205.

17. (a) Cunninghame, R. G.; Hanton, L. R.; Jenson, S. D.; Robinson, B. H.; Simpson, J. Organometallics **1987**, 1470. (b) Jenson, S. D.; Robinson, B. H.; Simpson, J. Organometallics **1987**, 1479.

18. Hansen, B. E.; Mancini, J. S. Inorg. Chem. **1983**, 2, 126.

19. (a) Arewgoda, C. M.; Robinson, B. H.; Simpson, J. J. Chem. Soc., Chem. Commun. **1982**, 284. (b) Arewgoda, C. M.; Robinson, B. H.; Simpson, J. J. Am. Chem. Soc. **1983**, 105, 1893. (c) Casagrande, L. V.; Chen, T.; Rieger, P. H.; Robinson, B. H.; Simpson, J.; Visco, S. J. Inorg. Chem. **1984**, 23, 2019.

20. For bma-related redox chemistry, see: (a) Mao, F.; Tyler, D. R.; Keszler, D. J. Am. Chem. Soc. **1989**, 111, 130. (b) Mao, F.; Philbin, C. E.; Weakley, T. J. R.; Tyler, D. R. Organometallics **1990**, 9, 1510.

21. Bard, A. J.; Faulkner, L. R. "Electrochemical Methods," Wiley: New York, **1980**. (b) Adams, R. N. "Electrochemistry at Solid Electrodes," Marcel Dekker: New York, **1969**.

22. For examples of redox-dependent structures involving cis- and trans-isomers and fac- and mer-isomers of mononuclear complexes, see: (a) Bond, A. M.; Colton, R.; McCormick, M. J. Inorg. Chem. **1977**, 16, 155. (b) Sullivan, B. P.; Meyer, T. J. Inorg. Chem. **1982**, 21, 1037. (c) Rieke, R. D.; Kojima, H.; Saji, T.; Rechberger, P.; Ofele, K. Organometallics **1988**, 7, 749. (d) Vallet, A.; Person, M.; Rollier, L.; Laviron, E. Inorg . Chem. **1987**, 26, 332. (e) Conner, K. A.; Walton, R. A. Inorg. Chem. **1986**, 25, 4422. (f) Lilga, M. A.; Ibers, J. A. Inorg. Chem. **1984**, 23, 3538. (g) Bagchi, R. N.; Bond, A. M.; Brain, G.; Colton, R.; Henderson, T. L. E.; Kevekordes, J. E. Organometallics **1984**, 3, 4.

23. (a) Arewgoda, M.; Rieger, P. H.; Robinson, B. H.; Simpson, J.; Visco, S. J. J. Am. Chem. Soc. **1982**, 104, 5633. (b) See also:

Dickson, R. S.; Peake, B. M.; Rieger, P. H.; Robinson, B. H.; Simpson, J. J. Organomet. Chem. **1979**, 172, C63.

24. Hoffman, D. M.; Hoffmann, R.; Fisel, C. R. J. Am. Chem. Soc. **1982**, 104, 3858.

25. Fenske, D. Chem. Ber. **1979**, 112, 363.

26. (a) Tyler, D. R.; Acc. Chem. Res. **1991**, 24, 325. (b) Tyler, D. R.; Mao, F. Coord. Chem. Rev. **1990**, 97, 119. (c) Mao, F.; Sur, S. K.; Tyler, D. R.; Organometallics **1991**, 10, 419. (d) Mao, F.; Tyler, D. R.; Rieger, A. L.; Rieger, P. H. J. Chem. Soc., Faraday Trans. **1991**, 87, 3113.

27. (a) Richmond, M. G.; Kochi, J. K. Inorg. Chem. **1986**, 25, 656. (b) Hinkelmann, K.; Heinze, J.; Schacht, H.-T.; Field, J. S.; Vahrenkamp, H. J. Am. Chem. Soc. **1989**, 111, 5078. (c) Ohst, H. H.; Kochi, J. K. J. Am. Chem. Soc. **1986**, 108, 2897.

28. Don, M. -J.; Richmond, M. G.; Inorg. Chem. **1991**, 30, 1703. (b) Dumond, D. S.; Richmond, M. G. J. Am. Chem. Soc. **1988**, 110, 7548. (c) Don, M.-J.; Richmond, M. G. Inorg. Chim. Acta **1990**, 173, 61. (d) Peake, B. M.; Ribinson, B. H.; Simpson, J. Watson, D. J. Inorg. Chem. **1977**, 16, 405. (e) Peake, B. M.; Rieger, P. H.; Robinson, B. H.; Simpson, J. Inorg. Chem. **1979**, 18, 1000.

29. Brown, T. L. in "Organometallic Radical Processes," Trogler, W. C., Elsevier: New York, **1990**, Chapter 3 and references therein.

30. Thorn, D. L.; Hoffmann, R. Inorg. Chem. **1978**, 17, 126.

31. For related studies on M_2L_6 dinuclear complexes, see: (a) Albright, T. A.; Hoffmann, R. J. Am. Chem. Soc. **1978**, 100, 7736. (b) DeKock, R. L.; Deshmukukh, P.; Dutta, T. K.; Fehlner, T. P.; Housecroft, C. E.; Hwang, J. L.-S. Organometallics **1983**, 2, 1108. (c) Anderson, A. B. Inorg. Chem. **1976**, 15, 2598.

32. The subjacent HOMO in the dinuclear complexes **8** (both isomers) and **9** consists of a Co-Co antibonding orbital derived from the out-of-phase overlap of hybridized dxz orbitals, with a minor contribution from the acetylene π^* bond. The switching of the HOMO and the subjacent HOMO in **8** and **9** from the that in Ref. 30 is immaterial, insomuch as the overall bonding in this class of dinuclear complexes is not adversely perturbed. The energy level for each subjacent HOMO in compounds **8** and **9** is calculated at ~-12.1 eV.

33. In agreement with the premise concerning the LUMO of **8**, the calculated energy (-10.4 eV) and the nodal properties of the LUMO of maleic anhydride closely match those reported here for the bma-substituted dinuclear compounds. See also: Hayakawa, K.; Mibu, N.; Osawa, E.; Kanematsu, K. J. Am. Chem. Soc. **1982**, 104, 7136.

34. Yang, K.; Bott, S. G.; Richmond, M. G. Organometallics **1994**, 13, in press.

35. (a) Wojcicki, A. Adv. Organomet. Chem. **1973**, 11, 87. (b) Calderazzo, F. Angew. Chem., Int. Ed. Engl. **1977**, 16, 299. (c) Kuhlman, E. J.; Alexander, J. J. Coord. Chem. Rev. **1980**, 33, 195.

CHAPTER IV

DISCUSSION

A. Syntheses and Kinetics Studies for $PhCCo_3(CO)_7$(bma) (2), $Co_3(CO)_6(\mu_2\text{-}\eta^2, \eta^1\text{-}C(Ph)C{=}C(PPh_2)C(O)OC(O))(\mu_2\text{-}PPh_2)$ (3), and $PhCCo_3(CO)_7[(Z)\text{-}Ph_2PCH{=}CHPPh_2]$ (4).

The reaction of $PhCCo_3(CO)_9$ (**1**) with the bidentate phosphine bma proceeds initially to give the diphosphine cluster $PhCCo_3(CO)_7$(bma) (**2**). Variable-temperature ^{31}P NMR measurements indicate that this cluster exists as a mixture of bridging and chelating isomers. At all temperatures examined, the bridging isomer has been found to be the predominant isomer in solution by ^{31}P NMR and ^{13}C NMR spectroscopy. However, X-ray diffraction analysis reveals that the solid-state structure is derived from the chelating isomer.

The noncoordinated C=C double bond of the maleic anhydride ring is believed to facilitate the observed bma equilibration process that is outlined in Scheme I. Starting with the bridged isomer, **2b**, and invoking an unimolecular mechanism that does not rely on CO loss, phosphine ligand displacement by the maleic anhydride C=C bond affords the saturated cluster **a**. Assuming that the coordinated olefinic bond in species **a** behaves similarly to a CO ligand in terms of migratory ability, an in-plane migration of two equatorial CO groups and the olefin moiety leads to cluster **b** with a bridging olefinic bond. Completion of the terminal-to-bridge ligand migration then yields the chelated alkenyl phosphine cluster **c**, which, upon

Scheme I

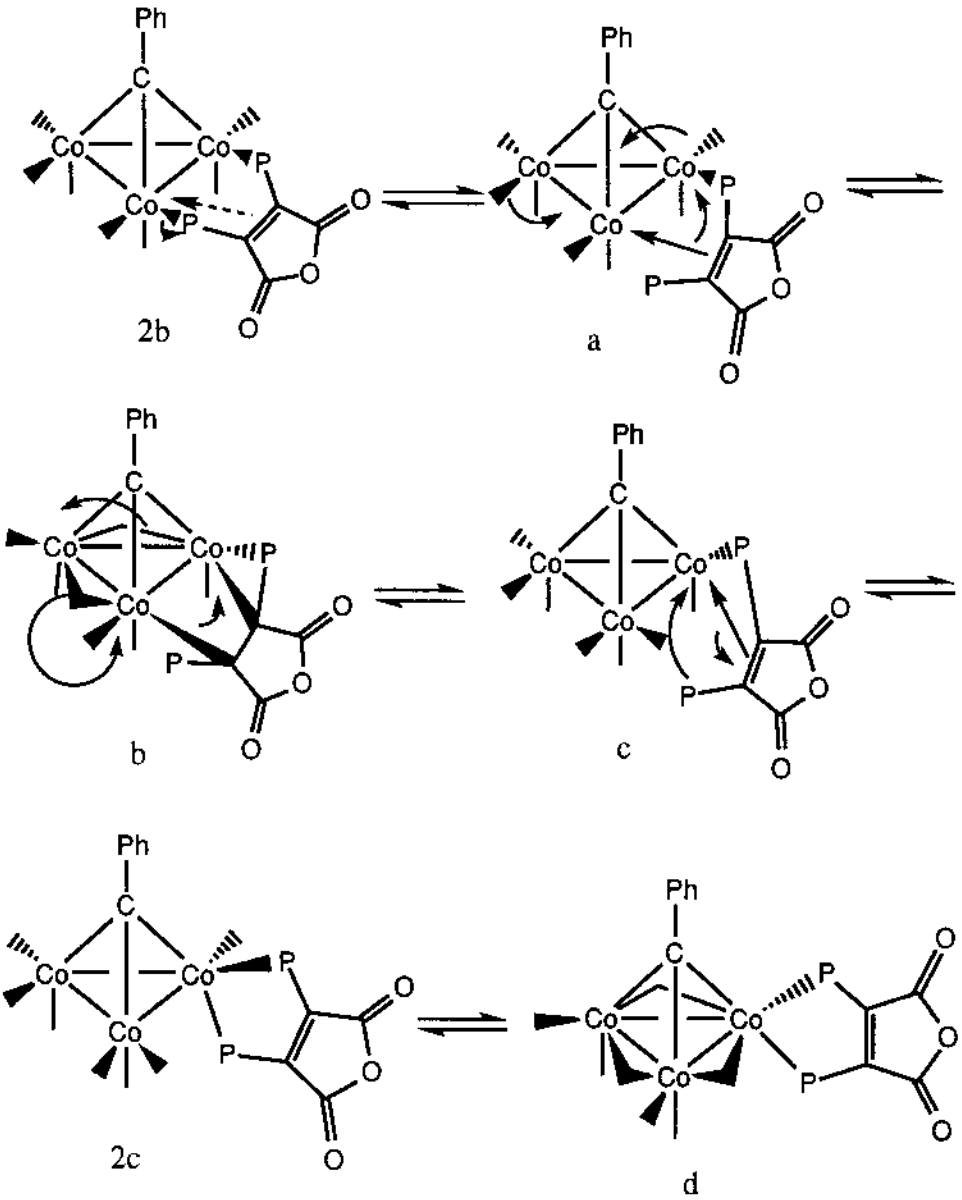

P = PPh_2

olefin displacement by the free, dangling PPh_2 moiety, gives the chelating diphosphine cluster **2c**. It is this chelating isomer, with its axial and equatorial PPh_2 groups, that was observed in the low-temperature ^{31}P NMR spectra of **2**. The determined X-ray structure of **2** is produced by one last terminal/bridge exchange of the equatorial CO groups in **2c**.

The proposed bma ligand equilibration is consistent with the fact that terminal/bridge CO exchange is known to be facile in this type of cluster and that the saturated diphosphine cluster $PhCCo_3(CO)_7$(dppe) does not exhibit such P-ligand movement. [1] Only the bridging isomer is observed in the dppe-substituted cluster since the requisite olefinic bond, which serves to tether the ligand to the cluster and preserves the electronic saturation at the cobalt centers in each of the intermediates, is absent.

The reactivity of **2** toward P-C(olefin) bond cleavage relative to that of the structurally similar cluster $PhCCo_3(CO)_7$[(Z)-Ph_2PCH=$CHPPh_2$] (**4**) was investigated by independent thermolysis and photolysis experiments. When **2** was heated in THF solution at 43.6 °C, it was converted to **3** in >95 % yield after 90 min ($t_{1/2}$ = ~ 18 min) while near-UV irradiation of **2** at 20 °C in THF solution gave **3** in quantitative yield. In contrast, when $PhCCo_3(CO)_7$ [(Z)-Ph_2PCH=$CHPPh_2$] was heated overnight at 43.6 °C, no new cobalt carbonyl containing material was observed and the starting cluster was recovered in 64% yield. Photolysis led only to the complete decomposition of **4**. It is important that no P-C bond cleavage products of any kind were observed in either reaction involving **4**. This suggests that if P-C(olefin) bond cleavage occurs, it is relatively inefficient in comparison to that of $PhCCo_3(CO)_7$(bma) and that the resulting product(s) must decompose before analysis.

Scheme II

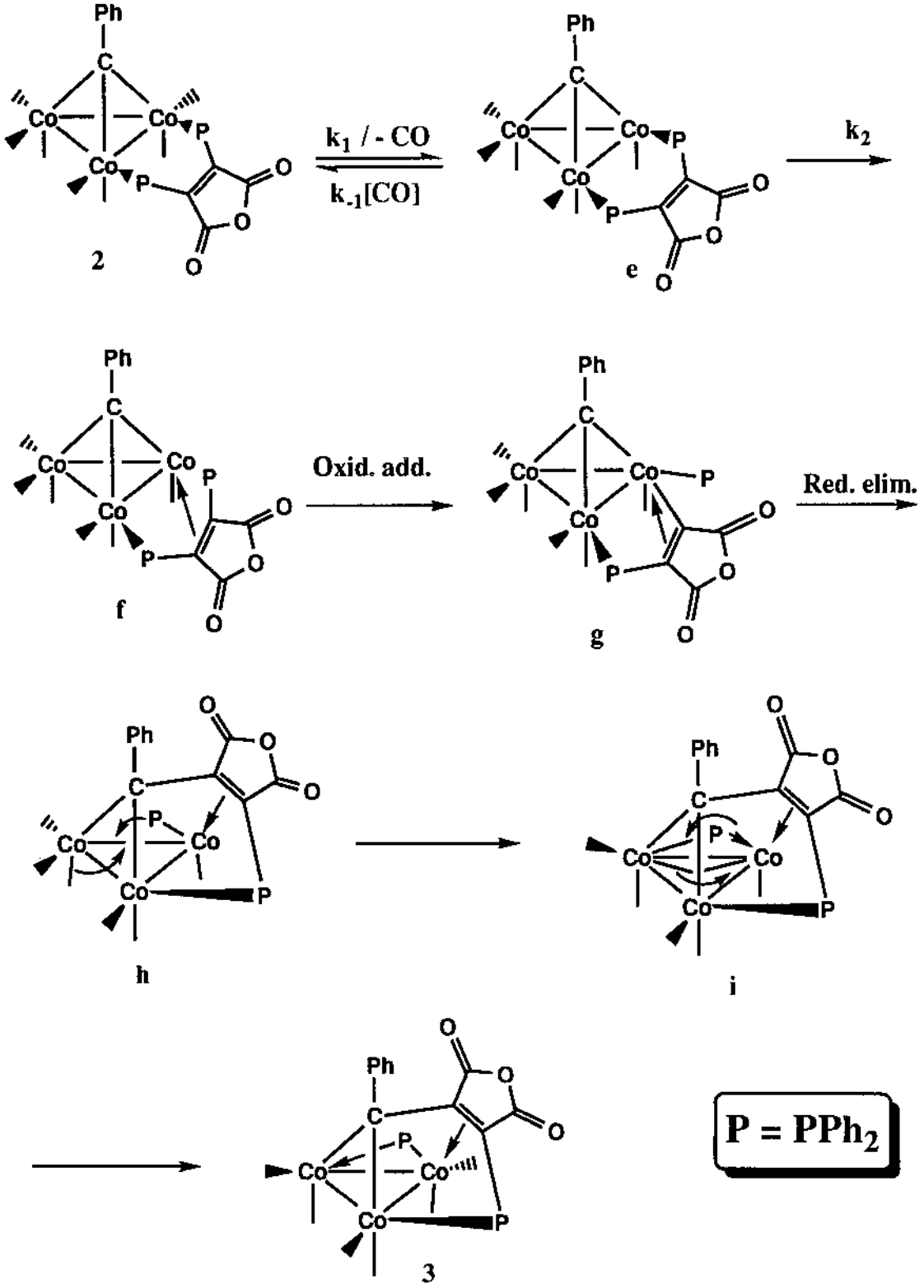

The formation of **3** from the bridging isomer of **2** is considered in Scheme II. As shown from the kinetic studies, dissociative CO loss from **2** represents the rate-determining step in the reactions leading to **3** and is expected to afford the unsaturated cluster **e**. The site of the lost CO has been shown in Scheme II to originate from a phosphine-substituted cobalt center. [2] Whether or not this is the initial site of CO loss is immaterial due to the rapid rates of intramolecular carbonyl scrambling in **2**, which would assist in the transfer of unsaturation to a bma-substituted cobalt atom. [3] Phosphine displacement by the non-coordinated C=C bond of the maleic anhydride ring would furnish species **f**. P-C(olefin) oxidative addition yields the terminal phosphido cluster **g**, which is followed by a reductive elimination of the benzylidyne and (diphenylphosphino)maleic anhydride groups to give **h**. [4] The final product, cluster **3**, is obtained after a terminal-to-bridge conversion of a phosphido group that is coupled with the migration of a CO ligand from the lone $Co(CO)_3$ group to the adjacent olefin-substituted cobalt center.

The oxidative addition step is selective in that only P-C(olefin) bond cleavage is observed. No evidence for P-C(aryl) bond cleavage was observed. These results are in keeping with the established reactivity trends concerning P-C bond scission; namely, electron-withdrawing substituents facilitate the cleavage of P-C bonds. [5] In the case of cluster **2**, the more strongly electron-withdrawing maleic anhydride group is the preferred site for the P-C bond scission.

B. X-Ray Diffraction Structures of $PhCCo_3(CO)_7$(bma) (2), $Co_3(CO)_6[\mu_2\text{-}\eta^2,\eta^1\text{-}C(Ph)\overline{C=C(PPh_2)C(O)OC(O)}](\mu_2\text{-}PPh_2)$ (3), and $PhCCo_3(CO)_7[(Z)\text{-}Ph_2PCH=CHPPh_2]$ (4).

Single crystals of **2**, **3**, and **4** were grown, and the molecular structure of each cluster was determined. The ORTEP diagram of **2** establishes the chelating disposition of the bma ligand and bridging disposition of the carbonyl groups. Several attempts were made to recrystallize the bridging isomer of **2**, but these were not successful and only the chelating isomer was observed. Additional proof concerning the preference of **2** to adopt a chelating bma ligand with bridging CO groups in the solid state is seen in the IR spectrum (KBr) of **2**, where an intense bridging CO band at 1885 cm^{-1} is observed. This same band is not present in solution as a result of rapid bma/CO ligand fluxionality, which serves to give the chelating isomer of **2** with rapidly exchanging carbonyl groups and the bridging isomer of **2**.

The polyhedral core of **2** consists of a triangular array of cobalt atoms capped by a μ_3-CPh moiety. Unequal Co-Co bond lengths are seen in **2**, with the bma-substituted Co-Co bonds being 0.094 Å longer than the unique Co(2)-Co(3) bond. The reason for this difference can be attributed to a sterically induced perturbation of the cluster core by the bma ligand. The mean value for the μ_3–C-Co (1.94 Å) and the Co-CO (1.76 Å) distances are consistent with those reported for related clusters. [6] The remaining distances and angles are unexceptional and require no comment.

The Co-Co bond distances in cluster **3** range from 2.412(2) to 2.696(2) Å, with a mean distance of 2.197 Å being observed for the μ_2–P-Co bonds. The μ_2–P-Co distances found are in good agreement with those of other phosphido-bridged cobalt clusters. [7] All other bond distances and angles are within normal limits and require no comment.

The internal polyhedron of **4** consists of a triangular array of cobalt atoms capped by a μ_3-benzylidyne group. The mean value for the Co-Co

(2.481 Å) and μ_3-C-Co (1.91 Å) bond lengths are similar to those reported for the parent cluster and related diphosphine-substituted derivatives. [7] The Co-CO bond distances range from 1.74 (1) to 1.80 (1) Å, with an average distance of 1.77 Å. The remaining bond lengths and angles are unexceptional and require no comment.

C. Synthesis and Reactivity of $Co_3(CO)_5(\mu\text{-}CO)(PMe_3)[\mu_2\text{-}\eta^2,\eta^1\text{-}C(Ph)\overline{C=C(PPh_2)C(O)OC(O)}](\mu_2\text{-}PPh_2)$ (5), $Co_3(CO)_5(PMe_3)[\mu_2\text{-}\eta^2,\eta^1\text{-}C(Ph)\overline{C=C(PPh_2)C(O)OC(O)}](\mu_2\text{-}PPh_2)$ (6), $Co_3(CO)_4(PMe_3)_2[\mu_2\text{-}\eta^2,\eta^1\text{-}C(Ph)\overline{C=C(PPh_2)C(O)OC(O)}](\mu_2\text{-}PPh_2)$ (7)

The tricobalt cluster $Co_3(CO)_6[\mu_2\text{-}\eta^2,\eta^1\text{-}C(Ph)\overline{C=C(PPh_2)C(O)OC(O)}](\mu_2\text{-}PPh_2)$ (**3**), reacts with 1.0 equivalent of PMe_3 to initially give the cluster $Co_3(CO)_5(\mu\text{-}CO)(PMe_3)[\mu_2\text{-}\eta^2,\eta^1\text{-}C(Ph)\overline{C=C(PPh_2)C(O)OC(O)}](\mu_2\text{-}PPh_2)$, (**5**), via site-selective PMe_3 addition to the PPh_2(maleic anhydride)-substituted cobalt center. This addition reaction is accompanied by cleavage of one of the Co-Co bonds in **3** and a formal change in how the μ_2-phosphido ligand distributes its three available bonding electrons to the ligated cobalt centers in **5**. The vast majority of similar cluster substitution reactions involves assistance from one or more of the ancillary CO groups, as outlined in Equation 4.1. [8,9] Here the formal transfer of the two electrons in the ruptured metal-metal bond is ultimately redistributed about the cluster polyhedron, giving rise to coordinately saturated metal centers. CO loss and reformation of the metal-metal bond complete the overall sequence for the net substitution of CO by the incoming ligand in many transition metal clusters.

Use of conventional electron counting formalism allows for the change in the coordination mode of the μ_2-PPh_2 moiety in **5** relative to **3** to

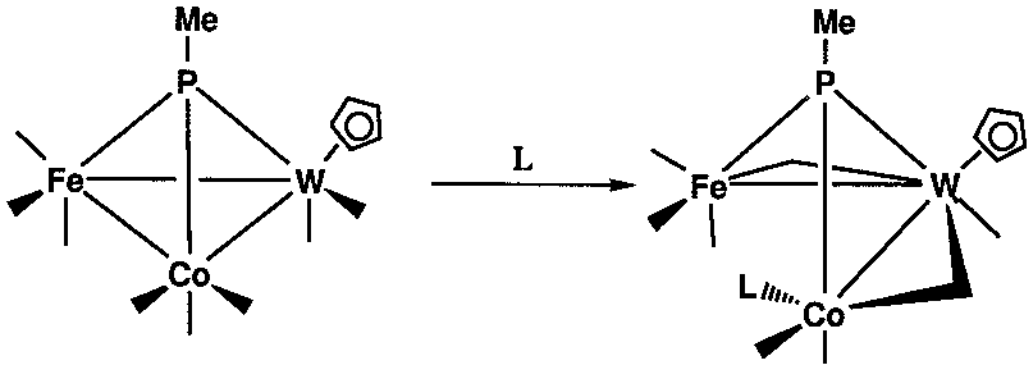

(4.1)

be easily rationalized. Initially, the phosphido ligand donates 2e- and 1e- to Co(2) and Co(1), respectively, in **3**, but this donation mode is ultimately reversed in the formation of **5**, as shown in Scheme III. Such a transformation, which enables all of the cobalt centers in **5** to achieve a coordinatively saturated state, is akin to the assistance rendered to the cluster by the CO groups in Equation 4.1 and related substitution reactions. The zwitterionic intermediate proposed in Scheme III is supported by the numerous zwitterionic clusters prepared by Carty and Deeming. [10] Furthermore, the observed polyhedral expansion in going from **3** to **5** can be explained by using Polyhedral Skeletal Electron Pair (PSEP) theory, [11] which allows for the prediction of an adopted molecular polyhedron upon ligand addition to a transition-metal cluster. Regarding cluster **3** as a four-vertex arachno cluster that possesses 7 skeletal electron pairs (SEP), it is expected and experimentally found that PMe_3 addition to **3** leads to the formation of the hypho cluster **5** with 8 SEP.

The formation of **6** from **5** is considered in Scheme IV. Starting with cluster **5**, the conversion of the bridging CO group between Co(2) and Co(3) into a terminal CO group on Co(2) affords the species **1**. Reformation of the metal-metal bond between Co(1) and Co(3), coupled with a change in the

Scheme III

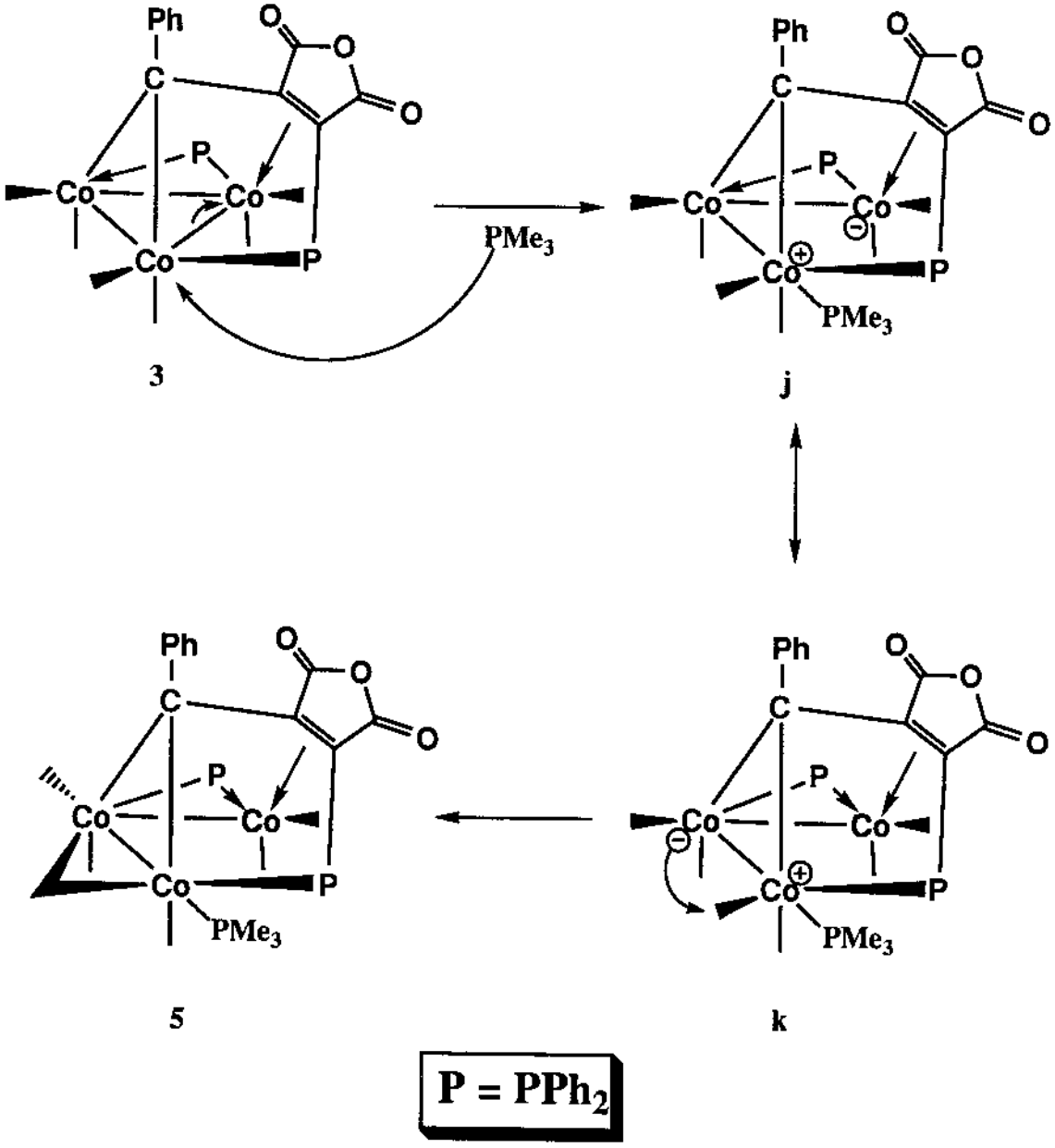

Scheme IV

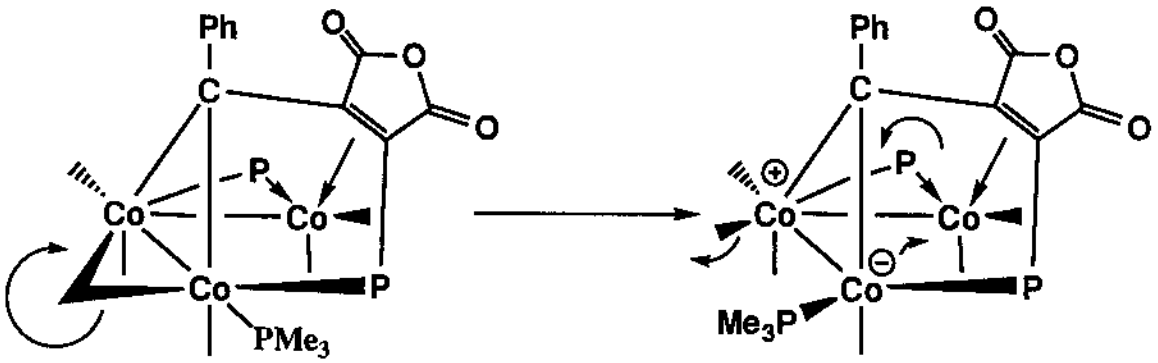

5 I

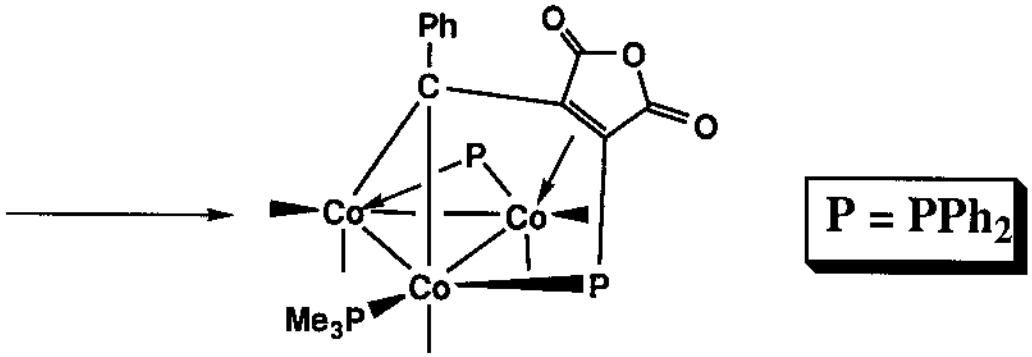

6

coordination mode of the μ_2-phosphido moiety, followed by the CO loss, ultimately gives **6** as the thermodynamic mono-substitution product. It is important to note that the coordination mode of μ_2-phosphido moiety in **6** is same as that in the cluster **3** (Scheme V). This flexibility in the ligand donation properties of the μ_2-phosphido group is presumed to be a key factor in promoting the observed polyhedral cluster expansion in **5**. The

Scheme V

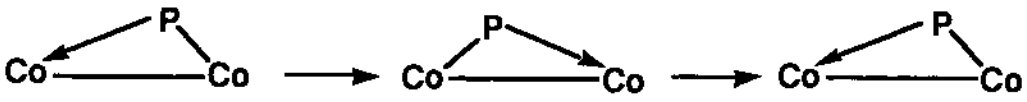

3 **5** **6**

P = PPh_2

interception of **5** as a kinetic product en route to the mono-substituted cluster **6** represents another example of metal-metal bond reactivity in a substitution reaction involving a polynuclear system.

The mono-substituted cluster **6** can undergo further reaction with additional PMe_3 to give the bis-substituted cluster **7**. The second PMe_3 adds to **6** in a site-selective fashion at the cobalt atom with the maleic anhydride double bond. It is interesting to note that in this CO substitution no evidence

has been found for the replacement of the maleic anhydride double bond by the incoming phosphine ligand. Furthermore, no CO insertion was observed in the reaction between **6** and PMe_3. In the case of zwitterionic hydrocarbyl complex $Co_2(CO)_4[\mu\text{-}\eta^2,\eta^2,\eta^1,\eta^1\text{–}PhC{=}C(H)PPh_2\overline{C{=}C(PPh_2)C(O)OC(O)}]$, the addition of PMe_3 leads to the quantitative CO insertion into the Co-C(hydrocarbyl) bond. Unlike the reaction between cluster **3** and 1.0 equivalent of PMe_3, no intermediates were found when **6** was treated with additional PMe_3.

D. X-Ray Diffraction Structures of $Co_3(CO)_5(\mu\text{-}CO)(PMe_3)[\mu_2\text{-}\eta^2,\eta^1\text{-}C(Ph)\overline{C{=}C(PPh_2)C(O)OC(O)}](\mu_2\text{-}PPh_2)$ (5), $Co_3(CO)_5(PMe_3)[\mu_2\text{-}\eta^2,\eta^1\text{-}C(Ph)\overline{C{=}C(PPh_2)C(O)OC(O)}](\mu_2\text{-}PPh_2)$ (6), and $Co_3(CO)_4(PMe_3)_2[\mu_2\text{-}\eta^2,\eta^1\text{-}C(Ph)\overline{C{=}C(PPh_2)C(O)OC(O)}](\mu_2\text{-}PPh_2)$ (7).

Single crystals of **5**, **6**, and **7** were grown, and the molecular structure of each cluster was determined. The ORTEP diagram of **5** establishes the disposition of the PMe_3 ligand and the cleavage of the Co(1)-Co(2) bond, the latter feature being supported by the 3.668(4) Å internuclear distance between these two atoms, and conversion of a terminal CO group at Co(3) into a semi-bridging CO group that serves to span Co(3) and Co(2). The bond distance between Co(2) and Co(3) (2.663 Å) is longer than that between Co(1) and Co(2) (2.523 Å).

The structural features of clusters **6** and **7** can be directly compared to those of the parent cluster **3**. Figure 4.1 shows the changes of Co-Co bond distances for clusters **3**, **5**, **6**, and **7**. The lengthening of the Co(2)-Co(3) bond is evident in clusters **6** and **7** (from 2.696 Å in **3** to 2.832 Å in **7**) upon the addition of PMe_3 . In comparison to clusters **6** and **7**, the distance

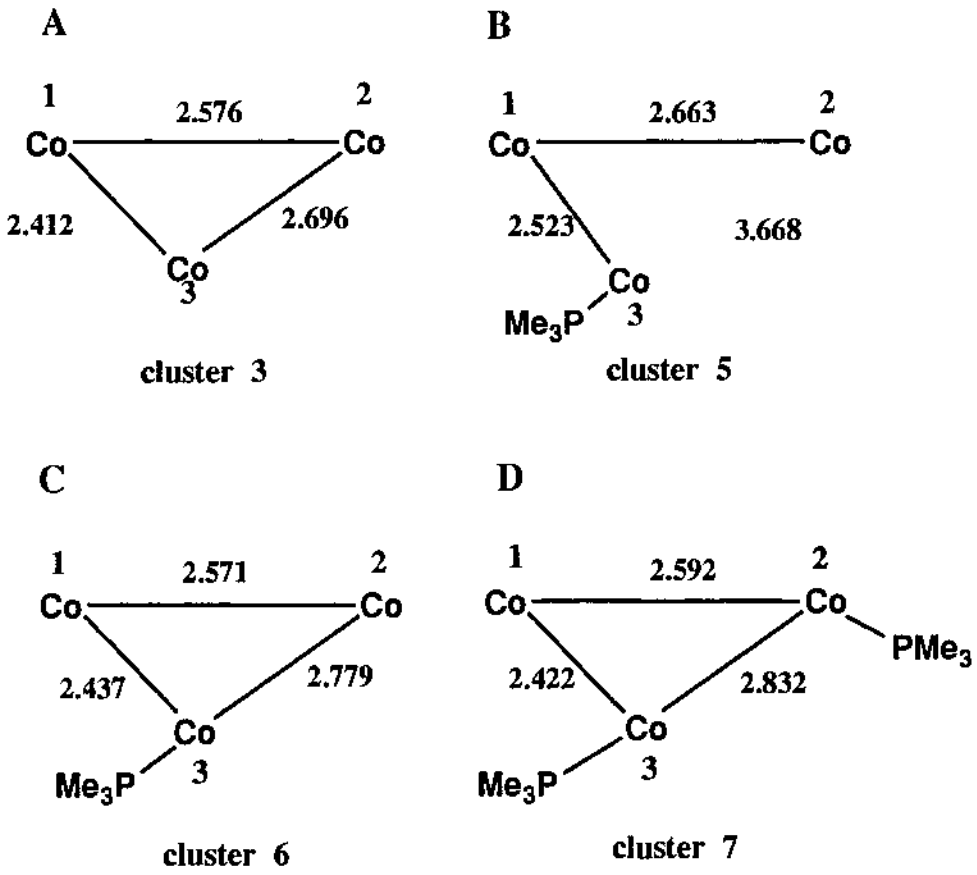

Figure 4.1 Comparison of the Co-Co bond lengths (Å) in (A) $Co_3(CO)_6[\mu_2$-η^2,η^1-C(Ph)C=C(PPh$_2$)C(O)OC(O)](μ_2-PPh$_2$) (**3**), (B) $Co_3(CO)_5$(μ-CO)(PMe$_3$)[μ_2-η^2,η^1-C(Ph)C=C(PPh$_2$)C(O)OC(O)](μ_2-PPh$_2$) (**5**), $Co_3(CO)_5$(PMe$_3$)[μ_2-η^2,η^1-C(Ph)C=C(PPh$_2$)C(O)OC(O)](μ_2-PPh$_2$) (**6**), and $Co_3(CO)_4$(PMe$_3$)$_2$[μ_2-η^2,η^1-C(Ph)C=C(PPh$_2$)C(O)OC(O)] (μ_2-PPh$_2$) (**7**).

Table 4.1 The Co—PPh_2 and Co←PPh_2 Bond Distances in Clusters **3**, **5**, **6**, and **7** (—PPh_2 refers to the phosphido ligand).

Clusters	Co—PPh_2 (Å)	Co←PPh_2 (Å)	Δ (Å)
3	2.264	2.129	0.135
5	2.188	2.129	0.059
6	2.253	2.135	0.118
7	2.241	2.139	0.102

between the Co(2) and the Co(3) centers in cluster **5** is much longer (3.668 Å), clearly supporting the breaking of the Co(2)-Co(3) bond in cluster **5**. The lengthening of Co(2)-Co(3) bond in clusters **5-7** can be attributed to the sterically induced perturbation by the PMe_3 ligand(s). It is of interest that the PMe_3 ligand(s) only slightly affects the distances of the Co(1)-Co(2) and Co(1)-Co(3) bonds in clusters **5-7**.

The phosphido-cobalt bond distances reveal an interesting trend. Table 4.1 summarizes the changes of the two-electron Co←PPh_2 donor bond and the one electron Co—PPh_2 covalent bond in clusters **3**, **5**, **6**, and **7**. It is apparent from Table 4.1 that the Co—PPh_2 covalent bond is longer than the corresponding Co←PPh_2 donor bond in all four clusters. The difference between the Co—PPh_2 and Co←PPh_2 bonds in clusters **3**, **5**, **6**, and **7** is 0.135, 0.059, 0.118, and 0.102 Å, respectively, which is consistent with the established coordination properties of phosphido ligand, where the M—PPh_2 covalent bond is usually longer than that of a tertiary phosphine-metal bond.

[12] The longer Co—PPh_2 bond in cluster **5** is significant, a fact that is in full agreement with the observed cluster expansion and reversed donation mode adopted by phosphido ligand in going from cluster **3** to **5** upon PMe_3 addition. The remaning distances and angles are unexceptional and require no comment.

E. Synthesis and Reactivity of $Co_2(CO)_4(\mu\text{-PhC}{\equiv}\text{CPh})$(bma) (8), $Co_2(CO)_4(\mu\text{-PhC}{\equiv}\text{CPh})[(Z)\text{-}Ph_2PCH{=}CHPPh_2]$ (9), and $Co_2(CO)_4[\eta^2,\eta^2,\eta^1,\eta^1\text{-}(Z)\text{-}Ph_2PC(Ph){=}(Ph)C\text{-}\overline{C{=}C(PPh_2)C(O)OC(O)}]$ (10).

The cobalt dinuclear complex $Co_2(CO)_6(\mu\text{-PhC}{\equiv}\text{CPh})$ reacts with the diphosphine ligand bma in the presence of Me_3NO at room temperature to yield $Co_2(CO)_4(\mu\text{-PhC}{\equiv}\text{CPh})$(bma), **8a**, which contains a chelating bma ligand. The identity of this compound has been established by IR and NMR (^{13}C and ^{31}P) spectroscopies. Equilibration of the chelating isomer to the bridging isomer of $Co_2(CO)_4(\mu\text{-PhC}{\equiv}\text{CPh})$(bma), **8b**, occurs upon thermolysis, which agrees with the reversible chelate-to-bridge bma ligand exchange observed in $PhCCo_3(CO)_7$(bma). [13] As in the case of $PhCCo_3(CO)_7$(bma), the uncoordinated C=C double bond of the bma ligand is believed to be crucial for the isomerization of the bma ligand in $Co_2(CO)_4(\mu\text{-PhC}{\equiv}\text{CPh})$(bma). Scheme VI shows a series of equilibria that would serve to equilibrate the bma ligand, starting from the chelating $Co_2(CO)_4(\mu\text{-PhC}{\equiv}\text{CPh})$(bma) isomer (**8a**). The inhibition of the isomerization reaction by added CO supports an initial step involving dissociative CO loss, which would generate the unsaturated species **m**. Coordination of the maleic anhydride C=C bond in concert with displacement of one of the PPh_2 groups affords species **n**. Terminal-to-bridge exchange of the coordinated C=C bond in **n** with a carbonyl group from the

$Co(CO)_3$ moiety then gives species **p**, via intermediate **o**. Displacement of the coordinated olefinic bond by the dangling PPh_2 group leads to the unsaturated bma-bridged complex **q**, which upon capture of CO furnishes the bridging isomer $Co_2(CO)_4(\mu\text{-PhC}\equiv\text{CPh})$(bma) (**8b**).

The absence of facile diphosphine isomerization in $Co_2(CO)_4(\mu\text{-PhC}\equiv\text{CPh})$[(Z)-$Ph_2PCH=CHPPh_2$] is of interest, as this highlights one of the unique reactivity differences between the bma ligand and normal diphosphine ligands devoid of an electron-withdrawing substitutent(s). Heating or photolyzing solutions of $Co_2(CO)_4(\mu\text{-PhC}\equiv\text{CPh})$[(Z)-$Ph_2PCH=CH$ PPh_2] lead only to decomposition, presumably due to the retarded ability of the (Z)-$Ph_2PCH=CHPPh_2$ diphosphine ligand to enter into the series of reactions outlined in Scheme **VI**. Analogous reactivity has been observed for $PhCCo_3(CO)_7$(P-P) [where P-P = bma, (Z)-$Ph_2PCH=CHPPh_2$] as discussed earlier. [13]

Reasonable pathways that account for the formation of **10** are considered in Scheme VII, starting from bridging isomer of **8b**. CO loss from the **8b** generates species **r**, which was an intermediate in Scheme VI. Exchange of the bma C=C bond for the coordinated PPh_2 group at the unsaturated cobalt center gives compound **s**, and sets up the molecule for the requisite P-C(olefin) bond oxidative addition step leading to species **t**. [5] The reaction temperature is important with respect to the transient species **r**. Only at higher temperatures does the oxidative addition reaction become competitive with the isomerization of the bma ligand and recapture of dissociated CO. The coupling of the alkyne and the maleic anhydride ligands occurs in the reductive elimination step that provides **u**. The terminal phosphido group in **u** next attacks the other end of the initial alkyne ligand to

Scheme VI

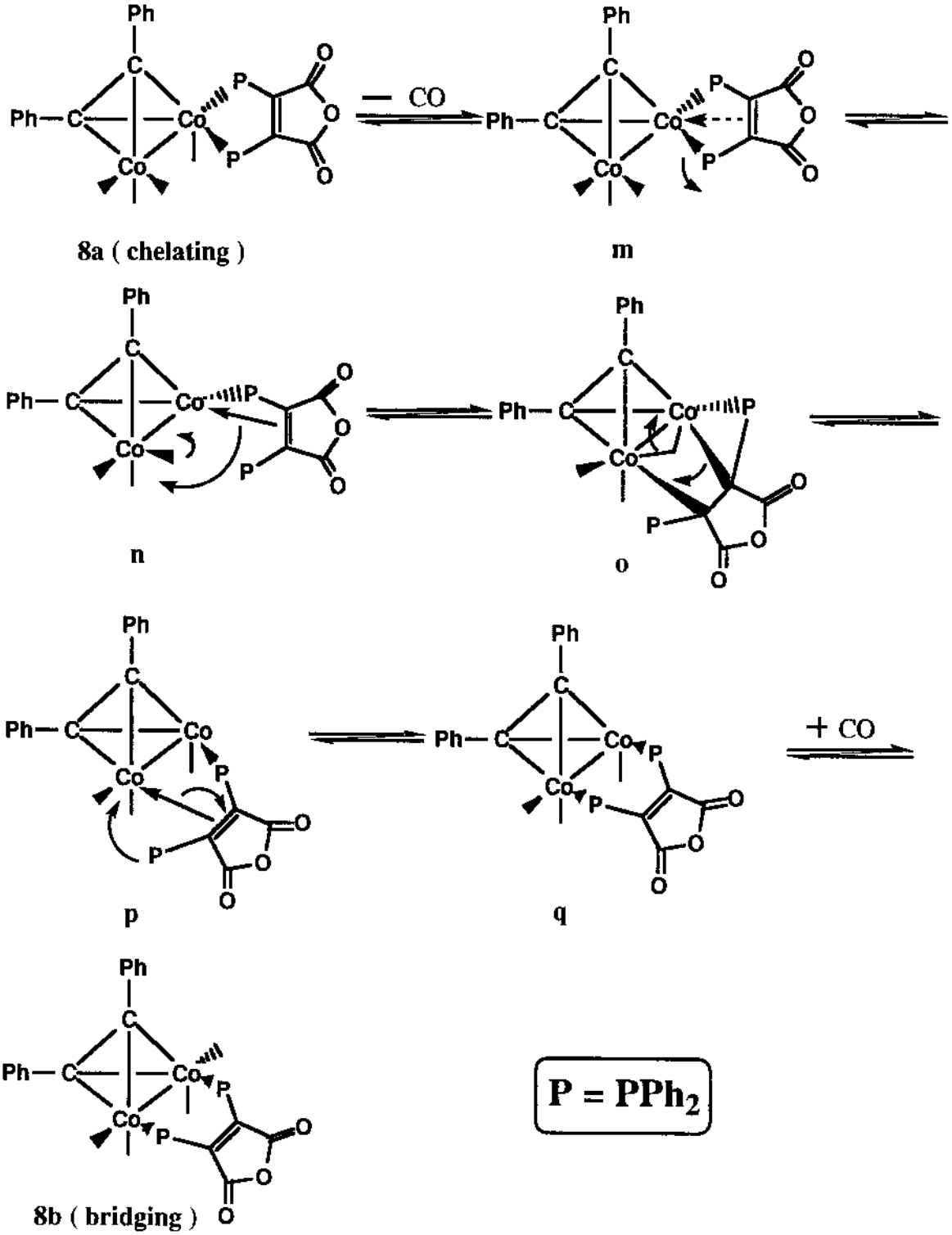

Scheme VII

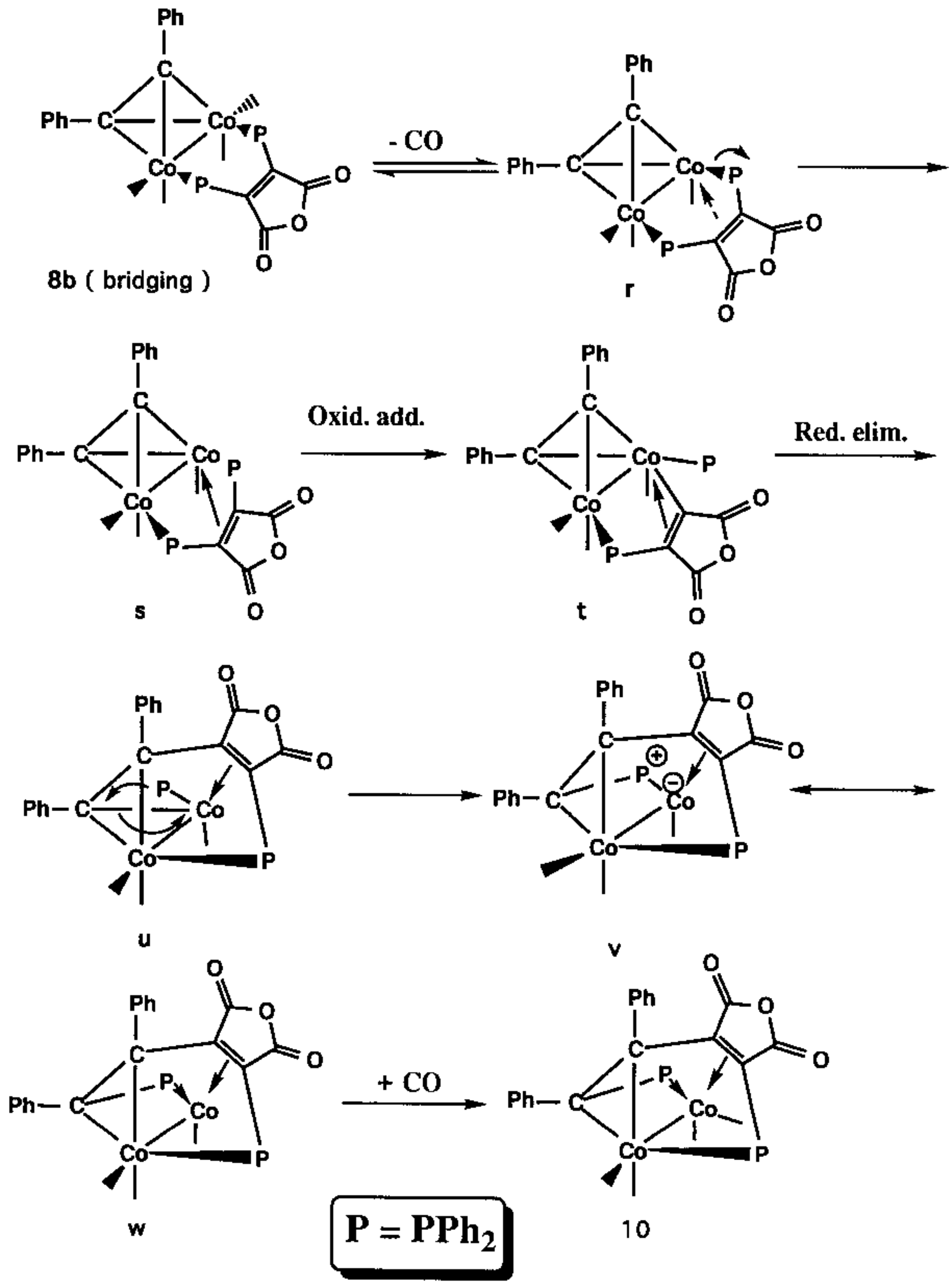

give the zwitterionic species **v**, which may also be viewed in terms of the non-charged resonance contributor shown in the lower left-hand corner of Scheme VII. [14] Capture of CO at the unsaturated cobalt center of **w** completes the scheme and affords the complex **10**.

The low yield associated with the production of **10** stands in contrast to the bma/cluster activation for $PhCCo_3(CO)_7$(bma). [13] Although the exact reason(s) for the low yield of **10** is unknown, it is likely that the oxidative addition of the P-C(olefin) bond and/or phosphido attack on the alkyne carbon are less favorable in the dinuclear case compared to the trinuclear cluster.

The nature of the ancillary P-ligand in **10** is related to complexes obtained from the reaction between $Co_2(CO)_4(\mu_2\text{-}PPh_2)_2$ and alkynes. [15,16] Double insertion of alkynes into the Co-phosphido bond leads to the metallocyclic complexes $Co_2\{\mu\text{-}Ph_2PCRCR'C(O)CR''CR'''PPh_2\}(CO)_4$. The nine-membered ring, which tethers both of the $Co(CO)_2$ groups, is identical to eight-electron ligand $\eta^2,\eta^2,\eta^1,\eta^1$-(Z)-$Ph_2PC(Ph)=(Ph)C\text{-}\overline{C=C(PPh_2)C(O)OC(O)}$ in **10**, except for the presence of the inserted carbonyl group.

F. X-Ray Diffraction Structures of $Co_2(CO)_4(\mu\text{-}PhC{\equiv}CPh)$(bma) (8b), $Co_2(CO)_4(\mu\text{-}PhC{\equiv}CPh)$[(Z)-$Ph_2PCH=CHPPh_2$] (9), and $Co_2(CO)_4[\eta^2,\eta^2,\eta^1,\eta^1$–(Z)-$Ph_2PC(Ph)=(Ph)C\text{-}\overline{C=(PPh_2)C(O)OC(O)}$] (10)

The dinuclear complexes $Co_2(CO)_4(\mu\text{-}PhC{\equiv}CPh)$(bma) (bridging), **8b**, and $Co_2(CO)_4(\mu\text{-}PhC{\equiv}CPh)$[(Z)-$Ph_2PCH=CHPPh_2$], **9**, are structurally similar with respect to the polyhedral (μ-alkyne)Co_2 core, the only significance difference between these two structures being the bonding mode adopted by the ancillary diphosphine ligand. Several attempts were made to grow single

crystals of the chelating isomer **8a**; however, these attempts were not successful, yielding only twinned and amorphous crystals, which necessitated the structural characterization of the bridging isomer of $Co_2(CO)_4(\mu$-PhC≡CPh)(bma). Both **8b** and **9** have a (μ-PhC≡CPh)Co_2 core, where the Co-Co bond length of 2.469(4) Å in $Co_2(CO)_4(\mu$-PhC≡CPh)(bma) (bridging) and 2.594(4) Å in **9** is comparable to other crystallographically characterized Co_2 complexes. [18] The 0.125 Å longer Co-Co bond in **9** (relative to **8b**) results from the chelating diphosphine ligand, which exerts a steric destabilization on the cobalt dinuclear complex, manifesting itself in an elongation of the Co-Co bond. The ancillary CO and diphosphine ligands occupy sites in the dinuclear complexes that give rise to the commonly observed "sawhorse" geometry associated with the Co_2L_6 fragment in **8b, 9**. [19] Considering each cobalt atom as defining a distorted octahedron, with a ligand sphere consisting of a shared diphenylacetylene ligand, CO/P ligands, and a Co-Co bond, allows for a ready description of the ancillary CO/P ligands at a given cobalt center. In **8b**, each cobalt atom possesses a pseudoequatorial phosphine and CO ligand and a single pseudoaxial CO group. Similar ligand arrangements have been observed in other diphosphine-bridged dinuclear complexes of this type. [20,21] Neglecting the alkyne ligand, a view down the Co-Co bond generates a nearly eclipsed Newman projection (i.e., "sawhorse" conformation) defined by the CO/P ligands at each cobalt center. The unique psuedoaxial ligand in such a projection is defined by the ligand that bisects the alkyne moiety. The dinuclear compound **9** is similar to **8b**, except that the chelating diphosphine ligand occupies a psuedoaxial (P(1)) and psuedoequatorial (P(2)) at the same cobalt center. The bond distances and angles in these two complexes exhibit no unusual properties that merit a

detailed discussion.

The structure of **10** consists of a $Co_2(CO)_4$ core that is ligated by the eight-electron ligand 2-[(Z)-1,2-diphenyl-2-(diphenylphosphino)ethenyl]-3-(diphenylphosphino)maleic anhydride. A picture of the isolated ligand is shown below. The Co-Co bond length of 2.594(4) Å is in agreement with

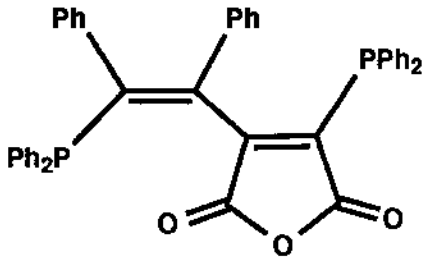

other complexes with a Co-Co single bond. [17] The two Co-P bond lengths of 2.244(6) Å for the Co(1)-P(1) bond and 2.179(6) Å for the Co(2)-P(2) bond are normal in comparison to other phosphine-substituted cobalt complexes, [22] but it is notable that the shorter Co-P distance corresponds to the PPh_2 group that is attached to the electron-withdrawing maleic anhydride ring. The alkene bonds of the ethene and maleic anhydride ligands are bound to different cobalt atoms in an η^2 fashion, with the adjacent PPh_2 group of each alkene being bound to the opposite cobalt atom in a typical η^1 fashion. The complexation of this eight-electron ligand to the two $Co(CO)_2$ moieties results in the formation of an eight-electron membered dimetallocyclic ring. The X-ray structure is important as it reveals that two phenyl groups that were originally from the diphenylacetylene ligand are situated cis to each other, as are the PPh_2 and (diphenylphosphino)maleic anhydride groups. The remaining bond distances and angles are unexceptional and require no comment.

G. Synthesis and Reactivity of $Co_2(CO)_4(\mu\text{-}PhC{\equiv}CH)(bma)$ (11), $Co_2(CO)_4(\mu\text{-}PhC{\equiv}CH)[(Z)\text{-}Ph_2PCH{=}CHPPh_2]$ (12), and $Co_2(CO)_4[\mu\text{-}\eta^2,\eta^2,\eta^1,\eta^1\text{-}PhC{=}C(H)PPh_2C{=}C(PPh_2)C(O)OC(O)]$ (13).

The reaction between the cobalt dinuclear complex $Co_2(CO)_6(\mu\text{-}PhC{\equiv}CH)$ and the diphosphine ligand bma in the presence of Me_3NO at room temperature affords the chelating isomer $Co_2(CO)_4(\mu\text{-}PhC{\equiv}CPh)(bma)$, **11a**. The identity of this compound has been established by IR and NMR (^{13}C and ^{31}P) spectroscopies. Conversion of the chelating isomer to bridging isomer of $Co_2(CO)_4(\mu\text{-}PhC{\equiv}CH)(bma)$, **11b**, occurs upon thermolysis. The bma ligand isomerization in $Co_2(CO)_4(\mu\text{-}PhC{\equiv}CH)(bma)$ can be easily explained on the basis of the same chemistry observed for $PhCCo_3(CO)_7(bma)$ and $Co_2(CO)_4(\mu\text{-}PhC{\equiv}CPh)(bma)$ (see Scheme I and Scheme VI). [13,23]

The thermolysis reactivity of the diphosphine complex $Co_2(CO)_4(\mu\text{-}PhC{\equiv}CH)[(Z)\text{-}Ph_2PCH{=}CHPPh_2]$ was also examined in refluxing 1,2-dichloroethane solvent in order to determine the reactivity differences between the bma ligand and normal diphosphine ligands devoid of an electron-withdrawing substitutent(s). Heating or photolyzing solutions of $Co_2(CO)_4(\mu\text{-}PhC{\equiv}CPh)[(Z)\text{-}Ph_2PCH{=}CHPPh_2]$ lead only to decomposition, presumably due to the retarded ability of the $(Z)\text{-}Ph_2PCH{=}CHPPh_2$ diphosphine ligand to enter into the series of reactions outlined in Scheme VI. Analogous reactivity has also been observed for $PhCCo_3(CO)_7(P\text{-}P)$ [where P-P = bma, $(Z)\text{-}Ph_2PCH{=}CHPPh_2$]. [13] Again, the absence of facile diphosphine isomerization in $Co_2(CO)_4(\mu\text{-}PhC{\equiv}CH)[(Z)\text{-}Ph_2PCH{=}CHPPh_2]$ is of interest, because it that highlights an unique reactivity difference between the bma ligand and the $(Z)\text{-}Ph_2PCH{=}CHPPh_2$ ligand.

Given the multidentate nature of the bma ligand (i.e., two phosphine

and one alkene groups), it is unreasonable to consider a scheme for the formation of **13** that involves the total dissociation of the bma ligand from $Co_2(CO)_4$(μ-PhC≡CH)(bma). The likely sequence of steps leading to **13** is considered in Scheme VIII, starting from bridging isomer of **11b.** CO loss from the **11b** generates species **x**. Exchange of the bma C=C bond for the coordinated PPh_2 group at the unsaturated cobalt center gives dinuclear species **y**, and sets up the molecule for the requisite P-C bond formation step leading to species **z**. Recapture of CO at the unsaturated cobalt center of **z** completes the scheme and affords the zwitterionic hydrocarbyl complex **13**. The coupling between the dangling -PPh_2 group and the coordinated μ-PhC≡CH ligand is regioselective, as only the terminal alkyne carbon is attacked. No evidence was found for the formation of the product derived from attack of the -PPh_2 group on the sterically protected alkyne carbon bearing the phenyl group. Intermediate **y** in Scheme VIII can be directly compared with the intermediate **s** in Scheme VII. There P-C(olefin) bond oxidation took place and no zwitterionic product (i.e., **13**) was formed. Although the exact reasons for the different reactivities exhibited by $Co_2(CO)_4$(μ-PhC≡CPh)(bma) and $Co_2(CO)_4$(μ-PhC≡CH)(bma) are not clear, it is likely that the oxidative addition of the P-C(olefin) bond and the coupling between -PPh_2 and alkyne are sterically controlled. Future studies are needed in order to fully understand the electronic and steric effects associated with the reactions between $Co_2(CO)_6$(μ-alkyne) and the bma ligand.

H. X-Ray Diffraction Structure of $Co_2(CO)_4[\mu\text{-}\eta^2,\eta^2,\eta^1,\eta^1\text{-}PhC{=}C(H)PPh_2\overline{C{=}C(PPh_2)C(O)OC(O)}]$ (13)

The structure of zwitterionic hydrocarbyl complex **13** was unequivi-

Scheme VIII

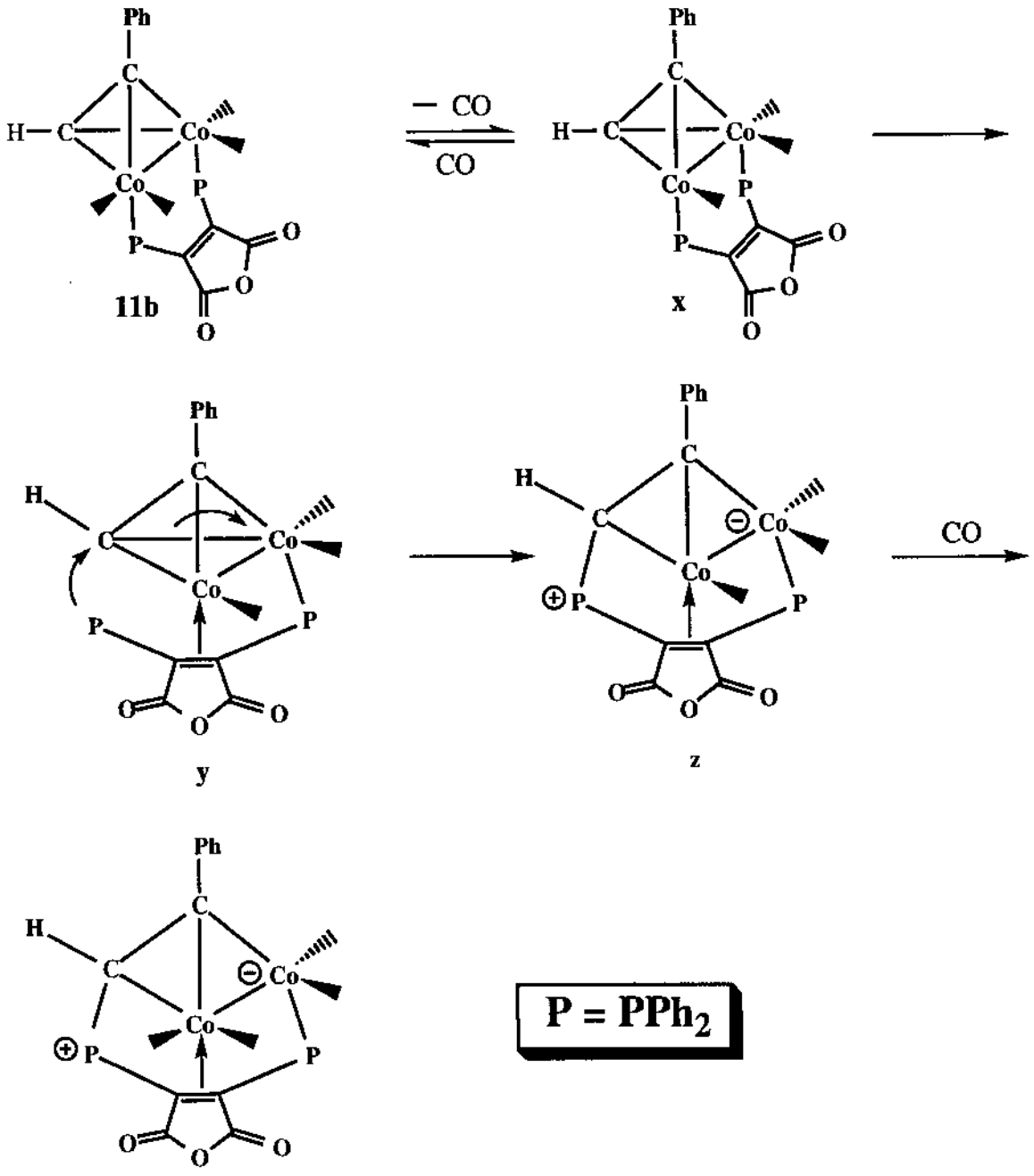

cally established by X-ray diffraction analysis, which revealed the migration of one of the phosphine moieties associated with the bma ligand to the terminal alkyne carbon of the coordinated phenylacetylene ligand. This regioselective transformation gives rise to the first μ-η^2,η^1–hydrocarbyl ligand complex formed from an intramolecular P-ligand attack on a coordinated alkyne moiety. The zwitterionic nature of **13** requires a negative charge on Co(2) and a positive charge on P(2); the latter center is best described as a phosphonium center given the tetrasubstituted nature of the P(2) atom. Of interest here is the utilization of the maleic anhydride bond as an η^2-donor ligand in the product, which allows each cobalt center to achieve a coordinatively saturated state. The Co-Co bond distance of 2.549 (Å) in **13** is comparable to other crystallographically characterized Co_2 dinuclear complexes. [17] The remaining bond distances and angles are unexceptional and require no comment.

I. Synthesis of $Co_2(CO)_3(PMe_3)[\mu$-$\eta^2,\eta^2,\eta^1,\eta^1$-PhC(CO)=C(H)$PPh_2$C=C(PPh$_2$)C(O)OC(O)] (14).

The zwitterionic hydrocarbyl complex **13** reacts with 1.0 equivalent of PMe_3 at room temperature to afford the new zwitterionic hydrocarbyl complex **14** in quantitive yield. The incoming PMe_3 ligand selectively attacks the cobalt atom that is coordinated by the maleic anhydride double bond, coupled with a presumed insertion of CO into the Co-alkyne bond. The CO insertion step is highly regioselective, as only the product observed is that from CO insertion into the Co-C(Ph)CH bond. The reaction involves no change in the formal oxidation state of either cobalt atom and can be classified as a phosphine-promoted intramolecular insertion reaction, the

type of which is well-documented. [24] Unfortunately, the mechanism associated with this CO insertion is not clear at this point. Kinetic measurements are prohibited due to the extremely fast rates associated with this reaction. The formation of **14** from **13** is novel. There is no literature precedent for the CO insertion into a metal-hydrocarbyl bond upon the addition of a phosphine ligand. It is interesting to note that no other substitution product was seen for this reaction.

J. X-Ray Diffraction Structure of $Co_2(CO)_3(PMe_3)[\mu\text{-}\eta^2,\eta^2,\eta^1,\eta^1\text{-}PhC(CO)=C(H)PPh_2C=C(PPh_2)C(O)OC(O)]$ (14).

The structure of **14** was unequivocally established by X-ray diffraction analysis. The structure features of **14** can be directly compared to those of **13**. The ORTEP diagram of **14** (Figure 3.16) confirms the migration of one CO group into the Co-C(Ph)CH bond of **13**. Like **13**, the zwitterionic structure of **14** requires a negative charge on Co(2) and positive charge on P(2), thereby allowing each cobalt atom to achieve a coordinatively saturated state.

The Co-Co bond distance of 2.650 (Å) in **14** is comparable to other crystallographically characterized Co_2 dinuclear complexes. [17] The 0.101 Å longer Co-Co bond in **14** relative to **13** results from a steric perturbation induced on the dinuclear core by the PMe_3 ligand. The remaining bond distances and angles are unexceptional and require no comment.

CHAPTER REFERENCES

1. (a) Downard, A. J.; Robinson, B. H.; Simpson, J. Organometallics **1986**, 5, 1122. (b) Unpublished variable-temperature ^{31}P NMR results.

2. Richmond, M. G.; Kochi, J. K. Inorg. Chem. **1986**, 25, 656.

3. Intramolecular CO exchange in $PhCCo_3(CO)_7(bma)$ is estimated to be 5×10^3 s^{-1} at room temperature.

4. The reductive coupling of the μ_3-benzlidyne and the (diphenylphosphino)maleic anhydride ligands reported here is akin to the alkylidyne-alkyne coupling observed in other trinuclear clusters. See: (a) Churchill, M. R.; Ziller, J. W.; Shapley, J. R.; Yeh, W.-Y. J. Organomet. Chem. **1988**, 353, 103. (b) Beanan, L. R.; Keister, J. B. Organometallics **1985**, 4, 1713. (c) Lentz, D.; Michael-Schulz, H. Inorg. Chem. **1990**, 29, 4396. (d) Nuel, D.; Dahan, F.; Mathieu, R. J. Am. Chem. Soc. **1985**, 107, 1658.

5. (a) Garrou, P. E. Chem. Rev. **1981**, 81, 229 and references therein. (b) Dubois, R. A.; Garrou, P. E. Organometallics **1986**, 5, 466.

6. (a) Colbran, S. B.; Robinson, B.; Simpson, J. Acta Crystallogr. **1986**, C42, 972. (b) Ahlgrén, M.; Pakkanen, T. T.; Tahvanainen, I. J. Organomet. Chem. **1987**, 323, 91. (c) Aitchison, A. A.; Farrugia, L. J. Organometallics **1987**, 6, 819. (d) Brice, M. D.; Penfold, B. R.; Robinson, W. T.; Taylor, S. R. Inorg. Chem. **1970**, 9, 362.

7. (a) Albright, T. A.; Kang, S.-K.; Arif, A. M.; Bard, A. J.; Jones, R. A.; Leland, J. K.; Schwab, S. T. Inorg. Chem. **1988**, 27, 1246. (b) Harley, A. D.; Whittle, R. R.; Geoffroy, G. L. Organometallics **1983**, 2, 60. (c) Baker, R. T.; Calabrese, J. C.; Krusic, P. J.; Therien, M. J.; Trogler, W. C. J. Am. Chem. Soc. **1988**, 110, 8392. (d) Regragui, R.; Dixneuf, P. H.; Taylor, N. J.; Carty, A. J. Organometallics **1990** 9, 2234. (e) Young, D. A. Inorg. Chem. **1981**, 20, 2049.

8. (a) Bogan, L. E.; Lesch, D. A.; Rauchfuss, T. B. J. Organomet. Chem. **1983**, 250, 429. (b) Adams, R. D.; Yang, L. W. J. Am. Chem. Soc. **1983**, 105, 1983. (c) Martin, L. R.; Einstein, F. W. B.; Pomeroy, R. K. Organometallics **1988**, 7, 294. (d) Tulyathan, B.; Geiger, W. E. J. Am. Chem. Soc. **1985**, 107, 5960. (e) Vahrenkamp, H. Adv. Organomet. Chem. **1983**, 22, 169 and references therein.

9. Planalp, R. P.; Vahrenkamp, H. Organometallics **1987**, 6, 492. (b) Schneider, J.; Minelli, M.; Huttner, G. J. Organomet. Chem. **1985**, 294, 75. (c) Darensbourg, D. J. in "The Chemistry of Metal Cluster Complexes," Shriver, D. F.; Kasez, H. D.; Adams, R. D. Eds.; VCH Publishers, Inc.: New York, **1990**, Chapter 4.

10. (a) Carty, A. J.; Mott, G. N.; Taylor, N. J.; Yule, J. E.; J. Am. Chem. Soc. **1978**, 100, 3051. (b) Carty, A. J.; Mott, G. N.; Taylor, N. J.; Ferguson, G.; Khan, M. A.; Roberts, P. J. J. Organomet. Chem. **1978**, 149, 345. (c) Cherkas, A. A.; Carty, A. J.; Sappa, E.; Pellinghelli, M. A.; Tiripicchio, A. Inorg. Chem. **1987**, 26, 3201. (d) Cherkas, A. A.; Mott, G. N.; Granby, R.; MacLauglin, S. A.; Yule, J. E.; Taylor, N. J.; Carty, A. J. Organometallics **1988**, 7, 1115. (e) Cherkas, A. A.; Doherty, S.; Cleroux, M.; Hogarth, G.; Randall, L. H.; Breckenridge, S. M.; Taylor, N. J.; Carty, A. J. Organometallics **1992**, 11, 1701. (f) Breckenridge, S. M.; Taylor, N. J.; Carty, A. J. Organometallics **1991**, 10, 837. (g) Henrick, K.; McPartlin, M.; Deeming, A. J.; Hasso, S.; Manning, P. J. Chem. Soc., Dalton Trans. **1982**, 899. (h) Boyar, E. R.; Deeming, A. J.; Kabir, S. E. J. Chem. Soc., Chem. Commun. **1986**, 577. (i) Deeming, A. J.; Kabir, S. S.; Nuel, D.; Powell, N. I. Organometallics **1989**, 8, 717. (j) Deeming, A. J. Adv. Organomet. Chem. **1986**, 26, 1.

11. (a) Wade, K. Adv. Inorg. Chem. Radiochem. **1976**, 18, 1. (b) Wade, K. in "Transition Metal Clusters," Johnson, B. F. G., Ed.; Wiley: New York, **1980**, Chapter 3. (c) Mingos, D. M. P. Acc. Chem. Res. **1984**, 17, 311.

12. Collman, J. P.; Hegedus, L. S.; Norton, J. R.; Finke, R. G. "Principles and Applications of Organotransition Metal Chemistry," University Science Books, Mill Valley, **1987**, Chapter 2, P75.

13. (a) Yang, K.; Smith, J. M.; Bott, S. G.; Richmond, M. G. Inorg. Chim. Acta. **1993**, 212, 1. (b) Yang, K.; Smith, J. M.; Bott, S. G.; Richmond, M. G. Organometallics **1993**, 12, 4779 and references therein.

14. Conole, G.; Hill, K. A.; McPartlin, M.; Mays, M. J.; Morris, M. J. J. Chem. Soc., Chem. Commun. **1989**, 688.

15. Caffyn, A. J. M.; Mays, M. J.; Solan, G. A.; Braga, D.; Sabatino, P.; Tiripicchio, A.; Tiripicchio-Camellini, M. Organometallics **1993**, 12, 1876.

16. Caffyn, A. J. M.; Mays, M. J.; Solan, G. A.; Conole, G.; Tiripicchio, A. J. Chem. Soc., Dalton, Trans. **1993**, 2345.

17. (a) Cotton, F. A.; Jamerson, J. D.; Stults, B. R. J. Am. Chem. Soc. **1976**, 98, 1774. (b) Miraz, H. A.; Vittal, J. J.; Puddephatt, R. J.; Frampton, C. S.; Manojlovic-Muir, L.; Xia, W.; Hill, R. H.

Organometallics **1993**, 12, 2767. (c) Gregson, D.; Howard, J. A. K. Acta, Cryst. **1983**, C39, 1024. (d) Lang, H.; Zsolnai, L. Chem. Ber. **1991**, 124, 259. (e) Gelling, A.; Jeffery, J. C.; Povey, D. C.; Went, M. J. J. Chem. Soc., Chem. Commun. **1991**, 349.

18. Richmond, M. G.; Kochi, J. K. Organometallics **1987**, 6, 254.

19. Thorn, D. L.; Hoffmann, R. Inorg. Chem. **1978**, 17, 126.

20. (a) Chia, L. S.; Cullen, W. R.; Franklin, M.; Manning, A. R. Inorg. Chem. **1975**, 14, 2521. (b) Bird, P. H.; Fraser, A. R.; Hall, D. N. Inorg. Chem. **1977**, 16, 1923. (c) Bianchini, C.; Dapporto, P.; Meli, A. J. Organomet. Chem. **1979**, 174, 205.

21. (a) Cunnighame, R. G.; Hanton, L. R.; Jenson, S. D.; Robinson, B. H.; Simpson, J. Organometallics **1987**, 1470. (b) Jenson, S. D.; Robinson, B. H.; Simpson, J. Organometallics **1987**, 1479.

22. (a) Don, M.-J.; Richmond, M. G.; Watson, W. H.; Krawiec, M.; Kashyap, R. P. J. Organomet. Chem. **1991**, 418, 231. (b) Yang, K.; Bott, S. G.; Richmond, M. G. J. Organomet. Chem. **1993**, 454, 273. (c) Brice, M. D.; Penfold, B. R.; Robinson, W. T.; Taylor, S. R. Inorg. Chem. **1970**, 9, 362. (d) Balavoine, G.; Collin, J.; Bonnet, J. J.; Lavinge, G. J. Organomet. Chem. **1985**, 280, 429.

23. Yang, K.; Bott, S. G.; Richmond, M. G. Organometallics **1994**, 13, in press.

24. (a) Wojcicki, A. Adv. Organomet. Chem. **1973**, 11, 87. (b) Calderazzo, F. Angew. Chem., Int. Ed. Engl. **1977**, 16, 299. (c) Kuhlman, E. J.; Alexander, J. J. Coord. Chem. Rev. **1980**, 33, 195.

BIBLIOGRAPHY

Abatjoglou, A. G.; Billig, E.; Bryant, D. R. Organometallics **1984**, 3, 923.

Albers, M. O.; Coville, N. J. Coord. Chem. Rev. **1984**, 53, 227.

Albright, T. A.; Hoffmann, R. J. Am. Chem. Soc. **1978**, 100, 7736.

Adams, R. D.; Babin, J. E.; Tasi, M.; Wolfe, T. A. Organometallics **1987**, 6, 2228.

Adams, R. D.; Chen, G.; Chen, L.; Wu, W.; Yin, J. Organometallics **1993**, 12, 3431.

Adams, R. D.; Horváth, I. T. Prog. Inorg. Chem. **1985**, 32, 127.

Adams, R. D.; Yang, L. W. J. Am. Chem. Soc. **1983**, 105, 1983.

Adams, R. N. "Electrochemistry at Solid Electrodes," Marcel Dekker: New York, **1969**.

Aggarwal, R. P.; Connelly, N. G.; Crespo, M. C.; Dunne, B. J.; Hopkins, P. M.; Orpen, A. G. J. Chem. Soc., Chem. Commun. **1989**, 33.

Aggarwal, R. P.; Connelly, N. G.; Crespo, M. C.; Dinne, B. J.; Hopkins, P. M.; Orpen, A. G. J. Chem. Soc., Dalton Trans. **1992**, 655.

Ahlgrén, M.; Pakkanen, T. T.; Tahvanainen, I. J. Organomet. Chem. **1987**, 323, 91.

Aime, S.; Botta, M.; Gobetto, R.; Osella, D. J. Organomet. Chem. **1987**, 320, 229.

Aime, S.; Milone, L.; Rosssetti, R.; Stanghellini, P. L. Inorg. Chim. Acta. **1977**, 25, 103.

Aitchison, A. A.; Farrugia, L. J. Organometallics **1987**, 6, 819.

Anderson, A. B. Inorg. Chem. **1976**, 15, 2598.

Arewgoda, M.; Rieger, P. H.; Robinson, B. H.; Simpson, J.; Visco, S. J. J. Am. Chem. Soc. **1982**, 104, 5633.

Arewgoda, C. M.; Robinson, B. H.; Simpson, J. J. Chem. Soc., Chem. Commun. **1982**, 284.

Arewgoda, C. M.; Robinson, B. H.; Simpson, J. J. Am. Chem. Soc. **1983**, 105, 1893.

Albright, T. A.; Burdett, J. K.; Whangbo, M. H. "Orbital Interactions in Chemistry," Wiley: New York, **1985**.

Albright, T. A.; Kang, S.-K.; Arif, A. M.; Bard, A. J.; Jones, R. A.; Leland, J. K.; Schwab, S. T. Inorg. Chem. **1988**, 27, 1246.

Alcock, N. W.; Bergamini, P.; Kemp, T. J.; Pringle, P. G. J. Chem. Soc., Chem. Commun. **1987**, 235.

Arduini, A. A.; Bahsoun, A. A.; Osborn, J. A.; Voelker, C. Angew. Chem., Int. Ed. Engl. **1980**, 19, 1024.

Avey, A.; Schut, D. M.; Weakley, T. J. R. Inorg. Chem. **1993**, 32, 233.

Bagchi, R. N.; Bond, A. M.; Brain, G.; Colton, R.; Henderson, T. L. E.; Kevekordes, J. E. Organometallics **1984**, 3, 4.

Bahsoun, A. A.; Osborn, J. A.; Voelker, C.; Bonnet, J. J.; Lavingne, G. Organometallics **1982**, 1, 1114.

Baker, R. T.; Calabrese, J. C.; Krusic, P. J.; Therien, M. J.; Trogler, W. C. J. Am. Chem. Soc. **1988**, 110, 8392.

Baker, R. T.; Krusic, P. J.; Tulip, T. H.; Calabrese, J. C.; Wreford, S. S. J. Am. Chem. Soc. **1985**, 107, 3346.

Balavoine, G.; Collin, J.; Bonnet, J. J.; Lavingne, G. J. Organomet. Chem. **1985**, 280, 429.

Bantel, H.; Powell, A. K.; Vahrenkamp, H. Chem. Ber. **1990**, 123, 1607.

Bard, A. J.; Faulkner, L. R. "Electrochemical Methods," Wiley: New York, **1980**.

Bird, P. H.; Fraser, A. R.; Hall, D. N. Inorg. Chem. **1977**, 16, 1923.

Basolo, F. Inorg. Chim. Acta. **1981**, 50, 65.

Beanan, L. R.; Keister, J. B. Organometallics **1985**, 4, 1713.

Bellon, P. L.; Benedicenti, C.; Caglio, G.; Manassero, M. J. Chem. Soc., Chem. Commun. **1973**, 946.

Benlaarab, H.; Chaudret, B.; Dahan, F.; Poilblanc, R. J. Organomet. Chem. **1987**, 320, C51.

Bennett, M. J.; Donaldson, P. B.; Inorg. Chem. **1977**, 16, 655.

Bergounhou, C.; Bonnet, J.-J.; Fompeyrine, P.; Lavingne, G.; Lugan, N.; Mansilla, F. Organometallics **1986**, 5, 60 and references therein.

Benvenutti, M. H. A.; Vargas, D.; Braga, D.; Grepioni, F.; Parisini, E.; Mann, B. E. Organometallics **1993**, 12, 2955.

Bergamini, P.; Sostero, S.; Traverso, O.; Kemp, T. J. J. Chem. Soc., Dalton Trans. **1989**, 2017.

Bianchini, C.; Dapporto, P.; Meli, A. J. Organomet. Chem. **1979**, 174, 205.

Bird, P. H.; Fraser, A. R. Hall, D. N. Inorg. Chem. **1977**, 16, 1923.

Bitterer, F.; Brauer, D. J.; Dörrenbach, F.; Stelzar, O. J. Organomet. Chem. **1990**, 399, C4.

Blickensderfer, J. R.; Kasez, H. D. J. Am. Chem. Soc. **1975**, 97, 2681.

Blickensderfer, J. R.; Knobler, C. B.; Kasez, H. D. J. Am. Chem. Soc. **1975**, 97, 2686.

Blum, O.; Frolow, F.; Milstein, D. J. Chem. Soc., Chem. Commun. **1991**, 258.

Bogan, L. E.; Lesch, D. A.; Rauchfuss, T. B. J. Organomet. Chem. **1983**, 250, 429.

Bond, A. M.; Colton, R.; McCormick, M. J. Inorg. Chem. **1977**, 16, 155.

Bor, G.; Dietler, U. K.; Pino, P.; Poe, A. J. Organomet. Chem. **1978**, 154, 301.

Bor, G.; Kettle, S. F. A.; Stanghellini, P. L. Inorg. Chim. Acta **1976**, 18, L18.

Boyar, E. R.; Deeming, A. J.; Kabir, S. E. J. Chem. Soc., Chem. Commun. **1986**, 577.

Bradford, C. W.; Nyholm, R. S. J. Chem. Soc., Chem. Commun. **1972**, 87.

Bradford, C. W.; Nyholm, R. S. J. Chem. Soc., Dalton Trans. **1973**, 529.

Brice, M. D.; Penfold, B. R.; Robinson, W. T.; Taylor, S. R. Inorg. Chem. **1970**, 9, 362.

Breckenridge, S. M.; Taylor, N. J.; Carty, A. J. Organometallics **1991**, 10, 837.

Brodie, N.; Poë, A. J.; Sekhar, V. C. J. Chem. Soc., Chem. Commun.

1985, 1090.

Brown, T. L. in "Organometallic Radical Processes," Trogler, W. C., Elsevier: New York, **1990**, Chapter 3 and references therein.

Browning, C. S.; Farrar, D. H.; Gukathasan, R. R.; Morris, S. A. Organometallics **1985**, 4, 1750.

Bruce, M. I. Coord. Chem. Rev. **1987**, 76, 1.

Bruce, M. I.; Horn, Ernst; Shawkataly, O. B.; Snow, M. R.; Tiekink, E. R. T.; Williams, M. L. J. Organomet. Chem. **1986**, 316, 187.

Bruce, M. I.; Shaw, G.; Stone, F. G. A. J. Chem. Soc., Dalton Trans. **1972**, 2094.

Bruce, M. I. J. Organomet. Chem. **1990**, 394, 365.

Bruce, M. I.; Humphrey, P. A.; Skelton, B. W.; White, A. H.; Williams, M. L. J. Organomet. Chem. **1985**, 394, 365.

Buhro, W. E.; Georgiou, S.; Hutchinson, J. P.; Gladysz, J. A. J. Am. Chem. Soc. **1985**, 107, 3346.

Burt, J. C.; Schmid, G. J. Chem. Soc., Dalton Trans. **1978**, 1385.

Cabeza, J. A.; Franco, R. J.; Llamazares, A.; Riera, V.; Pérez- Carreño, E.; Van der Maelen, J. F. Organometallics **1994**, 13, 55 and references therein.

Caffyn, A. J. M.; Mays, M. J.; Solan, G. A.; Braga, D.; Sabatino, P.; Tiripicchio, A.; Tiripicchio-Camellini, M. Organometallics **1993**, 12, 1876.

Caffyn, A. J. M.; Mays, M. J.; Solan, G. A.; Conole, G.; Tiripicchio, A. J. Chem. Soc., Dalton, Trans. **1993**, 2345.

Calderazzo, F. Angew. Chem., Int. Ed. Engl. **1977**, 16, 299.

Carty, A. J. Pure Appl. Chem. **1982**, 54, 113 and references therein.

Carty, A. J.; Taylor, N. J.; Smith, W. F. J. Chem. Soc., Chem. Commun. **1979**, 750.

Carty, A. J.; Mott, G. N.; Taylor, N. J.; Paik, H. N.; Smith, W.; Yule, J. G. J. Chem. Soc., Chem. Commun. **1976**, 41.

Carty, A. J.; Mott, G. N.; Taylor, N. J. J. Organomet. Chem. **1981**, 212, C54.

Carty, A. J.; Mott, G. N.; Taylor, N. J. J. Organomet. Chem. **1979**, 182,

C69.

Carty, A. J.; Taylor, N. J.; Smith, W. F.; Lappert, M. F.; Pye, P. L. J. Chem. Soc., Chem. Commun. **1978**, 1017.

Carty, A. J.; Mott, G. N.; Taylor, N. J.; Yule, J. E.; J. Am. Chem. Soc. **1978**, 100, 3051.

Carty, A. J.; Mott, G. N.; Taylor, N. J.; Ferguson, G.; Khan, M. A.; Roberts, P. J. J. Organomet. Chem. **1978**, 149, 345.

Casagrande, L. V.; Chen, T.; Reiger, P. H.; Robinson, B. H.; Simpson, J.; Visco, S. J. Inorg. Chem. **1984**, 23, 2019.

Caulton, K. G. Coord. Chem. Rev. **1975**, 14, 317.

Chaudiet, B. N.; Cole-Hamilton, D. J.; Nohr, R. S.; Wilkinson, G. J J. Chem. Soc., Dalton Trans. **1977**, 1546.

Cherkas, A. A.; Hagheri, N.; Carty, A. J.; Sappa, E.; Pellinghelli, M. A.; Tiripicchio, A. Organometallics **1990**, 9, 1887.

Cherkas, A. A.; Mott, G. N.; Granby, R.; MacLauglin, S. A.; Yule, J. E.; Taylor, N. J.; Carty, A. J. Organometallics **1988**, 7, 1115.

Cherkas, A. A.; Randall, L. H.; Taylor, N. J.; Mott, G. N.; Yule, J. E.; Guinamart, J. L.; Carty, A. J. Organometallics **1990**, 9, 1677.

Cherkas, A. A.; Carty, A. J.; Sappa, E.; Pellinghelli, M. A.; Tiripicchio, A. Inorg. Chem. **1987**, 26, 3201.

Chia, L. S.; Cullen, W. R.; Franklin, M.; Manning, A. R. Inorg. Chem. **1975**, 14, 2521.

Chini, P.; Heaton, B. Top. Curr. Chem. **1977**, 71, 53.

Churchill, M. R.; DeBoer, B. G.; Shapley, J. R.; Keister, J. B. J. Am. Chem. Soc. **1976**, 98, 2357.

Churchill, M. R.; Ziller, J. W.; Shapley, J. R.; Yeh, W.-Y. J. Organomet. Chem. **1988**, 353, 103.

Clark, H. C. Israel J. Chem. **1976/77**, 15, 210.

Colbran, S. B.; Robinson, B.; Simpson, J. Acta Crystallogr. **1986**, C42, 972.

Collman, J. P.; Hegedus, L. S.; Norton, J. R.; Finke, R. G. "Principles and Applications of Organotransition Metal Chemistry," University Science Books, Mill Valley, CA, **1987**, Chapter 2.

Conole, G.; Hill, K. A.; McPartlin, M.; Mays, M. J.; Morris, M. J. J. Chem. Soc., Chem. Commun. **1989**, 688.

Conner, K. A.; Walton, R. A. Inorg. Chem. **1986**, 25, 4422.

Cosslett, L.; Kane-Maguire, L. A. P. J. Organomet. Chem. **1979**, 178, C17.

Cotton, F. A.; Jamerson, J. D.; Stults, B. R. J. Am. Chem. Soc. **1976**, 98, 1774.

Cowley, A. H.; Norman, N. C. Quashie, S. J. Am. Chem. Soc. **1984**, 106, 5007.

Crow, J. P.; Cullen, W. R. Inorg. Chem. **1971**, 10, 2165.

Cunninghame, R. G.; Hanton, L. R.; Jenson, S. D.; Robinson, B. H.; Simpson, J. Organometallics **1987**, 1470.

Dahlinger, K.; Poë, A. J.; Sayal, P. K.; Sekhar, V. C. J. Chem. Soc., Dalton Trans. **1986**, 2145.

Darensbourg, D. J. in "The Chemistry of Metal Cluster Complexes," Shriver, D. F.; Kasez, H. D.; Adams, R. D. Eds.; VCH Publishers, Inc.: New York, **1990**, Chapter 4.

Darensbourg, D.; Bischoff, C. J. Inorg. Chem. **1993**, 32, 47.

Davies, J. A.; In "The Chemistry of the Metal-Carbon Bond," Hartley, F. R., Ed.; Wiley-Interscience: New York, **1982**, Chapter 21, p880.

Davis, S. G.; Gelfaud, L. G.; Sweigart, D. A. J. Chem. Soc., Chem. Commun. **1979**, 762.

de Boer, J. J.; van Doorn, J. A.; Osborn, J. A.; Masters, C. J. Chem. Soc., Chem. Commun. **1978**, 1005.

Deeming, A. J. Adv. Organomet. Chem. **1986**, 26, 1.]

Deeming, A. J.; Hasso, S. J. Organomet. Chem. **1976**, 112, C39.

Deeming, A. J.; Kabir, S. S.; Nuel, D.; Powell, N. I. Organometallics **1989**, 8, 717.

Deeming, A. J.; Kimber, R. E.; Underhill, M. J. Chem. Soc., Dalton Trans. **1973**, 2589.

Deeming, A. J.; Underhill, M. J. Chem. Soc., Dalton Trans. **1973**, 2727.

DeKock, R. L.; Deshmukukh, P.; Dutta, T. K.; Fehlner, T. P.; Housecroft, C. E.; Hwang, J. L.-S. Organometallics **1983**, 2, 1108.

Dickson, R. S.; Peake, B. M.; Rieger, P. H.; Robinson, B. H.; Simpson, J. J. Organomet. Chem. **1979**, 172, C63.

Dickson, R. S.; Fraser, P. J. Adv. Organomet. Chem. **1974**, 12, 323 and references therein.

Doherty, N. M.; Hogarth, G.; Knox, S. A. R.; Macpherson, K. A.; Melchior, F.; Orpen, A. G. J. Chem. Soc., Chem. Commun. **1986**, 540.

Doherty, S.; Cleroux, M.; Hogarth, G.; Randall, L. H.; Breckenridge, S. M.; Taylor, N. J.; Carty, A. J. Organometallics **1992**, 11, 1701.

Dolphin, D.; Wick, A. "Tabulation of Infrared Spectral Data," Wiley-Interscience: New York, **1977**.

Domaille, D. J.; Ittel, S. D.; Jesson, J. P.; Sweigart, D. A. J. Organomet. Chem. **1980**, 202, 191.

Dombek, B. D. J. Am. Chem. Soc. **1980**, 102, 6855.

Don, M.-J.; Richmond, M. G. Inorg. Chem. **1991**, 30, 1703.

Don, M.-J.; Richmond, M. G. Inorg. Chim. Acta **1990**, 173, 61.

Don, M.-J.; Richmond, M. G.; Watson, W. H.; Krawiec, M.; Kashyap, R. P. J. Organomet. Chem. **1991**, 418, 231.

Downard, A. J.; Robinson, B. H.; Simpson, J. Organometallics **1986**, 5, 1122.

Downard, A. J.; Robinson, B. H.; Simpson, J. Organometallics **1986**, 5, 1132, 1140.

Dubois, R. A.; Garrou, P. E.; Lavin, K. D.; Allock, H. R. Organometallics **1986**, 5, 460 and references therein.

Dubois, R. A.; Garrou, P. E. Organometallics **1986**, 5, 466.

Dumond, D. S.; Richmond, M. G. J. Am. Chem. Soc. **1988**, 110, 7548.

Edsworth, E. A. V.; Holloway, J. H.; Pilkington, N. J.; Rankin, D. W. H. Angew. Chem., Int. Ed. Engl. **1984**, 8, 630.

Eisch, J. J.; King, R. B.; "Organometallic Syntheses," Academic Press: New York, **1965**, pp. 70-71.

Elliot, D. J.; Holah, D. J.; Hughes, A. N.; Mirza, H. A.; Zawada, E. J. Chem. Soc., Chem. Commun. **1990**, 32.

Enemark, J. H.; Feltham, R. D. Coord. Chem. Rev. **1974**, 13, 339

Feltham, R. D.; Enemark, J. H. In "Topics in Inorganic and Organometallic Stereochemistry", Wiley: New York, **1981**, 12, 155.

Fenske, D. Chem. Ber. **1979**, 112, 363.

Fenske, D.; Becher, H. J. Chem. Ber. **1974**, 107, 117.

Fenske, D.; Becher, H. J. Chem. Ber. **1975**, 108, 2115.

Foley, H. C.; Finch, W. C.; Pierpoint, C. G.; Geoffroy, G. L. Organometallics **1982**, 1, 1379.

Garrou, P. E. Chem. Rev. **1985**, 171 and references therein.

Gastel, F. V.; MacLaughlin, S. A.; Lynch, M.; Carty, A. J.; Sappa, E. J. Organomet. Chem. **1987**, 326, C65.

Gates, R. A.; D'Agostino, K. A.; Sutin, K. A.; McGlinchey, M. J.; Janik, T. S.; Churchill, M. R. Organometallics **1990**, 9, 20.

Gelling, A.; Jeffery, J. C.; Povey, D. C.; Went, M. J. J. Chem. Soc., Chem. Commun. **1991**, 349.

Gordon, A. J.; Ford, R. A. "The Chemist's Companion," Wiley-Interscience: New York, **1972**.

Gragg, B. R.; Layton, W. J.; Niedenzu, K. J. Organomet. Chem. **1977**, 132, 29.

Gregson, D.; Howard, J. A. K. Acta Cryst. **1983**, C39, 1024.

Granozzi, G.; Tondello, E.; Bertoncello, R.; Aime, S.; Osella, D. Inorg. Chem. **1983**, 22, 744.

Hansen, B. E.; Mancini, J. S. Inorg Chem. **1983**, 2, 126.

Harley, A. D.; Whittle, R. R.; Geoffroy, G. L. Organometallics **1983**, 2, 60.

Harrington, P. J.; "Transition Metals in Total Synthesis," John Wiley & Sons: New York, **1990**, Chapter 9.

Hayakawa, K.; Mibu, N.; Ósawa, E.; Kanematsu, K. J. Am. Chem. Soc. **1982**, 104, 7136.

Heck, R. F. J. Am. Chem. Soc. **1963**, 85, 657.

Hendrickson, D. N.; Sohn, Y. S.; Gray, H. B. Inorg. Chem. **1971**, 10, 1559.

Henrick, K.; McPartlin, M.; Deeming, A. J.; Hasso, S.; Manning, P. J. Chem. Soc., Dalton Trans. **1982**, 899.

Hinkelmann, K.; Keinze, J.; Schacht, H.-T.; Field, J. S.; Vahrenkamp, H. J. Am. Chem. Soc. **1989**, 111, 5078.

Hitchcock, P. B.; McPartlin, M.; Mason, R. Chem. Commun. **1969**, 1367.

Hoffmann, R. Angew. Chem., Int. Ed. Engl. **1982**, 21, 711.

Hoffmann, R. J. Chem. Phys. **1963**, 39, 1397.

Hoffman, D. M.; Huffman, J. C.; Lappas, D.; Wierda, D. A. Organometallics **1993**, 12, 4312 and references therein.

Hoffman, D. M.; Hoffmann, R.; Fisel, C. R. J. Am. Chem. Soc. **1982**, 104, 3858.

Hoffmann, R.; Libscomb, W. N. J. Chem. Phys. **1962**, 36, 3179.

Hogarth, G. J. Organomet. Chem. **1991**, 407, 91.

Hogarth, G.; Knox, S. A. R.; Turner, M. L. J. Chem. Soc., Chem. Commun. **1990**, 145 and references therein.

Huttner, G.; Muller, H. P.; Frank, A.; Lorenz, H. Angew. Chem., Int. Ed. Engl. **1977**, 16, 482.

Jenson, S. D.; Robinson, B. H.; Simpson, J. Organometallics **1987**, 12, 1479.

John, G. R.; Kane-Maguire, L. A. P. J. Chem. Soc., Dalton Trans. **1979**, 873.

Koelle, U. J. Organomet. Chem. **1977**, 133, 53.

Kofen, W. G.; Backlawski, L. M. J. Org. Chem. **1976**, 41, 1879.

Knoll, K.; Huttner, G.; Zsolnai, L.; Jibril, I.; Wasincionek, M. J. Organomet. Chem. **1985**, 294, 91.

Knox, S. A. R.; Lloyd, B. R.; Morton, D. A. V.; Nicholls, S. M.; Orpen, G.; Viñas, J. M.; Weber, M.; Williams, G. K. J. Organomet. Chem. **1990**, 394, 385 and references therein.

Krafft, M. E.; Juliano, C. A.; Scott, I. L.; Wright, C.; McEachin, M. D. J. Am. Chem. Soc. **1991**, 113, 1693.

Krafft, M. E.; Scott, I. L.; Romero, R. H.; Feibelmann, S.; Van Pelt, C. E. J. Am. Chem. Soc. **1993**, 115, 7199.

Kuchen, W.; Buchward, H. Chem. Ber. **1959**, 92, 227.

Kuhlman, E. J.; Alexander, J. J. Coord. Chem. Rev. **1980**, 33, 195.

Lang, H.; Zsolnai, L. Chem. Ber. **1991**, 124, 259.

Langford, C. H.; Gray, H. B. In "Ligand Substitution Processes," New York: Benjamin, **1965**.

Lennon, P.; Madhavarao, M.; Rosan, A.; Rosenblum, M. J. Organomet. Chem. **1976**, 108, 93.

Lentz, D.; Michael-Schulz, H. Inorg. Chem. **1990**, 29, 4396.

Levason, W.; McAuliffe, C. A. Acc. Chem. Res. **1978**, 11, 363.

Levason, W.; McAuliffe, C. A. Adv. Inorg. Chem. Radiochem. **1972**, 14, 173.

Lewin, M.; Aizenshtat, Z.; Blum, J. J. Organomet. Chem. **1980**, 184, 255.

Lilga, M. A.; Ibers, J. A. Inorg. Chem. **1984**, 23, 3538.

Lu, K. L.; Chen, H. J.; Lu, P. Y.; Li, S. Y.; Hong, F. E.; Peng, S. M.; Lee, G. H. Organometallics **1994**, 13, 585.

Lugan, N.; Lavingne, G.; Bonnet, J.-J. Inorg. Chem. **1987**, 26, 585.

Lugan, N.; Lavingne, G.; Bonnet, J.-J.; Réau, R.; Neibecker, D.; Tkatchenko, I. J. Am. Chem. Soc. **1988**, 110, 5369.

MacLaughlin, S. A.; Carty, A. J. Taylor, N. J. Can. J. Chem. **1982**, 60, 88.

MacLaughlin, S. A.; Johnson, J. P.; Taylor, N. J.; Carty, A. J.; Sappa, E. Organometallics **1983**, 2, 352.

Mao, F.; Philbin, C. E.; Weakley, T. J. R.; Tyler, D. R. Organometallics **1990**, 9, 1510.

Mao, F.; Sur, S. K.; Tyler, D. R. Organometallics **1991**, 10, 419.

Mao, F.; Tyler, D. R.; Keszler, J. J. Am. Chem. Soc. **1989**, 111, 130.

Mao, F.; Tyler, D. R.; Rieger, A. L.; Rieger, P. H. J. Chem. Soc., Faraday Trans. **1991**, 87, 3113.

McAuliffe, C. A. Ed.; "Transition-Metal Complexes of Phosphrous, Arsenic, and Antimony Ligands," Wiley: New York, **1973**.

McCleverty, J. Chem. Rev. **1979**, 79, 53.15.

Manojlovic-Muir, L.; Brandes, D. A.; Puddephatt, R. J. Organomet. Chem. **1987**, 332, 201.

Mann, B. E.; Taylor, B. F. "^{13}C NMR Data for Organometallic Compounds," Academic Press: New York, 1981.

Marinetti, A.; Mathey, F. J. Am. Chem. Soc. **1982**, 104,

Martin, L. R.; Einstein, F. W. B.; Pomeroy, R. K. Organometallics **1988**, 7, 294.

Mason, R.; Sotofte, I.; Robinson, S. D.; Uttley, M. F. J. Organomet. Chem. **1972**, 46, C61.

Masters, C. Adv. Organomet. Chem. **1979**, 17, 61.

Mealli, C.; Proserpio, D. M. J. Chem. Ed. **1990**, 67, 399.

Melikyan, G. G.; Mineif, A.; Vostrowsky, O.; Bestmann, H. J. Synthesis **1991**, 633.

Mingos, D. M. P. Acc. Chem. Res. **1984**, 17, 311.

Miraz, H. A.; Vittal, J. J.; Puddephatt, R. J.; Frampton, C. S.; Manojlovic-Muir, L.; Xia, W.; Hill, R. H. Organometallics **1993**, 12, 2767.

Morris, R. J.; Girolami, G. S. Inorg. Chem. **1990**, 29, 4167.

Natarajan, K.; Zsolnai, L.; Huttner, G. J. Organomet. Chem. **1981**, 209, 85.

Nestle, M. O.; Hallgren, J. E.; Seyferth, D. Inorg. Synth. **1980**, 20, 226.

Nicholas, K. M.; Acc. Chem. Res. **1987**, 20, 207.

Nuel, D.; Dahan, F.; Mathieu, R. J. Am. Chem. Soc. **1985**, 107, 1658.

Noth, W. H. Inorg. Chem. **1975**, 14, 1566.

Ohst, H. H.; Kochi, J. K. J. Am. Chem. Soc. **1986**, 108, 2897.

Orpen, A. G. J. Chem. Soc., Chem. Commun. **1985**, 1310.

Ortiz, J. V.; Havias, Z.; Hoffmann, R. Helv. Chim. Acta. **1984**, 67, 1.

Osella, D.; Dutto, G.; Jaouen, G.; Vessiéres, A.; Raithby, P. R.; De Benedetto, L.; McGlinchey, M. J. Organometallics **1993**, 12, 4545.

Osella, D.; Fiedler, J. Organometallics **1992**, 11, 3875.

Osella, D.; Stein, E.; Jaouen, G.; Zanello, P. J. Organomet. Chem. **1991**, 401, 37.

Parshall, G. W. Acc. Chem. Res. **1970**, 3, 139.

Patel, V. D.; Taylor, N. J.; Carty, A. J. J. Chem. Soc., Chem. Commun. **1984**, 99.

Peake, B. M.; Robinson, B. H.; Simpson, J. Watson, D. J. Inorg. Chem. **1977**, 16, 405.

Peake, B. M.; Rieger, P. H.; Robinson, B. H.; Simpson, J. Inorg. Chem. **1979**, 18, 1000.

Planalp, R. P.; Vahrenkamp, H. Organometallics **1987**, 6, 492.

Poë, A. J.; Sekhar, V. C. Inorg. Chem. **1985**, 24, 4376.

Pregosin, P. S.; Kunz, R. W. In "NMR Basic Principles and Progress," Springer-Verlag: Heidelberg, **1979**, Vol. 16, p55.

Reed, J.; Schultz, A. J.; Pierpoint, C. G.; Eisenberg, R. Inorg. Chem. **1973**, 12, 2949.

Regragui, R.; Dixneuf, P. H.; Taylor, N. J.; Carty, A. J. Organometallics **1990** 9, 2234.

Rieke, R. D.; Kojima, H.; Saji, T.; Rechberger, P.; Öfele, K. Organometallics **1988**, 7, 749.

Richmond, M. G.; Kochi, J. K. Inorg. Chem. **1986**, 25, 656.

Richmond, M. G.; Kochi, J. K. Inorg. Chem. **1986**, 25, 1334.

Richmond, M. G.; Kochi, J. K. Inorg. Chem. **1987**, 26, 541.

Richmond, M. G.; Kochi, J. K. Organometallics **1987**, 6, 254.

Richmond, M. G.; Kochi, J. K. Organometallics **1987**, 6, 777.

Richter, F.; Beurich, H.; Vahrenkamp, H. J. Organomet. Chem. **1979**, 204, C10.

Rubin, Y.; Knobler, C. B.; Diederich, F. J. Am. Chem. Soc. **1990**, 112, 4966.

Sabo, S.; Chaudret, B.; Gervais, D. J. Organomet. Chem. **1983**, 258, C19.

Sandström, J. "Dynamic NMR Spectroscopy," Academic Press, New York, **1992**.

Shanan-Atidi, H.; Bar-Eli, K. H. J. Phys. Chem. **1970**, 74, 961.

Schneider, J.; Minelli, M.; Huttner, G. J. Organomet. Chem. **1985**, 294, 75.

Schreiber, S. L.; Klimas, M. T.; Sammakia, T. J. Am. Chem. Soc. **1987**, 109, 5749.

Seyferth, D.; Hoke, J. B.; Wheeler, D. R. J. Organomet. Chem. **1988**, 341, 421.

Shriver, D. F.; "The Manipulation of Air-Sensitive Compounds," McGraw-Hill: New York, **1969**.

Shriver, D. F.; Adams, R. D.; Kasez, H. D. "The Chemistry of Metal Cluster Complexes," VCH Publishers: New York, **1990**.

Schulman, C. L.; Richmond, M. G.; Watson, W. H.; Nagl, A. J. Organomet. Chem. **1989**, 368, 367.

Smith, G. P.; Patrick, R. Int. J. Chem. Kinet. **1983**, 15, 167.

Sommovigo, M.; Pasquali, M.; Leoni, P.; Braga, D.; Sabatino, P. Chem. Ber. **1991**, 124, 97 and references therein.

Sullivan, B. P.; Meyer, T. J. Inorg. Chem. **1982**, 21, 1037.

Sutin, K. A.; Kolis, J. W.; Miekuz, M., Bougeard, P.; Sayer, B. G.; Quilliam, M. A.; Faggiani, R.; Lock, C. J. L.; McGlinchey, M. J.; Jaouen, G. Organometallics **1987**, 6, 439.

Takats, J.; Washington, J.; Santarsiero, B. D. Organometallics **1994**, 13, 1078 and references therein.

Taube, D. J.; Ford, P. C. Organometallics **1986**, 5, 99.

Templeton, J. L. Adv. Organomet. Chem. **1989**, 29, 1.

Tester, R.; Varghese, V.; Montana, A. M.; Khan, M.; Nicholas, K. M. J. Org. Chem. **1990**, 55, 186.

Thorn, D. L.; Hoffmann, R. Inorg. Chem. **1978**, 17, 126.

Tulyathan, B.; Geiger, W. E. J. Am. Chem. Soc. **1985**, 107, 5960.

Tyler, D. R. Acc. Chem. Res. **1991**, 24, 325.

Tyler, D. R.; Mao, F. Coord. Chem. Rev. **1990**, 97, 119.

Tolman, C. A. Chem. Rev. **1977**, 77, 313.

Trofimenko, S. Inorg. Chem. **1973**, 12, 1215.

Xiao, S.-X.; Trogler, W. C.; Ellis, D. E.; Berkovitch-Yellin, Z. J. J. Am. Chem. Soc. **1983**, 105, 7033.

Vahrenkamp, H. Adv. Organomet. Chem. **1983**, 22, 169 and references therein.

Vallet, A.; Person, M.; Rollier, L.; Laviron, E. Inorg. Chem. **1987**, 26, 332.

Vidal, J. L.; Walker, W. E. Inorg. Chem. **1981**, 20, 249.

Wade, K. Adv. Inorg. Chem. Radiochem. **1976**, 18, 1.

Wade, K. in "Transition Metal Clusters," Johnson, B. F. G., Ed.; Wiley: New York, **1980**, Chapter 3.

Wang, J.; Sabat, M.; Lyons, L. J.; Shriver, D. F. Inorg. Chem. **1991**, 30, 382.

Watson, W. H.; Nagl, A.; Hwang, S.; Richmond, M. G. J. Organomet. Chem. **1993**, 445, 163.

Whyman, R. J. Chem. Soc., Dalton Trans. **1972**, 2294.

Wojcicki, A. Adv. Organomet. Chem. **1973**, 11, 87.

Wong, Y. S.; Paik, H. N.; Chieh, P. C.; Carty, A. J. J. Chem. Soc., Chem. Commun. **1975**, 309.

Yang, K.; Bott, S. G.; Richmond, M. G. J. Organomet. Chem. **1993**, 454, 273.

Yang, K.; Bott, S. G.; Richmond, M. G. Organometallics **1994**, 13, in press.

Yang, K.; Smith, J. M.; Bott, S. G.; Richmond, M. G. Organometallics **1993**, 12, 4779 and references therein.

Yang, K.; Smith, J. M.; Bott, S. G.; Richmond, M. G. Inorg. Chim. Acta. **1993**, 212, 1.

Young, D. A. Inorg. Chem. **1981**, 20, 2049.

Yuan, P.; Don, M. -J.; Richmond, M. G.; Schwartz, M. Inorg. Chem. **1991**. 30, 3704.

Yuan, P.; Richmond, M. G.; Schwartz, M. Inorg. Chem. **1991**, 30, 679.